

---

# Performance of Concrete Pavements,

---

## Volume II: Evaluation of Inservice

---

### Concrete Pavements

---

PB2001-101110



PUBLICATION NO. FHWA-RD-95-110

JUNE 1998



U.S. Department of Transportation  
**Federal Highway Administration**

Research and Development  
Turner-Fairbank Highway Research Center  
6300 Georgetown Pike  
McLean, VA 22101-2296



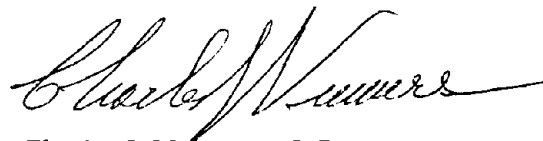
REPRODUCED BY:  
U.S. Department of Commerce  
National Technical Information Service  
Springfield, Virginia 22161

## FOREWORD

This report is part of a four-volume series titled "Performance of Concrete Pavements." The goal of this project was to improve design and construction procedures for conventional Portland Cement Concrete (PCC) pavements. During the field study in 1992 more than 300 test pavement sections located throughout North America were surveyed. The test pavements were previously constructed in individual State research studies. Fifteen States participated in the project: Arizona, California, Florida, Georgia, Illinois, Michigan, Minnesota, Missouri, New Jersey, New York, North Carolina, Ohio, Pennsylvania, West Virginia, Wisconsin and the Province of Ontario. About one-third of the sections were also surveyed in 1987 so some data is also available on trends with time. Data was also gathered on 96 PCC pavements from Europe and 21 PCC sections from Chile. The information was entered into the Rigid Pavement Performance (RIPPER) data base which is based on the SHRP LTPP data base. The RIPPER data base is available from the Federal Highway Administration.

The RIPPER data base was analyzed by researchers from Chile to develop the "Pavement Evaluator" program. These models will comprise part of the World Bank's HDM-4 system. The new models were tested with the Long Term Pavement performance (LTPP) data base. Information assimilated under this project also served as the basis for a set of supplemental AASHTO equations that were approved in 1997. A spreadsheet to perform these checks was built by the LTPP Implementation Program and will aid engineers to optimize PCC designs.

Volume I summarizes the pavement sections and performance data. Volume II presents the results design features. Volume III presents new equations for cracking, faulting, spalling, serviceability, and roughness. Volume IV documents data and key findings from the European and Chilean studies. These findings combined with results from the LTPP program will advance the "state of the practice" for PCC pavement materials, design, and construction procedures.



Charles J. Nemmers, P.E.  
Director, Office of Engineering  
Research and Development

## NOTICE

This document is disseminated under the sponsorship of the Department of Transportation in the interest of information exchange. The United States Government assumes no liability for its contents or use thereof. This report does not constitute a standard, specification or regulation.

The United States Government does not endorse products or manufacturers. Trade and Manufacturers' names appear in this report only because they are considered essential to the object of the document.

1. Report No. FHWA-RD-95-110		3. Recipient's Catalog No.	
4. Title and Subtitle PERFORMANCE OF CONCRETE PAVEMENTS  Volume II—Evaluation of Inservice Concrete Pavements		5. Report Date June 1998	
		6. Performing Organization Code	
7. Author(s) K. D. Smith, M. J. Wade, D. G. Peshkin, L. Khazanovich, H. T. Yu, M. I. Darter		8. Performing Organization Report No.	
9. Performing Organization Name and Address ERES Consultants, Inc. 505 W. University Avenue Champaign, IL 61820-3915		10. Work Unit No. (TRAIS) 3C1A	
		11. Contract or Grant No. DTFH61-91-C-00053	
12. Sponsoring Agency Name and Address Office of Engineering and Highway Operations R & D Federal Highway Administration 6300 Georgetown Pike McLean, VA 22101-2296		13. Type of Report and Period Covered Final Report October 1991-April 1996	
		14. Sponsoring Agency Code	
15. Supplementary Notes FHWA Contracting Officer's Technical Representative (COTR): Jim Sherwood, HNR-20 Special thanks are given to the following highway agencies for their assistance in the conduct of this study: Arizona, California, Florida, Georgia, Illinois, Michigan, Minnesota, Missouri, New Jersey, New York, Ohio, Ontario, Pennsylvania, Wisconsin, and West Virginia.			
16. Abstract <p>With the goal of improving future concrete pavement design and construction practices, this project evaluated the performance of 303 inservice concrete pavement sections located throughout North America. An extensive field testing program, consisting of pavement condition surveys, drainage surveys, falling weight deflectometer (FWD) testing, coring/boring operations, and roughness testing, was conducted in order to collect the information needed for analysis. Because many of these pavement sections are part of State-level studies on concrete pavements, a range of design variables (e.g., load transfer, slab thickness, joint spacing, drainage) thought to affect concrete pavement performance are present. Over one-third of the sections was evaluated under a preceding FHWA study, meaning that 5-year performance trends are available for some of the sections. Additional pavement performance data are also available for 96 European concrete pavement sections and for 21 Chilean concrete pavement sections. The average age and average cumulative ESAL loadings for the North American sections are 16 years and 7.1 million, respectively, compared to 21 years and 21.8 million for the European sections and 9 years and 5.9 million for the Chilean sections.</p> <p>This volume examines the performance of the North American concrete pavement sections included in the study. This examination primarily consists of an evaluation of the effect of concrete pavement design features on concrete pavement performance. Design features investigated include slab thickness, joint spacing, joint orientation, load transfer, joint sealant, base type, drainage, shoulder type, reinforcement, and pavement type. The results of an examination of the backcalculation results are also presented, as are the significant findings of an evaluation conducted on the performance of European and Chilean concrete pavements.</p> <p>This volume is the second of four volumes. The other volumes are:</p> <p>FHWA-RD-94-177 Volume I—Field Investigation FHWA-RD-95-111 Volume III—Improving Concrete Pavement Performance FHWA-RD-95-112 Volume IV—Appendixes</p>			
17. Key Words Concrete pavement, pavement design, pavement performance, pavement evaluation, pavement monitoring, performance trends, field testing, experimental pavements		18. Distribution Statement No restrictions. This document is available to the public through the National Technical Information Service, Springfield, Virginia 22161.	
19. Security Classif. (of this report) Unclassified	20. Security Classif. (of this page) Unclassified	21. No of Pages	22. Price

# SI\* (MODERN METRIC) CONVERSION FACTORS

## APPROXIMATE CONVERSIONS TO SI UNITS

## APPROXIMATE CONVERSIONS FROM SI UNITS

Symbol	When You Know	Multiply By	To Find	Symbol	Symbol	When You Know	Multiply By	To Find	Symbol
<b>LENGTH</b>					<b>LENGTH</b>				
in	inches	25.4	millimeters	mm	mm	millimeters	0.039	inches	in
ft	feet	0.305	meters	m	m	meters	3.28	feet	ft
yd	yards	0.914	meters	m	m	meters	1.09	yards	yd
mi	miles	1.61	kilometers	km	km	kilometers	0.621	miles	mi
<b>AREA</b>					<b>AREA</b>				
in <sup>2</sup>	square inches	645.2	square millimeters	mm <sup>2</sup>	mm <sup>2</sup>	square millimeters	0.0016	square inches	in <sup>2</sup>
ft <sup>2</sup>	square feet	0.093	square meters	m <sup>2</sup>	m <sup>2</sup>	square meters	10.764	square feet	ft <sup>2</sup>
yd <sup>2</sup>	square yards	0.836	square meters	m <sup>2</sup>	m <sup>2</sup>	square meters	1.195	square yards	yd <sup>2</sup>
ac	acres	0.405	hectares	ha	ha	hectares	2.47	acres	ac
mi <sup>2</sup>	square miles	2.59	square kilometers	km <sup>2</sup>	km <sup>2</sup>	square kilometers	0.386	square miles	mi <sup>2</sup>
<b>VOLUME</b>					<b>VOLUME</b>				
fl oz	fluid ounces	29.57	milliliters	mL	mL	milliliters	0.034	fluid ounces	fl oz
gal	gallons	3.785	liters	L	L	liters	0.264	gallons	gal
ft <sup>3</sup>	cubic feet	0.028	cubic meters	m <sup>3</sup>	m <sup>3</sup>	cubic meters	35.71	cubic feet	ft <sup>3</sup>
yd <sup>3</sup>	cubic yards	0.765	cubic meters	m <sup>3</sup>	m <sup>3</sup>	cubic meters	1.307	cubic yards	yd <sup>3</sup>
NOTE: Volumes greater than 1000 l shall be shown in m <sup>3</sup> .									
<b>MASS</b>					<b>MASS</b>				
oz	ounces	28.35	grams	g	g	grams	0.035	ounces	oz
lb	pounds	0.454	kilograms	kg	kg	kilograms	2.202	pounds	lb
T	short tons (2000 lb)	0.907	megagrams (or "metric ton")	Mg (or "t")	Mg (or "t")	megagrams (or "metric ton")	1.103	short tons (2000 lb)	T
<b>TEMPERATURE (exact)</b>					<b>TEMPERATURE (exact)</b>				
°F	Fahrenheit temperature	5(F-32)/9 or (F-32)/1.8	Celcius temperature	°C	°C	Celcius temperature	1.8C + 32	Fahrenheit temperature	°F
<b>ILLUMINATION</b>					<b>ILLUMINATION</b>				
fc	foot-candles	10.76	lux	lx	lx	lux	0.0929	foot-candles	fc
fl	foot-Lamberts	3.426	candela/m <sup>2</sup>	cd/m <sup>2</sup>	cd/m <sup>2</sup>	candela/m <sup>2</sup>	0.2919	foot-Lamberts	fl
<b>FORCE and PRESSURE or STRESS</b>					<b>FORCE and PRESSURE or STRESS</b>				
lbf	poundforce	4.45	newtons	N	N	newtons	0.225	poundforce	lbf
lbf/in <sup>2</sup>	poundforce per square inch	6.89	kilopascals	kPa	kPa	kilopascals	0.145	poundforce per square inch	lbf/in <sup>2</sup>


\* SI is the symbol for the International System of Units. Appropriate rounding should be made to comply with Section 4 of ASTM E380.

# TABLE OF CONTENTS

## Volume I Field Investigation

<b>1. INTRODUCTION</b> .....	1
Background .....	1
Project Scope and Objectives .....	2
Sequence of Report .....	3
<b>2. DATA COLLECTION PROCEDURES</b> .....	5
Introduction .....	5
Data Elements .....	6
Office Data Collection .....	6
Field Data Collection .....	6
Data Reduction Procedures .....	25
Data Base .....	34
<b>3. PERFORMANCE OF PAVEMENT SECTIONS</b> .....	35
Introduction .....	35
Performance Summary of Projects in Dry-Freeze Zone .....	37
Performance Summary of Projects in Dry-Nonfreeze Zone .....	58
Performance Summary of Projects in Wet-Freeze Zone .....	78
Performance Summary of Projects in Wet-Nonfreeze Zone .....	183
Overall Summary .....	222
<b>4. CLOSURE</b> .....	223
<b>REFERENCES</b> .....	225

*PROTECTED UNDER INTERNATIONAL COPYRIGHT  
ALL RIGHTS RESERVED  
NATIONAL TECHNICAL INFORMATION SERVICE  
U.S. DEPARTMENT OF COMMERCE*

Reproduced from  
best available copy. 

# TABLE OF CONTENTS

## Volume II Evaluation of Inservice Concrete Pavements

<b>1. INTRODUCTION</b> .....	1
Background .....	1
Research Objectives .....	2
Research Approach .....	2
Advisory Panel .....	3
Overview of Report .....	4
<b>2. OVERVIEW OF PROJECTS EVALUATED IN STUDY</b> .....	5
Introduction .....	5
Description of Projects .....	5
Overall Summary of Projects .....	35
<b>3. EFFECT OF DESIGN FEATURES ON PAVEMENT PERFORMANCE</b> .....	39
Introduction .....	39
Slab Thickness .....	39
Joint Spacing .....	55
Joint Orientation .....	71
Transverse Joint Load Transfer .....	77
Joint Sealant .....	92
Base Type .....	108
Drainage .....	136
Subgrade Type .....	158
Shoulder Type .....	161
Widened Lanes .....	177
Reinforcement .....	179
Maximum Course Aggregate Size .....	186
Pavement Type .....	190
<b>4. EXAMINATION OF BACKCALCULATION RESULTS</b> .....	207
Introduction .....	207
Fundamental Concept .....	208
The "Best Fit" Backcalculation Procedure .....	210
Backcalculation Procedure for Two-Layered Slab .....	214

# TABLE OF CONTENTS

## Volume II (continued)

Determination of In-Place Material Properties .....	221
<b>5. SUMMARY OF EUROPEAN AND CHILEAN CONCRETE PAVEMENT PERFORMANCE .....</b>	<b>231</b>
Introduction .....	231
Evaluation of European Concrete Pavement Performance .....	231
Evaluation of Pavement Performance for Each European Country .....	236
Overall Evaluation of European Pavement Performance .....	259
Evaluation of Chilean Concrete Pavement Performance .....	265
<b>6. SUMMARY AND CONCLUSIONS .....</b>	<b>281</b>
Overview of Report .....	281
Review of Significant Findings .....	282
Closure .....	298
<b>REFERENCES .....</b>	<b>299</b>

# TABLE OF CONTENTS

## Volume III Improving Concrete Pavement Performance

<b>1. INTRODUCTION</b> .....	1
Background .....	1
Research Objectives .....	2
Research Approach .....	2
Advisory Panel .....	3
Overview of Report .....	3
<b>2. DEVELOPMENT OF CONCRETE PAVEMENT     PERFORMANCE PREDICTION MODELS</b> .....	5
Introduction .....	5
General Description of Data Used in Model Development .....	7
Joint Faulting Model for Doweled Jointed Concrete Pavements .....	7
Joint Faulting Model for Nondoweled Jointed Concrete Pavements .....	23
Transverse Cracking Model for JPCP .....	34
Crack Deterioration Model for JRCP .....	82
Transverse Joint Spalling Model for JPCP .....	97
Transverse Joint Spalling Model for JRCP .....	114
Present Serviceability Rating Model .....	127
International Roughness Index (IRI) Model for JPCP .....	138
Example Application of Performance Prediction Models .....	140
Summary .....	145
<b>3. CONCRETE PAVEMENT DESIGN RECOMMENDATIONS</b> .....	147
Introduction .....	147
Effect of Site Conditions on Concrete Pavement Performance .....	147
Design Recommendations for Concrete Pavements .....	150
Concrete Pavement Type Selection Considerations .....	254
Summary .....	256



# TABLE OF CONTENTS

## Volume IV Appendixes

<b>APPENDIX A—PROJECT SUMMARY TABLES</b> .....	1
Introduction .....	1
General Information for the Projects Included in the Study (Table 5) .....	1
Structural Design Data (Table 6) .....	3
Joint Design Data (Table 7) .....	5
Outer Shoulder and Drainage Design Data (Table 8) .....	8
Traffic Data (Table 9) .....	11
Outer Lane Deflection Data (Table 10) .....	12
Edge Deflection Data (Table 11) .....	14
Primary Outer Lane Performance Data (Table 12) .....	16
Secondary Outer Lane Performance Data (Table 13) .....	18
Continuously Reinforced Concrete Pavement Performance Data (Table 14) .....	21
 <b>APPENDIX B—AN EVALUATION OF EUROPEAN CONCRETE PAVEMENTS</b> .....	 107
<b>1. INTRODUCTION</b> .....	107
Background .....	107
Analysis of Data .....	108
Description of Summary Report .....	109
<b>2. SUMMARY OF CONCRETE PAVEMENT PERFORMANCE BY     COUNTRY</b> .....	 111
Introduction .....	111
European COPES Data Base .....	111
Data Analysis .....	113
France .....	114
Italy .....	137
The United Kingdom .....	147
Belgium .....	164
Switzerland .....	182

# TABLE OF CONTENTS

## Volume IV (continued)

<b>3. SUMMARY OF OVERALL PAVEMENT PERFORMANCE</b> .....	203
Introduction .....	203
Design Features .....	203
Climatic Information .....	208
Traffic Data .....	208
Pavement Performance .....	210
Overall Summary of Important Findings .....	219
<b>4. CLOSURE</b> .....	221
Introduction .....	221
Review of Report Sequence .....	222
Additional Work .....	222
<b>APPENDIX C—AN EVALUATION OF CHILEAN CONCRETE PAVEMENTS</b> .....	225
<b>1. INTRODUCTION</b> .....	225
Background .....	225
Data Analysis .....	226
Description of Summary Report .....	226
<b>2. SUMMARY OF DESIGN AND CONSTRUCTION INFORMATION</b> .	227
Introduction .....	227
Chilean Program .....	227
Instrumentation .....	227
Design Features .....	229
Climatic Information .....	236
Traffic Data .....	237
Summary .....	241
<b>3. SUMMARY OF OVERALL PAVEMENT PERFORMANCE</b> .....	243
Introduction .....	243
Data Analysis .....	243
Pavement Performance .....	244
Overall Summary of Important Findings .....	260

# TABLE OF CONTENTS

## Volume IV (continued)

APPENDIX D—BIBLIOGRAPHY .....	263
APPENDIX E—REPRINT OF PAPER, <i>A PERFORMANCE EVALUATION OF PCC PAVEMENTS CONSTRUCTED ON PERMEABLE BASES</i> .....	275
REFERENCES .....	295

# LIST OF FIGURES

## Volume I Field Investigation

1.	General location of sections included in the study . . . . .	8
2.	Field survey form—general information collection form . . . . .	10
3.	Field survey form—pavement data collection form . . . . .	11
4.	Drainage survey sheet . . . . .	14
5.	Photographic record form . . . . .	18
6.	Sensor configurations used in the FWD testing . . . . .	22
7.	FWD testing pattern . . . . .	22
8.	Arrangement of pavement temperature measurement holes . . . . .	23
9.	Performance summary for MN 1 & 5 . . . . .	40
10.	Roughness and serviceability for MN 1 & 5 . . . . .	43
11.	Faulting and transverse cracking 5-year performance trends for MN 1 & 5 . . . . .	44
12.	Performance summary for MN 2 . . . . .	47
13.	Roughness and serviceability for MN 2 . . . . .	49
14.	5-year performance trends for MN 2 . . . . .	50
15.	Performance summary for MN 7 . . . . .	56
16.	Performance of dowel coatings on MN 7 . . . . .	57
17.	Roughness and serviceability for MN 7 . . . . .	59
18.	Performance summary for AZ 1 . . . . .	62
19.	Roughness and serviceability for AZ 1 . . . . .	64
20.	5-year performance trends for AZ 1 . . . . .	65
21.	Performance summary for CA 1 . . . . .	70
22.	Roughness and serviceability for CA 1 . . . . .	72
23.	5-year performance trends for CA 1 . . . . .	73
24.	Performance summary for IL 1 . . . . .	83
25.	Roughness for IL 1 . . . . .	84
26.	Performance summary for IL 2 . . . . .	87
27.	Roughness for IL 2 . . . . .	88
28.	Performance summary for MI 1 . . . . .	91
29.	Roughness and serviceability for MI 1 . . . . .	93
30.	5-year performance trends for MI 1 . . . . .	95
31.	Performance summary for MO 1 . . . . .	102
32.	Roughness and serviceability for MO 1 . . . . .	103
33.	Performance summary for NY 1 . . . . .	109
34.	Roughness and serviceability for NY 1 . . . . .	111
35.	5-year performance trends for NY 1 . . . . .	112
36.	Performance summary for NY 2 . . . . .	116
37.	Roughness and serviceability for NY 2 . . . . .	117
38.	5-year performance trends for NY 2 . . . . .	119
39.	Performance summary for OH 1 . . . . .	121

# LIST OF FIGURES

## Volume I (continued)

40.	Roughness measurements for OH 1 .....	123
41.	5-year performance trends for OH 1 .....	125
42.	Performance summary of OH 2 sections, joint faulting and spalling .....	130
43.	Performance summary of OH 2 sections, transverse and longitudinal cracking .....	131
44.	Roughness summary of OH 2 sections .....	132
45.	5-year performance trends of OH 2 sections .....	137
46.	Performance summary of ONT 1 sections .....	140
47.	Roughness and serviceability summary of ONT 1 sections .....	141
48.	5-year performance trends for ONT 1 sections .....	142
49.	Performance summary for PA 1 sections .....	148
50.	Roughness and serviceability for PA 1 sections .....	149
51.	5-year performance trends for PA 1 sections .....	150
52.	Performance summary for WV 1 .....	153
53.	Roughness and serviceability for WV 1 .....	154
54.	Performance summary for WI 1 .....	157
55.	Roughness and serviceability for WI 1 .....	159
56.	Performance summary for WI 2 and WI 7 .....	162
57.	Roughness and serviceability for WI 2 and WI 7 .....	164
58.	Performance summary for WI 3 .....	167
59.	Roughness and serviceability for WI 3 .....	168
60.	Performance summary for WI 4 .....	172
61.	Roughness and serviceability for WI 4 .....	173
62.	Performance summary for WI 5 .....	177
63.	Roughness and serviceability for WI 5 .....	178
64.	Performance summary for WI 6 .....	181
65.	Roughness and serviceability for WI 6 .....	182
66.	Performance summary for CA 3 .....	186
67.	Roughness and serviceability for CA 3 .....	188
68.	5-year performance trends for CA 3 .....	189
69.	Performance summary for CA 9 .....	193
70.	Roughness and serviceability for CA 9 .....	195
71.	Performance summary for JPCP sections for FL 4 .....	202
72.	Performance summary for CRCP/FRC sections for FL 4 .....	203
73.	Roughness and serviceability for JPCP sections for FL 4 .....	206
74.	Performance summary for GA 1 and GA 2 .....	211
75.	Roughness and serviceability for GA 1 and GA 2 .....	212
76.	Performance summary for NC 1 .....	216
77.	Roughness and serviceability for NC 1 .....	218
78.	5-year performance trends for NC 1 .....	220

# LIST OF FIGURES

## Volume II Evaluation of Inservice Concrete Pavements

1.	General location of projects included in the study	7
2.	Hinge joint design details for JRCP sections in Illinois	16
3.	Distribution of projects by age	37
4.	Distribution of projects by ESAL applications	37
5.	Distribution of slab thickness in sections	41
6.	Average transverse joint faulting versus slab thickness for all sections	52
7.	Effect of slab thickness on transverse cracking	53
8.	Loaded slab corner deflection by slab thickness for all sections	55
9.	Distribution of joint spacings for JPCP	56
10.	Distribution of joint spacings for JRCP	57
11.	Effect of joint spacing on JPCP transverse cracking	67
12.	Transverse cracking as a function of $L/\ell$ ratio for aggregate bases	68
13.	Transverse cracking as a function of $L/\ell$ ratio for dense-graded stabilized bases	68
14.	Faulting of randomly spaced joints	70
15.	Effect of joint spacing on JRCP transverse cracking	70
16.	Distribution of sections by joint orientation	72
17.	Effect of joint orientation on transverse joint faulting	75
18.	Effect of joint orientation on transverse joint spalling	75
19.	Effect of joint orientation on IRI	76
20.	Effect of joint orientation on corner breaking	77
21.	Distribution of doweled and nondoweled sections	78
22.	Distribution of dowel coatings	78
23.	Comparison of faulting for doweled and nondoweled sections	89
24.	Effect of dowel bar diameter on transverse joint faulting	90
25.	Effect of load transfer efficiency on transverse joint faulting	91
26.	Effect of dowel diameter on transverse joint spalling	91
27.	Transverse joint faulting for different dowel bar coatings	92
28.	Number of sections sealed with each sealant material (for all sections)	94
29.	Transverse joint spalling percentage by sealant type for all sections	105
30.	Sealant condition rating by joint sealant type for all sections	106
31.	Comparison of IRI for different joint sealant types	106
32.	Distribution of different base types	109
33.	Average transverse joint faulting for each base type	131
34.	Average transverse joint faulting by erodibility class	131
35.	Average joint spalling for each base type	132
36.	Transverse cracking by base type for JPCP	133
37.	Average deflections for each base type	133

# LIST OF FIGURES

## Volume II (continued)

38.	Effect of percentage of cement on transverse joint faulting . . . . .	134
39.	Effect of percentage of cement on corner deflections . . . . .	135
40.	Effect of percentage of asphalt cement on transverse joint faulting . . . . .	135
41.	Effect of percentage of asphalt cement on corner deflections . . . . .	136
42.	Distribution of drainage designs . . . . .	137
43.	Distribution of drainage designs for doweled and nondoweled pavements . . . . .	137
44.	Transverse joint faulting for each drainage design . . . . .	154
45.	Transverse joint spalling for each drainage design . . . . .	155
46.	Transverse cracking for each drainage design . . . . .	155
47.	Average age for each drainage design . . . . .	156
48.	Transverse joint faulting for various drainage coefficients . . . . .	157
49.	Effect of $P_{200}$ on transverse joint faulting . . . . .	158
50.	Effect of $C_U$ on transverse joint faulting . . . . .	159
51.	Distribution of subgrade types . . . . .	160
52.	Effect of subgrade type on transverse joint faulting of doweled pavements . . . . .	160
53.	Effect of subgrade type on transverse faulting of nondoweled pavements . . . . .	161
54.	Effect of edge support on edge deflection . . . . .	174
55.	Effect of edge support on transverse joint faulting . . . . .	174
56.	Effect of edge support on JPCP transverse cracking . . . . .	175
57.	Effect of load offset on calculated stress . . . . .	179
58.	Effect of steel percentage on deteriorated transverse cracking . . . . .	184
59.	Comparison between the "best fit" and AREA-based backcalculation procedures . . . . .	213
60.	Comparison of backcalculated PCC moduli for two sets of modular ratio; Unbonded interface between PCC plate and base . . . . .	219
61.	Comparison of backcalculated PCC moduli for two sets of modular ratio; Bonded interface between PCC plate and base . . . . .	219
62.	Percentage of sections vs. percentage of data kept . . . . .	220
63.	Comparison between backcalculated $E_{pcc}$ before and after screening . . . . .	222
64.	Comparison between backcalculated $k$ before and after screening . . . . .	222
65.	Backcalculated project average PCC moduli values . . . . .	227
66.	Backcalculated subgrade modulus of reactions, $k$ , values . . . . .	227
67.	Comparison of $k$ values determined in 1987 and 1992 . . . . .	228
68.	Effective slab thickness of stabilized base sections . . . . .	229
69.	Days per year (N) of heavy rainfall . . . . .	270

# LIST OF FIGURES

## Volume III Improving Concrete Pavement Performance

1.	Procedures used in the development of mechanistic-empirical statistical models . . . . .	6
2.	General location of sections included in study . . . . .	8
3.	Distribution of projects by age . . . . .	10
4.	Distribution of projects by ESAL applications . . . . .	10
5.	Two-dimensional scatter plot for doweled joint faulting model . . . . .	15
6.	Actual versus predicted faulting for the doweled faulting model . . . . .	20
7.	Predicted versus residual for the doweled faulting model . . . . .	20
8.	Sensitivity plot of the doweled faulting model with ESAL applications and bearing stress . . . . .	21
9.	Sensitivity plot of the doweled faulting model with ESAL applications and joint spacing . . . . .	21
10.	Sensitivity plot of the doweled faulting model with ESAL applications and $C_d$ . . . . .	22
11.	Sensitivity plot of the doweled faulting model with ESAL applications and freezing index . . . . .	22
12.	Sensitivity plot of the doweled faulting model with ESAL applications and mean annual precipitation . . . . .	23
13.	Two-dimensional scatter plot for nondoweled joint faulting model . . . . .	26
14.	Actual versus predicted faulting for the nondoweled faulting model . . . . .	30
15.	Predicted versus residual for the nondoweled faulting model . . . . .	30
16.	Sensitivity plot of the nondoweled faulting model with ESAL applications and slab thickness . . . . .	31
17.	Sensitivity plot of the nondoweled faulting model with ESAL applications and joint spacing . . . . .	31
18.	Sensitivity plot of the nondoweled faulting model with ESAL applications and $C_d$ . . . . .	32
19.	Sensitivity plot of the nondoweled faulting model with ESAL applications and freezing index . . . . .	32
20.	Sensitivity plot of the nondoweled faulting model with ESAL applications and the number of days above 90 °F . . . . .	33
21.	Sensitivity plot of the nondoweled faulting model with ESAL applications and annual precipitation . . . . .	33
22.	Comparison of PCC MR obtained by nondestructive testing and core testing . . . . .	39
23.	Distribution of hourly temperature gradient for CA 1 sections for an average year . . . . .	40
24.	Distribution of hourly temperature gradient for OH 2 sections for an average year . . . . .	41



# LIST OF FIGURES

## Volume III (continued)

25.	Distribution of hourly temperature gradient for GA 1 sections for an average year . . . . .	41
26.	Typical distribution of fatigue damage across a pavement slab . . . . .	55
27.	Preliminary fatigue analysis results given by ERES/COE fatigue model . . .	59
28.	Preliminary fatigue analysis results given by NCHRP 1-26 fatigue model . . . . .	59
29.	Preliminary fatigue analysis results given by Zero-Maintenance fatigue model . . . . .	60
30.	Preliminary fatigue analysis results given by ARE fatigue model . . . . .	60
31.	Edge load stress distribution across a pavement slab at mid-slab . . . . .	61
32.	Fatigue damage distribution across a pavement slab due to the loads placed at various distances away from the pavement edge . . . . .	62
33.	Effects of stress level and mean wheel location on p/c . . . . .	64
34.	Example fatigue damage calculation . . . . .	66
35.	Effects of temperature gradient shifts on critical stresses for fatigue damage . . . . .	67
36.	The effects of slab length on critical stresses in the pavement slab . . . . .	68
37.	Slab cracking data versus total ESAL applied . . . . .	70
38.	Slab cracking versus fatigue damage calculated using load stresses only . .	70
39.	Slab cracking versus fatigue damage calculated considering both load and curling stresses . . . . .	71
40.	Results of fatigue analysis performed using effective slab thickness . . . . .	72
41.	Results of fatigue analysis performed using design slab thickness . . . . .	73
42.	Fatigue analysis results with 4 °F (2.2 °C) shift applied to the temperature gradient . . . . .	75
43.	Fatigue analysis results with 8 °F (4.4 °C) shift applied to the temperature gradient . . . . .	75
44.	Final fatigue analysis results, including slab thickness and temperature gradient adjustments . . . . .	76
45.	The fatigue cracking model . . . . .	77
46.	Sensitivity of JPCP cracking model to slab thickness . . . . .	79
47.	Sensitivity of JPCP cracking model to joint spacing . . . . .	79
48.	Sensitivity of JPCP cracking model to shoulder spacing . . . . .	80
49.	Sensitivity of JPCP cracking model to bonding condition of base . . . . .	80
50.	Sensitivity of JPCP cracking model to climate . . . . .	81
51.	Sensitivity of JPCP cracking model to k-value . . . . .	81
52.	Sensitivity of JPCP cracking model to modulus of rupture . . . . .	82
53.	Comparison of predicted and actual slab cracking—section by section adjustments for built-in curling . . . . .	83

# LIST OF FIGURES

## Volume III (continued)

54.	Comparison of predicted and actual slab cracking—regional adjustments for built-in curling (DF=11°F [6.1°C]; DN=11.5 °F [6.4 °C]; WF=8°F [4.4 °C]; WN=8.5 °C[4.7 °C]) . . . . .	84
55.	Two-dimensional scatter plot for JRCP crack deterioration model . . . . .	88
56.	Actual versus predicted deteriorated cracking . . . . .	91
57.	Predicted versus residual deteriorated cracking . . . . .	91
58.	Sensitivity plot of the JRCP crack deterioration model showing effect of age and ESAL applications . . . . .	93
59.	Sensitivity plot for JRCP crack deterioration model showing effect of age and longitudinal reinforcement (stabilized base) . . . . .	93
60.	Sensitivity plot for JRCP crack deterioration model showing effect of age and longitudinal reinforcement (nonstabilized base) . . . . .	94
61.	Sensitivity plot for JRCP crack deterioration model showing effect of age and modulus of elasticity of concrete . . . . .	94
62.	Sensitivity plot for JRCP crack deterioration model showing effect of age and freezing index . . . . .	95
63.	Sensitivity plot for JRCP crack deterioration model showing effect of age and moisture index . . . . .	95
64.	Comparison of JRCP crack deterioration on selected Ohio sections with the model prediction . . . . .	96
65.	Two-dimensional scatter plot for JPCP spalling model . . . . .	101
66.	Actual versus predicted percentage of JPCP spalled joints . . . . .	105
67.	Actual versus residual percentage of JPCP spalled joints . . . . .	105
68.	Sensitivity plot of the JPCP joint spalling model for age and sealant type (FI = 1650) . . . . .	106
69.	Sensitivity plot of the JPCP joint spalling model for age and sealant type (FI = 1000) . . . . .	106
70.	Sensitivity plot of the JPCP joint spalling model for age and sealant type (FI = 0, Days90 = 10) . . . . .	107
71.	Sensitivity plot of the JPCP joint spalling model for age and sealant type (FI = 0, Days90 = 150) . . . . .	107
72.	Sensitivity plot of the JPCP joint spalling model for age and dowel protection . . . . .	108
73.	Sensitivity plot of the JPCP joint spalling model for age and freezing index (liquid sealant) . . . . .	108
74.	Sensitivity plot of the JPCP joint spalling model for age and freezing index (preformed sealant) . . . . .	109
75.	Sensitivity plot of the JPCP joint spalling model for age and freezing index (silicone sealant) . . . . .	109
76.	Sensitivity plot of the JPCP joint spalling model for age and freezing index (no sealant) . . . . .	110

# LIST OF FIGURES

## Volume III (continued)

77.	JPCP joint spalling distribution on Wisconsin sections . . . . .	110
78.	Comparison of JPCP spalling on selected Wisconsin sections with the model prediction . . . . .	111
79.	Comparison of JPCP spalling on selected Minnesota sections with the model prediction . . . . .	111
80.	Comparison of JPCP spalling on selected Arizona sections with the model prediction . . . . .	112
81.	Two-dimensional scatter plot for JRCP spalling model . . . . .	119
82.	Actual versus predicted percentage of JRCP spalled joints . . . . .	122
83.	Actual versus residual percentage of JRCP . . . . .	122
84.	Sensitivity plot of the JRCP joint spalling model for age, dowel coating, and sealant type (FI = 1500) . . . . .	123
85.	Sensitivity plot of the JRCP joint spalling model for age, dowel coating, and sealant type (FI = 200) . . . . .	123
86.	Sensitivity plot of the JRCP joint spalling model for age and joint spacing . . . . .	124
87.	Sensitivity plot of the JRCP joint spalling model for age and freezing index (liquid sealant, DOWELCOR = 0) . . . . .	124
88.	Sensitivity plot of the JRCP joint spalling model for age and freezing index (liquid sealant, DOWELCOR = 1) . . . . .	125
89.	Sensitivity plot of the JRCP joint spalling model for age and freezing index (preformed sealant, DOWELCOR = 0) . . . . .	125
90.	Sensitivity plot of the JRCP joint spalling model for age and freezing index (preformed sealant, DOWELCOR = 1) . . . . .	126
91.	Comparison of JRCP spalling on selected Minnesota sections with the model prediction . . . . .	126
92.	Two-dimensional scatter plot for JPCP PSR model . . . . .	129
93.	Actual versus predicted serviceability for the JPCP serviceability model . . .	131
94.	Predicted versus residuals for the JPCP PSR model . . . . .	131
95.	Sensitivity plot of the JPCP PSR model with faulting and transverse cracking . . . . .	132
96.	Sensitivity plot of the JPCP PSR model with transverse cracking and spalling . . . . .	132
97.	Sensitivity plot of the JPCP PSR model with faulting and spalling . . . . .	133
98.	Sensitivity plot of the JPCP PSR model with transverse cracking and longitudinal cracking . . . . .	133
99.	Two-dimensional scatter plot for JRCP PSR model . . . . .	134
100.	Actual versus predicted serviceability for the JRCP PSR model . . . . .	135
101.	Predicted versus residual for the JRCP PSR model . . . . .	136

# LIST OF FIGURES

## Volume III (continued)

102.	Sensitivity plot of the JRCP PSR model with faulting and transverse cracking . . . . .	136
103.	Sensitivity plot of the JRCP PSR model with transverse cracking and spalling . . . . .	137
104.	Sensitivity plot of the JRCP PSR model with faulting and spalling . . . . .	137
105.	Two-dimensional scatter plot for JPCP IRI model . . . . .	139
106.	Actual versus predicted PSR for the JPCP IRI model . . . . .	140
107.	Predicted versus residual for the JPCP IRI model . . . . .	141
108.	Sensitivity plot of the JPCP IRI model with faulting and transverse cracking . . . . .	141
109.	Sensitivity plot of the JPCP IRI model with transverse cracking and spalling . . . . .	142
110.	Sensitivity plot of the JPCP IRI model with faulting and spalling . . . . .	142
111.	Soil stabilization selection guidelines . . . . .	151
112.	Flow chart of drainage design recommendations based on $C_d$ (for pavements with design ESAL's greater than 5 million) . . . . .	157
113.	Cross section of a "bathtub" design . . . . .	159
114.	Example permeable base design . . . . .	159
115.	Daylighted pavement cross section . . . . .	160
116.	California drained LCB design . . . . .	161
117.	Effect of drainability on nondoweled joint faulting . . . . .	162
118.	Effect of drainability on doweled joint faulting . . . . .	162
119.	Typical cross section of subsurface drainage systems for crowned section and tied concrete shoulders . . . . .	167
120.	Typical cross section of subsurface drainage system for constant slope cross section and AC shoulders . . . . .	167
121.	Plot of New Jersey gradation . . . . .	168
122.	Recommended edge drain design . . . . .	171
123.	Recommended design for edge drain outlet . . . . .	172
124.	Smooth, long-radius bends and dual outlet system for cleanout and video camera inspection . . . . .	172
125.	A recommended headwall design . . . . .	174
126.	Geotextile wrapped drain . . . . .	175
127.	Partially wrapped drain . . . . .	175
128.	Nonwrapped drain . . . . .	175
129.	Geocomposite drain . . . . .	175
130.	Recommended installation detail for fin drains . . . . .	176
131.	Performance of sections on permeable and adjacent nonpermeable bases (nondoweled pavements). . . . .	183

# LIST OF FIGURES

## Volume III (continued)

132.	Performance of sections on permeable and adjacent nonpermeable bases (doweled pavements) . . . . .	183
133.	Effect of stabilized base on nondoweled joint faulting . . . . .	185
134.	Effect of stabilized base on JRCP crack deterioration . . . . .	185
135.	German JPCP design showing widened PCC slab and PCC shoulders. . . . .	193
136.	Types of PCC shoulder construction . . . . .	194
137.	Normalized edge load stress distribution across a slab under varying load locations . . . . .	197
138.	Effect of widened slab on doweled joint faulting . . . . .	198
139.	Sawcut rating as a function of compressive strength . . . . .	200
140.	Cracking performance as a function of $L/\ell$ . . . . .	202
141.	Example nonuniform joint spacing pattern (with skewed joints) . . . . .	205
142.	Illustration of load transfer concept . . . . .	208
143.	Effects of dowel diameter on faulting . . . . .	209
144.	Effect of sealing and sealant type on joint spalling . . . . .	211
145.	Cross section of joint sealant installation . . . . .	215
146.	Longitudinal contraction joint design . . . . .	217
147.	JRCP crack deterioration as a function of reinforcement content . . . . .	219
148.	Illustration of Illinois hinge joint design . . . . .	224
149.	Effects of JPCP slab thickness on mid-panel fatigue cracking for wet-freeze climatic region . . . . .	235
150.	Sensitivity of mid-panel fatigue cracking to joint spacing and slab thickness for wet-freeze climatic region . . . . .	237
151.	Effects of dynamic $k$ -value on stresses in pavement slabs for wet-freeze climatic region . . . . .	239
152.	Effects of subgrade dynamic $k$ on allowable traffic for the wet-freeze climatic region . . . . .	240
153.	Effects of subgrade $k$ and joint spacing on allowable traffic for wet-freeze climatic region . . . . .	241
154.	Effects of concrete strength and slab thickness on cracking performance of JPCP for wet-freeze climatic region . . . . .	242
155.	Effects of concrete strength and $E_{PCC}$ on cracking performance of JPCP for wet-freeze climatic region. . . . .	242
156.	Effects of the base-slab bond condition on cracking performance for wet-freeze climatic region . . . . .	244
157.	Effects of widened slab and tied PCC shoulder on cracking performance for wet-freeze climatic region . . . . .	246
158.	Effects of climate on slab thickness . . . . .	247

# LIST OF FIGURES

## Volume IV Appendixes

1.	Age of pavement sections in France . . . . .	120
2.	Range of slab thicknesses for sections in France . . . . .	120
3.	Distribution of base types for sections in France . . . . .	121
4.	Distribution in transverse joint spacings for sections in France . . . . .	122
5.	Type of drainage features for sections in France . . . . .	123
6.	Number of modernity elements incorporated into sections in France . . . . .	124
7.	Distribution of ESAL applications for sections in France . . . . .	126
8.	Typical load distribution of single axles in France . . . . .	127
9.	Typical load distribution of tandem axles in France . . . . .	127
10.	PSR vs. Age for sections in France . . . . .	130
11.	PSR vs. ESAL's for sections in France . . . . .	131
12.	PSR vs. (Age * ESAL's) for sections in France . . . . .	131
13.	Investigation of effect of base type in PSR vs. (Age * ESAL's) plot . . . . .	132
14.	Investigation of effect of slab thickness in PSR vs. (Age * ESAL's) plot . . . . .	132
15.	Investigation of effect of drainage in PSR vs. (Age * ESAL's) plot . . . . .	133
16.	Investigation of modernity element effect in PSR vs. (Age * ESAL's) plot . . . . .	134
17.	Sensitivity of French model to age and ESAL's . . . . .	135
18.	Sensitivity of French model to drainage conditions . . . . .	136
19.	Sensitivity of French model to slab thickness . . . . .	136
20.	Age of pavement sections in Italy . . . . .	139
21.	Range of slab thicknesses for sections in Italy . . . . .	140
22.	Distribution of base types for sections in Italy . . . . .	140
23.	Number of modernity elements incorporated into sections in Italy . . . . .	141
24.	Distribution of ESAL applications for sections in Italy . . . . .	142
25.	Typical load distribution of single axles in Italy . . . . .	143
26.	Typical load distribution of tandem axles in Italy . . . . .	144
27.	PSR vs. Age for sections in Italy . . . . .	145
28.	PSR vs. ESAL's for sections in Italy . . . . .	146
29.	PSR vs. (Age * ESAL's) for sections in Italy . . . . .	146
30.	Age of pavement sections in the United Kingdom . . . . .	151
31.	Range of slab thicknesses for sections in the United Kingdom . . . . .	151
32.	Distribution of base types for sections in the United Kingdom . . . . .	152
33.	Distribution of shoulder types for sections in the United Kingdom . . . . .	152
34.	Number of modernity elements incorporated into sections in the United Kingdom . . . . .	153
35.	Distribution of ESAL applications for sections in the United Kingdom . . . . .	154
36.	Typical load distribution of single axles in the United Kingdom . . . . .	155
37.	Typical load distribution of tandem axles in the United Kingdom . . . . .	155
38.	PSR vs. Age for sections in the United Kingdom . . . . .	157

# LIST OF FIGURES

## Volume IV (continued)

39.	PSR vs. ESAL's for sections in the United Kingdom . . . . .	158
40.	PSR vs. (Age * ESAL's) for sections in the United Kingdom . . . . .	158
41.	Investigation of effect of base type in PSR vs. ESAL's plot . . . . .	159
42.	Investigation of effect of slab thickness in PSR vs. ESAL's plot . . . . .	160
43.	Investigation of effect of shoulder type in PSR vs. ESAL's plot . . . . .	161
44.	Investigation of effect of joint spacing in PSR vs. ESAL's plot . . . . .	162
45.	Sensitivity of United Kingdom model to age and ESAL's . . . . .	163
46.	Sensitivity of United Kingdom model to slab thickness . . . . .	163
47.	Age of pavement sections in Belgium . . . . .	170
48.	CRCP designs in Belgium . . . . .	170
49.	Range of slab thicknesses for sections in Belgium . . . . .	171
50.	Distribution of base types for sections in Belgium . . . . .	171
51.	Number of modernity elements incorporated into sections in Belgium . . . . .	172
52.	Distribution of ESAL applications for sections in Belgium . . . . .	173
53.	Typical load distribution of single axles in Belgium . . . . .	174
54.	PSR vs. Age for sections in Belgium . . . . .	175
55.	PSR vs. ESAL's for sections in Belgium . . . . .	176
56.	PSR vs. (Age * ESAL's) for sections in Belgium . . . . .	176
57.	Investigation modernity element effect in PSR vs. (Age * ESAL's) plot . . . . .	177
58.	Investigation of effect of base type in PSR vs. (Age * ESAL's) plot . . . . .	178
59.	Investigation of effect of slab thickness in PSR vs. (Age * ESAL's) plot . . . . .	178
60.	Investigation of effect of pavement type in PSR vs. (Age * ESAL's) plot . . . . .	179
61.	Investigation of effect of freezing index in PSR vs. Age plot . . . . .	180
62.	Sensitivity of Belgian model to age and ESAL's . . . . .	181
63.	Sensitivity of Belgian models to slab thickness . . . . .	182
64.	Age of pavement projects in Switzerland . . . . .	187
65.	Range of slab thicknesses for projects in Switzerland . . . . .	188
66.	Distribution of base types for projects in Switzerland . . . . .	189
67.	Distribution of transverse joints spacings for projects in Switzerland . . . . .	190
68.	Distribution of drainage features for projects in Switzerland . . . . .	190
69.	Number of modernity elements for projects in Switzerland . . . . .	191
70.	Distribution of ESAL applications for projects in Switzerland . . . . .	192
71.	PSR vs. Age for projects in Switzerland . . . . .	194
72.	PSR vs. ESAL's for projects in Switzerland . . . . .	195
73.	PSR vs. (Age * ESAL's) for projects in Switzerland . . . . .	195
74.	Investigation of effect of joint spacing in PSR vs (Age * ESAL's) plot . . . . .	196
75.	Investigation of the effect of slab thickness in PSR vs. (Age * ESAL's) plot . . . . .	197
76.	Sensitivity of Swiss faulting model to ages and ESAL's . . . . .	199
77.	Sensitivity of Swiss faulting model to drainage conditions . . . . .	199
78.	Sensitivity of Swiss PSR model to age and ESAL's . . . . .	200

# LIST OF FIGURES

## Volume IV (continued)

79.	Sensitivity of Swiss PSR model to slab thickness . . . . .	200
80.	Age distribution of European COPES sections at the time of survey . . . . .	204
81.	Distribution of pavement types . . . . .	204
82.	Range of slab thicknesses . . . . .	206
83.	Comparison of slab thicknesses . . . . .	206
84.	Range of base types . . . . .	207
85.	Comparison of base types . . . . .	207
86.	Comparison of shoulder types . . . . .	209
87.	Comparison of modernity elements . . . . .	209
88.	Distribution of estimated 80-kN (18-kip) ESAL applications for the European COPES sections . . . . .	211
89.	Comparison of annual traffic . . . . .	211
90.	PSR vs. pavement age for all European COPES sections . . . . .	212
91.	PSR vs. ESAL applications for all European COPES sections . . . . .	212
92.	PSR vs. (Age * ESAL's) for all European COPES sections . . . . .	213
93.	PSR vs. ESAL applications by pavement type, overall sections . . . . .	213
94.	PSR vs. ESAL applications by slab thickness, overall sections . . . . .	215
95.	PSR vs. ESAL applications for doweled and undoweled sections, overall . . . . .	215
96.	PSR vs. ESAL applications by drainage condition, overall sections . . . . .	216
97.	PSR vs. ESAL applications by base type for all European COPES sections . . . . .	216
98.	PSR vs. ESAL applications by modernity elements, overall sections . . . . .	217
99.	PSR vs. (Age * ESAL's) by modernity elements, overall sections . . . . .	217
100.	Comparison of PSR vs. Age between European and U.S. sections . . . . .	218
101.	PSR vs. ESAL applications for the U.S. sections . . . . .	218
102.	Instrumentation devices in the test sections . . . . .	228
103.	Schematic layout of instrumentation . . . . .	228
104.	Age of Chilean concrete pavement sections . . . . .	229
105.	Range of slab thicknesses in Chilean sections . . . . .	231
106.	Distribution of base types in Chilean sections . . . . .	232
107.	Distribution of subbase types in Chilean sections . . . . .	232
108.	USCS classification chart, ASTM D-2487 . . . . .	233
109.	Subgrade type in Chilean sections . . . . .	234
110.	Distribution in transverse joint spacings in Chilean sections . . . . .	235
111.	Type of drainage features in Chilean sections . . . . .	235
112.	Number of modernity elements incorporated into Chilean sections . . . . .	237
113.	Days per year (N) of heavy rainfall . . . . .	238
114.	Distribution of ESAL applications in Chilean sections . . . . .	241
115.	Illustration of the curling/warping concept . . . . .	245
116.	Histogram of thermal gradients at a typical test section . . . . .	245
117.	Movement pattern of joint during a complete temperature cycle . . . . .	246



# LIST OF FIGURES

## Volume IV (continued)

118.	Variations in seasonal deflections for corner and interior loading conditions .....	249
119.	Openings of 10 consecutive joints .....	250
120.	Inclination of induced crack .....	252
121.	State of faulting in Chilean concrete pavements .....	253
122.	Faulting vs. ESAL's for Chilean sections .....	255
123.	Faulting vs. (Age * ESAL's) for Chilean sections .....	255
124.	Investigation of the effect of edge drains on faulting .....	256
125.	Investigation of the effect of k-value on faulting .....	256
126.	Comparison of predicted and actual cracking .....	258
127.	Cracking vs. age for Chilean sections .....	258
128.	Cracking vs. ESAL's for Chilean sections .....	259
129.	Cracking vs. (Age * ESAL's) for Chilean sections .....	259
130.	Investigation of the effect of slab length on cracking .....	261
131.	Investigation of the effect of $L/\ell$ on cracking .....	261
132.	Investigation of the effect of k-value on cracking .....	262

# LIST OF TABLES

## Volume I Field Investigation

1.	List of sections included in the study	7
2.	Listing of projects surveyed by automated methods	20
3.	Regression coefficients for $d_r^*$ versus $l_k$ relationships	31
4.	Summary of sections surveyed in 1987 and 1992	36
5.	Critical values for key performance indicators	37
6.	Experimental design matrix for MN 1 and MN 5	38
7.	Summary of 1987 and 1992 outer lane performance data for MN 1 and MN 5	39
8.	Experimental design matrix for MN 2	45
9.	Summary of 1987 and 1992 outer lane performance data for MN 2	46
10.	Design and outer lane performance data for MN 3, MN 4, and MN 6	52
11.	Experimental design matrix for selected sections on MN 7	53
12.	Summary of 1992 outer lane performance data for MN 7	55
13.	Summary of dowel performance on MN 7	55
14.	Experimental design matrix for AZ 1	60
15.	Traffic summary for AZ 1 sections	61
16.	Summary of 1987 and 1992 outer lane performance data for AZ 1	61
17.	Summary of 1987 and 1992 outer lane performance data for AZ 2	67
18.	Experimental design matrix for CA 1	67
19.	Summary of 1987 and 1992 outer lane performance data for CA 1	69
20.	Experimental design matrix for CA 2	75
21.	Summary of 1987 and 1992 outer lane performance data for CA 2	75
22.	Design and outer lane performance data for CA 6	76
23.	Design and outer lane performance data for CA 7 and CA 8	78
24.	Design and outer lane performance data for CA 11	79
25.	Summary of sections on IL 1	81
26.	Summary of 1992 performance data for IL 1	82
27.	Summary of sections on IL 2	85
28.	Summary of 1992 performance data for IL 2	86
29.	Experimental design matrix for MI 1	89
30.	Summary of 1987 and 1992 outer lane performance data for MI 1	90
31.	Design and outer lane performance data for MI 3, MI 5, and MI 6	96
32.	Experimental design matrix and performance summary for MI 4	97
33.	Experimental design matrix for MO 1	100
34.	Summary of 1992 outer lane performance data for MO 1	101
35.	Design and outer lane performance data for NJ 2	105
36.	Experimental design matrix for NJ 3	106
37.	Summary of 1987 and 1992 outer lane performance data for NJ 3	106

# LIST OF TABLES

## Volume I (continued)

38.	Experimental design matrix for NY 1 . . . . .	107
39.	Summary of 1987 and 1992 outer lane performance data for NY 1 . . . . .	108
40.	Experimental design matrix for NY 2 . . . . .	114
41.	Summary of 1987 and 1992 outer lane performance data for NY 2 . . . . .	115
42.	Experimental design matrix for OH 1 . . . . .	120
43.	Summary of 1987 and 1992 outer lane performance data for OH 1 . . . . .	122
44.	Experimental design matrix for selected sections on OH 2 . . . . .	127
45.	Summary of 1992 outer lane performance data for OH 2 sections with aggregate base . . . . .	128
46.	Summary of outer lane performance data for OH 2 sections with no base, ATB, and CTB . . . . .	129
47.	Summary of 1992 outer lane performance data for CRCP sections in OH 2 . . . . .	133
48.	Experimental design matrix for ONT 1 . . . . .	138
49.	Summary of 1987 and 1992 outer lane performance data for ONT 1 . . . . .	139
50.	Design and outer lane performance data for ONT 2 . . . . .	145
51.	Experimental design matrix for PA 1 . . . . .	145
52.	Summary of 1987 and 1992 outer lane performance data for PA 1 . . . . .	147
53.	Design and outer lane performance data for WV 1 . . . . .	152
54.	Experimental design matrix for WI 1 . . . . .	156
55.	Summary of 1992 outer lane performance data for WI 1 . . . . .	156
56.	Experimental design matrix for WI 2 and WI 7 . . . . .	160
57.	Summary of 1992 outer lane performance data for WI 2 and WI 7 . . . . .	161
58.	Experimental design matrix for WI 3 . . . . .	165
59.	Summary of 1992 performance data for WI 3 . . . . .	166
60.	Experimental design matrix for WI 4 . . . . .	170
61.	Experimental design matrix for WI 4 . . . . .	171
62.	Experimental design matrix for WI 5 . . . . .	175
63.	Summary of 1992 outer lane performance data for WI 5 . . . . .	176
64.	Experimental design matrix for WI 6 . . . . .	179
65.	Summary of 1992 outer lane performance data for WI 6 . . . . .	180
66.	Experimental design matrix for CA 3 . . . . .	184
67.	Summary of 1987 and 1992 outer lane performance data for CA 3 . . . . .	185
68.	Experimental design matrix for selected sections on CA 9 . . . . .	191
69.	Summary of 1992 outer lane performance data for CA 9 . . . . .	192
70.	Design and outer lane performance data for CA 10 . . . . .	196
71.	Design and outer lane performance data for FL 2 and FL 3 . . . . .	197
72.	Experimental design matrix for selected sections on FL 4 . . . . .	199
73.	Summary of 1992 outer lane performance data for FL 4 . . . . .	201
74.	Experimental design matrix for GA 1 and GA 2 . . . . .	208

# LIST OF TABLES

## Volume I (continued)

75.	Summary of 1992 outer lane performance data for Georgia sections . . . . .	210
76.	Experimental design matrix for NC 1 . . . . .	214
77.	Summary of 1987 and 1992 outer lane performance data for NC 1 . . . . .	215
78.	Design and outer lane performance data for NC 2 . . . . .	222

# LIST OF TABLES

## Volume II Evaluation of Inservice Concrete Pavements

1.	List of projects included in the study	6
2.	Experimental design matrix for AZ 1 (year built in parentheses)	8
3.	Traffic summary for AZ 1 sections	8
4.	Experimental design matrix for CA 1	9
5.	Experimental design matrix for CA 2	10
6.	Experimental design matrix for CA 3	11
7.	Summary of design data for CA 6	11
8.	Experimental design matrix for selected sections on CA 9	13
9.	Experimental design matrix for selected sections on FL 4	14
10.	Experimental design matrix for GA 1 and GA 2	15
11.	Experimental design matrix for IL 1	17
12.	Experimental design matrix for IL 2	17
13.	Experimental design matrix for MI 1	18
14.	Experimental design matrix for MN 1 and MN 5	20
15.	Experimental design matrix for MN 2	21
16.	Experimental design matrix for selected sections on MN 7	22
17.	Experimental design matrix for MO 1	23
18.	Experimental design matrix for NJ 3	24
19.	Experimental design matrix for NY 1	24
20.	Experimental design matrix for NY 2	25
21.	Experimental design matrix for NC 1	26
22.	Experimental design matrix for OH 1	27
23.	Experimental design matrix for selected sections on OH 2	28
24.	Experimental design matrix for ONT 1	29
25.	Experimental design matrix for PA 1	30
26.	Design data for WV 1	31
27.	Experimental design matrix for WI 1	31
28.	Experimental design matrix for WI 2 and WI 7	32
29.	Experimental design matrix for WI 3	33
30.	Experimental design matrix for WI 4	34
31.	Experimental design matrix for WI 5	34
32.	Experimental design matrix for WI 6	35
33.	Range of design features included in study	36
34.	Critical values for key performance indicators	40
35.	Summary of effect of slab thickness for MN 1	42
36.	Summary of effect of slab thickness for MN 2	44
37.	Summary of effect of slab thickness for AZ 1	45
38.	Summary of effect of slab thickness for CA 1	46
39.	Summary of effect of slab thickness for CRCP sections for IL 1	47

# LIST OF TABLES

## Volume II (continued)

40.	Summary of effect of slab thickness for OH 2 . . . . .	48
41.	Summary of effect of slab thickness for ONT 1 . . . . .	49
42.	Summary of selected 1992 deflection data . . . . .	54
43.	Summary of effect of joint spacing for CA 1 . . . . .	58
44.	Summary of effect of actual slab lengths on cracking for CA 1 . . . . .	59
45.	Summary of effect of joint spacing for IL 1 . . . . .	60
46.	Summary of effect of joint spacing for IL 2 . . . . .	61
47.	Summary of effect of joint spacing for MN 1/MN 5 . . . . .	61
48.	Summary of effect of joint spacing for MN 7 . . . . .	63
49.	Summary of effect of joint spacing for NY 2 . . . . .	64
50.	Summary of effect of joint spacing for OH 1 . . . . .	65
51.	Summary of effect of joint spacing for OH 2 . . . . .	66
52.	Summary of effect of joint orientation for FL 4 . . . . .	72
53.	Summary of effect of joint orientation for NC 1 . . . . .	73
54.	Summary of effect of joint orientation for NY 1 . . . . .	74
55.	Summary of effect of load transfer for FL 4 . . . . .	80
56.	Summary of effect of load transfer for GA 1 . . . . .	81
57.	Summary of effect of load transfer for MN 1 . . . . .	82
58.	Summary of effect of load transfer for MN 7 . . . . .	83
59.	Summary of dowel performance on MN 7 . . . . .	84
60.	Summary of effect of load transfer for NC 1 . . . . .	85
61.	Summary of effect of load transfer for NY 1 . . . . .	86
62.	Summary of effect of load transfer for WI 2/WI 7 . . . . .	87
63.	Summary of effect of load transfer for WI 6 . . . . .	88
64.	Pavement performance indicators related to sealing pavements . . . . .	93
65.	Summary of effect of joint sealant type for CA 3 . . . . .	95
66.	Summary of effect of joint sealing for CA 9 . . . . .	96
67.	Summary of effect of joint sealing on OH 2 . . . . .	99
68.	Summary of effect of joint sealant for WI 2/WI 7 . . . . .	100
69.	Summary of effect of joint sealing for WI 5 . . . . .	102
70.	Summary of effect of joint sealing for WI 6 . . . . .	103
71.	Summary of effect of joint sealing for WV 1 . . . . .	104
72.	Summary of effect of base type for AZ 1 . . . . .	110
73.	Summary of effect of base type for CA 1 . . . . .	111
74.	Summary of effect of base type for CA 2 . . . . .	112
75.	Summary of effect of base type for CA 6 . . . . .	113
76.	Summary of effect of base type for FL 4 . . . . .	114
77.	Summary of effect of base type for GA 1 . . . . .	115
78.	Summary of effect of base type for MI 1 . . . . .	116
79.	Summary of effect of base type for MN 1 . . . . .	118

# LIST OF TABLES

## Volume II (continued)

80.	Summary of effect of base type for MO 1 .....	119
81.	Summary of effect of base type for NC 1 .....	120
82.	Summary of effect of base type for NJ 3 .....	121
83.	Summary of effect of base type on JPCP for NY 1 .....	121
84.	Summary of effect of base type on JRCP for NY 1 .....	122
85.	Summary of effect of base type for OH 1 .....	123
86.	Summary of effect of base type for OH 2 .....	123
87.	Summary of effect of base type for ONT 1 .....	124
88.	Summary of effect of base type for PA 1 .....	126
89.	Summary of effect of base type for WV 1 .....	126
90.	Summary of effect of base type for WI 2 & 7 .....	128
91.	Summary of effect of base type for WI 3 .....	128
92.	Summary of effect of drainage for AZ 1 .....	138
93.	Summary of effect of drainage for CA 2 .....	139
94.	Summary of effect of drainage for CA 6 .....	140
95.	Summary of effect of drainage for CA 9 .....	141
96.	Summary of effect of drainage on JPCP for MI 1 .....	142
97.	Summary of effect of drainage on JRCP for MI 1 .....	143
98.	Summary of effect of drainage for NJ 3 .....	144
99.	Summary of effect of drainage for OH 2 (aggregate base) .....	145
100.	Summary of effect of drainage for OH 2 (stabilized base) .....	146
101.	Summary of effect of drainage for ONT 1 .....	147
102.	Summary of effect of drainage for PA 1 .....	147
103.	Summary of effect of drainage for WI 2 & 7 .....	149
104.	Summary of effect of drainage for WI 3 .....	150
105.	Summary of effect of drainage for WI 5 .....	151
106.	Summary of effect of shoulder type for AZ 1 .....	163
107.	Effect of shoulder type for CA 3 sections (preformed sealant) .....	164
108.	Effect of shoulder type for CA 3 sections (no sealant) .....	165
109.	Effect of shoulder type for FL 4 sections .....	166
110.	Summary of effect of shoulder type for MI 1 .....	167
111.	Summary of effect of shoulder type for MI 4 .....	168
112.	Summary of effect of shoulder type for MN 2 .....	169
113.	Summary of effect of shoulder type for NY 2 .....	169
114.	Summary of effect of shoulder type for OH 1 .....	170
115.	Effect of shoulder type for OH 2 sections .....	171
116.	Summary of effect of shoulder type for ONT 1 .....	172
117.	Maximum recommended tie bar spacings .....	176
118.	Improvement in pavement responses .....	177
119.	Summary of performance data for sections with widened lanes .....	178

# LIST OF TABLES

## Volume II (continued)

120.	Summary of effect of reinforcement for CA 1	180
121.	Summary of effect of reinforcement for IL 1	181
122.	Summary of effect of reinforcement for IL 2	182
123.	Overall performance of CRCP sections	185
124.	Summary of effect of maximum coarse aggregate size for MO 1	187
125.	Summary of effect of maximum coarse aggregate size for OH 2 sections constructed on aggregate base	188
126.	Summary of effect of maximum coarse aggregate size for OH 2 sections constructed on no base, ATB, and CTB	189
127.	Performance data summary for NC 1	192
128.	Performance data summary for OH 2	193
129.	Performance data summary for MI 1	195
130.	Performance data summary for WV 1	195
131.	Performance data summary for NY 1	196
132.	Performance data summary for NY 2	197
133.	Performance data summary for OH 1	198
134.	Performance data summary for MN 2	199
135.	Performance data summary for CA 1	200
136.	Performance data summary for IL 1	201
137.	Comparison of performance by pavement type	202
138.	Two sets of the moduli ratios, $E_{pcc}/E_{base}$	218
139.	Results of backcalculation for sections with high percentage of dropped data	221
140.	Distribution of sections by country and pavement type	232
141.	Summary of design features and performance data	237
142.	Design information for Chilean concrete pavement sections	267
143.	Performance data for Chilean sections	276
144.	Summary of effect of design features	293



# LIST OF TABLES

## Volume III Improving Concrete Pavement Performance

1.	Range of design features included in study . . . . .	9
2.	Distribution of the pavement sections used in the development of doweled joint faulting model . . . . .	11
3.	Simplified design matrix for the selection of the overall drainage coefficient, $C_d$ . . . . .	14
4.	Estimates of the coefficients and the associated SEE and P-values for the doweled joint faulting model . . . . .	19
5.	Distribution of the pavement sections used in the development of nondoweled joint faulting model . . . . .	24
6.	Estimates of the coefficients and the associated SEE and P-values for the nondoweled joint faulting model . . . . .	29
7.	Distribution of the JPCP sections and designs used in the development of fatigue cracking model . . . . .	36
8.	Thermal gradients determined for all study sections . . . . .	42
9.	Distribution of the pavement sections and designs used in the development of JRCP crack deterioration model . . . . .	85
10.	Distribution of the pavement sections and designs used in the development of JPCP spalling model . . . . .	98
11.	Spalling of JPCP sections located in a cold climate . . . . .	112
12.	Distribution of the pavement sections and designs used in the development of JRCP spalling model . . . . .	115
13.	Distribution of the pavement sections used in the development of PSR model . . . . .	128
14.	Estimates of the coefficients and the associated SEE and P-values for JPCP PSR distress model . . . . .	130
15.	Estimates of the coefficients and the associated SEE and P-values for JRCP PSR model . . . . .	135
16.	Estimates of the coefficients and the associated SEE and P-values for JPCP IRI model . . . . .	140
17.	Example application of prediction models to check adequacy of concrete pavement design . . . . .	144
18.	Critical values for key performance indicators . . . . .	145
19.	Potential for moisture accelerated damage indicated by the MAD index . . .	155
20.	Simplified design matrix for the selection of the overall drainage coefficient, $C_d$ . . . . .	155
21.	Potential for moisture damage indicated by $C_d$ . . . . .	156
22.	Pavement cross section recommendations for enhancing overall drainability	158
23.	Wisconsin standard gradation for permeable aggregate base . . . . .	164
24.	Quality of drainage based on time to drain . . . . .	165
25.	Gradations used in permeable bases . . . . .	168

# LIST OF TABLES

## Volume III (continued)

26.	Typical dense-graded aggregate separator layer gradation . . . . .	170
27.	Performance of PCC pavement base types . . . . .	180
28.	Performance of permeable base sections . . . . .	182
29.	Performance of pavement sections without a base course . . . . .	186
30.	General recommendations on use of shoulder type/edge support . . . . .	192
31.	Summary of performance data for sections with widened lanes . . . . .	196
32.	Recommended maximum joint spacings for JPCP designs . . . . .	204
33.	Summary of effect of joint orientation . . . . .	206
34.	Recommended dowel usage & diameters . . . . .	210
35.	Strain capacity of field-molded joint sealants . . . . .	212
36.	Effect of coarse aggregate size on deteriorated transverse cracking . . . . .	220
37.	Summary of three field developed models for deteriorated transverse cracking or JRCP . . . . .	221
38.	Minimum recommended percent longitudinal reinforcement for JRCP (50 percent level of reliability) . . . . .	222
39.	Effect of reinforcement content on CRCP performance . . . . .	226
40.	Effect of steel reinforcement depth on CRCP performance . . . . .	228
41.	Summary of three prediction models for punchouts and roughness in CRCP	229
42.	Minimum reinforcement contents for CRCP on aggregate base courses and in a wet-freeze climate (50 percent level of reliability) . . . . .	230
43.	Minimum reinforcement contents for CRCP on stabilized base courses and in a wet-freeze climate (50 percent level of reliability). . . . .	231
44.	Comparison of predicted and actual failures (punchouts and deteriorated cracks) from various CRCP sections . . . . .	232
45.	JPCP slab thickness design table for dry-freeze climate (50 percent design reliability) . . . . .	249
46.	JPCP slab thickness design table for dry-nonfreeze climate (50 percent design reliability) . . . . .	250
47.	JPCP slab thickness design table for wet-freeze climate (50 percent design reliability) . . . . .	251
48.	JPCP slab thickness design table for wet-nonfreeze climate (50 percent design reliability) . . . . .	252
49.	Summary of PCC pavement types . . . . .	255
50.	Summary of structural design recommendations for medium- and heavy- trafficked roadways . . . . .	258
51.	Summary of transverse joint design recommendations for medium- and heavy- trafficked roadways . . . . .	259
52.	Summary of longitudinal lane-lane contraction joint design recommendations for medium- and heavy-trafficked roadways . . . . .	260

# LIST OF TABLES

## Volume IV Appendixes

1.	Field testing summary for the sections in the dry-freeze climatic zone . . . .	23
2.	Field testing summary for the sections in the dry-nonfreeze climatic zone .	24
3.	Field testing summary for the sections in the wet-freeze climatic zone . . . .	25
4.	Field testing summary for the sections in the wet-nonfreeze climatic zone .	26
5.	General information for the projects included in the study . . . . .	31
6.	Structural design data . . . . .	32
7.	Joint design data . . . . .	44
8.	Outer shoulder and drainage design data . . . . .	55
9.	Traffic data . . . . .	66
10.	Outer lane deflection data . . . . .	68
11.	Edge deflection data . . . . .	77
12.	Primary outer lane performance data . . . . .	86
13.	Secondary outer lane performance data . . . . .	96
14.	Continuously Reinforced Concrete Pavement performance data . . . . .	106
15.	Distribution of sections by country and pavement type . . . . .	108
16.	Listing of sections included in European COPES analysis . . . . .	111
17.	Design information for COPES concrete pavement sections in France . . . . .	115
18.	Performance data for outer traffic lane of COPES concrete pavement sections in France . . . . .	117
19.	Design information for COPES concrete pavement sections in Italy . . . . .	138
20.	Performance data for outer traffic lane of COPES concrete pavement sections in Italy . . . . .	138
21.	Design information for COPES concrete pavement sections in the United Kingdom . . . . .	149
22.	Performance data for outer traffic lane of COPES concrete pavement sections in the United Kingdom . . . . .	150
23.	Design information for COPES concrete pavement sections in Belgium . . .	166
24.	Performance data for outer traffic lane of COPES concrete pavement sections in Belgium . . . . .	168
25.	Design information for COPES concrete pavement sections in Switzerland .	183
26.	Performance data for outer traffic lane of COPES concrete pavement sections in Switzerland . . . . .	185
27.	PSR for COPES concrete pavement sections in Switzerland . . . . .	193
28.	Design information for Chilean concrete pavement sections . . . . .	230
29.	Traffic composition on Chilean sections . . . . .	239
30.	Maximum uplift of corners . . . . .	248
31.	Load transfer for 80-kN (18-kip) load . . . . .	251
32.	Performance data for Chilean sections . . . . .	254

## List of Acronyms and Abbreviations

AASHTO	American Association of State Highway and Transportation Officials
AC	Asphalt Concrete
ADT	Average Daily Traffic
AGG	Dense-Graded Aggregate Base
ATB	Asphalt-Treated Base
$C_d$	Drainage Coefficient
CESAL	Cumulative Equivalent Single Axle Load
COE	Corps of Engineers
COPEs	Concrete Pavement Evaluation System
CRCP	Continuously Reinforced Concrete Pavement
CTB	Cement-Treated Base
CSB	Cement-Stabilized Base
$C_u$	Coefficient of Uniformity
DF	Dry-Freeze
DNF	Dry-Nonfreeze
$D_o$	Load Plate Sensor
E	Concrete Elastic Modulus
ESAL	Equivalent Single-Axle Load
ESAR	Equivalent Single Axle Radius
FI	Freezing Index
FHWA	Federal Highway Administration
FRC	Fiber Reinforced Concrete
FWD	Falling Weight Deflectometer
GRB	Granular Base
IRI	International Roughness Index
JPCP	Jointed Plain Concrete Pavement
JRCP	Jointed Reinforced Concrete Pavement
k	Modulus of Subgrade Reaction
LCB	Lean Concrete Base
LDF	Load Distribution Factor
LEF	Load Equivalency Factor
LTE	Load Transfer Efficiency
LTPP	Long-Term Pavement Performance
MR	Modulus of Rupture
NOAA	National Oceanic and Atmospheric Administration
PAGG	Permeable Aggregate Base (nontreated)
PATB	Permeable Asphalt-Treated Base
P/C	Pass to Coverage Ratio
PCA	Portland Cement Association
PCC	Portland Cement Concrete
PCTB	Permeable Cement-Treated Base

## List of Acronyms and Abbreviations (continued)

PIARC	Permanent International Association of Road Congresses
PSR	Present Servicability Rating
P-value	Probability Value
PVC	Polyvinylchloride
SC	Soil Cement Base
SCS	Soil Conservation Service
SHRP	Strategic Highway Research Program
SEE	Standard Error of the Estimate
SI	International System of Units
TF	Truck Factor
TMI	Thornthwaite Moisture Index
USCS	Unified Soil Classification System
WF	Wet-Freeze
WNF	Wet-Nonfreeze
WWF	Welded-Wire Fabric



# 1. INTRODUCTION

## Background

The need to improve the design and performance of highway pavements is not only indisputable, it is continuous. The introduction and use of innovative designs, new materials, and new construction practices, coupled with increased truck loading of pavement facilities, dictate the need for the monitoring of highway pavement performance so that deficiencies can be identified and addressed by updating current design and construction practices. While such pavement monitoring has been conducted since the earliest days of road building, it has been only in the last two decades that formalized pavement monitoring programs have been implemented. One example of such a monitoring program is the Long-Term Pavement Performance (LTPP) study that was launched by the Strategic Highway Research Program (SHRP) in 1987 and is now being administered by the Federal Highway Administration (FHWA).<sup>(1)</sup> This program is monitoring the performance of both asphalt concrete (AC) and portland cement concrete (PCC) pavements over a 20-year period with the single-minded goal of improving the performance of new pavements.

Before the LTPP program was launched, the FHWA in 1986 sponsored a research study on the evaluation of 95 concrete pavement sections located throughout North America. The goal of the study was to obtain feedback information on the performance of these inservice concrete pavements, many of which are experimental projects containing a variety of design features (e.g., slab thickness, base type, load transfer) that allow for an evaluation of the effect of the design features on pavement performance. That study, completed in 1990, provided much useful information on the performance of concrete pavements, including the development of prediction models for several concrete pavement performance indicators (faulting, spalling, cracking, and serviceability loss). The results are fully documented in a six-volume report.<sup>(2-7)</sup>

One shortcoming of that study was that the findings and results were limited to the pavement designs present in the data base. For example, the data collected under the original study represent a "snapshot" in the performance life of the pavement section. That is, there was no time series performance data that could provide an indication of the section's rate of deterioration, or how the pavement performed over time. Furthermore, many of the sections that incorporated recent design innovations were too new or had not carried enough traffic for drawing meaningful conclusions.

To address these deficiencies while building upon and extending the original study, the FHWA sponsored this followup study in 1991. Not only were the original 95 pavement sections reinspected and reevaluated after receiving 5 more years of traffic loading, but an additional 208 pavement sections were added to the study, thus greatly strengthening the data base used for analysis. Furthermore, many of the new sections that were added to the study contained newer design elements, such as

widened lanes or permeable bases. The result is a total of 303 concrete pavement sections—located throughout North America and representing a broad range of pavement designs—available for analysis. In addition, 96 concrete pavement sections from several European countries (France, Italy, the United Kingdom, Belgium, and Switzerland) and 21 concrete pavement sections from Chile are included.

## **Research Objectives**

The objectives of this project are to:

- Reevaluate the 95 projects originally surveyed in 1987 to reveal performance trends and to determine deterioration rates.
- Determine the impact of different pavement types, design features, materials, and construction variables on pavement performance, based on additional data collection and testing, data analysis, and performance evaluations.
- Improve design procedures and performance prediction models for jointed concrete pavements, using the expanded data base. Where possible, evaluate the performance of the various rigid pavement types to provide improved guidance on pavement type selection.

In short, the overall objective of this study can be stated as the development of improved guidance on the design and construction of concrete pavements through the field evaluation of the performance of inservice concrete pavements.

## **Research Approach**

The work conducted under this project can be divided into essentially three distinct phases. The first phase of the project included the collection of performance data for each of the 303 sections included in the study. This field data collection effort consisted of the following major elements:

- A pavement distress survey to quantify the type, amount, and severity of distress occurring on each section.
- A pavement drainage survey to characterize the drainage capabilities of each section.
- Falling Weight Deflectometer (FWD) deflection testing to determine the concrete elastic modulus (E) and the modulus of subgrade reaction (k) of some of the sections, and to characterize the load transfer across transverse joints.
- Coring and boring operations to obtain layer thicknesses and to obtain samples for later laboratory testing.
- Pavement roughness testing using a South Dakota-type road profiler.

A more detailed description of the field data collection activities is reported in volume I.



The second phase of the project consisted of reducing the data collected under the field testing program and, along with pertinent design, construction and traffic data obtained from the participating State Highway Agencies, developing a data base for later analyses. The ORACLE data base management system was selected for this task because of its use on the FHWA LTPP program.<sup>(8)</sup> The data were extensively cleaned and verified in order to ensure their validity for analysis. The data were also presented in a spreadsheet format, which was used extensively for data analysis and model development. A summary of the data for each pavement section is presented in appendix A of volume IV.

The third and final phase of the project was data analysis. Several different analyses were conducted, including an evaluation of the effect of design features on concrete pavement performance, the development of pavement performance prediction models, and the development of guidelines for improving concrete pavement performance.

### **Advisory Panel**

An advisory panel consisting of experienced highway engineers was assembled to provide guidance to the research team in the collection and evaluation of concrete pavement performance data. The advisory panel assisted throughout the project, from arranging for traffic control to providing design and construction information to reviewing project documentation. Members of the advisory panel include:

- Mr. Jamshid Armaghani, Florida Department of Transportation.
- Mr. Chuck Arnold, Michigan Department of Transportation.
- Mr. Roger Green, Ohio Department of Transportation.
- Mr. Terry Rutkowski, Wisconsin Department of Transportation.
- Mr. Larry Scofield, Arizona Department of Transportation.
- Mr. Gordon Wells, California Department of Transportation.
- Mr. Bill Trimm, Missouri Department of Transportation.

In addition, while not serving on the advisory panel, engineers from other highway agencies were also very helpful and cooperative in providing traffic control and inventory data for pavement sections evaluated within their State. These individuals include:

- Mr. Walt Brubaker, West Virginia Parkways Economic Development and Tourism Authority
- Mr. Gaylord Cumberledge, Pennsylvania Department of Transportation.
- Mr. Wouter Gulden, Georgia Department of Transportation.
- Mr. Tom Kazmierowski, Ontario Ministry of Transportation
- Mr. David Lippert, Illinois Department of Transportation.
- Mr. Victor Mottola, New Jersey Department of Transportation.
- Mr. Robert Perry, New York Department of Transportation.
- Mr. David Rettnar, Minnesota Department of Transportation.

## Overview of Report

The results of this project are presented in a four-volume final report. This report focuses on the evaluation of pavement design features on concrete pavement performance and contains five chapters (in addition to this one). Chapter 2 summarizes briefly the sections included in the study and gives an overview of the range of designs and design features available for analysis. Chapter 3 provides an evaluation of the effect of pavement design features (e.g., slab thickness, joint spacing, load transfer) on concrete pavement performance. Chapter 4 investigates the backcalculation of the deflection data collected under the study and introduces the "equivalent thickness" concept. Chapter 5 summarizes the results of an investigation conducted on the performance of concrete pavements in Europe and in Chile. Finally, chapter 6 provides an overall summary of the report.

## 2. OVERVIEW OF PROJECTS EVALUATED IN STUDY

### Introduction

The 303 concrete pavement sections evaluated under this study represent a variety of designs. Most of the sections are jointed plain (JPCP) or jointed reinforced concrete pavements (JRCP), although a few continuously reinforced concrete pavements (CRCP) are also included. The sections are located throughout the United States, with the majority located in the upper midwest. In addition, two projects from Canada are also included in the study.

A range of design features is present on the pavement sections. For example, slab thickness ranges from 7.5 in (190 mm) to 15 in (381 mm) and joint spacing varies from 7 ft (2.1 m) to 30 ft (9.1 m) for JPCP and from 21 ft (6.4 m) to 46.5 ft (14.2 m) for JRCP. In addition, many of the pavements contain dowel bars at the transverse joints for load transfer, while many others rely upon aggregate interlock. Also, many different base types are present, including dense-graded aggregate bases (AGG), cement-treated bases (CTB), asphalt-treated bases (ATB), lean concrete bases (LCB), and many different permeable base designs (untreated permeable aggregate base [PAGG], cement-treated permeable [PCTB], and asphalt-treated permeable [PATB]).

This chapter presents general design information for the different projects evaluated in this study. Each of the different projects is briefly summarized, and the various design features described. The purpose of this chapter is to introduce the pavement sections used in the analyses and to indicate the range of design variables available. Additional design information and pavement performance details are found in appendix A of volume III and in the project interim report (reference 8).

### Description of Projects

As previously indicated, a total of 303 pavement sections from 50 pavement projects are included in this study. Table 1 lists the projects included in the study, while figure 1 depicts the general location of each project. A brief description of the characteristics of each project follows.

#### Arizona 1 (S.R. 360, Phoenix)

A series of experimental concrete pavement sections were constructed on State Route 360 in Phoenix, Arizona, over a number of years during the 1970's and early 1980's.<sup>(9,10)</sup> Experimental design features include base type, slab thickness, shoulder type, and drainage. All of the sections are nondoweled JPCP with random, skewed transverse joints spaced at 13-15-17-15-ft (4.0-4.6-5.2-4.6-m) intervals. The longitudinal centerline joint contains 24-in (610-mm) long, No. 4 (13-mm) tie bars spaced 30 in (760 mm) apart. AZ 1-1 contains an AC shoulder whereas the other section contain PCC shoulder (paved separately from the mainline pavement). The subgrade varies from

Table 1. List of projects included in the study.

Project ID	Location	Climatic Zone	1987 Project?
AZ 1	RT 360, Phoenix, AZ	DNF	Y
AZ 2	I-10, Phoenix, AZ	DNF	Y
CA 1	I-5, Tracy, CA	DNF	Y
CA 2	I-210, Los Angeles, CA	DNF	Y
CA 3	US 101, Geyserville, CA	WNF	Y
CA 6	RT 14, Solemint, CA	DNF	Y
CA 7	I-5, Sacramento, CA	DNF	Y
CA 8	US 101, Thousand Oaks, CA	DNF	Y
CA 9	I-680, Milpitas, CA	DNF	N
CA 10	US 101, Ukiah, CA	WNF	N
CA 11	I-5, Thornton, CA	DNF	N
FL 2	I-75, Brandon, FL	WNF	Y
FL 3	I-75, Bradenton, FL	WNF	Y
FL 4	US 41, Ft. Meyers, FL	WNF	N
GA 1	I-85, Newnan, GA	WNF	N
GA 2	I-85, LaGrange, GA	WNF	N
IL 1	US 50, Carlyle, IL	WF	N
IL 2	US 20, Freeport, IL	WF	N
MI 1	US 10, Clare, MI	WF	Y
MI 3	I-94, Marshall, MI	WF	Y
MI 4	I-69, Charlotte, MI	WF	Y
MI 5	I-94, Paw Paw, MI	WF	Y
MI 6	Davison Freeway, Detroit, MI	WF	N
MN 1	I-94, Rothsay, MN	DF	Y
MN 2	I-90, Albert Lea, MN	DF	Y
MN 3	I-90, Austin, MN	DF	Y
MN 4	TH 15, New Ulm, MN	DF	Y
MN 5	I-94, Rothsay, MN	DF	Y
MN 6	TH 15, Truman, MN	DF	Y
MN 7	TH 36, Roseville, MN	DF	N
MO 1	I-35, Bethany, MO	WF	N
NJ 1	RT 130, Yardville, NJ	WF	Y
NJ 2	I-676, Camden, NJ	WF	Y
NY 1	RT 23, Catskill, NY	WF	Y
NY 2	I-88, Otego, NY	WF	Y
NC 1	I-95, Rocky Mount, NC	WNF	Y
NC 2	I-85, Greensboro, NC	WNF	Y
OH 1	RT 23, Chillicothe, OH	WF	Y
OH 2	SR 2, Vermilion, OH	WF	Y
ONT 1	HWY 3N, Windsor, ONT	WF	Y
ONT 2	HWY 427, Toronto, ONT	WF	Y
PA 1	RT 66/RT 422, Kittanning, PA	WF	Y
WV 1	I-77, Charleston, WV	WF	N
WI 1	I-90, Stoughton, WI	WF	N
WI 2	USH 18/151, Mt. Horeb, WI	WF	N
WI 3	STH 14, Middleton, WI	WF	N
WI 4	STH 164, Waukesha, WI	WF	N
WI 5	STH 50, Kenosha, WI	WF	N
WI 6	STH 29, Green Bay, WI	WF	N
WI 7	USH 18/151, Barneveld, WI	WF	N

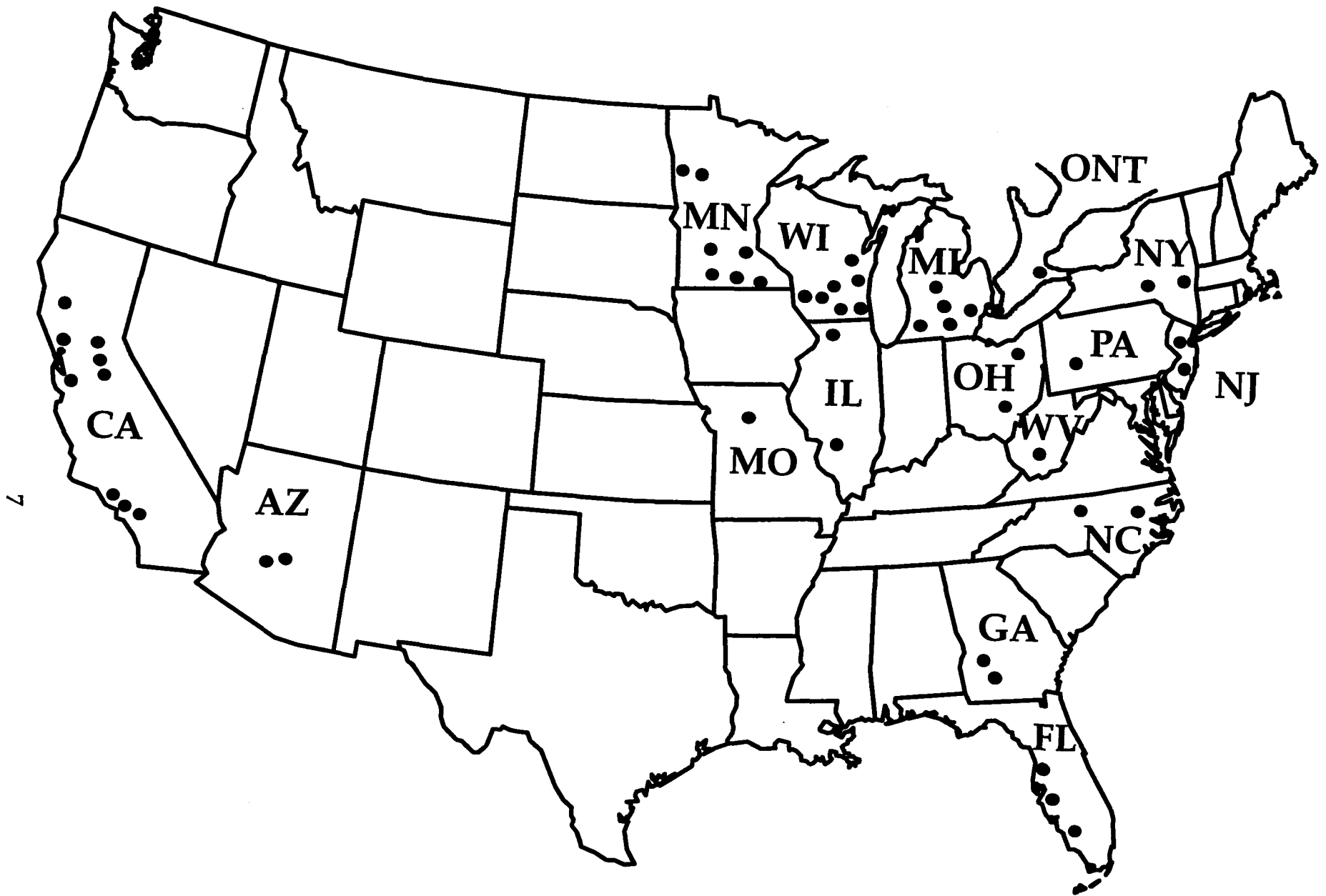


Figure 1. General location of projects included in the study.

an AASHTO A-4 to an A-6. These sections were included in the 1987 evaluation and are summarized in table 2.

Table 2. Experimental design matrix for AZ 1 (year built in parentheses).

		No Edge Drains		Edge Drains
		AC Shoulder	PCC Shoulder	PCC Shoulder
9-in JPCP	6-in CTB (4.3% cement)	AZ 1-1 (1972)		
	4-in LCB (6.9% cement)		AZ 1-6 (1981)	AZ 1-7 (1981)
11-in JPCP	No Base		AZ 1-5 (1979)	
13-in JPCP	No Base		AZ 1-2 (1975) AZ 1-4 (1979)	

1 in = 25.4 mm

Note: AZ 1-1 has a 4-in (102-mm) aggregate subbase on an A-4 subgrade.  
All other sections have no subbase and an A-6 subgrade.

Since each of these sections was constructed in different years, they each have accumulated different ESAL applications. The cumulative 18-kip (80-kN) ESAL applications for each section are given in table 3.

Table 3. Traffic summary for AZ 1 sections.

Section	Year Built	ESAL's, millions (outer lane)	
		1987	1992
AZ 1-1	1972	4.0	7.0
AZ 1-2	1975	3.4	6.5
AZ 1-4	1979	2.4	5.6
AZ 1-5	1979	2.8	6.0
AZ 1-6	1981	2.0	5.1
AZ 1-7	1981	1.5	4.7

Arizona 2 (I-10, Phoenix)

This single pavement section, included in the 1987 evaluation, is located on I-10 in Phoenix. Built in 1983, this section represents one of the few JPCP sections in a dry climate that incorporates dowel bars in its design. The pavement consists of a 10-in (254-mm) slab over a 5-in (127-mm) lean concrete base (LCB) course containing 6.9 percent cement. Transverse joints are skewed and spaced at intervals of 13-15-17-15 ft (4.0-4.6-5.2-4.6-m). The subgrade is an AASHTO A-6. Through 1992, this section has sustained approximately 9.6 million 18-kip (80-kN) ESAL applications.

California 1 (I-5, Tracy)

A set of experimental sections was constructed on I-5 near Tracy, California in 1971. Four different pavement designs were included to study the effect of slab thickness, joint spacing, and base type on pavement performance.<sup>(11-13)</sup> In addition, one section was constructed with high-strength concrete. All of the CA 1 sections are nondoweled JPCP designs with random, skewed, and nonsealed transverse joints. Also, no tie bars were used in the longitudinal centerline joint. The subgrade soils range from an AASHTO A-1-a to an A-2-4. This project was included in the 1987 evaluation and is depicted in the experimental matrix shown in table 4.

Table 4. Experimental design matrix for CA 1.

		12-13-19-18-ft Jts		5-9-11-7-ft Jts	8.4-in CRCP		
		8.4-in JPCP	11.4-in JPCP	8.4-in JPCP	Long. Bars	Long + Trans Bars	Welded Wire Fabric
Normal Strength Concrete (5.5 bag)	CTB (4%)	CA 1-3 CA 1-4	CA 1-5 CA 1-6	CA 1-1 CA 1-2	CA 1-11 CA 1-12	CA 1-13 CA 1-14	CA 1-15 CA 1-16
	LCB (4 bag)	CA 1-7 CA 1-8					
High Strength Concrete (7.5 bag)	CTB (4%)	CA 1-9 CA 1-10					

1 in = 25.4 mm  
1 ft = 0.305 m

Built in 1971  
Cumulative ESAL's = 11.9 million

Notes: All sections have a 5.4-in (137-mm) base and a 24-in (610-mm) aggregate subbase.  
CA 1-5 and CA 1-14 are SHRP LTPP study sections.

California 2 (I-210, Los Angeles)

In 1980, two different concrete pavement designs were constructed on I-210 near Los Angeles to evaluate the effect of base type on concrete pavement performance.<sup>(12)</sup> The only variable in these sections is base type and permeability; one section contains a permeable cement-treated base (PCTB), whereas the other section has an CTB.

However, for the permeable base section, a thin layer of asphalt concrete was placed between the slab and the base, essentially causing the design to perform as if it had a nonpermeable base.

Common to both sections is an 8.4-in (213-mm) JPCP slab with transverse joints spaced at 12-13-19-18-ft (3.7-4.0-5.8-5.5-m) intervals. The transverse joints contain no dowel bars and are not sealed. The subgrade soil is an AASHTO A-4 material. The simplified design matrix for the project is shown in table 5. These sections were also evaluated in 1987.

Table 5. Experimental design matrix for CA 2.

	Base Type	
	7.8-in Dense AC/PCTB (6-8% cement)	5.4-in CTB (5% cement)
8.4-in JPCP 12-13-19-18-ft Joints	CA 2-2	CA 2-3

1 in = 25.4 mm  
1 ft = 0.305 m

Built in 1980  
Cumulative ESAL's = 9.1 million

Notes: CA 2-2 has 3-in (76-mm) aggregate subbase.  
CA 2-3 has 6-in (152-mm) aggregate subbase.

### California 3 (U.S. 101, Geyserville)

In 1975, the California Department of Transportation constructed an experimental project on U.S. 101 near Geyserville to study the effects of shoulder type on pavement performance.<sup>(12)</sup> Seven different sections were constructed, including sections with tied PCC shoulders, nontied PCC shoulders, and various types of asphalt concrete shoulders. Some of these sections have sealed transverse joints, in contrast to the then-current practice in California of not sealing joints. Several of these sections were included in the 1987 evaluation.

Common to these pavements is a 9-in (229-mm) JPCP slab over a 5.4-in (137-mm) CTB and a 6-in (152-mm) aggregate subbase. The transverse joints are spaced at 12-13-19-18-ft (3.7-4.0-5.8-5.5-m) intervals and do not contain dowel bars. The subgrade soil classification varies from an AASHTO A-4 to an AASHTO A-6 material. The tied PCC shoulder design consists of 22-in (560-mm) long, No. 4 (13-mm) bars at 30-in (760-mm) centers. The shoulders were paved separately from the mainline pavement. Through 1992, these sections have sustained approximately 5.7 million ESAL applications. The design matrix for this project is shown in table 6.



Table 6. Experimental design matrix for CA 3.

		9-in Nondoweled JPCP 5.4-in CTB (5% cement) 12-13-19-18 ft Joints		
		Tied PCC Shoulder	Nontied PCC Shoulder	AC Shoulder
Transverse Joint Seal Type	Preformed	CA 3-1 CA 3-6	CA 3-3 CA 3-8	
	None	CA 3-2 CA 3-7	CA 3-5 CA 3-10	CA 3-4 CA 3-9

1 in = 25.4 mm  
1 ft = 0.305 m

Built in 1975  
Cumulative ESAL's = 5.7 million

Note: All sections have 6-in (152-mm) aggregate subbase and A-4 subgrade.

California 6 (RT. 14, Solemint)

Two separate concrete pavement sections, located on RT. 14 near Solemint in the greater Los Angeles area, were evaluated under this study. One section, constructed in 1971, is a 9-in (229-mm) JPCP section that contains transverse joints spaced at 12-13-19-18-ft (3.7-4.0-5.8-5.5-m) intervals and is constructed over a CTB. An adjacent section, constructed in 1980, is built on a permeable asphalt-treated base (PATB) and includes transverse joints spaced at 12-13-15-14 ft (3.7-4.0-4.6-4.3 m) intervals. While only the former section was surveyed in 1987, both sections were evaluated in 1992. The design of these sections is given in table 7.

Table 7. Summary of design data for CA 6.

	CA 6-1	CA 6-2
Pavement Type	JPCP	JPCP
Year Built	1971	1980
Thickness, in	9 in	9 in
Joint Spacing, ft	12-13-19-18	12-13-15-14
Dowel Diameter, in	None	None
Base Type	5.4-in CTB (4% cement)	4.2-in PATB (2%, AR-4000)
Subgrade	A-2-4	A-2-4
ESAL's, millions	13.3	9.8

Notes: CA 6-1 has a 24-in aggregate subbase.  
CA 6-2 has 33-in aggregate subbase.

1 in = 25.4 mm  
1 ft = 0.305 m

### California 7 (I-5, Sacramento)

Constructed in 1979 on I-5 near Sacramento, this single section includes a 10.2-in (259-mm) JPCP a CTB. The joints are randomly spaced at 12-13-19-18 ft (3.7-4.0-5.8-5.5 m) intervals, skewed, and are not doweled. The AASHTO A-7 subgrade is lime stabilized to a depth of 5.4 in (137 mm). This project was included in the 1987 evaluation and has sustained approximately 19.6 million 18-kip (80-kN) ESAL's.

This project is one of the earliest projects incorporating California's then-current drainage design. The drainage design consists of a 12-in (305-mm) PATB beneath the asphalt shoulder. Longitudinal edge drains (1.5-in [38-mm] diameter) are located 15.6 in (396 mm) below the pavement surface (and within the PATB). Drainage fabric was placed at the PATB-subgrade interface to guard against migration of fines.

### California 8 (U.S. 101, Thousand Oaks)

This 10.2-in (259-mm) JPCP section is constructed with widened outer lanes. Built in 1983 on U.S. 101 near Thousand Oaks, the slab rests on a 5.4-in (137-mm) thick ATB course and an AASHTO A-7 subgrade material. The pavement has skewed, random joints (12-13-15-14-ft [3.7-4.0-4.6-4.3-m] intervals) and contains longitudinal edge drains. The section was included in the 1987 evaluation and has sustained approximately 9.1 million 18-kip (80-kN) ESAL applications.

### California 9 (I-680, Milpitas, CA)

This experimental project, located on I-680 in Milpitas, was conducted by the California Department of Transportation to evaluate the effect of joint sealing on the performance of concrete pavements.<sup>(12)</sup> The project was constructed in 1974 and evaluated four different joint seal materials. The experiment also includes a section containing a longitudinal edge drain and a control section containing no edge drain and no joint sealant. Table 8 shows the design matrix for the sections evaluated.

### California 10 (U.S. 101, Ukiah)

This project is a single section that is located on U.S. 101 near Ukiah. It is a 9-in (229-mm) JPCP design constructed over a 4-in (102-mm) PATB. The transverse joints are spaced at 12-15-13-14-ft (3.7-4.6-4.0-4.3-m) intervals and do not contain dowel bars or joint sealant. The section was constructed in 1990 and has sustained about 1 million 18-kip (80-kN) ESAL's through 1992.

### California 11 (I-5, Thornton)

Built in 1979, this project is located on I-5 near Thornton. The pavement is an 8.4-in (213-mm) JPCP constructed on a lean concrete base (LCB). The joints do not contain dowel bars and are spaced at 12-13-19-18-ft (3.7-4.0-5.8-5.5-m) intervals. The project been subjected to approximately 19 million 18-kip (80-kN) ESAL applications through 1992.

Table 8. Experimental design matrix for selected sections on CA 9.

		9-in Nondoweled JPCP 5.4-in CTB (5% cement) 12-13-19-18-ft Joints	
		No Drains	Drains
Joint Sealant Type	Polyurethane	CA 9-2	
	Hot-Pour	CA 9-3	
	PVC Coal Tar	CA 9-4	
	Preformed	CA 9-5	
	None	CA 9-10	
			CA 9-8

1 in = 25.4 mm  
1 ft = 0.305 m

Built in 1974  
Cumulative ESAL's = 10.5 million

Note: All sections contain a 6-in (152-mm) aggregate subbase.

#### Florida 2 (I-75, Brandon)

Constructed in 1986, this single section is part of six-lane I-75 in Hillsborough County, near Brandon. The design of this section consists of a 13-in (330-mm) JPCP with a 14-ft (4.3-m) widened outside lane placed over a 6-in (152-mm) sand base course. The transverse joints contain 1.25-in (32-mm) diameter, epoxy-coated dowel bars, and are spaced at 12-18-19-13-ft (4.9-5.5-5.8-4.0-m) intervals. The subgrade is classified as an AASHTO A-3 material. This project was included in the 1987 evaluation and has sustained 9.5 million 18-kip (80-kN) ESAL applications through 1992.

#### Florida 3 (I-75, Bradenton)

This single section, constructed in 1982, is located on I-75 near Bradenton, in Manatee County. The design for this section is a 9-in (229-mm) JPCP with tied PCC shoulders, and random, skewed joints spaced at 16-17-23-22 ft (4.9-5.2-7.0-6.7 m) intervals. The transverse joints contain 1.00-in (25-mm) diameter, epoxy-coated dowels and are sealed with a silicone joint sealant. The base consists of 6 in (152 mm) of lean concrete, and the subgrade is an AASHTO A-3 material. Through 1992, this section has been subjected to 13 million 18-kip (80-kN) ESAL applications.

#### Florida 4 (U.S. 41, Ft. Meyers)

This project is located in the southbound lanes of U.S. 41 between Punta Gorda and Ft. Meyers and was constructed to evaluate the feasibility of constructing a two-course pavement system.<sup>(14,15)</sup> While this project originally contained 33 test sections when constructed in 1978, the sections included in this study are shown in table 9.

Table 9. Experimental design matrix for selected sections on FL 4.

	3-in JPCP 15-ft Skewed Jts		3-in JPCP 15-ft Square Jts		3-in JPCP 20-ft Square Jts		9-in JPCP 20-ft Square Jts	
	6-in Shell Stab. Subgrade		6-in Cement- Treated Subgrade		6-in Shell Stab. Subgrade		6-in Cement- Treated Subgrade	
	Dowels	No Dowels	Dowels	No Dowels	1 in Dowels	No Dowels	Dowels	No Dowels
9 in LCB "A" $f'_c = 2000 \text{ lb/in}^2$		FL 4-2		FL 4-7	FL 4-10			
9 in LCB "B" $f'_c = 1250 \text{ lb/in}^2$		FL 4-3 FL 4-4 FL 4-5		FL 4-8	FL 4-11			
9 in LCB "C" $f'_c = 750 \text{ lb/in}^2$		FL 4-6		FL 4-9				
No Base								FL 4-1

1 in = 25.4 mm  
 1 ft = 0.305 m  
 1 lb/in<sup>2</sup> = 0.0069 MPa

Built in 1978  
 Cumulative ESAL's = 4.5 million

Note: Sections FL 4-4 and FL 4-5 contain tied lean concrete shoulders.

With the exception of FL 4-1 (representative of Florida's then-standard concrete pavement design), all sections in the project are two-layer structures consisting of a lean concrete base and a thin (2 or 3 in [51 or 76 mm]) concrete surface layer. Three different lean concrete base types were used in this study, each with a different compressive strength. Other variables that can be evaluated under this study are joint spacing (15 ft [4.6 m] versus 20 ft [6.1 m]), load transfer, pavement type, joint orientation, and type of subgrade stabilization. The project has sustained about 4.5 million 18-kip (80-kN) ESAL applications through 1992.

### Georgia 1 (I-85, Newnan) and Georgia 2 (I-85, La Grange)

In 1971, an experimental project was constructed by the Georgia Department of Transportation in the southbound lanes of I-85 near Newnan. Consisting of 10 different test sections, the purpose of this project is to evaluate the effects of dowels and base type on the performance of JPCP.<sup>(16)</sup>

All 10 GA 1 sections are 9-in (229-mm) JPCP with 20-ft (6.1-m) skewed joints that are sealed with a hot-poured sealant material. The base types include a 1-in (25-mm) AC layer over a 5-in (127-mm) CTB, a 6-in (152-mm) CTB, and a 4-in (102-mm) ATB. Dowels, when included, were 1.13 in (29 mm) in diameter, 18 in (457 mm) long, spaced at 15-in (381-mm) intervals, and coated with red lead paint. Replicate sets of sections were also constructed for all base types, except for the 6-in (127-mm) CTB section, which represented the standard DOT design at the time. All GA 1 sections

were constructed on an AASHTO A-4 subgrade. All GA 1 sections were diamond ground in 1985 primarily to restore ride quality due to rough initial construction.

An adjacent concrete pavement section, GA 2, was included in this evaluation because it contains a lean concrete base. GA 2, located about 20 mi (32 km) south of GA 1 in the southbound lanes of I-85, was constructed in 1977. It is also a 9-in (229-mm) JPCP with 20-ft (6.1-m) perpendicular joints and contains 1.13-in (29-mm) diameter dowel bars. It was constructed on an AASHTO A-2-6 subgrade. The experimental design matrix for the GA 1 and GA 2 projects is shown in table 10.

Table 10. Experimental design matrix for GA 1 and GA 2.

	9-in JPCP 20-ft Skewed Joints		9-in JPCP 20-ft Joints
	1.13-in Dowel Bars	No Dowels	1.13-in Dowel Bars
1-in AC (4-5% AC-20) 5-in CTB (6% cement)	GA 1-1 GA 1-3	GA 1-2 GA 1-4	
6-in CTB (6% cement)	GA 1-5	GA 1-10	
4-in ATB (4.5% AC-20)	GA 1-6 GA 1-8	GA 1-7 GA 1-9	
6-in LCB (6.9% cement)			GA 2

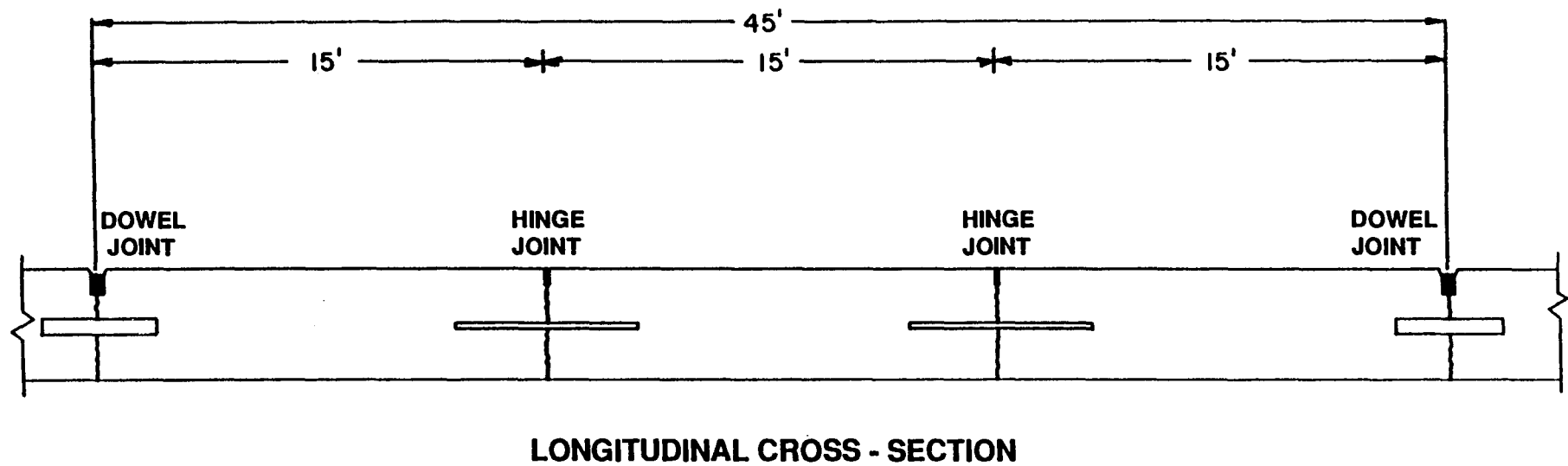
1 in = 25.4 mm  
1 ft = 0.305 m

GA 1 built in 1971, GA 2 in 1977  
GA 1 ESAL's = 19.1 million (6.5 million since grinding)  
GA 2 ESAL's = 12.1 million

### Illinois 1 (U.S. 50, Carlyle)

This project, constructed in 1986, is located approximately 20 mi (32.2 km) south of I-70 on U.S. 50, near Carlyle. Twenty-nine pavement sections are included in the project, consisting of CRCP, JRCP, and JPCP designs of varying thicknesses, sections with and without underdrains, sections with and without edge joint seals, and sections with different joint spacings (JRCP only).<sup>(17)</sup>

For the current study, only seven sections were selected for evaluation, as the main focus was an evaluation of the "hinge joint" design. Four sections are JRCP designs and three are CRCP designs. Three of the JRCP sections are "hinge joint" designs (illustrated in figure 2) in which conventional doweled joints (1.5-in [38-mm] epoxy-coated dowels) are located at each end of the 40-ft (12.2-m) slab, with one or two intermediate joints placed within the slabs. These intermediate joints are sawed as conventional joints, but are located where additional reinforcing steel has been placed. The concept is to force transverse cracks (which are expected to occur in a



16

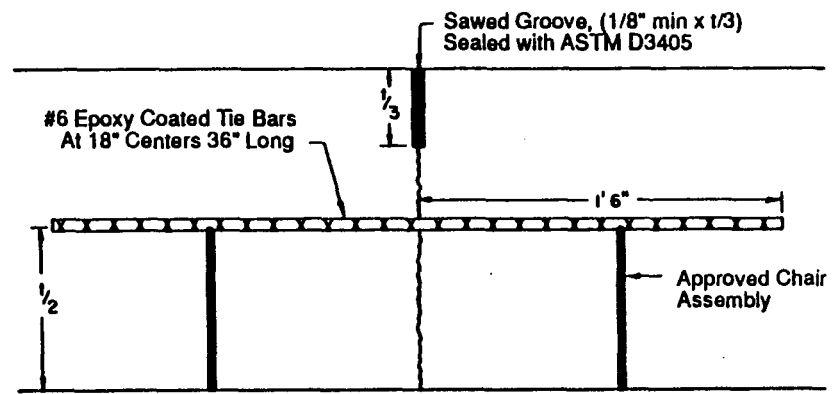
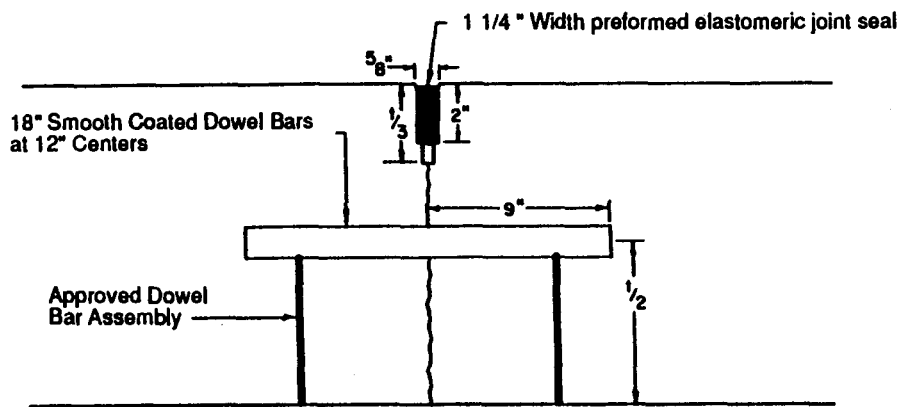


Figure 2. Hinge joint design details for JRCP sections in Illinois.

JRCP design) to develop at the sawed joints, where the additional reinforcing steel will hold the sawed joint tight. The conventional JRCP design contains 0.13 percent reinforcing steel, whereas the hinged JRCP design contains an effective 0.29 percent reinforcing steel. Table 11 summarizes the selected sections from IL 1.

Table 11. Experimental design matrix for IL 1.

		Underdrains No Edge Joint Seal
7-in CRCP (0.70% Steel, No. 5 Bars)		IL 1-9
8-in CRCP (0.73% Steel, No. 6 Bars)		IL 1-2
9-in CRCP (0.72% Steel, No. 6 Bars)		IL 1-1
8.5-in JRCP 40-ft Slabs 1.5-in Dowels	20-ft hinge (mesh)	IL 1-13
	20-ft hinge (no mesh)	IL 1-14
	13.3-ft hinge (mesh)	IL 1-15
	Conventional, No hinge (wire mesh)	IL 1-16

1 in = 25.4 mm

1 ft = 0.305 m

Notes: All sections contain a 4-in (102-mm) LCB.

Built in 1986

Cumulative ESAL's = 1.7 million

### Illinois 2 (U.S. 20, Freeport)

The project, constructed in 1986, is located on U.S. 20 near Freeport.<sup>(17)</sup> Four pavement sections are included in the project, each a 10-in (254-mm) thick JRCP constructed over a 4-in (102-mm) LCB. Similar to IL 1, these sections contain a hinge joint design (illustrated in figure 2). Table 12 shows the sections included in the study.

Table 12. Experimental design matrix for IL 2.

10-in JRCP 4-in LCB				
	Conventional No Hinge Wire Mesh 0.11% Steel	20-ft Hinge No Mesh 0.25% Steel	20-ft Hinge Wire Mesh 0.25% Steel	13.3-ft Hinge No Mesh 0.25% Steel
40-ft Joints 1.5-in Dowels	IL 2-8	IL 2-5	IL 2-6	IL 2-7

1 in = 25.4 mm

1 ft = 0.305 m

Built in 1986

Cumulative ESAL's = 1.3 million

Michigan 1 (US 10, Clare)

Michigan 1 is an experimental project constructed on U.S. 10 near Clare. Built in 1975, the purpose is to evaluate the effects of base type, drainage, joint spacing, joint skew, and dowels on the performance of jointed concrete pavements.<sup>(18)</sup> The project includes both plain and reinforced jointed concrete pavements with 9-in (229-mm) slabs. Through 1992, this project has carried about 1.3 million ESAL's. The experimental design matrix for the sections surveyed on MI 1 is shown in table 13.

Table 13. Experimental design matrix for MI 1.

	Drained		Nondrained	
	Skewed Joints	Nonskewed Joints	Skewed Joints	Nonskewed Joints
	No Dowels	1.25-in Epoxy-Coated Dowels	No Dowels	1.25-in Epoxy-Coated Dowels
9-in JPCP 12-13-17-16-ft Jts 4-in AGG		MI 1-7a MI 1-7a5		MI 1-7b MI 1-7b5
9-in JPCP 12-13-19-18-ft Jts 4-in PATB (2-3% of 85-100 pen)	MI 1-4a MI 1-4a10 MI 1-4a12			
9-in JPCP 12-13-19-18-ft Jts 4-in ATB (6-8% of 250-300 pen)	MI 1-10a MI 1-10a3		MI 1-10b MI 1-25	
9-in JRCP (0.15% steel) 71.2-ft Jts 4-in AGG		MI 1-1a MI 1-1a2		MI 1-1b MI 1-1b2

1 in = 25.4 mm  
1 ft = 0.305 m

Built in 1975  
Cumulative ESAL's = 1.3 million

Note: All sections constructed on a 10-in (254-mm) aggregate subbase and A-2-4 subgrade.

Michigan 3 (I-94, Marshall)

Michigan 3, located on I-94 near Marshall, is a single section that was constructed in 1986 using recycled aggregate. The pavement is a 10-in (254-mm) JRCP placed over the 4-in (102-mm) PAGG, and includes a 41-ft (12.5-m) joint spacing with 1.25-in (38-mm) dowels. This section contains a PCC shoulder that was paved separately from the mainline and tied to mainline pavement. The subgrade is an AASHTO A-2-4 material. The project was included in the 1987 evaluation and has sustained about 11.5 million ESAL's through 1992.



#### Michigan 4 (I-69, Charlotte)

This project, located on I-69 near Charlotte, was constructed in 1972 to evaluate the differences in performance of JRPC provided with different shoulder types.<sup>(19)</sup> Two sections were selected for this study, both of which are 9-in (229-mm) JRPC designs with transverse joints that are spaced at 71.2-ft (21.7-m) intervals and that contain 1.25-in (32-mm) diameter dowels. However, section 4-1 contains a tied PCC shoulder (paved separately from mainline) while section 4-2 contains an AC shoulder. These sections have been subjected to about 6.3 million ESAL's through 1992.

#### Michigan 5 (I-94, Paw Paw)

This single section was constructed in 1984 using recycled aggregate. Located on I-94 near Paw Paw, this section has a permeable aggregate base course and tied, nonreinforced concrete shoulders. The JRPC slab is 10 in (254 mm) thick with doweled transverse joints spaced at 41-ft (12.5-m) intervals. The subgrade on the project is an AASHTO A-2-4 material. This section is identical to MI 3, except MI 5 has tied, nonreinforced concrete shoulders (paved separately from mainline) whereas MI 3 contains tied, reinforced concrete shoulders. Through 1992, this section has carried about 8.5 million ESAL applications.

#### Michigan 6 (Davison Freeway, Detroit)

This single section is a 10-in (254 mm) JPCP located on the Davison Freeway near downtown Detroit. This section of Davison Freeway is a sunken urban highway (approximately 25 ft [7.6 m] below the ground level), with retaining walls and curbs on both sides of the roadway. It was constructed in 1942 and contains nondoweled joints spaced at 25-ft (7.6-m) intervals. The pavement rests on a 5-in (127-mm) granular base course placed on the clay subgrade. This project was included because it represents an older JPCP design that has been subjected to heavy traffic loadings (approximately 34 million through 1992).

#### Minnesota 1 and Minnesota 5 (I-94, Rothsay)

This experimental project on I-94 near Rothsay, Minnesota, was constructed in 1970 to evaluate the effect of base type, slab thickness, and load transfer on jointed reinforced concrete pavement performance.<sup>(20,21)</sup> The variables include aggregate (AGG), asphalt-treated (ATB, 5 percent of AC-10), and cement-treated (CTB, 5 percent cement) bases; 8- and 9-in (203- and 229-mm) JRPC slabs (0.09 and 0.08 percent steel, respectively); and doweled (1-in [25-mm] diameter bars) and nondoweled joints. Each design section rests on an A-6 subgrade.

Minnesota 5, a pavement section located near the MN 1 project, is included in the study because it is typical of Minnesota's concrete pavement design of the 1960's. This section was built in 1969 and consists of a 9-in (229-mm) thick JRPC (0.04 percent steel) with doweled transverse joints spaced at 39-ft (11.8-m) intervals. It has a 3-in (76-mm) thick aggregate base and rests on an AASHTO A-6 subgrade.

The design matrix for these sections is shown in table 14. Through 1992, these sections have carried about 7.4 million ESAL applications.

Table 14. Experimental design matrix for MN 1 and MN 5.

		8-in JRCP (0.09% Steel)		9-in JRCP (0.08% Steel)	
		No Dowels	1-in (25-mm) Dowels	No Dowels	1-in (25-mm) Dowels
Constructed 1970 27-ft Skewed Joints	6-in AGG	MN 1-3* MN 1-23*	MN 1-4 MN 1-24	MN 1-1* MN 1-21*	MN 1-2 MN 1-22
	5-in ATB (5% AC-10)	MN 1-5 MN 1-15	MN 1-6 MN 1-16	MN 1-7 MN 1-13	MN 1-8 MN 1-14
	5-in CTB (5% cement)	MN 1-11* MN 1-17*	MN 1-12 MN 1-18	MN 1-9* MN 1-19*	MN 1-10 MN 1-20
Constructed 1969 39-ft Joints	3-in AGG				MN 5 (0.04% Steel)

1 in = 25.4 mm  
1 ft = 0.305 m

Cumulative ESAL's = 7.4 million

Notes: \* Sections diamond ground and edge beam (tied and doweled) added in 1984.  
Sections 1-1 through 1-12 were also surveyed in 1987.

### Minnesota 2 (I-90, Albert Lea)

A second experimental project in Minnesota is located on I-90, west of Albert Lea. the purpose of this experimental project is to evaluate the effect of tied concrete shoulders and widened traffic lanes on concrete pavement performance.<sup>(22,23)</sup> This project was included in the 1987 study and was reevaluated in 1992.

The MN 2 pavement sections were constructed in 1977. Design variables include pavement type (JRCP and JPCP), shoulder type, and slab thickness. All sections have a widened inner lane (15 ft [4.6 m] wide) and are constructed on an aggregate base course over an AASHTO A-6 subgrade. With the exception of the inner lanes of MN 2-1 and 2-2, the sections all contain 1-in (25-mm) diameter dowel bars. MN 2-1 and 2-2 contain tied and keyed PCC shoulders (paved separately from mainline) whereas MN 2-3 and 2-4 contain AC shoulders. Through 1992, the sections have sustained about 4.2 million ESAL applications. The experimental design matrix is shown in table 15.

Table 15. Experimental design matrix for MN 2.

	8-in Slab	9-in Slab	
	PCC Shoulder	AC Shoulder	PCC Shoulder
JPCP 13-16-14-19 ft Skewed Joints	MN 2-2		MN 2-1
JRCP (0.09% steel) 27-ft Skewed Joints		MN 2-3 MN 2-4	

1 in = 25.4 mm  
1 ft = 0.305 m

Constructed in 1977  
Cumulative ESAL's = 4.2 million

Notes: MN 2-1 and 2-3 have 6-in (152-mm) AGG base.  
MN 2-2 and 2-4 have 5-in (127-mm) AGG base.

Minnesota 3 (I-90, Austin)

This project, constructed in 1984 as part of I-90 in Austin, consists of a single pavement section. It is included in this study because it has a 14-ft (4.3 -m) widened outside lane and a 13.5-ft (4.1-m) widened inside lane. The pavement slab is a doweled, 9-in (229-mm) JRCP with 27-ft (8.2-m) skewed joints that rests on an aggregate base course and an AASHTO A-4 subgrade. The project has carried approximately 3.7 million ESAL's through 1992.

Minnesota 4 (TH 15, New Ulm)

Minnesota 4 is a single pavement section located on Trunk Highway 15 near New Ulm. Built in 1986, this project is included in the study because of the 14-ft (4.3-m) widened outer lane. The pavement, located on a two-lane highway, is a 7.5-in (190-mm) JPCP constructed over an aggregate base course. The transverse joints are doweled, skewed, and spaced at 13-16-14-17-ft (4.0-4.9-4.3-5.2-m) intervals. The subgrade is an AASHTO A-2-6 material. Through 1992, this project has carried about 0.9 million ESAL applications.

Minnesota 6 (TH 15, Truman)

Minnesota 6, built in 1983, is a single pavement section located on Trunk Highway 15 near Truman. This project, a two-lane highway, is included because it contains a permeable asphalt-treated base (PATB) course and a 14-ft (4.3-m) widened outer lane. The pavement is a doweled, 8-in (203-mm) JRCP with 27-ft (8.2-m) skewed joints. The section is constructed on an AASHTO A-2-4 subgrade and has carried 2 million ESAL applications through 1992.

Minnesota 7 (TH 36, Roseville)

This experimental project, located on Trunk Highway 36 in Roseville, was constructed in 1958 with a range of design variables to determine the combination that provided the best performance.<sup>(24)</sup> Design variables for the study included pavement type (JRCP vs. JPCP), joint spacing (33 ft [10.1 m] vs. 65 ft [19.8 m] for JRCP and 15 ft [4.6 m] vs. 20 ft [6.1 m] for JPCP), load transfer (doweled vs. nondoweled, JPCP only), and base type (two types of aggregate bases). However, because the JRCP slabs were at some time sawed into shorter panel lengths, and because extensive joint repairs had been performed on the JRCP test sections, only the JPCP sections were evaluated under this study.

For each doweled pavement section, three different types of 1-in (25-mm) diameter dowels were used: oiled, rust-proofed, and sleeved dowels. These dowels were placed at alternating joints within the section. The design matrix for the sections originally selected for the study is shown in table 16. These sections have been subjected to about 6.9 million ESAL applications through 1992.

Table 16. Experimental design matrix for selected sections on MN 7.

		9-in JPCP 15-ft Joints	9-in JPCP 20-ft Joints
AGG Base B	No Dowels	MN 7-10 MN 7-18	MN 7-9 MN 7-17
	1-in Dowels	MN 7-15 MN 7-23	MN 7-16 MN 7-24

1 in = 25.4 mm  
1 ft = 0.305 m

Constructed in 1958  
Cumulative ESAL's = 6.9 million

Note: AGG Base B consists of 3-in gravel, 3-in sand-gravel, 3-in gravel, and 9-in sand-gravel.

Missouri 1 (I-35, Bethany)

This project, constructed in 1977, consists of eight sections. Located in the northbound lanes of I-35, near Bethany, this project was constructed to evaluate the effect of coarse aggregate size and base type on pavement performance.<sup>(25)</sup> Common to all sections are a 9-in (229-mm) JRCP and 1.25-in [32-mm] noncoated dowel bars at transverse joints spaced at 61.5-ft (18.7-m) intervals. The shoulder design throughout the project consists of 5-in (127-mm), permeable open-graded aggregate subbase and 8-in (203-mm) dense-graded aggregate surface. A 3-ft (0.9-m) wide segment of the shoulder adjacent to either side of the mainline pavement has a 2-in (51-mm) AC surface. The experimental design matrix for this project is provided in table 17.

Table 17. Experimental design matrix for MO 1.

		4-in AGG	4-in ATB (5%, 60-70 pen)	4-in PATB (3%, 60-70 pen)	4-in CTB (4.5% cement)
9-in JRCP  0.1% Steel	2-in Max Size Aggregate	MO 1-1			
	1-in Max Size Aggregate	MO 1-4 MO 1-8	MO 1-5	MO 1-6	MO 1-7
61.5-ft Joints	0.75-in Max Size Aggregate	MO 1-2			
		MO 1-3			

1 in = 25.4 mm  
1 ft = 0.305 m

Constructed in 1977  
Cumulative ESAL's = 13.7 million

Notes: Section MO 1-1 contains non-D-cracking susceptible aggregate.  
MO 1-2 and 1-8 contain moisture barrier.  
MO 1-4, MO 1-5, MO 1-6, and MO 1-7 are SHRP LTPP sections.

### New Jersey 2 (Route 130, Yardville)

A part of Route 130 near Yardville, New Jersey is one of the oldest sections included in this study. Once a major access route to New York City, it was constructed in 1951 and is still typical of New Jersey's current standard concrete pavement design. The pavement is a 10-in (254-mm) JRCP that rests on an aggregate base and subbase material. The slabs are 78.5-ft (23.9-m) long and are constructed with expansion joints at that interval. Load transfer is provided by stainless steel-wrapped dowel bars, 1.25-in (32-mm) in diameter. Through 1992, this section has carried 38.2 million ESAL applications.

### New Jersey 3 (I-676, Camden)

This experimental project is located on I-676 near Camden. Built in 1979, the project is a drainage study evaluating the performance of pavement sections with open-graded aggregate bases (PAGG) and bituminous-stabilized open-graded base layers (PATB). Both sections included in this project have 9-in (229-mm) JRCP slabs, 78.5-ft (23.9-m) transverse joint spacings (every joint is an expansion joint), 1.25-in (32-mm) diameter stainless steel-wrapped dowel bars, and AC shoulders. A filter fabric is placed full-width beneath both of the open-graded layers and above the lime-flyash stabilized subgrade. The sections have sustained about 12.6 million ESAL applications through 1992. The simplified design matrix is presented in table 18.

Table 18. Experimental design matrix for NJ 3.

	<b>4-in PAGG</b>	<b>4-in PATB (2.5%, AC-20)</b>
<b>9-in JRCP 0.16% Steel 78.5-ft Expansion Joints</b>	NJ 3-1	NJ 3-2

1 in = 25.4 mm  
1 ft = 0.305 m

Built in 1979  
Cumulative ESAL's = 12.6 million

New York 1 (Route 23, Catskill)

Route 23 between Catskill and Cairo, New York, is the site of an experimental project constructed in 1968. The purpose of this project (which consists of 30 sections representing 8 different designs) is to evaluate the effects of load transfer, joint orientation, base type, joint spacing, and pavement type on pavement performance.<sup>(26,27)</sup>

The designs included in this project are shown in table 19. All slabs are 9 in (229 mm) thick and the subgrade for the project varies from an AASHTO A-1-a to A-2-4 material. Load transfer, where applicable, is provided by ACME two-part malleable iron devices. The sections have sustained about 5.5 million ESAL's through 1992.

Table 19. Experimental design matrix for NY 1.

		Perpendicular Joints		Skewed Joints
		Load Transfer	No Load Transfer	No Load Transfer
<b>9-in JPCP 20-ft Joints</b>	<b>4-in AGG</b>	NY 1-6*		
	<b>3-in ATB (2.5-4%, 60-70 pen)</b>	NY 1-1*	NY 1-7 NY 1-8a*	NY 1-8b*
	<b>4-in Soil Cement (8-10% cement)</b>		NY 1-5a	NY 1-5b
<b>9-in JRCP 0.20% Steel 61-ft Joints</b>	<b>4-in AGG</b>	NY 1-4*		
	<b>3-in ATB (2.5-4%, 60-70 pen)</b>	NY 1-2 NY 1-3*		

1 in = 25.4 mm  
1 ft = 0.305 m

Built in 1968  
Cumulative ESAL's = 5.5 million

Notes: Sections marked with "\*" were included in 1987 evaluation.  
All sections contain an 8-in (203-mm) aggregate subbase and AC shoulders.

New York 2 (I-88, Otego)

In 1975, an experimental project was constructed on I-88 near Otego, New York. The purpose of the study was to evaluate the performance of jointed plain concrete pavements (which had fared well on NY 1) under Interstate traffic loading conditions.<sup>(28)</sup> Design variables include pavement type, joint spacing, and shoulder type. In addition, the effect of sealing the lane-shoulder joint was investigated.

Four pavement sections were evaluated in 1987 and again in 1992. All slabs are 9 in (229 mm) thick and contain epoxy-coated I-beams for load transfer. Aggregate bases are common to all sections, as is the AASHTO A-1-a subgrade. Three sections also contain tied PCC shoulders that were paved separately from the mainline pavement. The simplified design matrix for this project is shown in table 20.

Table 20. Experimental design matrix for NY 2.

	PCC Shoulder	AC Shoulder
9-in JPCP 20-ft Joints Sealed Lane-Shoulder Jt	NY 2-3	
9-in JPCP 20-ft Joints Nonsealed Lane-Shoulder Jt	NY 2-9	
9-in JPCP 26.7-ft Joints	NY 2-11	
9-in JRCP 0.2% Steel 63.5-ft Joints		NY 2-15

1 in = 25.4 mm  
1 ft = 0.305 m

Built in 1975  
Cumulative ESAL's = 5.8 million

Notes: NY 2-3 & 2-15 have 4-in (102-mm) aggregate base.  
NY 2-9 & 2-11 have 6-in (152-mm) aggregate base.

North Carolina 1 (I-95, Rocky Mount)

Several experimental pavement sections were constructed on I-95 near Rocky Mount, North Carolina, in 1967.<sup>(29,30)</sup> Design variables in the project include base type, pavement type, joint spacing, slab thickness, joint skew, and load transfer. The subgrade soil for these sections varies from AASHTO A-4 to A-7-6. In addition, an adjacent CRCP section was constructed as part of the project. These sections, evaluated in 1987 and again in 1992, have sustained approximately 16.0 million ESAL applications through 1992. The design matrix for the project is depicted in table 21.

Table 21. Experimental design matrix for NC 1.

	9-in JPCP 30-ft Jts			8-in JRCP 0.17% Steel 60-ft Jts	8-in CRCP 0.6% Steel
	Skewed Joints	Perpendicular Joints		Perpendicular Joints	
	No Dowels	1-in Dowels	No Dowels	1-in Dowels	
4-in AGG	NC 1-1	NC 1-4	NC 1-8	NC 1-7	NC 1-9
6-in Soil Cement (8% cement)		NC 1-2	NC 1-3		
4-in CTB (6% cement)			NC 1-5		
4-in ATB (4% AC-20)			NC 1-6		

1 in = 25.4 mm  
1 ft = 0.305 m

Built in 1968  
Cumulative ESAL's = 16.0 million

Note: All sections include a daylighted aggregate base.

### North Carolina 2 (I-85, Greensboro)

This single section, located on I-85 near Greensboro, is included in the study because of its doweled, JPCP design and tied concrete shoulders. It is also a section being monitored by the North Carolina Department of Transportation to evaluate the effect of the lean concrete base on pavement performance.<sup>(31)</sup>

Constructed in 1982, the pavement consists of 11-in (279-mm) JPCP slabs placed on a lean concrete base. The subgrade for the project is an AASHTO A-4 material. The transverse joints are spaced at 18-25-23-19 ft (5.5-7.6-7.0-5.8 m) intervals, contain 1.38-in (35-mm) diameter dowels, and are sealed with a silicone sealant. Fin drains are also provided in the pavement structure. Through 1992, this section has sustained approximately 14.2 million ESAL applications.

### Ohio 1 (Route 23, Chillicothe)

This experimental project, located on U.S. 23 near Chillicothe, was constructed in 1973 to evaluate the effect of different design variables on pavement performance.<sup>(32)</sup> The experimental variables for this project include base type, joint spacing, pavement type, and dowel coatings. All slabs are 9 in (229 mm) thick and the subgrade ranges from an AASHTO A-4 to an AASHTO A-6 material. This project, which was evaluated in both 1987 and 1992, has carried about 6.1 million ESAL applications. The experimental design matrix is shown in table 22.



Table 22. Experimental design matrix for OH 1.

		7.5-in AGG	4-in ATB (5.7%, AC-20)
9-in JRCP 0.09% Steel 21-ft Jts	1.25-in Standard Dowels	OH 1-10*	OH 1-3*
	1.25-in Plastic- Coated Dowels	OH 1-6*	
9-in JRCP 0.09% Steel 40-ft Jts	1.25-in Standard Dowels	OH 1-1* OH 1-2 OH 1-8 OH 1-9*	OH 1-4*
	1.25-in Plastic- Coated Dowels	OH 1-7*	
9-in JPCP 17-ft Skewed Jts	No Dowels		OH 1-5

1 in = 25.4 mm  
1 ft = 0.305 m

Built in 1973  
Cumulative ESAL's = 6.1 million

Note: Sections marked with "\*" were included in 1987 evaluation.

### Ohio 2 (S.R. 2, Vermilion)

In 1974, an experimental project was constructed on State Route 2 near Vermilion to study the factors that influence the development of D-cracking.<sup>(33)</sup> The factors examined include the type (quality) and maximum size of coarse aggregate, drainage, base type, joint spacing, joint sealing, pavement type, and slab thickness. The project contains 104 test sections, each about 240-ft (73.2-m) long. Of the 104 sections, two were included in the original 1987 study. A total of 52 sections (including the original 2 surveyed in 1987) were evaluated in 1992. The reduced design matrix for this project, showing the sections evaluated under this study, is provided in table 23. These sections have sustained an estimated 6.5 million ESAL's through 1992.

### Ontario 1 (Highway 3N, Windsor)

This project was constructed on Highway 3N near Windsor, Ontario, in 1982. It features the following experimental factors: variations in base type, slab thickness, shoulder type, and surface textures.<sup>(34,35)</sup> The subgrade at the project site is an AASHTO A-7-6. All sections contain subdrainage and transverse skewed joints spaced in a repeated pattern of 12-13-19-18 ft (3.7-4.0-5.8-5.5 m). The transverse joints are sealed with a hot-poured joint sealant material and do not contain dowel bars. Two sections contain an LCB (7.2 percent cement), one section contains a PATB (no separator layer beneath base and edge drains placed in dense-graded shoulder base), and one section contains no base course.

Table 23. Experimental design matrix for selected sections on OH 2.

Base Type	Seal Type	20-ft JPCP				40-ft JRCP									60-ft JRCP		9-in CRCP		
		No Drains		Drains		No Drains			Daylighted			Drains			Drains		No Drains	Day-lighted	Drains
		Max. Agg. Size, in		Max. Agg. Size, in		Max. Agg. Size, in			Max. Agg. Size, in			Max. Agg. Size, in			Max. Agg. Size, in		Max. Agg. Size, in		
		0.5	1.5	0.5	1.5	0.5	1.0	1.5	0.5	1.0	1.5	0.5	1.0	1.5	0.5	1.5	1.5	1.5	1.5
None	None																		
	HP	2-1 2-4	2-2 2-3																
	Pref																		
6-in AGG	None				2-13			2-73			2-59			2-22				2-CRC 2-Sa 2-Sb	
	HP			2-17	2-12	2-75	2-74	2-69 2-72	2-55	2-56	2-54 2-57	2-24	2-23	2-20 2-21	2-18	2-11			
	Pref				2-14					2-58					2-9				
4-in ATB (4-7%)	None							2-42						2-53			2-47		2-48
	HP					2-44		2-43 2-45				2-50		2-49 2-51					
	Pref							2-41						2-52					
4-in CTB (4.4%)	None							2-93						2-104			2-98		2-99
	HP					2-95		2-94 2-96				2-101		2-100 2-102					
	Pref							2-92						2-103					

28

1 in = 25.4 mm  
1 ft = 0.305 m

Built in 1974  
Cumulative ESAL's = 6.1 million

Notes: OH 2-9, 2-11, 2-12, 2-13, 2-14, 2-17, 2-18, 2-CRC, 2-Sa, and 2-Sb have 4 to 8.5 in tapered base.  
OH 2-1, 2-2, 2-3, and 2-4 are 15-in slabs (skewed joints) with no dowels, others are 9-in slabs with 1.25-in dowels (no dowels in CRCP).  
OH 2-1, 2-2, and 2-11 have tied PCC shoulders, others have AC shoulders.  
OH 2-21, 2-22, 2-51, 2-54, 2-72, 2-73, and 2-102 contain durable Sy2 coarse aggregate; others contain D-cracking susceptible aggregate.

These sections were evaluated in both 1987 and 1992. Through 1992, they have sustained approximately 2.1 million ESAL applications. The actual traffic on this project was much greater than estimated during original design (pavement designed for 3.5 million ESAL's over 20-year design life). The experimental design matrix for this project is shown in table 24.

Table 24. Experimental design matrix for ONT 1.

	AC Shoulder		PCC Shoulder	
	8-in JPCP No Dowels	12-in JPCP No Dowels	7-in JPCP No Dowels	8-in JPCP No Dowels
4-in PATB (2% AC)	ONT 1-2			
5-in LCB (7.2% cement)			ONT 1-4	ONT 1-3
No Base		ONT 1-1		

1 in = 25.4 mm

1 ft = 0.305 m

Built in 1982

Cumulative ESAL's = 2.1 million

Note: All sections contain longitudinal edge drains and no subbase.

### Ontario 2 (Highway 427, Toronto)

This project is a single JPCP section located on Highway 427 in Toronto. Highway 427 is a principal access route into downtown Toronto. At the location of the survey section, the highway has four lanes in the direction of survey, and has carried 56 million ESAL applications in the heaviest-traveled lane. Constructed in 1971, the section features a 9-in (229-mm) PCC slab constructed on a 6-in (152-mm) CTB containing 5 percent cement. The joints are skewed, spaced at 12-13-19-18-ft (3.7-4.0-5.8-5.5-m) intervals, and contain 1-in (25-mm) dowel bars. Longitudinal edge drains were added in 1982.

### Pennsylvania 1 (Route 66 and Route 422, Kittanning)

In 1980, an experimental JPCP consisting of bases of varying permeabilities was constructed on Routes 66 and 422 near Kittanning to investigate the performance of the alternative base types.<sup>(36)</sup> The base types tested include CTB, PATB, uniformly graded aggregate, well-graded aggregate, and dense-graded aggregate. All sections have a 10-in (254 mm) pavement slab with 46.5-ft (14.2-m) joint spacing and 1.25-in (32-mm) epoxy-coated dowels. The subgrade type varies from A-2-4 to A-4. All sections contain AC shoulders.

The section with a CTB (PA 1-1) is constructed on Route 422 and is not replicated on Route 66. All remaining sections were constructed on Route 66 and replicated in both directions of the divided roadway. Section PA 1-1 has accumulated 1.1 million ESAL applications, while the other sections have sustained about 0.8 million ESAL applications. The experimental design for this project is shown in table 25.

Table 25. Experimental design matrix for PA 1.

	6-in CTB (6% cement)	5-in PATB (2% asphalt)	8-in Uniform-Graded AGG (Permeable)	8-in Well-Graded AGG (Permeable)	13-in Dense-Graded AGG
10-in JRCP (0.09% Steel) 46.5-ft Joints	PA 1-1	PA 1-2	PA 1-3	PA 1-4	PA 1-5

1 in = 25.4 mm  
1 ft = 0.305 m

Built in 1980  
PA 1-1 cumulative ESAL's = 1.1 million  
PA 1-2 through PA 1-5 cumulative ESAL's = 0.8 million

### West Virginia 1 (I-77, Charleston)

While not part of an experimental project, three sections were evaluated on the West Virginia Turnpike (I-77), south of Charleston. These sections include two 10-in (254-mm) JRCP sections with 40-ft (12.2-m) joint spacing (WV 1-1, and WV 1-2), built in the early and mid-1980's and containing PCC shoulders. The third section is a 10-in (254-mm) JPCP with 15-ft (4.6-m) joint spacing and a widened outside lane (WV 1-3). WV 1-3 was added as a truck climbing lane adjacent to an existing 60-ft (18.3-m) JRCP. All sections contain 1.25-in (32-mm) epoxy-coated dowel bars. Table 26 shows summarizes the key design variables for these sections.

### Wisconsin 1 (I-90, Stoughton)

This experimental project, constructed in 1990, is located in the westbound lanes of I-90 near Stoughton. This project was constructed by the Wisconsin Department of Transportation to evaluate the feasibility of using various types of PCTB beneath concrete pavements to provide both a construction platform and positive drainage.<sup>(37)</sup>

The pavement is a 11-in (279-mm) JPCP with skewed joints spaced at 19-18-20-17-ft (5.8-5.5-6.1-5.2-m) intervals. The joints contain 1.5-in (38-mm) dowel bars and are sealed with a preformed joint sealant material. The outside traffic lane is 14 ft (4.3 m) wide, and the sections contain AC shoulders.

Table 26. Design data for WV 1.

	WV 1-1	WV 1-2	WV 1-3
<b>Pavement Type</b>	JRCP (0.1% Steel)	JRCP (0.1% Steel)	JPCP
<b>Year Built</b>	1986	1981	1989
<b>Thickness, in</b>	10.0 (254 mm)	10.0 (254 mm)	10.0 (254 mm)
<b>Joint Spacing, ft</b>	40 (12.2 m)	40 (12.2 m)	15 (4.6 m)
<b>Dowel Diameter, in</b>	1.25 (32 mm)	1.25 (32 mm)	1.25 (32 mm)
<b>Base Type</b>	6-in (152-mm) AGG	6-in (152-mm) CTB (5% cement)	6-in (152-mm) AGG
<b>Subgrade</b>	AASHTO A-4	AASHTO A-4	AASHTO A-4
<b>ESAL's, millions</b>	6.5	8.9	3.7

1 in = 25.4 mm  
1 ft = 0.305 m

Note: WV 1-3 was added as truck climbing lane to an existing 60-ft JRCP. The section contains edge drains and 15-ft outer lane.

Three different pavement sections were constructed, each containing a different amount of cement added to the PCTB: one section contained 150 lb/yd<sup>3</sup> (89 kg/m<sup>3</sup>), another contained 200 lb/yd<sup>3</sup> (119 kg/m<sup>3</sup>), and a third section contained 250 lb/yd<sup>3</sup> (148 kg/m<sup>3</sup>). The 4-in (102 mm) permeable layer is placed over a 4-in (102 mm) dense-graded aggregate base. Through 1992, the pavement has sustained approximately 1.3 million ESAL applications. Table 27 shows the experimental design matrix for the WI 1 sections.

Table 27. Experimental design matrix for WI 1.

	Cement Content of 4-in PCTB		
	5.2 Percent	6.8 Percent	8.3 Percent
<b>11-in JPCP 19-18-20-17 ft Joints 1.5-in Dowels AC Shoulders</b>	WI 1-1	WI 1-2	WI 1-3

1 in = 25.4 mm  
1 ft = 0.305 m

Built in 1990  
Cumulative ESAL's = 1.3 million

Wisconsin 2 (U.S. 18/151, Mt. Horeb) and Wisconsin 7 (U.S. 18/151, Barneveld)

These two projects, constructed in 1988, are located adjacent to each other on U.S. 18/151 and are considered together because of the way that they complement each other in terms of their ability to compare design features. The WI 2 sections are located near Mt. Horeb (in Dane County), while the WI 7 sections are located near Barneveld (in adjacent Iowa County). Both projects were opened to traffic at the same time and have accumulated 1.3 million ESAL applications through 1992.

The basic design for these projects is a 9-in (229-mm) JPCP with 12-13-19-18-ft (3.7-4.0-5.8-5.5-m) skewed, random joints and AC shoulders. Considering the projects together, design variables that can be evaluated include load transfer; base type (4-in [102-mm] PCTB, 4-in [102-mm] PATB, 4-in [102-mm] PAGG, and 6-in [152-mm] AGG); drainage (none, longitudinal, and transverse); and joint sealant (none and preformed). All sections contain an aggregate subbase course with thicknesses ranging from 12 to 16 in (305 to 406 mm). The design matrix for the WI 2 and WI 7 projects is shown in table 28.

Table 28. Experimental design matrix for WI 2 and WI 7.

		9-in JPCP 12-13-19-18 ft Joints				
		Longitudinal Drains			Trans. Drains	No Drains
		4-in PCTB	4-in PATB	4-in PAGG	6-in AGG	6-in AGG
1.25-in Epoxy-Coated Dowels	Preformed Seals					WI 2-5
	No Seal	WI 2-1	WI 2-2	WI 2-3	WI 7-10	WI 2-4
No Dowels	Preformed Seals	WI 7-3	WI 7-5	WI 7-1		WI 7-8
	No Seal	WI 7-4	WI 7-6	WI 7-2	WI 7-7	WI 7-9

1 in = 25.4 mm  
1 ft = 0.305 m

Built in 1988  
Cumulative ESAL's = 1.3 million

Notes: WI 2-4, 2-5, 7-7, 7-8, 7-9, & 7-10 have 12-in AGG subbase; others have 16-in AGG subbase.  
WI 2-2, WI 7-4, WI 7-6, and WI 7-10 are SHRP LTPP study sections.

Wisconsin 3 (STH 14, Middleton)

This experimental project, a two-lane highway, is located on STH 14 near Middleton. Built in 1988, the project consists of three, nondoweled 8-in (203-mm) JPCP sections with AC shoulders and joints spaced at 12-13-19-18-ft (3.7-4.0-5.8-5.5-m)

intervals. Two design features are evaluated under this project: drainage (no drain versus longitudinal fin drain) and base type (3.5-in [89-mm] permeable asphalt-treated base versus 6-in [152-mm] dense-graded aggregate base). The experimental design matrix for this project is given in table 29.

Table 29. Experimental design matrix for WI 3.

		8-in JPCP 12-13-19-18-ft Skewed Jts No Dowels	
		3.5-in PATB (2%)	6-in AGG
Longitudinal Fin Drain		WI 3-1	WI 3-2
No Drain			WI 3-3

1 in = 25.4 mm  
1 ft = 0.305 m

Built in 1988  
Cumulative ESAL's = 1.2 million

Notes: WI 3-1 has 6-in (152-mm) aggregate subbase.  
Other sections have no subbase.  
All sections have AC shoulders and A-3 subgrade.

#### Wisconsin 4 (STH 164, Waukesha)

This project consists of five sections in the northbound lanes and one section in the southbound lanes of STH 164 in Waukesha. Constructed in 1988, the pavement design is a 9-in (229-mm) JPCP with AC shoulders placed on a 6-in (152-mm) dense-graded aggregate base. The joints are spaced at 20-ft (6.1-m) intervals and do not contain dowel bars.

The experimental design for this project is shown in table 30. Unfortunately, five of the experimental sections (4-1 through 4-5) are located in the center lane of a three-lane roadway in an urban location and could not be evaluated. Thus, only one section (4-6, in the southbound direction) was included in the evaluation, having sustained an estimated 1.5 million ESAL applications.

#### Wisconsin 5 (STH 50, Kenosha)

An experimental project constructed in 1988 on STH 50 near Kenosha consists of six 10-in (254-mm) JPCP sections with AC shoulders constructed on a 6-in (152-mm) dense-graded aggregate base. Transverse joints are spaced at 12-13-19-18-ft (3.7-4.0-5.8-5.5-m) intervals and do not contain dowel bars. The design features of interest on this project include joint sealing and drainage. The experimental design matrix for this project is shown in table 31.

Table 30. Experimental design matrix for WI 4.

		9-in JPCP 20-ft Joints 6-in AGG No Dowels	
		Longitudinal Edge Drain	No Edge Drain
Transverse Joint Drain	Joint Seal	WI 4-3	
	No Seal	WI 4-4	
No Transverse Joint Drain	Joint Seal	WI 4-2	WI 4-1
	No Seal	WI 4-6	WI 4-5

1 in = 25.4 mm  
1 ft = 0.305 m

Built in 1988

Table 31. Experimental design matrix for WI 5.

		Type of Drainage		
		Fin Drain	Edge Drain	No Drain
10-in JPCP 12-13-19-18 ft Skewed Joints No Dowels 6-in AGG	Silicone Sealant	WI 5-1	WI 5-3	WI 5-5
	No Sealant	WI 5-2	WI 5-4	WI 5-6

1 in = 25.4 mm  
1 ft = 0.305 m

Built in 1988  
Cumulative ESAL's = 1.4 million

Wisconsin 6 (STH 29, Green Bay)

This experimental project is located on STH 29 west of Green Bay. Built in 1988, the project consists of four experimental sections. All sections are 10-in (254-mm) JPCP designs with 12-13-19-18-ft (3.7-4.0-5.8-5.5-m) joint spacing. Each section is constructed on a 4-in (102-mm) permeable aggregate base over a 4-in (100-mm) dense-graded aggregate subbase. The sections have a 14-ft (4.3-m) wide outer lane and AC shoulders.

The experimental design factors that are being evaluated under this study are dowel bars and joint sealant. Where used, the joint sealant material is a preformed compression seal and the dowel bars are 1.5-in (38-mm) in diameter and coated with epoxy. Table 32 shows the design features evaluated in this project.



Table 32. Experimental design matrix for WI 6.

	<b>10-in JPCP</b> <b>12-13-19-18-ft Skewed Joints</b> <b>4-in PAGG Base</b> <b>Longitudinal Edge Drains</b>	
	1.5-in Dowels	No Dowels
Preformed Joint Seal	WI 6-3	WI 6-2
No Joint Sealant	WI 6-4	WI 6-1

1 in = 25.4 mm

1 ft = 0.305 m

Built in 1988

Cumulative ESAL's = 4.2 million

Notes: All sections contain a 4-in (102-mm) aggregate subbase.  
 All section have a 14-ft wide outer lane and AC shoulders.

### Overall Summary of Projects

A total of 50 concrete pavement projects, representing 303 pavement sections, were evaluated under this study. A variety of design features (i.e., slab thickness, joint spacing, load transfer, and so on) are included on these projects. The range of design features encountered in these projects is summarized in table 33. This table shows that a significant range of variables exists, although often these ranges occur over different projects located in different climates.

These projects also vary considerably in age and in cumulative traffic loadings (ESAL's) that they have sustained. Figures 3 and 4 illustrate the range of age and ESAL loadings of the pavement sections. Figure 3 shows that most of the sections are between 15 and 25 years old, with about 20 sections greater than 25 years old. Figure 4 indicates that the majority of the sections have sustained less than 10 million ESAL applications, and only four sections have carried more than 20 million.

Table 33. Range of design features included in study.

Design Feature	Range of Design Feature	Distribution of Design Feature	
		Categories	Number in Category
Slab Thickness	7 to 15 in	< 8 in 8 to 9.9 in 10 to 11.9 in ≥ 12 in	3 234 41 25
Joint Spacing—JPCP	5 to 30 ft	< 10 ft 10 to 14.9 ft 15 to 19.9 ft ≥ 20	2 7 103 49
Joint Spacing—JRCP	21 to 78.5 ft	< 25 ft 25 to 39.9 ft 40 to 59.9 ft ≥ 60 ft	3 29 61 24
Joint Orientation		Nonskewed Joints Skewed Joints	130 148
Joint Load Transfer		Doweled Joints Nondoweled Joints	154 124
Joint Sealant		None Hot-Poured Silicone Preformed PVC Coal Tar Polyurethane	54 118 17 86 2 1
Base Type		None AGG CTB ATB LCB PAGG PCTB PATB	8 107 70 42 40 14 7 15
Drainage		None Daylighted Edge Drains Only Edge/Trans. Drains Permeable Base Fin Drains	168 36 55 4 36 4
Shoulder Type		AC PCC Gravel	246 56 1
JRCP Reinforcement	0.04 to 0.25%	< 0.1 percent 0.1 to 0.14 percent 0.15 to 0.19 percent ≥ 0.20 percent	45 54 9 9
Pavement Type		JPCP JRCP CRCP	161 117 25
Climate		Dry-Freeze Dry-Nonfreeze Wet-Freeze Wet-Nonfreeze	40 30 171 62

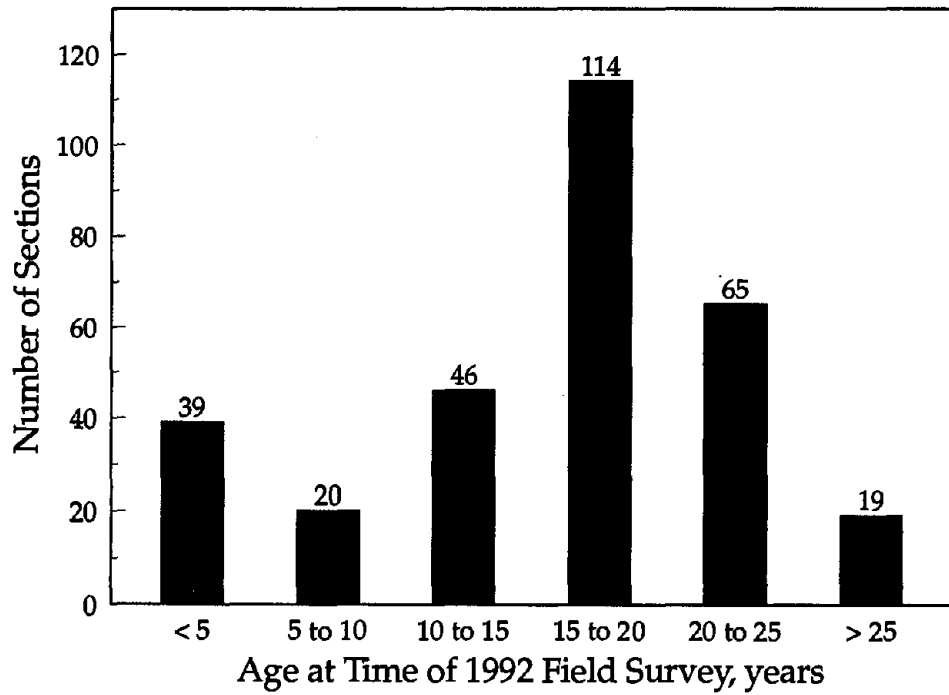


Figure 3. Distribution of projects by age.

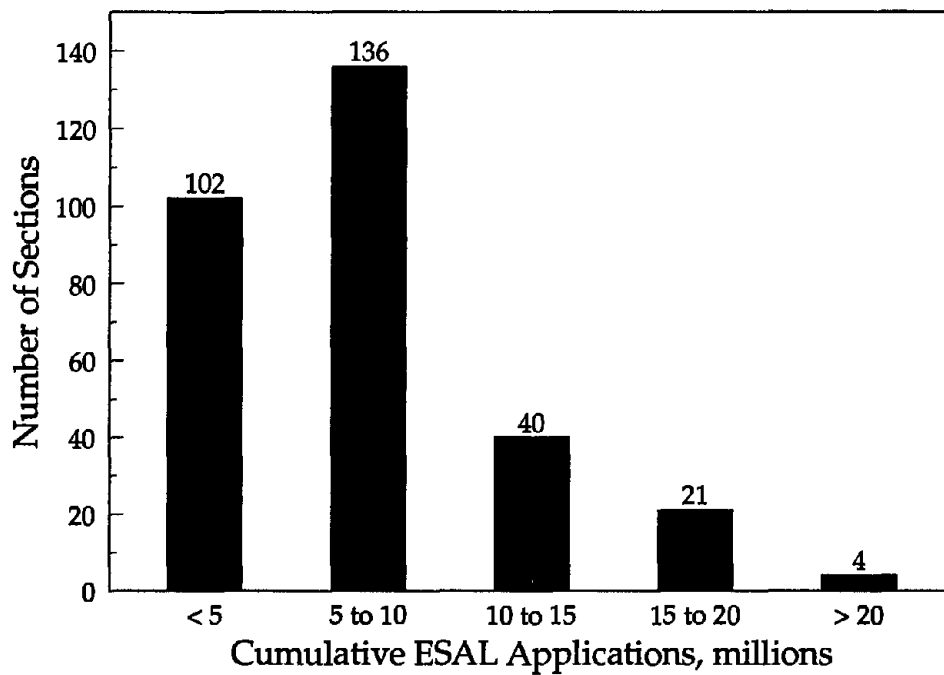


Figure 4. Distribution of projects by ESAL applications.



### 3. EFFECT OF DESIGN FEATURES ON PAVEMENT PERFORMANCE

#### Introduction

As described in chapter 2, a range of design features is present on the 303 pavement sections evaluated under this study. This chapter examines the effect of those design features on the overall performance of the concrete pavement sections. Of particular interest are those projects that vary one design feature while holding all others constant; this allows the effect of that feature on pavement performance to be determined. For example, a doweled pavement section can be compared with an adjacent nondoweled pavement section (of otherwise similar design) to determine the effect of dowels on joint faulting and overall rideability. Similarly, a section constructed thicker than an adjacent section can be evaluated to determine if increased slab thickness reduces slab cracking or other structural defects.

However, many of the projects evaluated under this study vary more than one design feature at a time. This variation makes the comparison difficult and may cloud the effect that each individual design feature has on pavement performance. In these cases, the effect of the combination of design features must be considered.

Pertinent performance data from projects varying the appropriate design feature are examined and presented in the following sections. The design features that are considered in this evaluation include the following:

- Slab thickness.
- Joint spacing.
- Joint orientation.
- Joint load transfer.
- Joint sealant.
- Base type.
- Drainage.
- Shoulder type.
- Widened lanes.
- Reinforcement.
- Pavement type.

To assist in evaluating the performance of the pavement sections, table 34 provides critical levels of deterioration—values at which the pavement is considered to be in need of some sort of rehabilitation—for each distress.

#### Slab Thickness

The effect of slab thickness on pavement performance has been of interest to engineers since pavements were first designed to carry loads. For any pavement

Table 34. Critical values for key performance indicators.

Performance Indicator	JPCP	JRCP
Joint Faulting	0.13 in	0.26 in
Transverse Cracking	10% slabs cracked	70 deteriorated (M-H) cracks/mi
Longitudinal Cracking	500 ft/mi (all levels)	500 ft/mi (all levels)
Joint Spalling	15-20% joints spalled, or 50 spalls/mi	20-30% joints spalled, or 25 spalls/mi
PSR	3.0-3.5	3.0-3.5
IRI	125-175 in/mi	125-175 in/mi

1 in = 25.4 mm; 1 ft = 0.305 m; 1 mi = 1.61 km

type, the interest in reducing thickness is driven by economics; that is, the thinner the pavement, the less expensive it is to construct. The interest in increasing thickness is a recognition of the positive effect that additional structure has on a pavement's load-carrying capability; the thicker the pavement, the more loads it should be able to carry and hence the longer it should last. Both theoretical and field studies that consider slab thickness as a variable are, quite simply, seeking to find the balance between economics and performance. However, if D-cracking or ASR are present, increasing slab thickness may not increase the pavement's service life.

In this project, most of the other features whose contribution to performance is studied are not directly considered in the design process. For example, joint spacing, load transfer, joint sealing, shoulder type, and base type, as well as others, are design features for which often no clear-cut, definitive design guidance exists, but for which guidance is needed. Slab thickness is different. Slab thickness is a direct output of most (if not all) pavement design procedures, including AASHTO, PCA, and many other methods. When slab thickness becomes a design variable, in effect one returns to an examination of the relationship between structure and load-carrying capability, such as was studied at the AASHO Road Test. Hopefully, one of two effects is observed: whether there is some additional, unexpected performance benefit from constructing slabs thicker than needed to carry loads (such as less faulting, cracking, or spalling), or whether thinner slabs can carry loads as well as thicker ones under some circumstances.

### Review of Project Data

Figure 5 shows the range in slab thickness for all of the concrete pavement sections studied in this project. The predominant slab thickness is 9 in (229 mm); the range in thicknesses is from 7 to 15 in (178 to 381 mm). The average slab thickness for all sections is 9.3 in (236 mm). The average for each pavement type follows:

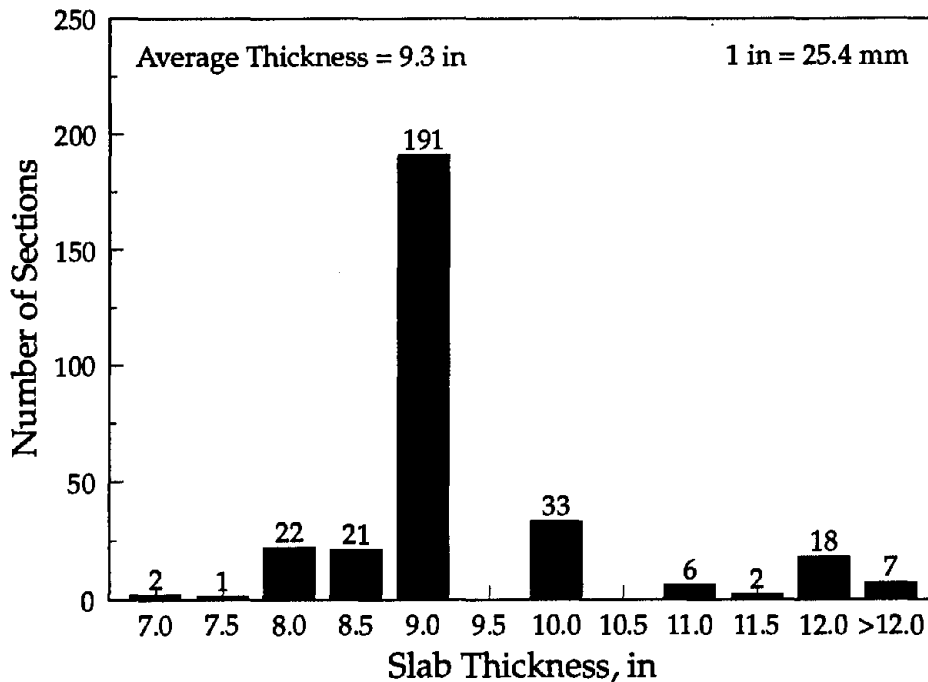


Figure 5. Distribution of slab thickness in sections.

- Average JPCP thickness = 9.5 in (241 mm).
- Average JRCP thickness = 9.0 in (229 mm).
- Average CRCP thickness = 8.6 in (218 mm).

Thus, the reinforcing steel is used to offset some slab thickness. The thickness is reduced by about 0.5 in (13 mm) from JPCP to JRCP and from JRCP to CRCP.

There are eight projects in this study in which slab thickness is varied, each of which is reviewed in this section (with the exception of NC 1, which includes too many confounding variables to make its inclusion useful). In the following review of those sections, an attempt is made to identify the performance differences among the slabs of different sizes to see if the contributions of thickness can be isolated.

#### *Minnesota 1*

This project, located on I-94 near Rothsay, was intended to study the effect of a number of design variables on the performance of reinforced concrete pavements. The variation in slab thickness at this site included sections that were constructed 8 and 9 in (203 and 229 mm) thick and reinforced with 0.09 and 0.08 percent reinforcing steel, respectively. Other variables on this project included three different base types (AGG, ATB, and CTB) and both doweled and nondoweled skewed transverse joints. The transverse joint spacing was 27 ft (8.2 m) for all sections. A plastic parting strip was used to form the centerline joints. The nondoweled sections on AGG and CTB (of both thicknesses) received a tied and doweled edge "beam" in 1984 to reduce the

widespread pumping that was taking place. On the same sections, the outer truck lane was also diamond ground. At the time of the 1992 survey, the outer lane of this project had carried an estimated 7.4 million ESAL's.

The performance of these sections is summarized in table 35. Sections are grouped so that the performance of those with similar base type and load transfer are summarized together. Looking first at the sections that did not have dowels, there does appear to be a benefit provided by the thicker slabs. With the ATB and CTB sections, the average faulting was significantly less on the thicker sections than on the thinner sections; the average faulting was the same on the AGG base sections. For all three base types, much more deteriorated transverse cracking occurred on the 8-in (203-mm) sections than on the 9-in (229-mm) sections. The spalling results are inconclusive: the same on the AGG base sections, slightly higher on the thicker slab on the CTB, and slightly lower on the thicker slab on the ATB. There was very little difference in average PSR or IRI from one thickness to the other.

Table 35. Summary of effect of slab thickness for MN 1.

		No Dowels		25 mm (1 in) Dowels	
		203 mm (8 in)	229 mm (9 in)	203 mm (8 in)	229 mm (9 in)
AGG		<u>1-3, 1-23*</u>	<u>1-1, 1-21*</u>	<u>1-4, 1-24</u>	<u>1-2, 1-22</u>
	Faulting, in	0.16	0.16	0.10	0.13
	Det. Tr. Crks/mi	61	0	85	34
	Long. Crks, ft/mi	285	0	191	0
	% Joints Spalled	42	42	43	55
	PSR	3.2	3.2	3.3	3.3
IRI, in/mi	143	153	123	161	
ATB		<u>1-5, 1-15**</u>	<u>1-7, 1-13**</u>	<u>1-6, 1-16</u>	<u>1-8, 1-14</u>
	Faulting, in	0.20	0.14	0.11	0.09
	Det. Tr. Crks/mi	89	41	29	90
	Long. Crks, ft/mi	3317	5081	3374	6077
	% Joints Spalled	88	79	94	96
	PSR	3.3	3.4	3.2	3.5
IRI, in/mi	169	151	167	137	
CTB		<u>1-11, 1-17*</u>	<u>1-9, 1-19*</u>	<u>1-12, 1-18</u>	<u>1-10, 1-20</u>
	Faulting, in	0.21	0.11	0.13	0.13
	Det. Tr. Crks/mi	8	4	45	29
	Long. Crks, ft/mi	2752	361	627	0
	% Joints Spalled	49	53	66	59
	PSR	3.3	3.5	3.3	3.3
IRI, in/mi	145	141	143	142	

1 in = 25 mm

1 ft = 0.305 m

1 mi = 1.6 km

Common Design Features:

JRCP with 27-ft joint spacing

Built in 1970

1992 ESAL's = 7.4 million

\* Sections received edge beams (tied and doweled) and diamond ground in 1984.

\*\* Section diamond ground in 1984, no edge beams added.



On the doweled sections, the results are different. The average transverse joint faulting is similar for both the thin and the thicker sections. In terms of average deteriorated transverse cracking, it is higher on the thicker sections with both the ATB bases and lower on the thicker sections with the CTB and AGG bases. Little difference in percent of spalled joints was noticed, with two base types showing slightly higher spalling on the thicker sections and one showing slightly lower spalling on the thicker sections. The average PSR values for both slab thicknesses are very similar and the trends with the average IRI do not reveal any advantage to constructing slabs of either thickness.

Although thicker slabs are intended to provide enhanced performance by contributing to reductions in deteriorated transverse cracking, transverse joint spalling, and perhaps lower faulting, this is not clearly supported by either the faulting or the joint spalling results at MN 1. However, the advantage of the slightly thicker slabs does appear to be borne out in the lower average number of deteriorated transverse cracks that is seen in all of the projects except for the doweled sections on the ATB. Again with the exception of those sections on the ATB, the thicker sections also have substantially lower amounts of longitudinal cracking than do the thinner sections. However, most cracking occurred shortly after construction, as the plastic parting strip at the centerline joint was ineffective at preventing random longitudinal cracking.

#### *Minnesota 2*

This project is located on I-90 near Albert Lea. The pavement was constructed in 1977 and had carried an estimated 4.2 million ESAL's in the outer lane through 1992. Overall, the project includes four sections in which slab thickness, shoulder type, and pavement type are primary variables. The inner lanes of MN 2-1 and 2-2, which are widened, are not doweled. Elsewhere, load transfer is provided by 1-in (25-mm) diameter dowel bars. Joint spacing is an indirect variable, as the sections with AC shoulders are also reinforced and have a 27-ft (8.2-m) transverse joint spacing. However, in this analysis, only sections with tied PCC shoulders (paved separately from the mainline pavement) and the 13-16-14-19-ft (4.0-4.9-4.3-5.8-m) joint spacing are considered.

The results of the 1992 performance evaluation are summarized in table 36. As shown, only a slight difference is observed between the performance of these two sections with the exception of the amount of longitudinal cracking, which is believed to be due to improper construction of the longitudinal joint and not to structural deficiencies. The overall performance of MN 2-1, the 9-in (229-mm) section, is slightly better than that of the thinner section, but not by an appreciable amount.

#### *Arizona 1*

The AZ 1 sections were constructed during a period from 1972 to 1981 on S.R. 360 (Superstition Freeway) in Phoenix. The sections are all JPCP with variable joint spacing (13-15-17-15 ft [4.0-4.6-5.2-4.6 m]) and no load transfer. They include 9-in

Table 36. Summary of effect of slab thickness for MN 2.

	MN 2-2	MN 2-1
	203 mm (8 in)	229 mm (9 in)
Faulting, in	0.08	0.08
Det. Tr. Crks/mi	5	0
Long. Crks, ft/mi	150	932
% Joints Spalled	21	7
PSR	3.9	4.0
IRI, in/mi	142	140

1 in = 25 mm  
 1 ft = 0.305 m  
 1 mi = 1.6 km

Common Design Features:

Doweled JPCP  
 13-16-14-19-ft joint spacing  
 Built in 1977  
 1992 ESAL's = 4.2 million

(229-mm) thick slabs on CTB and LCB, and 11 in and 13 in (279 and 325 mm) thick slabs on grade. One of the 9 in (229 mm) sections (AZ 1-1) has an AC shoulder, but the rest have PCC shoulders (paved separately from the mainline pavement. One of the 9-in (229-mm) sections also has edge drains. The longitudinal centerline joint contains 24-in (610-mm) long, No. 4 (13-mm) tie bars spaced 30 in (760 mm) apart.

The performance of these sections is summarized in table 37. The worst performing section is also the oldest one and the one that has carried the most traffic. It is also the only section that does not have tied PCC shoulders. If the performance of that section is not included in the comparison, it can be seen that the 9-in (229-mm) thick slabs on a stabilized base are performing as well as, if not better than, the thicker sections that do not have a base. This is the case when considering faulting, deteriorated transverse cracks, and transverse joint spalling. In comparing the performance of the two thicker slabs, there is not a large difference in distresses when going from 11 to 13 in (279 to 330 mm). The 9-in (229-mm) sections have carried, on average, about 12 percent fewer ESAL's than the thicker ones.

The performance of the AZ 1 sections suggests little difference between the thinner slabs on a stabilized base and the thicker slabs constructed directly on the subgrade. While this effect is certainly somewhat obscured by the different ages and cumulative ESAL's, this site includes three different designs that have each provided about the same level of performance. The relatively mild climate and low annual rainfall in Arizona may be one reason for the similarities in performance.

### California 1

The experimental sections of CA 1, constructed in 1971, are located on I-5 near Tracy. The sections are nondoweled JPCP and are constructed on two different base types (CTB and LCB). Two different slab thicknesses (8.4 and 11.4 in [213 and 290 mm]) and a conventional and a short transverse joint spacing pattern (12-13-19-18 ft

Table 37. Summary of effect of slab thickness for AZ 1.

	9 in (229 mm)			11 in (279 mm)	13 in (330 mm)	
	CTB	LCB			1-2	1-4
	1-1*	1-6	1-7†	1-5		
Faulting, in	0.08	0.01	0.02	0.03	0.01	0.02
Det. Tr. Crks/mi	0	0	0	0	69	0
Long. Crks, ft/mi	278	0	0	0	0	20
% Joints Spalled	24	3	8	18	12	3
PSR	3.9	3.5	3.6	3.9	4.2	3.8
IRI, in/mi	105	123	135	102	111	122
Age in 1992	20	11	11	13	17	13
ESAL's, millions	7.0	5.1	4.7	6.0	6.5	5.6

1 in = 25 mm  
 1 ft = 0.305 m  
 1 mi = 1.6 km

Common Design Features:

Nondoweled JPCP  
 13-15-17-15-ft joint spacing  
 \* Section has AC shoulder  
 † Section has edge drains

[3.7-4.0-5.8-5.5 m] and 5-8-11-7 ft [1.5-2.4-3-4-2.1 m]) are represented. The sections do not contain tie bars at the centerline joint and the joints are not sealed. Additional variations in pavement design at this project include two sections constructed with a higher strength concrete mix and three different CRCP designs.

The 1992 performance of these sections is summarized in table 38, after the sections had carried an estimated 11.9 million ESAL's. Because of performance differences between the sections located in the northbound and southbound lanes, the results are presented separately (the odd-numbered sections in this table are located in the northbound direction and the even-numbered sections are located in the southbound direction).

A direct comparison of the effect of slab thickness on performance is made by comparing CA 1-3 and 1-4 to CA 1-5 and 1-6; the other sections either have a different base type or joint spacing. In terms of faulting, percent spalled joints, and even PSR, there is very little difference in the performance of these sections of different thickness. The primary difference is in the amount transverse cracking, which is much higher on the thinner sections than it is on the thicker sections. The high rate of cracking was found to be predominantly located in the longer slabs (18 and 19 ft [5.5 and 5.8 m]), which are apparently too long for the stiff base on which they were placed. The lack of tie bars and joint sealant at the longitudinal centerline joint resulted in separation and faster deterioration.

Interestingly, the best performing sections at this site in terms of faulting are the 8.4 in (213 mm) sections on an LCB; these sections performed better than either the short-jointed design or the thicker slabs. However, this design is also subject to the same transverse cracking that plagues the other sections on this project.

Table 38. Summary of effect of slab thickness for CA 1.

		12-13-19-18-ft Joints (3.6-4.0-5.8-5.5-m)				5-8-11-7-ft Joints (1.5-2.4-3.4-2.1-m)	
		8.4 in (213 mm)		11.4 in (290 mm)		8.4 in (213 mm)	
CTB (4% cement)	Faulting, in	<u>1-3</u> 0.08	<u>1-4</u> 0.10	<u>1-5</u> 0.11	<u>1-6</u> 0.11	<u>1-1</u> 0.05	<u>1-2</u> 0.07
	% Slabs Cracked	18	53	0	34	1	8
	Long. Crks, ft/mi	812	0	65	0	0	507
	% Joints Spalled	1	3	3	1	1	1
	PSR	3.3	3.3	3.2	3.5	3.3	2.7
	IRI, in/mi	111	157	141	166	129	210
LCB (9.4% cement)	Faulting, in	<u>1-7</u> 0.02	<u>1-8</u> 0.04				
	% Slabs Cracked	24	60				
	Long. Crks, ft/mi	210	85				
	% Joints Spalled	9	6				
	PSR	3.1	3.5				
	IRI, in/mi	120	106				
CTB (4% cement)	Faulting, in	<u>1-9*</u> 0.11	<u>1-10*</u> 0.13				
	% Slabs Cracked	63	71				
	Long. Crks, ft/mi	551	70				
	% Joints Spalled	3	0				
	PSR	3.1	2.7				
	IRI, in/mi	130	210				

1 in = 25 mm

1 ft = 0.305 m

1 mi = 1.6 km

Common Design Features:

Nondoweled JPCP with 5.4-in base  
Built in 1971

1992 ESAL's = 11.9 million

\* Sections constructed using high strength concrete mix.

Generally, the thinner slabs appear to be about as effective as the thicker slabs in reducing faulting. The thicker slabs did show a much reduced incidence of transverse cracking, which suggests that if the design is prone to cracking (as was found with the longer slabs) the additional thickness can provide some resistance to reducing the occurrence of those cracks.

### Illinois 1

This project, constructed in 1986, is located on U.S. 50 near Carlyle. Of the 29 sections at this site, covering a wide variety of joint types, reinforcement types, drainage, and sealing, there are CRCP sections that are 7, 8, and 9 in (178, 203, and 229 mm) thick. These CRCP sections are all constructed on an LCB, have longitudinal underdrains, and contain a range in reinforcement from 0.70 to 0.73 percent.

The performance of these three CRCP sections is summarized in table 39. At the time of the 1992 survey, these sections had carried approximately 1.7 million ESAL's. There is essentially no difference in performance among these three sections after 6 years of exposure to traffic and environmental loadings. For a fixed amount of reinforcement (which these slight variations can be considered to be), for different slab thicknesses one would expect to see more failures per mile (1.6 km) and perhaps more deteriorated cracks per mile (1.6 km) in the thinner slabs than in the thicker slabs. Since neither of these have yet occurred, one cannot possibly draw any conclusions regarding the effect of slab thickness on performance.

Table 39. Summary of effect of slab thickness for CRCP sections for IL 1.

	7 in (178 mm), 0.70 % Steel	8 in (203 mm), 0.73% Steel	9 in (229 mm), 0.72% Steel
Avg. Crack Spacing, ft	$\frac{1-9}{3.5}$	$\frac{1-2}{3.0}$	$\frac{1-1}{3.4}$
Avg. Crack Width, in	—	—	—
Deteriorated Cracks/mi	—	—	—
Failures/mi	0	0	0
PSR	—	—	—
IRI, in/mi	123	114	103

1 in = 25 mm  
1 ft = 0.305 m  
1 mi = 1.6 km

Common Design Features:

CRCP with 4-in LCB  
Built in 1986  
1992 ESAL's = 1.7 million

### Ohio 2

The project on S.R. 2 near Vermilion, Ohio 2, includes over 100 sections in which the following design features are varied:

- Type and maximum size of coarse aggregate.
- Pavement drainage.
- Slab thickness.
- Joint spacing.
- Joint sealing .
- Base type.
- Pavement type.

These sections are each about 240 ft (73 m) long. All but four of the jointed sections are 9-in (229-mm) thick JRCP with 1.25-in (32-mm) diameter dowels. Those four exceptions consist of 15-in (381-mm) thick, nondoweled JPCP placed on grade. The transverse joints of these sections are skewed and spaced at 20-ft (6.1-m) intervals. When these sections were evaluated in 1992, they were 18 years old and had carried approximately 6.5 million ESAL's.

It is difficult to select the most appropriate sections to compare with these thicker slabs. The design that is most similar is probably the 9-in (229-mm) JRCP on an aggregate base with 20-ft (6.1-m) joint spacing (the same as the thick JPCP sections). These sections also contain aggregate from the same source. Therefore, the performance of the 15-in (381-mm) JPCP sections is compared to the thinner JRCP sections in table 40.

Table 40. Summary of effect of slab thickness for OH 2.

	15-in (381-mm) JPCP					9-in (229-mm) doweled JRCP, AGG Base				
	2-1*	2-2*	2-3	2-4	Avg	2-12	2-13	2-14	2-17	Avg
Faulting, in	0.07	0.08	0.14	0.30	0.15	n/a	0.13	0.03	0.24	0.13
Det. Tr. Crks/mi	0	0	11	0	3	0	102	22	317	110
Long. Crks, ft/mi	158	572	148	0	219	220	0	0	0	55
% Joints Spalled	0	52	96	0	37	100	79	100	0	70
PSR	n/a	n/a	n/a	n/a	n/a	n/a	n/a	n/a	n/a	n/a
IRI, in/mi	131	143	99	93	117	171	157	183	239	187

1 in = 25 mm  
 1 ft = 0.305 m  
 1 mi = 1.6 km

\* Sections contain tied PCC shoulders;  
 all other sections contain AC shoulders.

Common Design Features:

Nondoweled JPCP  
 20-ft joint spacing  
 Built in 1974  
 1992 ESAL's = 6.5 million

Keeping in mind that the thinner slabs are doweled, the faulting of the two different designs is similar, with the faulting of the JPCP sections slightly higher. Far fewer deteriorated transverse cracks were exhibited on the thicker sections, which may be attributable both to the increased slab thickness and the absence of dowel bars (the dowel bars may have corroded and locked up the transverse joints on the thinner sections). Transverse joint spalling on the thicker slabs is about half of what it is on the thinner slabs, but this may again be attributed to joint problems caused by the load transfer devices.

Overall, the thicker JPCP slabs on grade appear to be performing better than the thinner JRCP sections on an AGG base. The dowels have likely contributed to the better performance of the 9 in (229 mm) sections but the increased thickness probably contributed to the reduced number of deteriorated transverse cracks.

### Ontario 1

In 1982, the Ontario Ministry of Transportation constructed an experimental pavement on Highway 3N, near Windsor. Four different designs were constructed that incorporated variations in the following features:

- Base type
- Slab thickness
- Shoulder type
- Surface texture

The basic design consisted of nondoweled JPCP with random, skewed transverse joints at 12-13-19-18-ft (3.7-4.0-5.8-5.5-m) intervals. Two sections have an AC shoulder and two have a PCC shoulder. The sections consist of a 12-in (305-mm) thick slab placed on grade, a 7- and 8-in (178-and 203-mm) thick slab on an LCB, and an 8-in (203-mm) thick slab on a PATB (no separator layer beneath base and edge drains placed in dense-graded shoulder base). The performance of these sections in 1992, after 2.1 million ESAL's, is summarized in table 41.

Table 41. Summary of effect of slab thickness for ONT 1.

Shoulder Type	AC		PCC	
	12 in (305 mm)	8 in (203 mm)	8 in (203 mm)	7 in (178 mm)
Base Type	None	PATB	LCB	LCB
	<u>1-1</u>	<u>1-2</u>	<u>1-3</u>	<u>1-4</u>
Faulting, in	0.11	0.10	0.14	0.13
Det. Tr. Crks/mi	0	0	28	48
Long. Crks, ft/mi	40	105	621	516
% Joints Spalled	0	1	0	0
PSR	3.9	3.9	3.9	3.9
IRI, in/mi	146	135	147	164

1 in = 25 mm  
 1 ft = 0.305 m  
 1 mi = 1.6 km

Common Design Features:

Nondoweled JPCP  
 13-19-18-12-ft joints  
 Built in 1982  
 1992 ESAL's = 2.1 million

From the standpoint of rideability, there is very little difference in performance from one section to the next. They have identical PSR values and the IRI values are also similar. The predominant pavement distress on these sections is longitudinal cracking, which is usually not related to structural deficiencies. The thicker slab has the lowest amount of longitudinal cracking, however.

The faulting levels of these four sections are approximately the same as well, with the lowest faulting provided by the 8-in (203-mm) section on the permeable layer. However, the thicker slab on grade is faulting about the same amount. Neither the 12-in (305-mm) section nor the 8-in (203-mm) section on the PATB show any deteriorated transverse cracks; the two sections on an LCB, which are 8 and 7 in (203 and 178 mm) thick, both exhibit some deteriorated transverse cracks.

The different sections in this project illustrate the fact that similar performance can be arrived at by a variety of approaches. The thin sections on the stiff base (sections 1-3 and 1-4) did not perform as well as the other two sections, despite employing a tied PCC shoulder. While it is not believed that the transverse or longitudinal cracking that did occur are due to load, it seems safe to conclude that the thicker slab can help to minimize the deleterious effects of any cracking that might occur. The comparable performance of the 8-in (203-mm) slab on a permeable base and the 12-in (305-mm) slab on grade suggests the importance of drainage to performance and the possible trade-offs that can be made between slab thickness and drainage. However, the performance would likely be better if a separator layer had been used or if the permeable base material had been extended to the edge drains.

### Related Research

Very little research has been carried out to specifically study the effect of slab thickness on performance. While studies that date back to at least the 1920's have considered certain aspects of the relationship between slab thickness and pavement performance (such as the performance of trapezoidal sections, stresses in pavements, and stresses in pavements of different thicknesses subjected to loads), there do not appear to be any studies in which thicker (or thinner) than necessary pavements have been constructed to study how they perform. Perhaps the single most important exception to this is the work done at the AASHO Road Test. On the concrete pavement sections at the AASHO Road Test, slab thickness was varied from 2.5 to 12.5 in (63 to 317 mm). These sections were placed either on daylighted granular bases of varying thickness or directly on the subgrade.

One of the results of this study is the development of a model that relates slab thickness to ESAL's, based on the change in serviceability due to load. In the current version of the AASHTO design model, this same basic relationship between slab thickness and projected ESAL loadings is still used. However, in the AASHTO rigid pavement structural design model, the design slab thickness can be adjusted by altering a number of variables, of which perhaps the most significant is the reliability factor. For any design, holding all other inputs constant and increasing the reliability factor will result in a thicker slab. In effect, what this does is take for granted a result that was sought in these experimental sections: that a slab constructed thicker than needed to carry the design traffic will perform better. Test sections in which this was done are essentially designed with a higher reliability factor. If they have not performed better, it suggests that there are factors other than slab thickness that can have a controlling factor on pavement performance.

### Overall Evaluation

The conventional wisdom is that increasing slab thickness improves pavement performance. This is bolstered by the pavement design procedures in use today, in which variables such as traffic, climatic inputs, and material properties are an input to obtain slab thickness as an output. If additional thickness is then added to a design developed by such a procedure while all other inputs are held constant, it is only



logical that performance should be improved. Such improved performance would be seen in an increase in the loads that the pavement could carry. This philosophy has been borne out by numerous theoretical analyses which show that slab stresses are reduced through the use of thicker slabs and tied shoulders or widened lanes, and reduced stresses logically contribute to better performance. One of the objectives of the earliest research into concrete pavement designs was to identify those factors that contributed to load carrying capacity, and slab thickness has almost always emerged as a primary contributing factor.

At most sites in this project, the ability of thicker pavements to carry additional loads was not directly studied. Some studies looked at the ability of an extra inch (25 mm) or more to contribute to reductions in faulting and pumping. Others approached the use of thicker slabs as a construction expediency, considering it more cost-effective to construct a 13-in (330-mm) slab than a 9-in (229-mm) slab on a 4-in (102-mm) cement-treated base. Still others looked at the trade-off between thicker slabs and AC shoulders and thinner slabs with tied PCC shoulders. Most of these comparisons confound variables, such as when a thin, reinforced slab is compared with a thicker, plain slab.

With that said, there does not appear to be a significant advantage in terms of faulting to constructing thicker slabs among the sections that were studied. For the most part, average faulting is similar and overall ride is also very comparable for both thin and thick sections. A similar trend is shown in figure 6, which illustrates the relationship between slab thickness and average transverse joint faulting (divided by ESAL's to account for traffic) for all of the sections studied under this project. When the effect of traffic is introduced, a better trend between slab thickness and faulting is observed, particularly for the nondoweled sections.

There does seem to be an observable difference between the performance of the thinner and thicker slabs at some of the sites, especially in regards to cracking. At MN 1, AZ 1, CA 1, and OH 2, fewer deteriorated transverse cracks are present on the thicker sections than on the thinner sections. The conditions that contribute to the develop of such cracking are believed to be present for both sets of pavements, but the thicker slabs are better able to resist the deterioration. At ONT 1, the results of the difference in slab thickness cannot be separated from other confounding variables, whereas at MN 2 there does not appear to be any difference in performance between the 8- and 9-in (203- and 229-mm) slabs.

The CRCP pavements of different thicknesses at IL 1 have not yet started to deteriorate and no differences are observed at that site either. At several of the sites where longitudinal cracking is a problem, the positive contribution of the thicker slabs to reducing the amount of cracking is also noted, although this effect is not observed at all such sites. At MN 1, the increased longitudinal cracking is not believed to be due entirely to the thinner pavement sections, as the plastic parting strips used at the longitudinal centerline joints were ineffective.

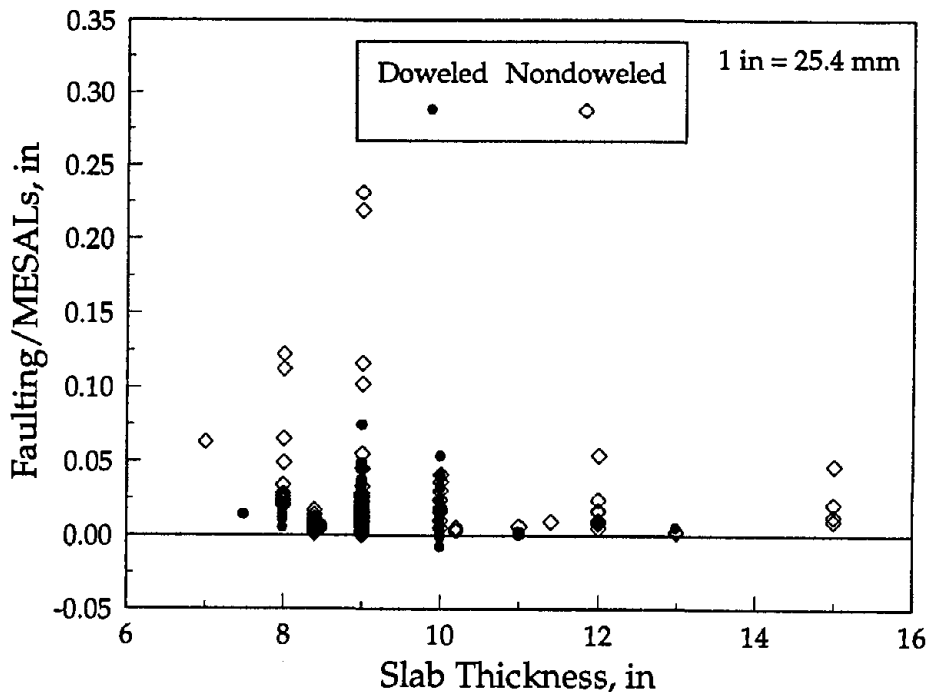


Figure 6. Average transverse joint faulting versus slab thickness for all sections.

Figure 7 shows this same relationship between deteriorated transverse cracking and slab thickness for all sections in the study, separated by base type. This figure illustrates that the sections constructed on a stiff bases, such as CTB and LCB, show more transverse cracking, on average, than other base types. Some sections constructed on an aggregate base are also showing high cracking levels. Very little cracking is observed on the sections with a permeable base, although they are not as old as many of the other sections. A similar plot for JRCP did not show any significant trends, mainly because the JRCP sections have a small range in slab thickness from 8 to 10 in (203 to 254 mm).

One distress, pumping, is not directly addressed in the summary tables (although it is indirectly considered in the faulting measurement). Pumping did not seem to be significantly influenced by slab thickness. Consider, for example, OH 2, where the thick sections with AC shoulders that were constructed on grade pumped more than most thin sections with an aggregate base. The addition of a tied PCC shoulder, however, prevented the occurrence of pumping on the OH 2 sections with otherwise similar designs. All sections pumped at CA 1, regardless of their thickness, and only one 9-in (229-mm) section pumped at AZ 1. The pumping observations at MN 1 are evenly divided between the thinner and thicker sections, and no pumping is evident at MN 2 and ONT 1.

At some of these projects, FWD deflection data were collected for some of the sections. Table 42 summarizes slab edge, center, and corner deflection data (these data are reported in full in appendix A of volume IV; sections for which no deflection data are reported were not tested). As is discussed earlier, a reported benefit of

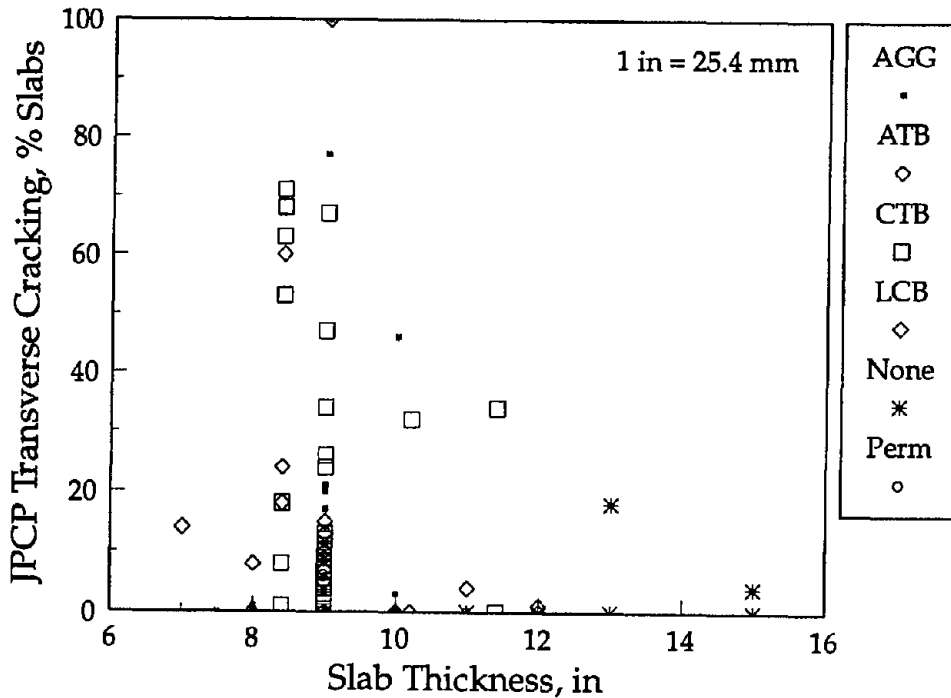


Figure 7. Effect of slab thickness on transverse cracking.

thicker slabs is a reduction in stresses due to loads, all other factors held constant. Factors in particular that would affect these results include different support conditions and load transfer, both of which were varied in some cases as slab thickness was varied. What one expects to find is lower deflections on the thicker sections, and for the most part this is true, especially when there are large differences in slab thickness, as is seen in AZ 1, CA 1, and OH 2.

The relationship between loaded slab corner deflections and slab thickness for all sections is shown in figure 8 and appears to support this relationship as well. The thicker slabs uniformly have lower corner deflections whereas the data for the thinner slabs are inconclusive. The effect of slab thickness is more apparent on the nondoweled sections. These results suggest that there continues to be strong mechanistic-based reasons for building thicker slabs, but that the performance benefits of the additional thickness is not always documented.

For the slab thickness comparisons, the difference in slab thickness was greater than 1 in (25 mm) in only four of the seven sections. These include the sections studied at AZ 1, CA 1, OH 2, and ONT 1. At three of these sites a benefit of the thicker slabs was observed, while at the fourth the effect was confounded. This result suggests that the benefits of adding only an inch of thickness may be obscured by many other effects, such as the inherent variability in performance, variations in thickness typically observed in field construction, or other chance variations (e.g., applied loads, support conditions, and material and construction quality).

Table 42. Summary of selected 1992 deflection data.

Section	Slab Thick, in	Deflections, mils								
		Slab Edge			Slab Center			Slab Corner		Temp, °F
		High	Low	Ave	High	Low	Avg	Loaded	Unloaded	
AZ 1-1	9.0	8.5	5.5	7.1	3.7	2.8	3.3	6.4	5.9	86
AZ 1-2	13.0	3.4	2.3	3.0	2.8	1.5	2.2	3.4	3.1	86
AZ 1-4	13.0	5.5	1.8	3.1	2.5	1.7	1.9	2.6	2.4	81
AZ 1-5	11.0	7.3	4.4	5.8	3.9	2.4	2.8	5.9	5.5	86
AZ 1-6	9.0	4.5	4.5	4.5	3.9	1.6	2.7	2.8	2.6	80
AZ 1-7	9.0	5.4	2.2	3.7	6.0	2.0	3.1	6.0	5.7	84
CA 1-1	8.4	—	—	—	9.8	4.8	7.3	33.3	7.1	—
CA 1-2	8.4	10.0	5.8	7.8	6.4	4.5	5.2	19.1	7.3	81
CA 1-3	8.4	—	—	—	8.2	3.3	4.4	35.5	6.3	—
CA 1-4	8.4	11.4	6.8	8.9	6.7	3.2	4.6	21.4	13.2	77
CA 1-5	11.4	—	—	—	3.1	2.1	2.6	5.7	4.3	—
CA 1-6	11.4	4.9	3.5	4.1	3.0	2.2	2.4	5.3	3.0	84
CA 1-7	8.4	—	—	—	4.6	3.4	3.9	6.7	4.2	—
CA 1-9	8.4	—	—	—	6.0	3.8	5.1	19.6	3.5	—
CA 1-10	8.4	7.8	5.5	6.5	5.2	4.4	4.7	10.4	5.8	84
OH 2-1	15.0	3.7	3.2	3.5	2.1	1.7	1.9	6.9	1.9	85
OH 2-2	15.0	4.3	3.4	4.0	2.0	1.6	1.8	8.5	2.0	83
OH 2-3	15.0	4.2	3.4	3.8	2.2	2.0	2.0	8.3	2.1	85
OH 2-4	15.0	4.0	3.0	3.4	2.2	1.8	2.0	8.1	2.0	84
OH 2-12	9.0	21.8	9.3	12.7	12.4	4.2	7.2	—	—	79
OH 2-13	9.0	9.7	4.7	6.6	8.0	4.5	6.1	12.3	5.1	78
OH 2-14	9.0	17.8	8.7	12.4	12.3	6.4	9.2	16.8	9.8	77
OH 2-17	9.0	7.6	7.0	7.4	9.5	5.7	7.4	19.2	6.3	78
ONT 1-1	12.0	—	—	—	4.0	2.6	3.0	—	—	—
ONT 1-2	8.0	12.1	4.9	7.9	7.2	4.4	5.3	16.0	3.1	79
ONT 1-3	8.0	—	—	—	5.0	3.8	4.7	—	—	—
ONT 1-4	7.0	5.0	5.0	5.0	5.8	3.4	4.5	6.3	5.9	84

1 in = 25 mm

MN 1 and NC 1 only have data for 9-in (229-mm) sections.

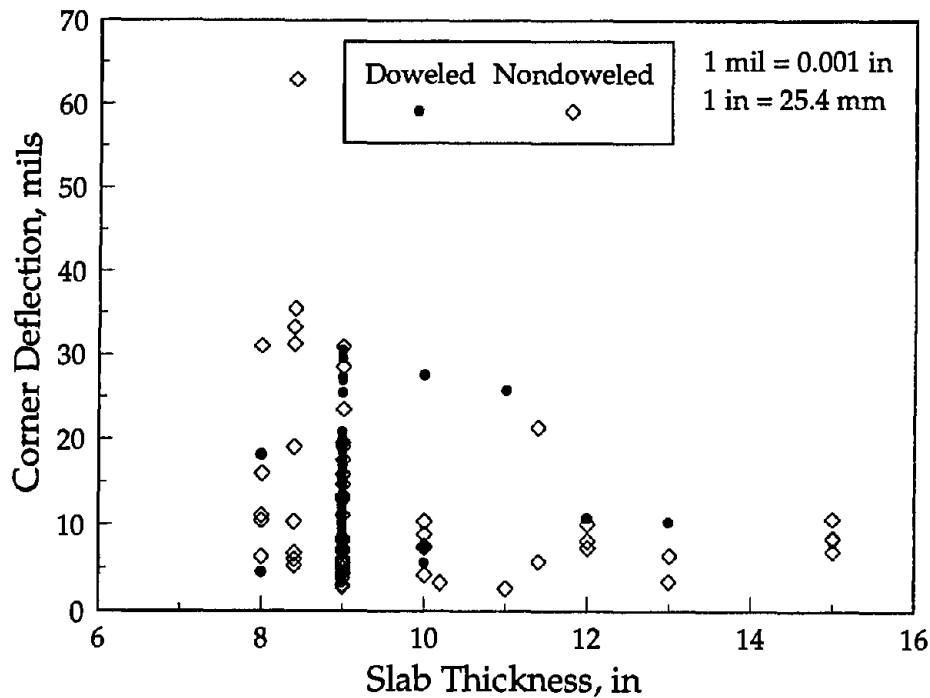


Figure 8. Loaded slab corner deflection by slab thickness for all sections.

### Joint Spacing

Joint spacing has long been a controversial issue in the design of jointed concrete pavements. While it is generally recognized that joint spacing can have a large effect on performance, little guidance is available for the selection of the most effective joint spacing for a particular design. A common "rule of thumb" is that the slab length in feet should not exceed 2 times the slab thickness in inches. For example, the slab length on a pavement with a slab thickness of 8 in (200 mm) should not exceed 16 ft (4.9 m). Others recommended that the slab length in feet not exceed 1.75 times the slab thickness.<sup>(38)</sup> NCHRP Synthesis 211 provides additional guidance for designing joints.<sup>(39)</sup>

Joint spacing requirements are different for JPCP and JRCP. In the design of JPCP, transverse joints are spaced at closer intervals so as to prevent the development of uncontrolled transverse cracks; typically, the joints in JPCP are spaced at intervals between 15 and 20 ft (4.6 and 6.1 m). Shorter joint spacing may be required for JPCP constructed on stabilized bases because of greater thermal curling stresses, although greater moisture stresses may allow longer joint spacings. On JRCP, the joints may be spaced farther apart since the pavement contains reinforcing steel intended to hold tight any transverse cracks that may occur. Joint spacing on JRCP is typically in the range of 20 to 50 ft (6.1 to 15.2 m). Current recommendations are that slab lengths should not exceed 15 ft (4.5 m) for JPCP and should not exceed 30 ft (9 m) for JRCP.<sup>(2)</sup>

Within a given project, transverse joints may be installed in a random pattern. This pattern is a series of three or four joints placed at varying intervals that are

repeated in a regular pattern. For example, a random joint spacing of 12-13-19-18 ft (3.6-4.0-5.8-5.5 m) indicates that joints are spaced at 12-, 13-, 19-, and 18-ft (3.6-, 4.0-, 5.8-, and 5.5-m) intervals and that pattern is repeated throughout the project. Where applicable, random joint spacings are also evaluated in this section.

Review of Project Data

Figures 9 and 10 illustrate the range of joint spacings for JPCP and JRCP, respectively (for sections with a random joint spacing, the average spacing of the pattern is used). The average joint spacing is 16.7 ft (5.1 m) for JPCP and 42.2 ft (12.9 m) for JRCP, although a range of joint spacings is available for each pavement type. This section reviews the performance data from the applicable projects that incorporate varying joint spacings and allow meaningful comparisons. However, no comparisons on the effect of joint spacing are conducted across pavement type. A more detailed evaluation of the performance of different pavement types is provided later in this chapter.

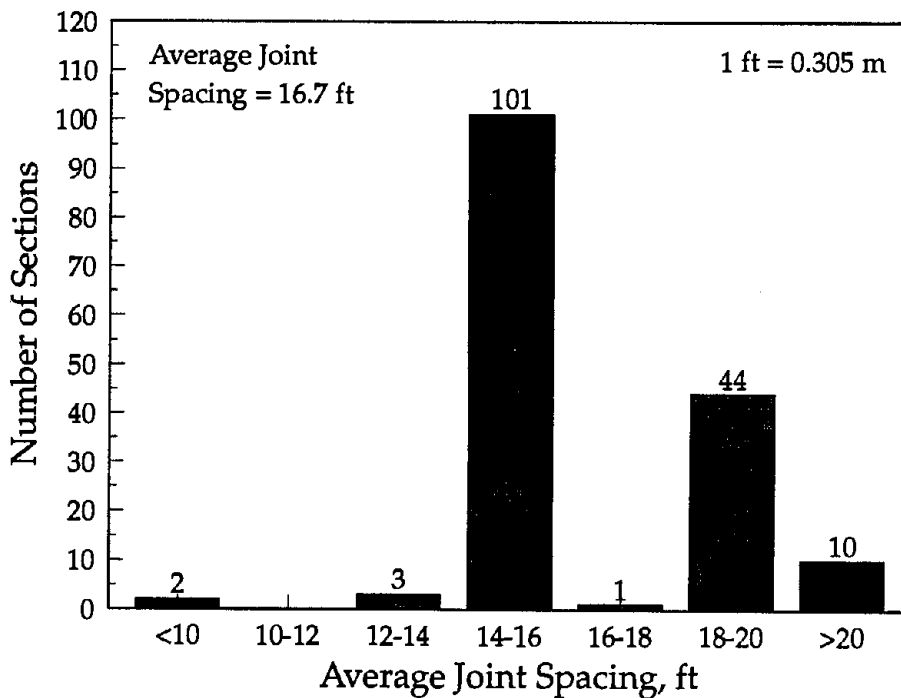


Figure 9. Distribution of joint spacings for JPCP.

*California 1*

The California 1 project, located on I-5 near Tracy, includes two similar JPCP designs in which joint spacing is varied. The conventional design, represented by sections CA 1-3 and CA 1-4, contains a random joint spacing of 12-13-19-18 ft (3.6-4.0-5.8-5.5 m). An experimental design, represented by sections CA 1-1 and CA 1-2, has a random joint spacing of 5-8-11-7 ft (1.5-2.4-3.4-2.1 m).

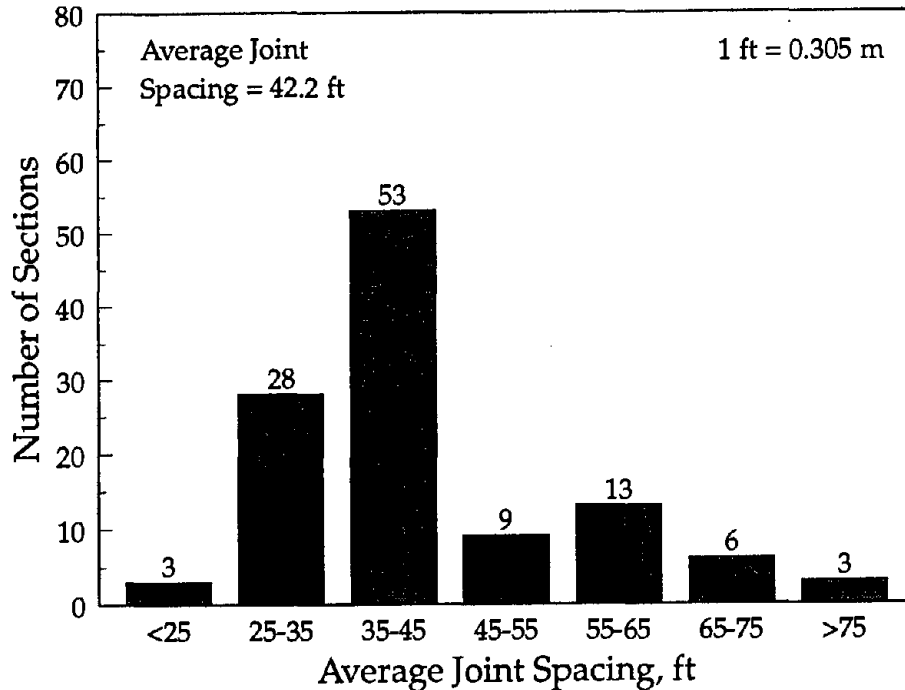


Figure 10. Distribution of joint spacings for JRCP.

The performance data for these sections are summarized in table 43. This table shows that the shorter joint spacing had a definite effect on reducing the amount of transverse cracking. The sections with shorter joint spacing had very little transverse cracking (1 and 8 percent), whereas the sections with longer joint spacing had significant slab cracking (18 and 53 percent). However, there are directional effects also, as the amount of cracking is greater in the southbound direction than in the northbound direction; this could be due to differences in traffic loading or to differences in construction or curing conditions.

The transverse joint faulting is slightly lower for the sections with short joint spacing, although the difference is not significant. Very little transverse joint spalling was evident on the designs, with the percentage of joints exhibiting joint spalling virtually the same for each section.

Although the sections with shorter joint spacing have less cracking and faulting, they are considerably rougher than the sections with longer joint spacing. One explanation is the greater number of joints in the shorter joint spacing design, which adversely affects the rideability. For example, the 8-11-7-5-ft (1.5-2.4-3.4-2.1-m) design (average joint spacing of 7.75 ft [2.4 m]) has 681 joints per mile (1.6 km), whereas the 12-13-19-18-ft (3.6-4.0-5.8-5.5-m) design (average joint spacing of 15.5 ft [4.7 m]) has 340 joints per mile (1.6 km). Assuming an average faulting of 0.05 in (1.3 mm) for the short joint spacing design and an average faulting of 0.08 in (2.0 mm) for the long joint spacing design, the cumulative faulting is 34.0 in/mi (536.6 mm/km) for the short joint spacing design (681 joints times 0.05 in [1.3 mm]) and 27.2 in/mi (429.3

Table 43. Summary of effect of joint spacing for CA 1.

Section ID	Year Built	ESAL's, millions		Joint Faulting, in		% Slabs Cracked		% Joints Spalled		IRI, in/mi (PSR)	
		1987	1992	1987	1992	1987	1992	1987	1992	1987	1992
CA 1-1 (NB) 8-11-7-5 ft Jts	1971	7.6	11.9	0.06	0.05	1	1	2	1	- (2.9)	129 (3.3)
CA 1-2 (SB) 8-11-7-5 ft Jts	1971	7.6	11.9	-	0.07	-	8	-	1	- (2.7)	210 (2.7)
CA 1-3 (NB) 12-13-19-18 ft Jts	1971	7.6	11.9	0.10	0.08	9	18	3	1	- (3.0)	111 (3.3)
CA 1-4 (SB) 12-13-19-18 ft Jts	1971	7.6	11.9	-	0.10	-	53	-	3	- (3.3)	157 (3.3)

1 in = 25.4 mm  
 1 ft = 0.305 m  
 1 mi = 1.61 km

Common Design Features: 8.4 in JPCP  
 5.4 in CTB on 24-in AGG  
 No Dowels

mm/km) for the long joint spacing design (340 joints times 0.08 in [2.0 mm]). Thus, even though the faulting on the short joint spacing design is less, the greater number of joints in the design has an adverse affect on the overall rideability.

Although longitudinal cracking was present on both designs, its occurrence on the long-jointed design is attributed to longitudinal joint forming techniques. However, on the short-jointed design, longitudinal cracking developed in the center of the outer traffic lane and primarily on the very short (5- and 7-ft [1.5- and 2.1-m] slabs. This distress is similar to what is often observed on short full-depth repairs that have been placed on distressed PCC pavements and is believed to be due to the short slab behaving more like a beam than like a slab.

It is also interesting to consider the effect of the actual slab lengths of the random joint spacing pattern on pavement performance. Table 44 provides a breakdown of slab cracking by each slab length in the random joint spacing pattern of each design. This table shows that the majority of cracking in each section occurs in the longer slab lengths of the random joint spacing pattern. It also indicates that there is a distinct difference in the performance of the northbound and southbound sections.

### Illinois 1

This project, located on U.S. 50 near Carlyle, includes JRPC designs in which joint spacing is varied. Section IL 1-16 represents the conventional design, which has doweled contraction joints spaced at 40-ft (12.2-m) intervals and contains 0.13 percent longitudinal steel in the form of wire mesh reinforcement. Three experimental sections, designated as IL 1-13, IL 1-14, and IL 1-15, maintain the same 40-ft (12.2-m)



Table 44. Summary of effect of actual slab lengths on cracking for CA 1.

Section ID	% Slabs Cracked By Slab Length							
	5 ft	7 ft	8 ft	11 ft	12 ft	13 ft	18 ft	19 ft
CA 1-1 (NB) 8-11-7-5-ft Jts	0	0	0	1	-	-	-	-
CA 1-2 (SB) 8-11-7-5-ft Jts	0	1	2	5	-	-	-	-
CA 1-3 (NB) 12-13-19-18-ft Jts	-	-	-	-	0	2	2	0
CA 1-4 (SB) 12-13-19-18-ft Jts	-	-	-	-	7	6	21	19

1 in = 25.4 mm  
1 ft = 0.305 m

Common Design Features: 8.4 in nondoweled JPCP  
1992 ESAL's = 11.9 million

doweled contraction joint spacing, but also contain *hinge* joints placed between the contraction joints. These hinge joints are weakened plane joints that are sawed over No. 6 (19-mm) deformed tie bars placed at either mid- or third-points in the slab. For example, sections IL 1-13 and IL 1-14 contain a hinge joint at the mid-panel of the slab, or 20 ft (6.1 m) away from the contraction joints. Section IL 1-15 contains two hinge joints at the third points in the slab, or at distance of 13.3 ft (4.1 m) away from each contraction joint. The purpose of the hinge joint design is to control the development of cracks in reinforced concrete pavements by sawing a weakened plane joint at critical locations in the slab; reinforcing steel is then concentrated at the hinge joints so that the joint is held tight and not allowed to deteriorate.

Table 45 summarizes the performance data for these sections. The sections with the hinge joint design are exhibiting far less deteriorated cracking than the conventional 40-ft (12.2-m) design. This is the result of both shorter effective joint spacing on the hinge joint design (which thereby relieves warping and curling stresses) and also the greater concentration of steel at those hinge joint locations. However, the conventional design was smoother riding than the hinge joint design, perhaps because of the fewer number of joints in the section.

### Illinois 2

This project is located on U.S. 20 near Freeport and contains designs similar to those on Illinois 1. The conventional section, IL 2-8, contains doweled contraction joints spaced at 40-ft (12.2-m) intervals and 0.11 percent longitudinal steel. Two of the three experimental sections (IL 2-5 and IL 2-6) contain a hinge joint at the mid-panel of the slab, or 20 ft (6.1 m) away from the contraction joints. The third experimental section, section IL 2-7, contains two hinge joints at the third points in the slab, or at distance of 13.3 ft (4.1 m) away from each contraction joint.

Table 45. Summary of effect of joint spacing for IL 1.

Section ID	Year Built	ESAL's, millions	Joint Faulting, in	Det. Cracks/mi	% Joints Spalled	IRI, in/mi
IL 1-13 20 ft Hinge Jts 0.29% Steel	1986	1.7	0.01	0	4	153
IL 1-14 20-ft Hinge Jts 0.29% Steel	1986	1.7	0.01	20	10	173
IL 1-15 13.3-ft Hinge Jts 0.29% Steel	1986	1.7	0.01	0	3	168
IL 1-16 No Hinge Jts 0.13% Steel	1986	1.7	0.01	100	8	119

1 in = 25.4 mm  
1 ft = 0.305 m  
1 mi = 1.61 km

Common Design Features: 8.5-in JRCF with 4-in LCB  
40-ft contraction joints  
1.5-in dowels

The performance data for these sections are summarized in table 46. While all of these sections are in excellent condition, the conventional section, with longer joint spacing and less steel reinforcing, exhibits a significant amount of deteriorated transverse cracking whereas the hinge joint sections show no such cracking. Faulting or spalling has not reached objectionable levels on any of the sections, although section IL 2-6 displays more spalling and IL 2-7 slightly more faulting than the other sections. The roughness of the sections are all very similar, with section IL 2-7 (which had the greatest faulting) providing the smoothest ride.

#### *Minnesota 1/Minnesota 5*

Minnesota 1, located on I-94 near Rothsay, is an experimental project that looks at the effect of different slab thicknesses, base types, and load transfer design on JRCF performance. While the joint spacing for all MN 1 sections is 27 ft (8.2 m), an adjacent project (MN 5) constructed at about the same time contains joints placed at 39-ft (11.9-m) intervals, thereby allowing an evaluation of the effect of joint spacing on JRCF performance.

The performance of the comparable MN 1/MN 5 sections is summarized in table 47. This table shows that while significant faulting has developed on all sections (probably because of the small dowel diameter), the sections with shorter joint spacing exhibit less deteriorated cracking and less spalling than the section with the longer joint spacing. The section with longer joint spacing has about twice as many deteriorated cracks and is exhibiting severe spalling at nearly every transverse joint.

Table 46. Summary of effect of joint spacing for IL 2.

Section ID	Year Built	ESAL's, millions		Joint Faulting, in		Det. Cracks/mi		% Joints Spalled		IRI, in/mi	
IL 2-5 20-ft Hinge Jts 0.25% Steel	1986	1.3		0.01		0		2		121	
IL 2-6 20-ft Hinge Jts 0.25% Steel	1986	1.3		0.02		0		12		127	
IL 2-7 13.3-ft Hinge Jts 0.25% Steel	1986	1.3		0.03		0		3		96	
IL 2-8 No Hinge Jts 0.11% Steel	1986	1.3		-0.01		42		8		131	

1 in = 25.4 mm  
1 ft = 0.305 m  
1 mi = 1.61 km

Common Design Features: 10-in JRCP with 4-in LCB  
40-ft contraction joints  
1.5-in dowels

Table 47. Summary of effect of joint spacing for MN 1/MN 5.

Section ID	Year Built	ESAL's, millions		Joint Faulting, in		Det. Cracks/mi		% Joints Spalled		IRI, in/mi (PSR)	
		1987	1992	1987	1992	1987	1992	1987	1992	1987	1992
		MN 1-2 27 ft Jts 0.08% Steel	1970	5.5	7.4	0.10	0.15	23	45	14	61
MN 1-22 27 ft Jts 0.08% Steel	1970	5.5	7.4	—	0.12	—	23	—	50	—	143 (3.2)
MN 5 39 ft Jts 0.04% Steel	1969	5.5	7.4	0.09	0.13	53	79	36	95	— (3.3)	139 (3.5)

1 in = 25.4 mm  
1 ft = 0.305 m  
1 mi = 1.61 km

Common Design Features: 9-in JRCP  
6-in AGG base  
1-in dowels

The reason for this difference in performance is believed to be due to the greater movement that occurs in the section with longer slab lengths; that is, the section with longer joint spacing will exhibit more slab movement (joint/crack opening and closing) as the slab responds to a changes in temperature. These greater movements

serve to open transverse joints wider, thereby allowing more incompressibles to infiltrate the joint system. The combination of larger slab movements and a greater number of incompressibles that collect in the joint result in more joint spalling.

In addition to the opening of joints, the greater slab movements are partially accommodated by the opening of mid-panel cracks. Although the steel in JRCP is intended to hold tight those mid-panel cracks that develop, when the steel is inadequate for the amount of movement encountered (as appears to be the case here, as the reinforcement for MN 5 is only 0.04 percent), the steel may rupture and be unable to hold the crack tightly together. With the steel reinforcement ruptured, the cracks become working and rapidly break down under traffic loading.

From a rideability standpoint, there does not appear to be much difference in performance between these sections. In fact, the roughest section is one with 27-ft (8.2-m) joints.

### *Minnesota 7*

Minnesota 7 is an experimental project constructed on Trunk Highway 36 in Roseville. Constructed in 1958, it contains two JPCP designs with different joint spacings: one design with 15-ft (4.6-m) joints and one with 20-ft (6.1-m) joints. Both doweled and nondoweled designs are represented within each joint spacing design.

The performance data for these sections are summarized in table 48. Within each load transfer category, this table shows that the 15- and 20-ft (4.6- and 6.1-m) sections are performing in a similar fashion. For example, for the nondoweled sections, the average faulting of the sections with 15-ft (4.6-m) joint spacing is about the same as that of the sections with 20-ft (6.1-m) joint spacing. In addition, the joint spalling of the nondoweled sections is not significantly different. However, although the amount is not considered significant, one 20-ft (6.1-m) nondoweled section exhibits some slab cracking, whereas none of the 15-ft (4.6-m) nondoweled sections do. The absence of cracking on the longer section may partly be explained by the low traffic loadings that the pavement has sustained over its 34-year life.

The doweled sections exhibit trends similar to the nondoweled sections. Again, there is little difference in performance between the 15- and 20-ft (4.6- and 6.1-m) sections. As with the nondoweled designs, one 20-ft (6.1-m) section is observed to exhibit a small amount of cracking, but it is not a significant amount. An examination of the rideability of the pavement sections does not indicate any significant differences in the performance of the sections with different joint spacings.

Although not included in this study, this project also includes JRCP sections with 33- and 65-ft (10- and 20-m) joint spacings. A study conducted by the Minnesota Department of Transportation revealed that the sections with the shorter joint spacings (15 and 20 ft [4.6 and 6.1 m]) are performing much better than the sections with longer joint spacings.<sup>(24)</sup> However, no appreciable difference in performance was noticed between the sections with 15- and 20-ft (4.6- and 6.1-m) joint spacings.

Table 48. Summary of effect of joint spacing for MN 7.

Section ID	Year Built	ESAL's, millions	Joint Faulting, in	% Slabs Cracked	% Joints Spalled	IRI, in/mi (PSR)
MN 7-10 15-ft Jts No Dowels	1958	6.9	0.07	0	50	162 (3.3)
MN 7-18 15-ft Jts No Dowels	1958	6.9	0.16	0	31	158 (3.5)
MN 7-9 20-ft Jts No Dowels	1958	6.9	0.07	6	39	169 (3.4)
MN 7-17 20-ft Jts No Dowels	1958	6.9	0.15	0	31	194 (2.9)
MN 7-15 15-ft Jts 1-in Dowels	1958	6.9	0.01	0	59	193 (3.1)
MN 7-23 15-ft Jts 1-in Dowels	1958	6.9	0.01	0	31	183 (3.3)
MN 7-16 20-ft Jts 1-in Dowels	1958	6.9	0.01	0	75	201 (3.0)
MN 7-24 20-ft Jts 1-in Dowels	1958	6.9	0.01	6	39	179 (3.2)

1 in = 25.4 mm  
 1 ft = 0.305 m  
 1 mi = 1.61 km

Common Design Features: 9-in JRPC  
 18-in AGG base

*New York 2*

This project is located on I-88 near Otego and contains two JPCP pavements with different joint spacings. Sections NY 2-3 and NY 2-9 are 9-in (229-mm) JPCP with transverse joints spaced at 20-ft (6.1 m) intervals. Section 2-11 is a 9-in (229-mm) JPCP with transverse joints spaced at 26.7-ft (8.1-m) intervals. All sections are constructed on aggregate bases and contain 1-in (25-mm) I-beams for load transfer.

The performance data for these sections are shown in table 49. The sections are performing similarly in terms of all of the distress categories: joint faulting, slab cracking, joint spalling, and overall rideability. In this case, there is no clear evidence that supports the belief that longer joint spacings result in more transverse cracking, at least for pavements on aggregate bases. One possible explanation for this is that the joint spacings under review in this study are considered somewhat extreme for

Table 49. Summary of effect of joint spacing for NY 2.

Section ID	Year Built	ESAL's, millions		Joint Faulting, in		% Slabs Cracked		% Joints Spalled		IRI, in/mi (PSR)	
		1987	1992	1987	1992	1987	1992	1987	1992	1987	1992
NY 2-3 20-ft Jts	1975	1.6	5.8	0.01	0.01	13	21	0	0	- (4.2)	108 (-)
NY 2-9 20-ft Jts	1975	1.6	5.8	0.02	0.01	9	9	0	0	- (4.0)	91 (3.9)
NY 2-11 26.7-ft Jts	1975	1.6	5.8	0.01	0.01	13	20	0	0	- (4.1)	98 (4.1)

1 in = 25.4 mm  
 1 ft = 0.305 m  
 1 mi = 1.61 km

Common Design Features: 9-in JPCP  
 4- to 6-in AGG base  
 1-in I-Beams

most JPCP designs. That is, if a 20-ft (6.1-m) joint spacing is considered excessive and expected to result in the development of significant slab cracking, the use of a 26.7-ft (8.1-m) joint spacing is also excessive and should also develop significant cracking. Thus, both joint spacings are too long for most JPCP and are in a range where significant differences in cracking are not expected.

*Ohio 1*

Located on U.S. 23 near Chillicothe, this project contains two JPCP designs with different joint spacings. Sections OH 1-3, OH 1-6, and OH 1-10 all have 21-ft (6.4-m) joint spacings while sections OH 1-1, OH 1-4, OH 1-7, and OH 1-9 all have 40-ft (12.2-m) joint spacings. Although two different base types are present, replicates of each design were constructed so that direct comparison of sections with different joint spacings is possible.

Table 50 summarizes the performance data for these sections, grouped to allow comparisons between similar designs. No significant difference between the faulting of the two designs is observed, but the amount of deteriorated transverse cracking is generally greater on the sections with the 40-ft (12.2-m) joint spacing than on those with the 21-ft (6.4-m) joint spacing. However, several of the short-jointed sections still developed significant transverse cracking, which may speak to the inadequacy of the amount of longitudinal reinforcing steel (0.09 percent) on these sections.

*Ohio 2*

This project is located on State Route 2 near Vermilion. The project consists of a total of 104 test sections in which—among other items—maximum coarse aggregate size, joint spacing, joint sealant, base type, and drainage are evaluated. However, only about half of those sections are included as part of the evaluation.

Table 50. Summary of effect of joint spacing for OH 1.

Section ID	Year Built	Base Type	Dowel Coating	ESAL's, millions		Joint Faulting, in		Det. Cracks/mi		% Joints Spalled		IRI, in/mi (PSR)	
				1987	1992	1987	1992	1987	1992	1987	1992	1987	1992
OH 1-3 21-ft Jts	1973	ATB	Std	4.1	6.1	0.06	0.03	0	0	13	13	- (4.2)	152 (-)
OH 1-4 40-ft Jts	1973	ATB	Std	4.1	6.1	0.07	0.02	29	132	0	0	- (4.1)	156 (-)
OH 1-10 21-ft Jts	1973	AGG	Std	4.1	6.1	0.10	0.03	0	168	0	0	- (4.2)	182 (-)
OH 1-1 40-ft Jts	1973	AGG	Std	4.1	6.1	0.13	0.02	0	88	0	0	- (4.2)	224 (-)
OH 1-9 40-ft Jts	1973	AGG	Std	4.1	6.1	0.14	0.07	106	251	0	0	- (4.2)	154 (-)
OH 1-6 21-ft Jts	1973	AGG	Plastic	4.1	6.1	0.03	0.01	31	220	0	0	- (4.2)	196 (-)
OH 1-7 40-ft Jts	1973	AGG	Plastic	4.1	6.1	0.07	0.01	235	279	0	0	- (4.2)	135 (-)

1 in = 25.4 mm  
 1 ft = 0.305 m  
 1 mi = 1.61 km

Common Design Features: 9-in JRCP  
 0.09 percent steel  
 1.25-in dowels

The effect of joint spacing on pavement performance can be evaluated for several of the JRCP designs. Both designs are 9 in (229 mm) thick and constructed on an aggregate base course. Both 40-ft (12.2-m) and 60-ft (18.3-m) joint spacings are available for comparison.

The performance data for these sections is provided in table 51, grouped by maximum coarse aggregate size (the aggregate source is the same for all sections). For the sections with 1.5-in (38-mm) coarse aggregate, the section with 60-ft (18.3-m) joint spacing (OH 2-11) is exhibiting transverse joint spalling at every joint due to the development of D-cracking; this severe spalling prevented the measurement of joint faulting. OH 2-20, constructed with the same D-cracking susceptible aggregate as OH 2-11 but with 40-ft (12.2-m) joints, also exhibits significant joint spalling due to D-cracking, but about half of that of OH 2-11. This may be due to the less movement associated with the shorter joint spacing. Section OH 2-21, constructed with a more durable aggregate, shows no joint spalling.

All sections constructed with 1.5-in (38-mm) aggregate displayed a significant amount of deteriorated transverse cracks, although the section with 60-ft (12.2-m) joints shows less cracking than those sections with 40-ft (12.2-m) joints. Also, the overall rideability of the long-jointed section is better than the short-jointed section.

Table 51. Summary of effect of joint spacing for OH 2.

Section ID	Year Built	ESAL's, millions	Max. Agg. Size, in	Joint Faulting, in	Det. Cracks/mi	% Joints Spalled	IRI, in/mi
OH 2-11 60-ft Jts	1974	6.5	1.5	-	88	100	161
OH 2-20 40-ft Jts	1974	6.5	1.5	0.08	132	57	201
OH 2-21 40-ft Jts	1974	6.5	1.5	0.04	132	0	180
OH 2-18 60-ft Jts	1974	6.5	0.5	0.17	418	0	296
OH 2-24 40-ft Jts	1974	6.5	0.5	0.00	154	0	161

1 in = 25.4 mm  
 1 ft = 0.305 m  
 1 mi = 1.61 km

Common Design Features: 9-in JRCP with 6-in AGG  
 Edge drains  
 1.25 in dowels

The sections with 0.5-in (13-mm) maximum coarse aggregate size are all constructed with a durable coarse aggregate and therefore show no transverse joint spalling. However, both sections show a significant number of deteriorated transverse cracks, probably due to the small coarse aggregate size being less effective at providing aggregate interlock load transfer at transverse cracks. The section with the 60-ft (18.3-m) transverse joint spacing is exhibiting significantly more deteriorated transverse cracks than its 40-ft (12.2-m) counterpart, and is also much rougher.

### Overall Evaluation of Joint Spacing

The effect of joint spacing on both JRCP and JPCP performance has been examined on several projects in which direct comparisons are possible. In general, the shorter jointed sections on JPCP showed less transverse cracking. The longer jointed JPCP sections experienced higher thermal stresses and are therefore more prone to cracking. However, due to the increased number of joints on the shorter jointed sections, more roughness is often observed. Ultimately, there must be a trade-off between the two components. In terms of other distress types (e.g., faulting, spalling, and longitudinal cracking), joint spacing did not play a critical role in their occurrence. These distress types are often more associated with other design features.

Figure 11 illustrates the effect of joint spacing on transverse cracking of JPCP sections. For sections with random joint spacings, the data are broken out by each particular slab length. That is, a section with a random joint spacing of 12-13-18-19 ft (3.7-4.0-5.5-5.8 m) contains four different points on the graph, one for each particular joint spacing. Sections with a uniform joint spacing, on the other hand, are only represented once in the graph.



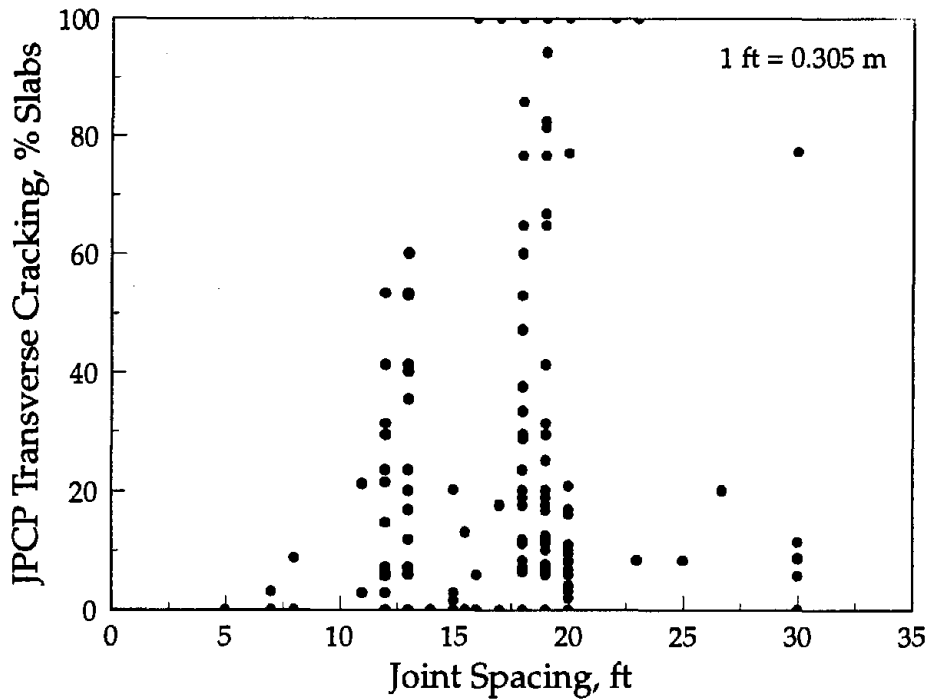


Figure 11. Effect of joint spacing on JPCP transverse cracking.

This overall evaluation of the sections produces similar results as that within individual projects. Although there is some scatter in the data, the sections with shorter joint spacings do exhibit less transverse cracking. The percentage of slabs with transverse cracks seems to increase for joint spacings greater than 17 ft (5.2 m), as well as the variation between the sections. Some variation, however, is due to differences in design and traffic and not specifically to different joint spacings.

Similar trends are shown in figures 12 and 13, which illustrate the percentage of slabs with transverse cracks as a function of the  $L/l$  ratio (slab length over the radius of relative stiffness), where  $l$  is defined as follows:

$$l = \left[ \frac{Eh^3}{12(1 - \mu^2)k} \right]^{0.25} \quad (1)$$

where:

- $l$  = Radius of relative stiffness, in.
- $E$  = Modulus of elasticity, lbf/in<sup>2</sup>.
- $h$  = Slab thickness, in.
- $\mu$  = Poisson's ratio.
- $k$  = Modulus of subgrade reaction, lbf/in<sup>2</sup>/in.

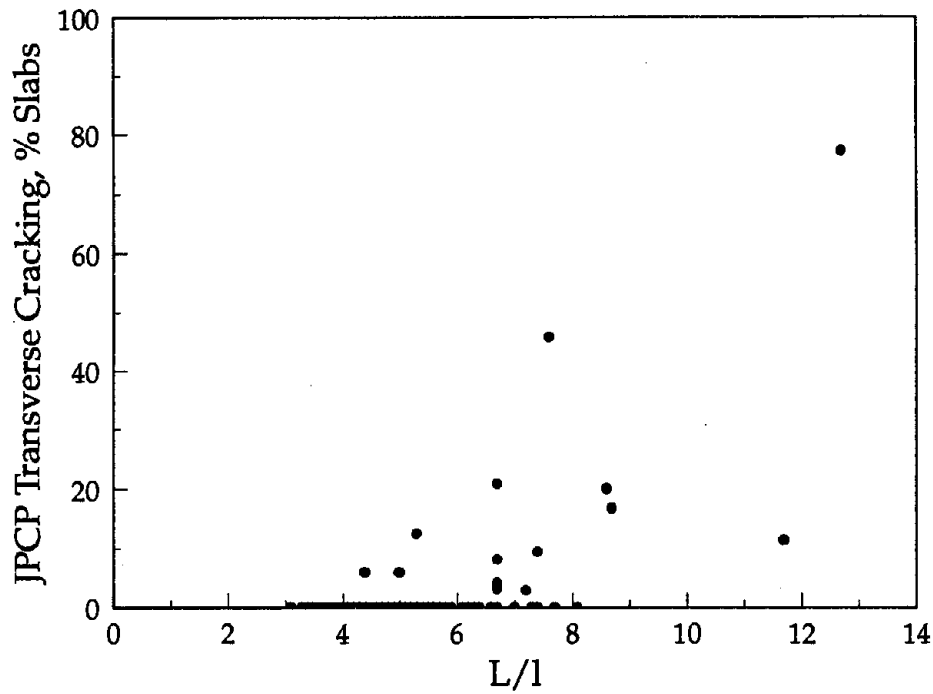


Figure 12. Transverse cracking as a function of  $L/\ell$  ratio for aggregate bases.

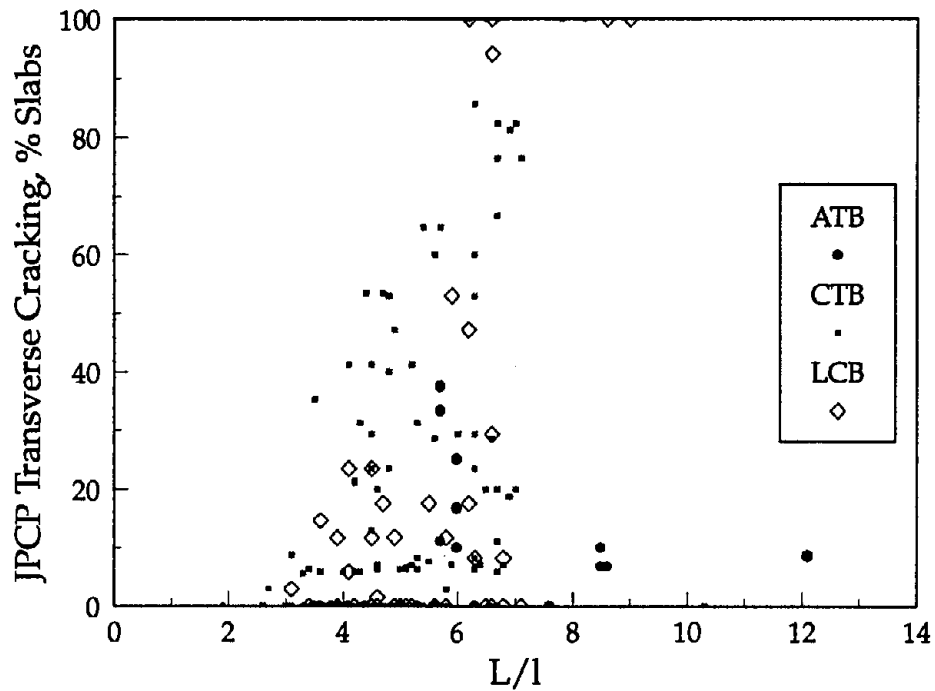


Figure 13. Transverse cracking as a function of  $L/\ell$  ratio for dense-graded stabilized bases.

Figure 12 shows the relationship for sections constructed on an aggregate base, and figure 13 is for sections on a stabilized base. For both plots, this ratio does appear to have an effect on transverse cracking.

For sections on an aggregate base, the critical value is around six. At this point, transverse cracking begins to occur on a higher percentage of the slabs. Before this critical point, however, transverse cracking does not predominate, with many sections showing no cracking at all. Of the sections with an L/l ratio less than five, none have more than 10 percent cracked slabs. The two sections with the high L/l ratios (greater than 10) are from North Carolina and have a joint spacing of 30 ft (9.1 m).

The sections constructed on a stabilized base have more cracking at the same L/l ratio as compared to those on an aggregate base. For sections on a stabilized base, the critical value is around four. Although transverse cracking steadily increases with L/l, cracking is more predominant after this critical value, with some sections showing cracking on 100 percent of the slabs. The sections on CTB and LCB are performing about the same in terms of transverse cracking. Sections on ATB, on the other hand, seem to be showing less cracking at the same L/l ratios. As before, the sections with L/l ratios greater than 10 have joint spacings of 30 ft (9.1 m).

Another interesting investigation is the effect of random joint spacing on concrete pavement performance. Figure 14 illustrates the average faulting between slabs of different lengths, with the first number indicating the length of the approach slab and the second number indicating the length of the leave slab. The random joint spacing pattern (12-13-19-18 ft [3.7-4.0-5.8-5.5 m]) illustrated in this figure is a common pattern. This study contains sections from California, Michigan, Wisconsin, and Ontario in which this pattern was used. Because of the occurrence of transverse cracking on the longer slabs in this pattern, California changed to a 12-13-15-14-ft (3.7-4.0-4.6-4.3-m) pattern in the late 1970's.

Many researchers believe that the difference in lengths between adjacent slabs creates differential curling, thus resulting in faulting at the transverse joints. This belief is not supported by these data; faulting at the 19-18-ft (5.8-5.5-m) joint is as great as at the 18-12-ft (5.5-3.7-m) joint. The trend here is higher faulting on sections with longer approach slabs.

Figure 15 illustrates the number of deteriorated cracks on the JRCP sections as a function of joint spacing. The correlation is not as apparent as for the JPCP sections. Transverse cracking on JRCP sections is controlled by different mechanisms. Transverse cracks are expected on JRCP and are controlled through the use of reinforcing steel. Thus, deterioration of the transverse cracks is thought to be related more to the amount of reinforcing steel than to the joint spacing. The effect of joint spacing on spalling at transverse joints was also not apparent.

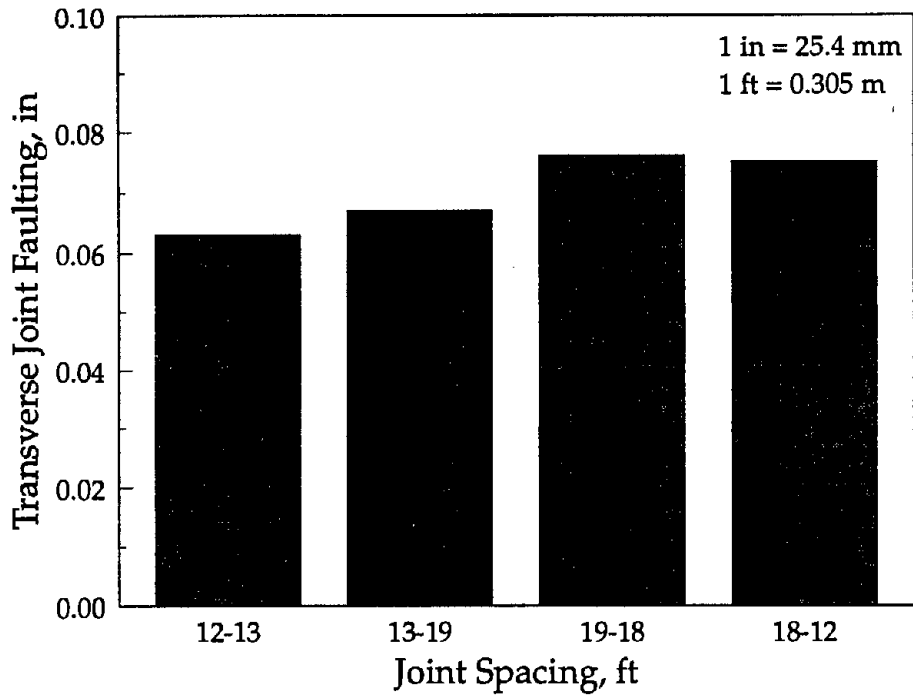


Figure 14. Faulting of randomly spaced joints.

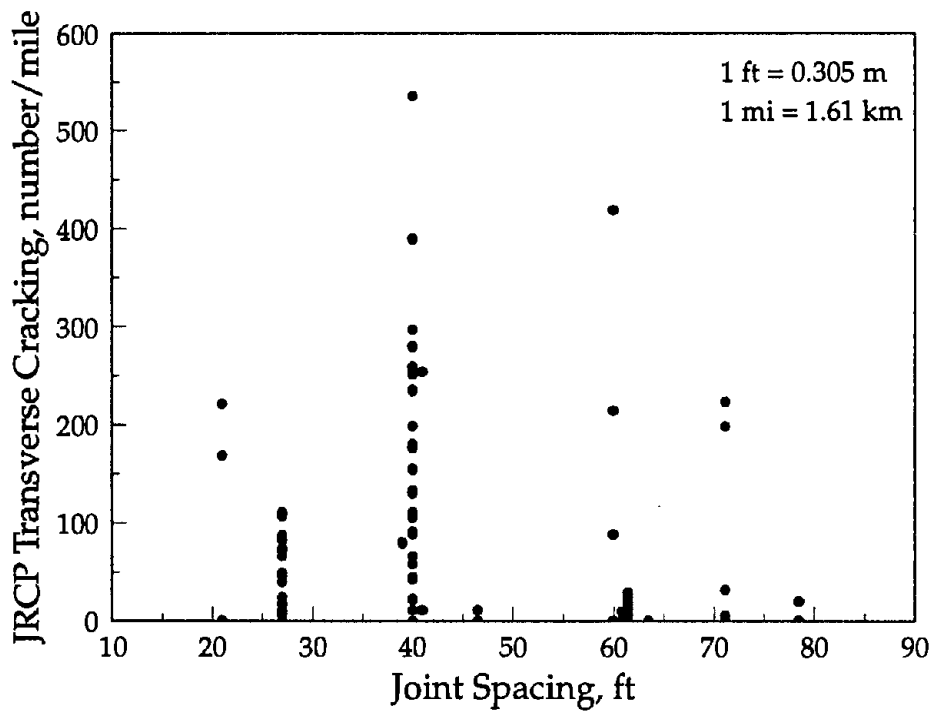


Figure 15. Effect of joint spacing on JRC transverse cracking.

As far as roughness, a correlation between joint spacing and IRI is not evident. The data are widely scattered regardless of the joint spacing. Again, even though the joint spacing does appear to affect transverse cracking, the effect does not transcend to the measured roughness.

As with IRI, joint spacing on both JPCP and JRCP did not appear to have an effect on transverse joint faulting. Again, this result is not surprising, as faulting is more related to dowel bars and the degree of aggregate interlock than to joint spacing.

### **Joint Orientation**

Joint orientation, or joint skew, refers to the angle of the transverse joint with respect to the centerline of the mainline pavement. Perpendicular joints are constructed at a right angle to the centerline, whereas skewed joints are placed at an angle to the centerline, usually offset about 2 ft (0.6 m) per 12-ft (3.7-m) lane. Skewed joints are placed counterclockwise in the direction of traffic such that the obtuse angle at the outside edge is on the leave side of the joint.

Skewing of transverse joints is thought to reduce the number of critical wheel loads at the joint from two to one, thus reducing stresses and deflections, and ultimately, faulting of the joints. Skewed joints are also thought to provide less impact reaction in vehicles crossing the joints. Skewed joints are often placed in conjunction with randomly spaced joints and are expected to be most beneficial to nondoweled pavements. Recent studies indicate that skewed joints are not necessary on doweled concrete pavements.<sup>(38, 39)</sup>

### Review of Project Data

Figure 16 illustrates the distribution of the available sections. A good distribution of perpendicular and skewed joints are available for each pavement type. Skewed joints are common on the nondoweled sections. No nondoweled JRCP sections are available with perpendicular joints. The best means of evaluating the effect of joint orientation is through comparisons of similar sections within the same project, one with perpendicular joints and one with skewed joints. However, these comparisons are only available for a limited number of projects.

#### *Florida 4*

This experimental project, located in the southbound lanes of U.S. 41 between Punta Gordo and Ft. Myers, contains a comparison between perpendicular and skewed joints, although the comparison is complicated by different stabilized subgrades. All sections are 3-in (76-mm) JPCP bonded to a 9-in (229-mm) LCB. Three different LCB types were used, each with a different cement content and compressive strength. The transverse joints are spaced at 15-ft (4.6-m) intervals and do not contain any load transfer devices. The sections with skewed joints are constructed on a shell-stabilized subgrade, and the sections with perpendicular joints are constructed on a cement-treated subgrade.

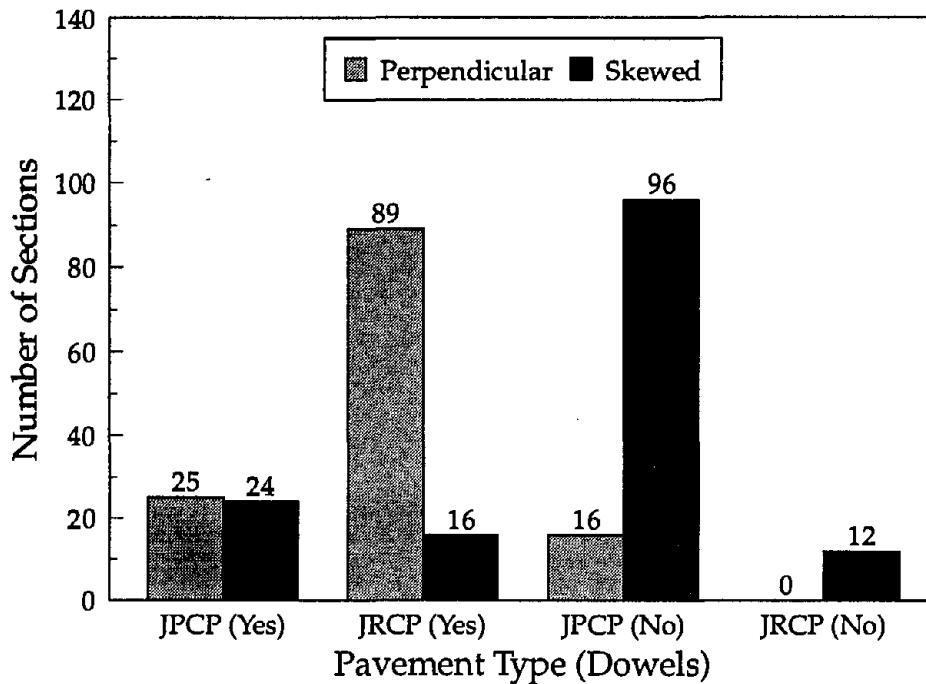


Figure 16. Distribution of sections by joint orientation.

Table 52 provides a summary of the performance data for evaluating the effect of joint orientation. The sections with skewed joints have lower faulting levels and higher serviceability levels for all three comparisons. However, the comparison is complicated by different types of stabilized subgrades. Other distress measurements do not point in favor of either perpendicular or skewed nondoweled joints.

Table 52. Summary of effect of joint orientation for FL 4.

Section	Skewed Joints	ESAL's, millions	Faulting, in	% Slabs Cracked	Long. Crk., ft/mi	% Joints Spalled	IRI, in/mi (PSR)
FL 4-2	yes	4.5	0.02	0	0	1	139 (3.8)
FL 4-7	no	4.5	0.07	0	0	1	110 (3.7)
FL 4-3	yes	4.5	0.04	0	546	0	122 (3.7)
FL 4-8	no	4.5	0.08	0	0	0	106 (3.6)
FL 4-6	yes	4.5	0.05	0	0	0	95 (3.7)
FL 4-9	no	4.5	0.11	1	1513	0	125 (3.2)

1 in = 25.4 mm  
 1 ft = 0.305 m  
 1 mi = 1.61 km

Common Design Features: 3-in JPCP bonded to 9-in LCB  
 15-ft joint spacing, nondoweled  
 Built in 1978

## North Carolina 1

This experimental project, located on I-95 near Rocky Mount, contains a direct comparison of the effect of joint orientation. NC 1-1 was constructed with skewed joints, and NC 1-8 was constructed with perpendicular joints. Both sections are 9-in (229-mm) JPCP with a 4-in (102-mm) aggregate base that runs to the ditchline (daylighted). The transverse joints are spaced at 30-ft (9.1-m) intervals and do not contain any load transfer devices.

The performance data for these sections are shown in table 53. The sections with skewed joints have significantly less faulting, transverse cracking, and roughness. Neither section experienced any longitudinal cracking or transverse joint spalling. Based on these data, skewing the transverse joints results in better performance than constructing perpendicular joints. However, the load transfer efficiency was 65 percent on the section with skewed joints and 100 percent on the section with perpendicular joints.

Table 53. Summary of effect of joint orientation for NC 1.

Section	Skewed Joints	ESAL's, millions		Faulting, in		% Slabs Cracked		IRI, in/mi (PSR)	
		1987	1992	1987	1992	1987	1992	1987	1992
NC 1-1	yes	9.0	16.0	0.12	0.13	3	11	— (3.4)	111 (3.3)
NC 1-8	no	9.0	16.0	0.22	0.23	37	77	— (3.7)	131 (3.3)

1 in = 25.4 mm  
 1 ft = 0.305 m  
 1 mi = 1.61 km

Common Design Features: 9-in JPCP and 4-in AGG  
 30-ft nondoweled joints  
 Built in 1967

Faulting has remained essentially the same since 1987 for both sections. Transverse cracking increased from 3 to 11 percent of the slabs on NC 1-1 and from 37 to 77 percent on NC 1-8. Thus, for this project at least, transverse cracking initiates sooner and increases at a faster rate on the section with perpendicular joints.

## New York 1

This project, located on Route 23 between Catskill and Cairo, provides a direct comparison between skewed joints (NY 1-8b) and perpendicular joints (NY 1-8a). Both sections are 9-in (229-mm) JPCP with a 3-in (76-mm) ATB. The transverse joints are spaced at 20-ft (6.1-m) intervals and do not contain any load transfer devices.

A summary of the performance data for these two sections is highlighted in table 54. Both sections are performing remarkable well after 24 years of service. Distress measurements are about the same for both sections, with slightly more faulting and

slightly less transverse cracking on the section with skewed joints. The 5-year trends are also similar. Faulting has remained the same on both sections, and transverse cracking has increased slightly.

Table 54. Summary of effect of joint orientation for NY 1.

Section	Skewed Joints	ESAL's, millions		Faulting, in		% Slabs Cracked		IRI, in/mi (PSR)	
		1987	1992	1987	1992	1987	1992	1987	1992
NY 1-8a	no	3.1	5.5	0.01	0.01	3	10	— (4.1)	112 (4.2)
NY 1-8b	yes	3.1	5.5	0.03	0.03	0	7	— (3.8)	111 (3.9)

1 in = 25.4 mm  
 1 ft = 0.305 m  
 1 mi = 1.61 km

Common Design Features: 9-in JPCP and 3-in ATB  
 20-ft nondoweled joints  
 Built in 1968

### Overall Evaluation of Joint Orientation

Comparisons of sections within individual projects indicate improved performance (especially in terms of faulting) on two of the three projects. Skewed joints on FL 4 had less faulting and a higher PSR than perpendicular joints. Likewise, experimental sections on NC 1 had less faulting, transverse cracking, and roughness for skewed joints. However, sections with skewed and perpendicular joints exhibited similar levels of distress on NY 1.

An overall evaluation of skewed and perpendicular transverse joints was also conducted. Figure 17 provides a comparison of skewed and perpendicular joints for different pavement types and load transfer mechanisms. For sections with skewed transverse joints, faulting levels are lower on JPCP but considerably higher on JRCP. Skewing of the joints is generally thought to provide the most benefit on nondoweled sections, as is the case for JPCP. None of the nondoweled JRCP sections were constructed with perpendicular joints.

The same trend is evident for transverse joint spalling, as seen in figure 18. Skewed joints are showing less spalling on JPCP and more spalling on JRCP as compared to perpendicular sections. Spalling was exhibited at more than 50 percent of the transverse joints on JRCP for both doweled and nondoweled sections.

Figure 19 compares the IRI values of skewed and perpendicular joints. The sections with perpendicular joints are rougher than the sections with skewed joints, as observed by the higher IRI values. The doweled JRCP sections with skewed joints, which had more faulting and spalling at the transverse joints, had less roughness. Apparently, skewed joints were effective at improving the ride quality by offering a smoother transition across the joint even though they did not reduce the occurrence of distress.



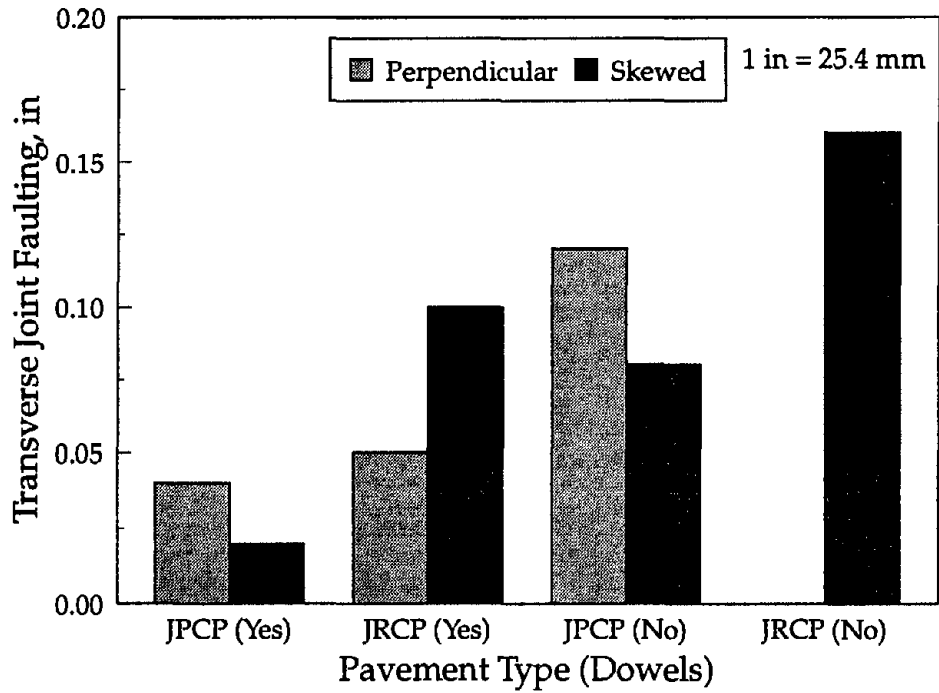


Figure 17. Effect of joint orientation on transverse joint faulting.

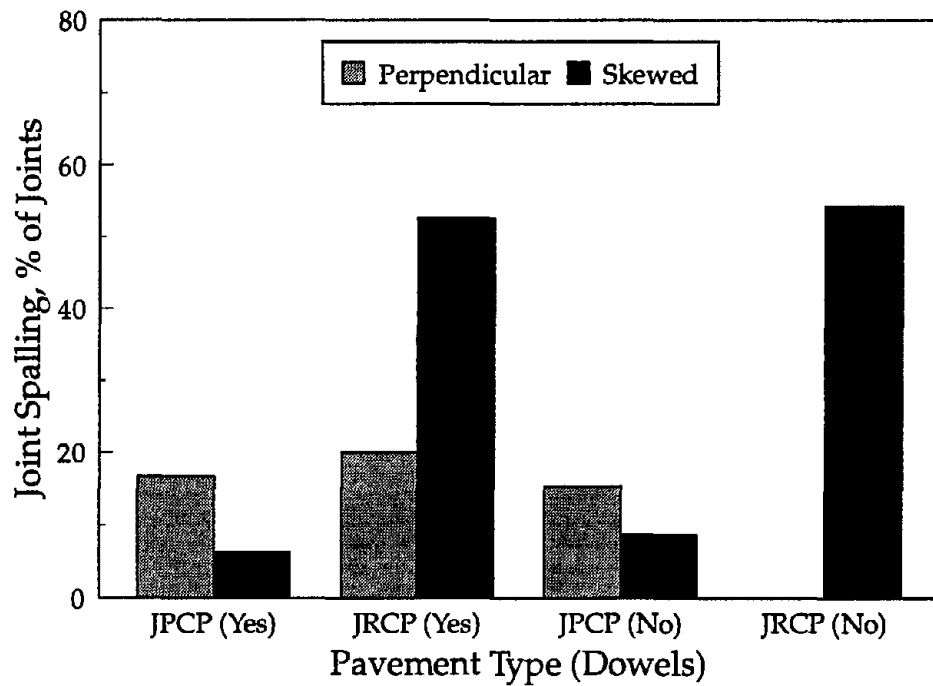


Figure 18. Effect of joint orientation on transverse joint spalling.

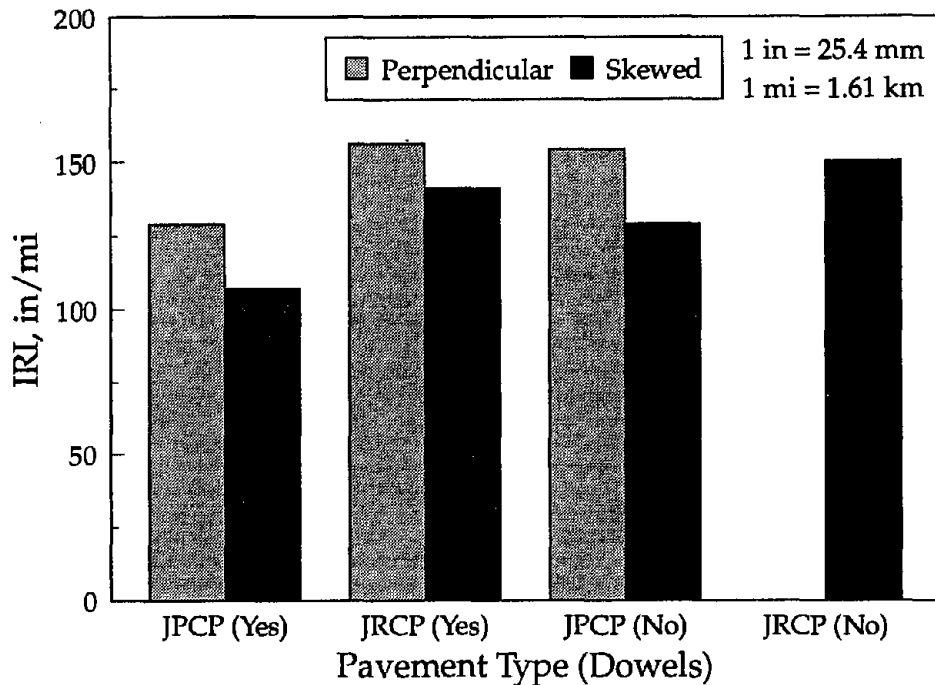


Figure 19. Effect of joint orientation on IRI.

Sections with skewed joints have considerably more corner breaks than those with perpendicular joints, as illustrated in figure 20. More corner breaks were evident for both doweled and nondoweled sections and on both the approach and leave side of the joint. The nondoweled sections with perpendicular joints did not exhibit any corner breaks. Although skewed joints were effective at reducing some distress types and improving the ride quality, corner breaks were more common.

An important aspect of skewed joints is the magnitude of the skew. Joints are skewed to reduce the number of critical loads at the joint and to reduce the impact reaction of vehicles. However, increasing the skew also increases the risk of corner breaks on the leave side of the slab. Most States use a skew of somewhere between 1 and 4 ft (0.3 to 1.2 m) per 12-ft (3.7-m) lane, with 2 ft (0.6 m) being the most common. The sections in this study all have skews of either 1 or 2 ft (0.3 or 0.6 m) per 12-ft (3.7-m) lane. Recent data shows that skewed joints should be limited to a 1 in 10 skew.<sup>(38)</sup>

Overall, skewed joints on JPCP seem to be effective at reducing faulting, spalling, and roughness. On JRCP, these distresses are not reduced, and in many cases are higher on sections with skewed joints. For both pavement types, however, more corner breaks have occurred on sections with skewed joints.

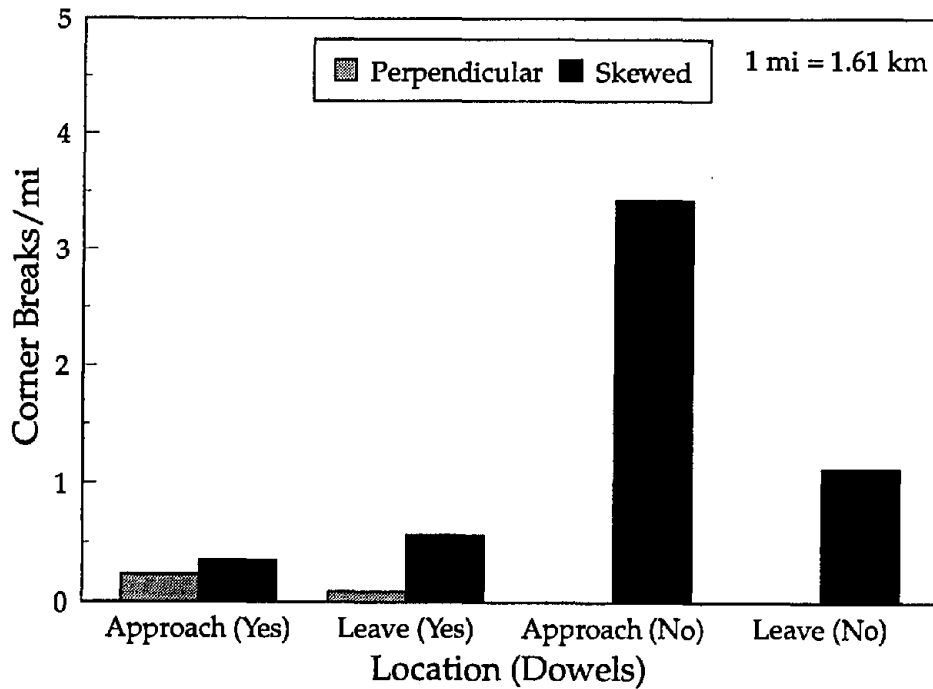


Figure 20. Effect of joint orientation on corner breaking.

### Transverse Joint Load Transfer

Transverse joint load transfer is the mechanism through which wheel loads are conveyed from one slab to the next. It is an important consideration in the design of concrete pavements because the effective transfer of the wheel load from one slab to the next will reduce significantly the magnitude of the stresses and deflections in the slab at the joints. This load transfer, in turn, will help reduce such joint distresses as pumping, faulting, and corner breaks.

Load transfer across a transverse joint is achieved either through the aggregate interlock between the abutting joint faces or through the use of mechanical load transfer devices, such as dowel bars. Traditionally, dowel bars have been used in JRCP because that design is constructed with longer joint spacing and it is implicitly acknowledged that joint movements will be such that aggregate interlock cannot be relied upon. However, the use of dowel bars on JPCP is more controversial, as some believe that aggregate interlock can be maintained because of the shorter joint spacings that lead to smaller joint movements. Nevertheless, the trend in recent years has been toward the use of dowel bars for most high-type roadways.

### Review of Project Data

The distribution of doweled and nondoweled sections is illustrated in figure 21. Approximately 55 percent of the sections contain load transfer devices. Another important factor for doweled joints is the dowel coating. This distribution is shown in figure 22. Six different dowel coatings were used.

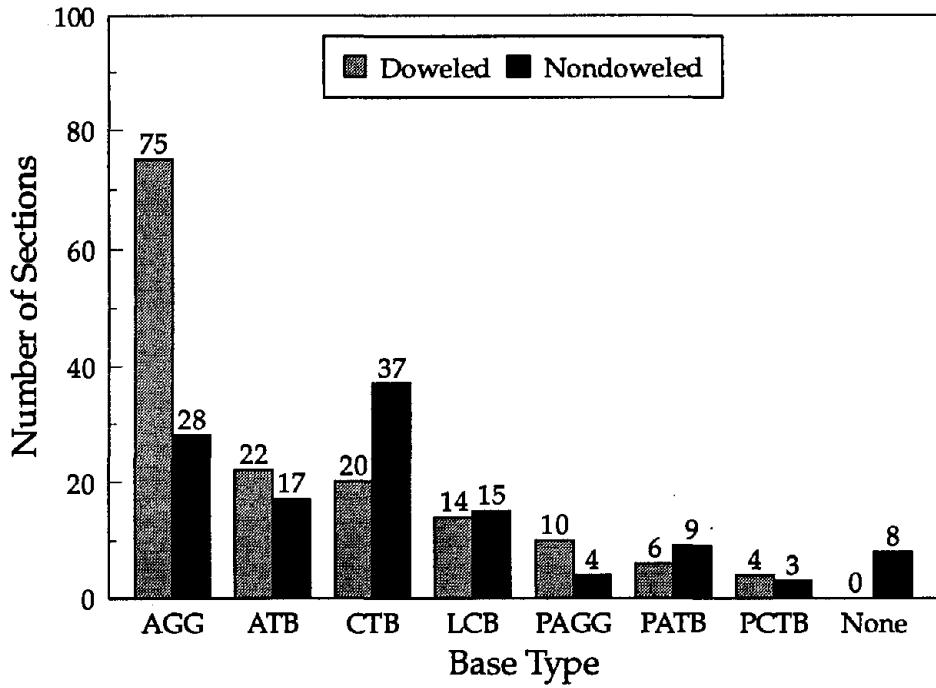


Figure 21. Distribution of doveled and nondoweled sections.

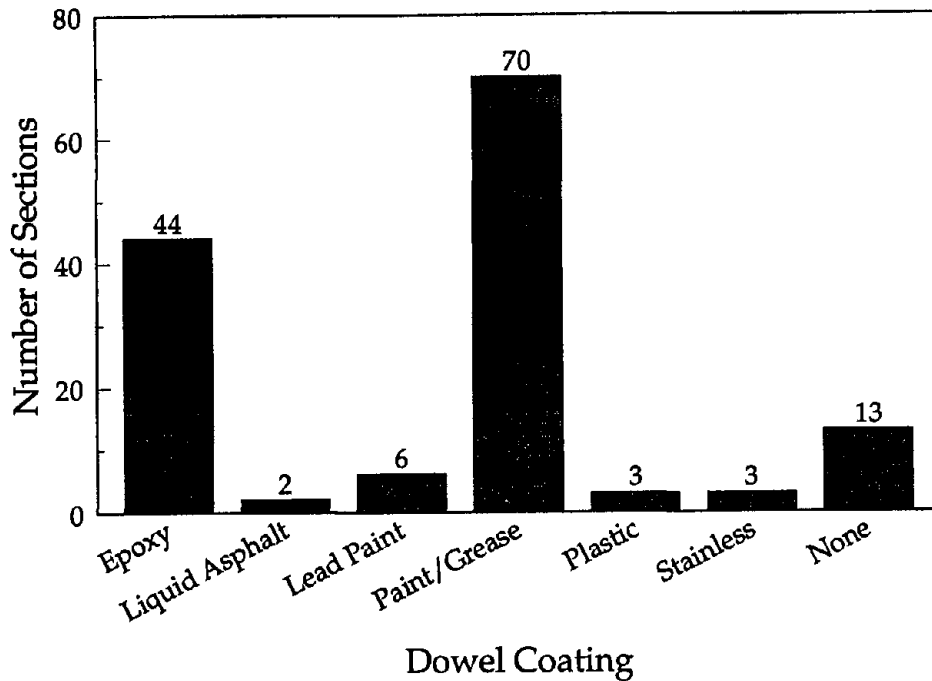


Figure 22. Distribution of dowel coatings.

This section reviews the performance data from the applicable projects that incorporate different load transfer mechanisms and for which meaningful comparisons are possible. In addition to dowel bars, two other mechanical load transfer devices (ACME two-part malleable iron load transfer devices and I-beams) are included, located on several New York sections.

#### *Florida 4*

The Florida 4 project, located on U.S. 41 near Ft. Meyers, contains several designs in which the effect of load transfer can be evaluated. However, it is first important to recall that these sections are composite designs in which a thin 3-in (76-mm) surface is bonded to a 9-in (229-mm) lean concrete base. The dowel bars, when present, are placed at the mid-depth of the total 12-in (305-mm) pavement thickness.

Section FL 4-10, containing 1-in (25-mm) dowel bars and constructed on lean concrete base type "A" (design strength of 2000 lb/in<sup>2</sup> [14 MPa]) can be compared to section FL 4-2, which contains no dowel bars. Similarly, section FL 4-11, which contains 1-in (25-mm) dowel bars and constructed on LCB type "B" (design strength of 1250 lb/in<sup>2</sup> [14 MPa]) can be compared to sections FL 4-3, 4-4, and 4-5. However, joint spacing is confounded in these comparisons in that the doweled sections contain 20-ft (6.1-m) joints and the nondoweled sections contain 15-ft (4.6-m) joints.

The performance data for these sections are summarized in table 55. This table shows no discernable difference between the performance of the doweled and nondoweled sections. For those pavements constructed on LCB A, the nondoweled section actually has less faulting than the doweled section, although the difference is probably not significant. The faulting for the sections constructed on LCB B are about the same for all designs. In terms of roughness and serviceability, there are no significant differences in the ride quality of one design over the other.

One possible explanation for the similarities in performance between the doweled and nondoweled designs is the cross-sectional design. All pavements have a relatively thick pavement structure (effective 12-in [254-mm] slab) and are placed on a shell stabilized subgrade. This total pavement structure, along with the relatively few ESAL applications that the pavement has experienced over its 14-year life, are believed to be the reasons that no significant differences exist between the faulting of the different designs.

#### *Georgia 1*

This experimental project, constructed in 1971 and located on I-85 near Newnan, evaluates the effect of base type and load transfer on pavement performance. A direct evaluation of load transfer is possible, although all of the sections were diamond ground in 1985 due to poor ride quality during initial construction, meaning that the effectiveness of dowel bars in controlling faulting can be assessed only since that grinding.

Table 55. Summary of effect of load transfer for FL 4.

Section	Year Built	ESALs, millions	Joint Faulting, in	% Slabs Cracked	% Joints Spalled	IRI, in/mi (PSR)
FL 4-2 15-ft Joints No Dowels LCB "A"	1978	4.5	0.02	0	1	139 (3.8)
FL 4-10 20-ft Joints 1 in Dowels LCB "A"	1978	4.5	0.04	0	0	112 (3.6)
FL 4-3 15-ft Joints No Dowels LCB "B"	1978	4.5	0.04	0	0	122 (3.7)
FL 4-4 15-ft Joints No Dowels LCB "B"	1978	4.5	0.04	0	0	98 (3.9)
FL 4-5 15-ft Joints No Dowels LCB "B"	1978	4.5	0.04	0	3	110 (3.6)
FL 4-11 20-ft Joints 1 in Dowels LCB "B"	1978	4.5	0.05	0	4	116 (3.6)

1 in = 25.4 mm  
1 ft = 0.305 m  
1 mi = 1.61 km

Common Design Features: Composite JPCP  
3-in surface/9-in bonded base  
Shell-stabilized subgrade

Table 56 summarizes the performance data for the Georgia 1 sections. This table shows that the faulting for the doweled sections is less than that of the nondoweled sections, although there is not a large difference between the values. Overall, these sections are performing so well that there is virtually no other distress, and the IRI values indicated that these sections are among the smoothest-riding sections included in the study.

#### Minnesota 1

Minnesota 1, located on I-94 near Rothsay, is an experimental project that examines the effect of different slab thicknesses, base types, and load transfer designs on JRCF performance. Direct comparisons of sections with and without dowel bars are possible for 8- and 9-in (203- and 229-mm) slabs and for ATB, CTB, and aggregate bases.

Table 56. Summary of effect of load transfer for GA 1.

Section	Year Built	ESALs, millions		1992 %LTE	Joint Faulting, in	% Slabs Cracked	% Joints Spalled	IRI, in/mi (PSR)
		Since 1971	Since 1985					
GA 1-1 1 in AC/5 in CTB 1.13-in Dowels	1971	19.1	6.5	—	0.01	0	0	60 (4.1)
GA 1-2 1 in AC/5 in CTB No Dowels	1971	19.1	6.5	—	0.04	0	0	70 (4.1)
GA 1-3 1 in AC/5 in CTB 1.13-in Dowels	1971	19.1	6.5	31	0.03	0	0	54 (4.1)
GA 1-4 1 in AC/5 in CTB No Dowels	1971	19.1	6.5	26	0.03	0	0	51 (4.1)
GA 1-5 6 in CTB 1.13-in Dowels	1971	19.1	6.5	90	0.03	0	0	51 (4.0)
GA 1-10 6 in CTB No Dowels	1971	19.1	6.5	50	0.05	0	0	54 (4.0)
GA 1-6 4 in ATB 1.13-in Dowels	1971	19.1	6.5	56	0.01	0	0	43 (4.1)
GA 1-7 4 in ATB No Dowels	1971	19.1	6.5	42	0.02	0	0	49 (4.0)
GA 1-8 4 in ATB 1.13-in Dowels	1971	19.1	6.5	—	0.01	0	2	50 (4.1)
GA 1-9 4 in ATB No Dowels	1971	19.1	6.5	—	0.01	0	0	56 (4.1)

1 in = 25.4 mm  
 1 ft = 0.305 m  
 1 mi = 1.61 km

Common Design Features: 9 in JPCP  
 20 ft Skewed Joints  
 All sections ground in 1985

The performance of the MN 1 sections is summarized in table 57. The table indicates that faulting is more severe on the sections without dowel bars. The difference is even greater than that shown in the table, as the nondoweled sections on aggregate and cement-treated bases were diamond ground in 1984 (tied and doweled edge beam was also added), eliminating faulting that reportedly often exceeded 0.5 in (13 mm). Dowel bars appear to be more effective at reducing faulting on the 8-in (203-mm) sections as compared to the 9-in (229-mm) sections. The type of base does not seem to have a significant effect on the effectiveness of dowel bars.

Table 57. Summary of effect of load transfer for MN 1.

Section	ESALs, millions	Slab Thick, in	Base Type	Dowels	1992 %LTE	Joint Faulting, in	Det. Cracks/mi	% Joints Spalled	IRI, in/mi	PSR
MN 1-3*	7.4	8	AGG	None	—	0.17	49	56	161	3.4
MN 1-4	7.4	8	AGG	1.0	—	0.11	83	48	105	3.3
MN 1-23*	7.4	8	AGG	None	—	0.15	73	28	126	3.0
MN 1-24	7.4	8	AGG	1.0	—	0.09	86	38	140	3.2
MN 1-5	7.4	8	ATB	None	—	0.19	73	84	186	3.5
MN 1-6	7.4	8	ATB	1.0	—	0.08	8	96	186	3.1
MN 1-15	7.4	8	ATB	None	—	0.21	106	92	151	3.0
MN 1-16	7.4	8	ATB	1.0	—	0.14	49	92	149	3.3
MN 1-11*	7.4	8	CTB	None	—	0.16	8	77	125	3.5
MN 1-12	7.4	8	CTB	1.0	—	0.12	81	80	124	3.5
MN 1-17*	7.4	8	CTB	None	—	0.25	8	20	164	3.2
MN 1-18	7.4	8	CTB	1.0	—	0.15	8	52	161	3.2
MN 1-1*	7.4	9	AGG	None	12	0.13	0	68	156	3.3
MN 1-2	7.4	9	AGG	1.0	37	0.15	45	61	179	3.5
MN 1-21*	7.4	9	AGG	None	—	0.19	0	16	151	3.1
MN 1-22	7.4	9	AGG	1.0	—	0.12	23	50	143	3.2
MN 1-7	7.4	9	ATB	None	38	0.11	16	65	174	3.6
MN 1-8	7.4	9	ATB	1.0	39	0.10	70	96	109	3.8
MN 1-13	7.4	9	ATB	None	—	0.17	65	92	128	3.1
MN 1-14	7.4	9	ATB	1.0	—	0.08	110	96	166	3.1
MN 1-9*	7.4	9	CTB	None	31	0.11	0	38	155	3.6
MN 1-10	7.4	9	CTB	1.0	59	0.12	18	76	117	3.5
MI 1-19*	7.4	9	CTB	None	—	0.12	8	69	127	3.5
MN 1-20	7.4	9	CTB	1.0	—	0.15	39	31	167	3.1

1 in = 25.4 mm  
 1 ft = 0.305 m  
 1 mi = 1.61 km

Common Design Features: Constructed in 1970  
 JRCP  
 27-ft Joints

\* Sections were diamond ground and edge beam (tied and doweled) was added in 1984.

Although available for only three sections, the load transfer efficiencies at the transverse joints are significantly higher on the doweled sections in two of the cases. However, the load transfer efficiency for the doweled joints is quite low, indicating that the 1.0-in (25-mm) dowels are not effective and perhaps that corrosion of the



noncoated dowel bars has occurred. Furthermore, although faulting levels are lower on the doweled sections, they are still high in comparison to other doweled pavements, which again may be due to the small dowel size and corrosion. Moreover, more deteriorated transverse cracks and often more transverse joint spalling were manifested on the doweled sections, which may be an indication of joint lock-up.

The higher faulting levels on the nondoweled sections did not produce more roughness. The IRI and PSR values are not well correlated with the use of dowel bars. Direct comparisons indicate that ride quality is better on some sections with dowel bars, whereas on other sections it is worse.

### Minnesota 7

This experimental project, located on Trunk Highway 36 in Roseville, contains several direct comparisons of the effect of dowel bars. Sections were constructed with and without dowel bars, with different types of dowels (oiled, rust-protected, and sleeved), and with different joint spacings (15 and 20 ft [4.6 and 6.1 m]). All sections are 9-in (229-mm) JPCP with an aggregate base. The sections were constructed in 1958 and have been exposed to 6.9 million ESALs as of 1992.

Table 58 provides a summary of the performance data for these sections. The use of dowel bars has resulted in a significant reduction in the amount of faulting. The average faulting on the nondoweled sections is 0.11 in (2.8 mm), whereas it is only 0.01 in (0.25 mm) on the doweled sections. However, load transfer efficiencies are only slightly higher on the doweled sections.

Table 58. Summary of effect of load transfer for MN 7.

Section	ESALs, millions	Joint Spacing, ft	Dowel Dia, in	1992 %LTE	Joint Faulting, in	% Slabs Cracked	% Joints Spalled	IRI, in/mi	PSR
MN 7-10	6.9	15	None	86	0.07	0	50	162	3.3
MN 7-18	6.9	15	None	—	0.16	0	31	158	3.5
MN 7-15	6.9	15	1.0	92	0.01	0	59	193	3.1
MN 7-23	6.9	15	1.0	—	0.01	0	31	183	3.3
MN 7-9	6.9	20	None	84	0.07	6	39	169	3.4
MN 7-17	6.9	20	None	—	0.15	0	31	194	2.9
MN 7-16	6.9	20	1.0	93	0.01	0	75	201	3.0
MN 7-24	6.9	20	1.0	—	0.01	6	39	179	3.2

1 in = 25.4 mm  
 1 ft = 0.305 m  
 1 mi = 1.61 km

Common Design Features: Constructed in 1958  
 9-in JPCP  
 3-in AGG Base  
 15-in AGG Subbase

Other distress types appear to be unaffected by the use of dowel bars. Almost no transverse cracking has occurred on either the doweled or nondoweled sections. Joint spalling, roughness, and serviceability vary regardless of whether dowel bars are used. In fact, the IRI values on MN 7-15 and 7-23, which are doweled, are 193 and 183 even though there is little faulting and no transverse cracking.

An investigation of the type of dowels and their effect on performance is shown in table 59. In terms of faulting, the oiled and rust-proofed dowels provide better performance than the sleeved dowels. The joints containing sleeved dowels were badly deteriorated, and many had been repaired. These results are similar to findings reached by the Minnesota Department of Transportation on this project, in which sections with sleeved dowels were found to exhibit poor performance.<sup>(24)</sup>

Table 59. Summary of dowel performance on MN 7.

Dowel Type	Faulting, in			% Joints Spalled		
	15-ft Joints	20-ft Joints	Average	15-ft Joints	20-ft Joints	Average
Oiled	0.012	0.006	0.009	9	36	23
Rust-Proofed	0.012	0.008	0.011	64	55	59
Sleeved	0.025	0.022	0.024	70	90	80

1 in = 25.4 mm  
1 ft = 0.305 m

### North Carolina 1

This experimental project is located on I-95 near Rocky Mount. Sections with and without dowels are provided for two different base types: a 4-in (102-mm) aggregate base and a 6-in (152-mm) soil cement base containing 8 percent cement. All sections are 9-in (229-mm) JPCP with a transverse joint spacing of 30 ft (9.1 m). The sections were constructed in 1967 and have encountered 16 million ESALs through 1992.

The performance data for NC 1 are provided in table 60. For the sections on an aggregate base, faulting is reduced through the use of dowel bars. However, the average faulting on the doweled section is still 0.13 in (3.3 mm), which is unacceptable for Interstate highways. For the sections on a soil cement base, faulting is slightly higher on the doweled section. Therefore, dowel bars are not effective at reducing faulting on these sections. The ineffectiveness of the dowel bars is thought to be due to the small diameter of the dowel bars (1 in [25 mm]).

Table 60. Summary of effect of load transfer for NC 1.

Section	ESALs, millions	Base Type	Dowels	1992 %LTE	Joint Faulting, in	% Slabs Cracked	% Joints Spalled	IRI, in/mi	PSR
NC 1-4	16.0	AGG	1.0	94	0.13	0	0	110	3.2
NC 1-8	16.0	AGG	None	100	0.23	77	0	131	3.3
NC 1-2	16.0	Soil-Cement	1.0	100	0.16	6	3	114	3.3
NC 1-3	16.0	Soil-Cement	None	100	0.14	6	3	116	3.4

1 in = 25.4 mm  
 1 ft = 0.305 m  
 1 mi = 1.61 km

Common Design Features: Constructed in 1967  
 9-in JPCP  
 30-ft Joints

Conversely, the load transfer efficiencies at the transverse joints are all greater than 90 percent. This high level of load transfer does not correspond with the high faulting levels. One possible explanation is the joints may have been closed due to expansion, as deflection testing was conducted when the temperature was near 80 °F (27 °C).

The nondoweled section on an aggregate base has considerably more transverse cracking than the corresponding doweled section. However, cracking is not a common occurrence on other nondoweled sections within this project, so this is believed to be due to other factors (e.g., poor subgrade compaction or construction problems). Transverse joint spalling is the same for the doweled and nondoweled sections. Likewise, roughness and serviceability do not appear to be affected by the use of dowel bars.

### *New York 1*

This project, located on Route 23 between Catskill and Cairo, contains a direct comparison of the use of load transfer devices. NY 1-1 contains ACME two-part malleable iron load transfer devices, whereas NY 1-8a does not contain any load transfer devices. Both sections are 9-in (229-mm) JPCP with a 3-in (76-mm) ATB and a 20-ft (6.1-m) joint spacing. As of 1992, the sections have been exposed to 5.5 million ESALs since being constructed in 1968.

The sections are performing similarly in terms of distress levels, as shown in table 61. Both sections are exhibiting very little distress considering they are 24 years old. However, the light traffic levels on these sections may not provide a true indication of the effect of the load transfer devices. Other studies conducted in New York indicated that the ACME load transfer devices corroded and did not provide long-term load transfer, often failing within 5 years.<sup>(40)</sup>

Table 61. Summary of effect of load transfer for NY 1.

Section	ESALs, millions	Load Transfer	Joint Faulting, in	% Slabs Cracked	% Joints Spalled	IRI, in/mi	PSR
NY 1-1	5.5	ACME	0.02	7	6	106	3.7
NY 1-8a	5.5	None	0.01	10	0	112	4.2

1 in = 25.4 mm  
 1 ft = 0.305 m  
 1 mi = 1.61 km

Common Design Features: Constructed in 1968  
 9-in JPCP with 3-in ATB  
 20-ft Joints

*Wisconsin 2/Wisconsin 7*

These projects are located adjacent to each other and allow for comparisons to be made between the different projects. Both projects are located on U.S. 18/151, with WI 2 located near Mt. Horeb and WI 7 located near Barneveld. These projects contain a range of different variables, including load transfer, base type, drainage, and joint sealant. Several comparisons can be made regarding the effects of dowel bars. All sections are 9-in (229-mm) JPCP with transverse joints spaced at 12-13-19-18-ft (3.7-4.0-5.8-5.5-m) intervals. At the time of the survey in 1992, the sections were 4 years old and had been exposed to 1.3 million ESALs.

Six different comparisons of the effect of dowel bars can be made for these projects. Table 62 shows the performance data for each comparison. Because of the short life and limited distress on the sections, it is difficult to draw definitive conclusions. However, some trends are already apparent. For instance, faulting on the nondoweled sections is higher than that on the doweled section for all six comparisons. Although the differences were not significant at the time of the survey, the differences are expected to continue to increase with time. The load transfer efficiency is also much lower on the nondoweled sections, which is further reason to expect faulting to increase on the nondoweled sections.

Of particular concern are the extremely low load transfer efficiencies on the nondoweled sections constructed on permeable bases. Apparently, these bases do not contribute to the load transfer across the joints due to their gradation. Although these low load transfer efficiencies have not yet affected the faulting of the pavements, it is expected that they soon will. Dowel bars may be a necessity for pavements with permeable bases.

Crovetti also conducted an analysis of these pavement sections using FWD data.<sup>(41)</sup> The results indicated that joint deflection load transfer was consistently high on the doweled sections regardless of base type, joint sealant, and drainage design. In addition, the section constructed on a nonstabilized open-graded base with doweled and unsealed transverse joints was found to have poor support due to base layer densification.<sup>(41)</sup>

Table 62. Summary of effect of load transfer for WI 2/WI 7.

Section	ESALs, millions	Base Type	Dowel Dia., in	Joint Seal	1992 %LTE	Joint Faulting, in	% Slabs Cracked	1997 %Joints Spalled	IRI, in/mi	PSR
WI 2-1	1.3	PCTB	1.25	None	100	0.01	0	0	122	4.1
WI 7-4	1.3	PCTB	None	None	45	0.04	0	3	147	4.0
WI 2-2	1.3	PATB	1.25	None	100	0.01	0	3	106	4.0
WI 7-6	1.3	PATB	None	None	29	0.02	0	3	98	4.0
WI 2-3	1.3	PAGG	1.25	None	100	0.01	0	3	112	4.0
WI 7-2	1.3	PAGG	None	None	10	0.03	6	3	136	4.3
WI 7-10	1.3	AGG*	1.25	None	-	0.01	0	0	113	4.2
WI 7-7	1.3	AGG*	None	None	-	0.02	0	0	117	4.3
WI 2-4	1.3	AGG**	1.25	None	100	0.01	0	0	121	4.0
WI 7-9	1.3	AGG**	None	None	94	0.04	0	0	114	3.9
WI 2-5	1.3	AGG**	1.25	Pref.	100	0.01	0	0	122	3.9
WI 7-8	1.3	AGG**	None	Pref.	100	0.04	0	3	116	3.9

- \* Transverse Joint Drains
- \*\* No Positive Drainage
- 1 in = 25.4 mm
- 1 ft = 0.305 m
- 1 mi = 1.61 km

Common Design Features: Constructed in 1988  
 9-in JPCP  
 12-13-19-18-ft Joints

Transverse joint spalling is slightly higher on several nondoweled section, which may also be related to the use of dowel bars. However, the small differences in spalling make it difficult to fully analyze the effect of dowel bars on spalling. Other distress types (transverse cracking, roughness, and serviceability) are similar for the doweled and nondoweled sections.

*Wisconsin 6*

This experimental project, located on STH 29 west of Green Bay, contains two direct comparisons involving the use of dowel bars. All sections are 10-in (254-mm) JPCP with a 4-in (102-mm) permeable aggregate base, widened outside lanes, and AC shoulders. Transverse joints are spaced at 12-13-19-18-ft (3.7-4.0-5.8-5.5-m) intervals. The sole difference in the two comparisons is the joint sealant: two sections contain no joint sealant and two sections contain a preformed sealant.

The performance of the WI 6 sections are shown in table 63. The doweled sections are exhibiting much less faulting than the nondoweled sections after only 4 years of service. Faulting is negligible on the doweled sections but is already approaching critical levels on the nondoweled sections. More spalling is also observed at the transverse joints of the nondoweled sections. However, the

nondoweled sections have lower IRI values and higher PSR values, indicating a smoother riding pavement.

Table 63. Summary of effect of load transfer for WI 6.

Section	ESALs, millions	Base Type	Dowel Dia., in	Joint Seal	Joint Faulting, in	% Slabs Cracked	% Joints Spalled	IRI, in/mi	PSR
WI 6-4	4.2	PAGG	1.25	None	0.00	0	11	102	3.8
WI 6-1	4.2	PAGG	None	None	0.07	0	9	88	4.0
WI 6-3	4.2	PAGG	1.25	Pref.	0.00	0	6	81	3.8
WI 6-2	4.2	PAGG	None	Pref.	0.04	0	3	77	3.9

1 in = 25.4 mm  
 1 ft = 0.305 m  
 1 mi = 1.61 km

Common Design Features: Constructed in 1988  
 10-in JPCP  
 12-13-19-18-ft Joints

### Overall Evaluation of Transverse Joint Load Transfer

The investigation of the effect of transverse joint load transfer through direct comparisons on individual projects provided some interesting results. The most obvious and expected result was the reduction in faulting caused by the addition of dowel bars. However, the presence of small diameter dowel bars was not always effective in significantly reducing faulting. For instance, several doweled sections containing 1-in (25-mm) dowels were observed to have developed significant faulting, whereas less faulting was observed on sections with larger dowel diameters. The reduction in bearing stresses in moving to a 1.25- or 1.5-in (32- or 38-mm) dowel bar is quite substantial, which in turn can significantly reduce faulting.

Another important consideration is the coating of the dowel, which is expected to prevent corrosion of the load transfer device. If the dowels are not coated or ineffectively coated, corrosion of the dowel can occur, leading to a reduction in the effective diameter of the dowel and the freezing of the joint.

Taken together, sections with small diameter dowels or no protective coating did not always reap the expected benefits of positive load transfer. On these sections, load transfer efficiencies and faulting levels were usually not greatly improved through the use of dowels. NCHRP Synthesis 211 states that the use of dowel bars is critical when slab lengths exceed about 15 ft (4.5 m) because aggregate interlock begins to become ineffective at greater slab lengths.<sup>(39)</sup> Kelleher and Larson also stress the importance of dowel bars, which should also be corrosion resistant, to reduce the rate of faulting.<sup>(38)</sup>

Some increase in the amount of spalling at the transverse joints was also noticed through the addition of dowel bars. Other distress measurements, such as transverse

and longitudinal cracking, did not seem to be influenced by the addition of dowels. Likewise, roughness and serviceability values were not significantly improved by the use of dowel bars.

An overall comparison of the effect of dowel bars provided similar results. For instance, the addition of dowel bars was found to have a significant impact on the amount of faulting. This result, distributed by base type, is shown graphically in figure 23. With the exception of the sections constructed on an LCB, dowel bars were an effective means of reducing faulting. The reduction in faulting was quite significant for sections constructed on an aggregate base, ATB, or CTB. Although no doweled sections were constructed directly on grade, a significant reduction in faulting would be expected through the addition of dowel bars.

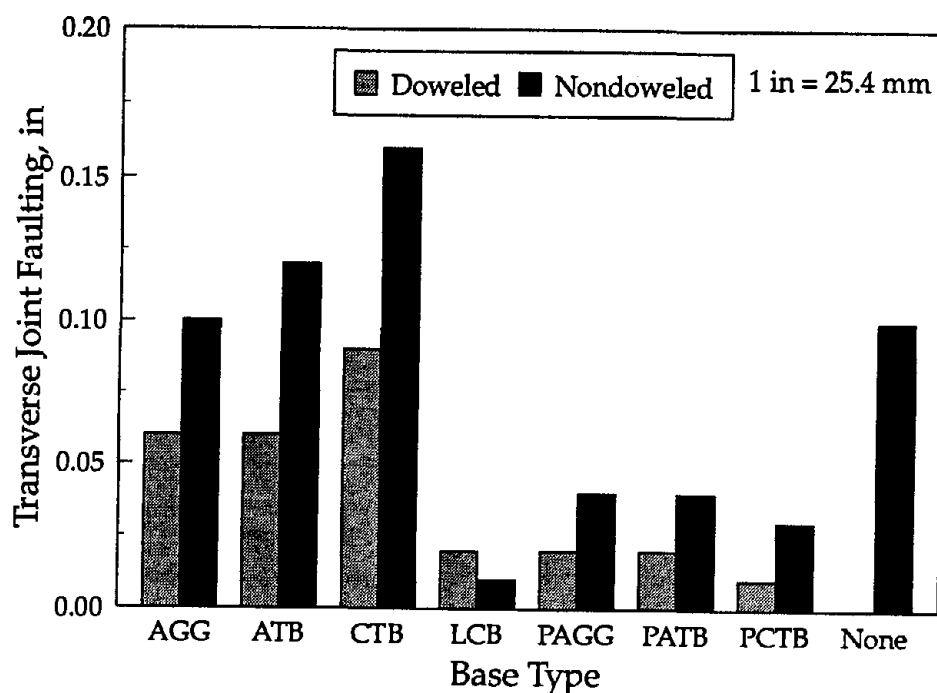


Figure 23. Comparison of faulting for doweled and nondoweled sections.

The sections constructed on permeable bases (PAGG, PATB, or PCTB) did not show as much of a reduction in faulting through the use of dowel bars as compared to other base types. However, those sections are also not as old as the sections on other base types, and should begin to show a greater difference as more traffic is applied to these pavements. Through the better drainage capabilities of the permeable bases, all of which also contain longitudinal edge drains, the potential for pumping and subsequent faulting is greatly reduced.

Figure 24 also illustrates the effect of dowel bars on transverse joint faulting, but the doweled sections are further broken out by the dowel bar diameter. Again, the doweled sections exhibit less faulting than the nondoweled sections. Although some deviations are noticed, a trend between the dowel diameter and faulting is apparent.

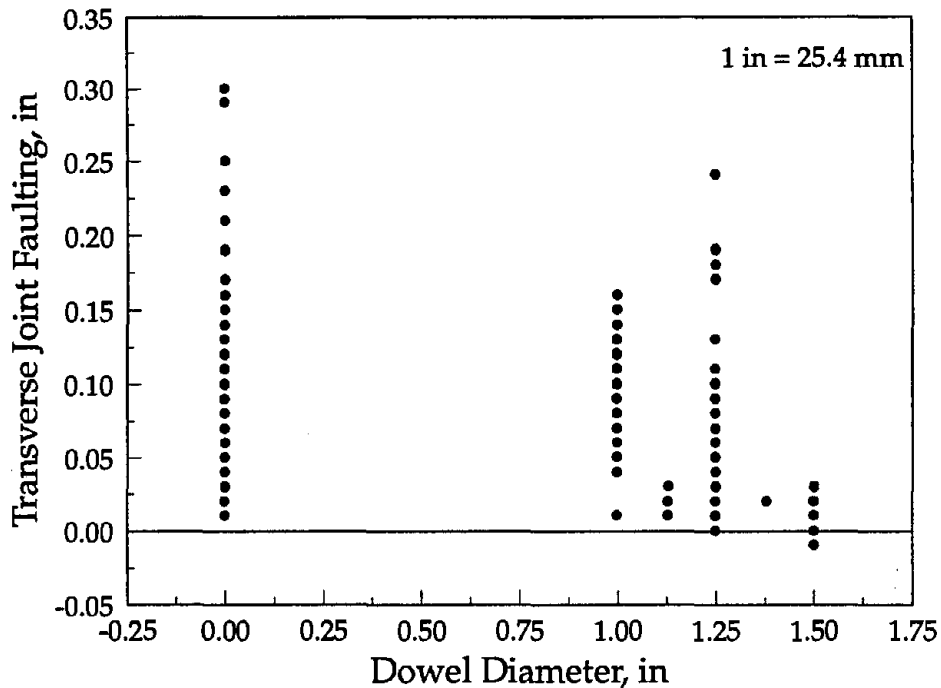


Figure 24. Effect of dowel bar diameter on transverse joint faulting.

Some variation is expected due to differences in design and climate among the sections. However, sections with dowel bar diameters greater than 1.25 in (32 mm) have very little faulting regardless of the conditions.

The degree of load transfer directly influences the deflections and faulting at the transverse joint. Figure 25 illustrates faulting as a function of load transfer efficiency. There is a large amount of scatter in the data, especially for the nondoweled sections. With the exception of a few data points, a trend is apparent for the doweled sections. The sections with less than 60 percent efficiency have higher faulting levels on average, with many sections having faulting levels greater than 0.10 in (2.5 mm).

A similar type of plot for spalling at transverse joints is shown in figure 26. The trend is not as apparent as for faulting. However, the sections with the largest diameter dowel bars do have less spalling than other sections. Similar plots were developed for IRI, corner deflection, and load transfer efficiency. These plots seemed to suggest that dowel bar diameter had little influence on these measurements, as the data were widely scattered throughout these plots.

Another factor that deserves further consideration is the effect of the dowel bar coating on concrete pavement performance. Figure 27 illustrates the average faulting for each particular dowel bar coating. Some coatings, such as epoxy, lead paint, and plastic, seem to be more effective at reducing faulting (or at least dowel bar corrosion, which eventually leads to faulting). Other coatings, however, are no more effective than no coatings. The results for the liquid asphalt coatings are only based on two sections, which may not provide an accurate assessment of these coatings.



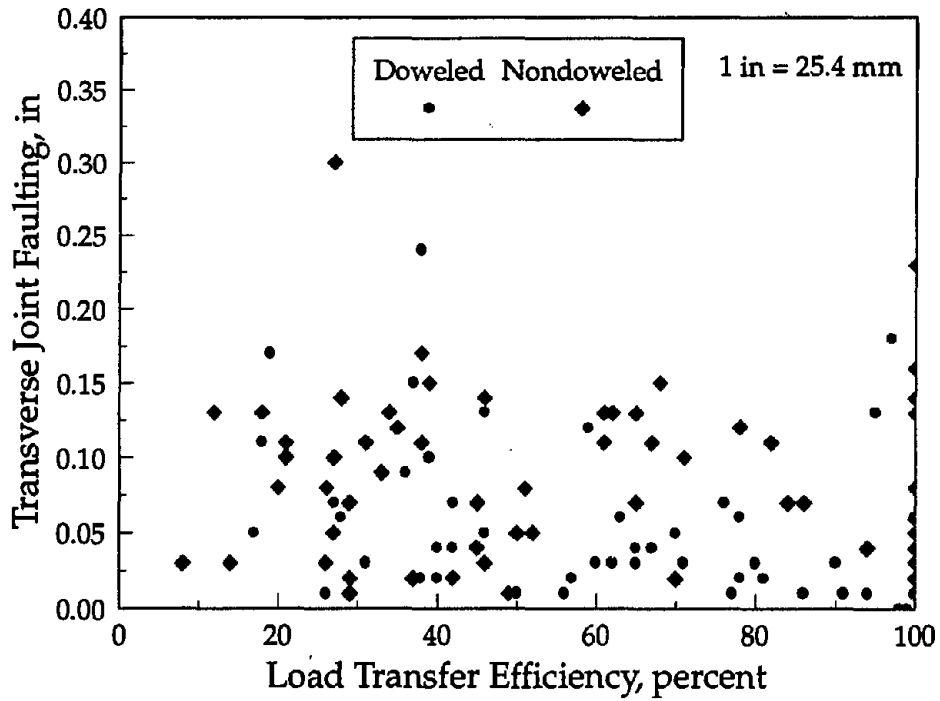


Figure 25. Effect of load transfer efficiency on transverse joint faulting.

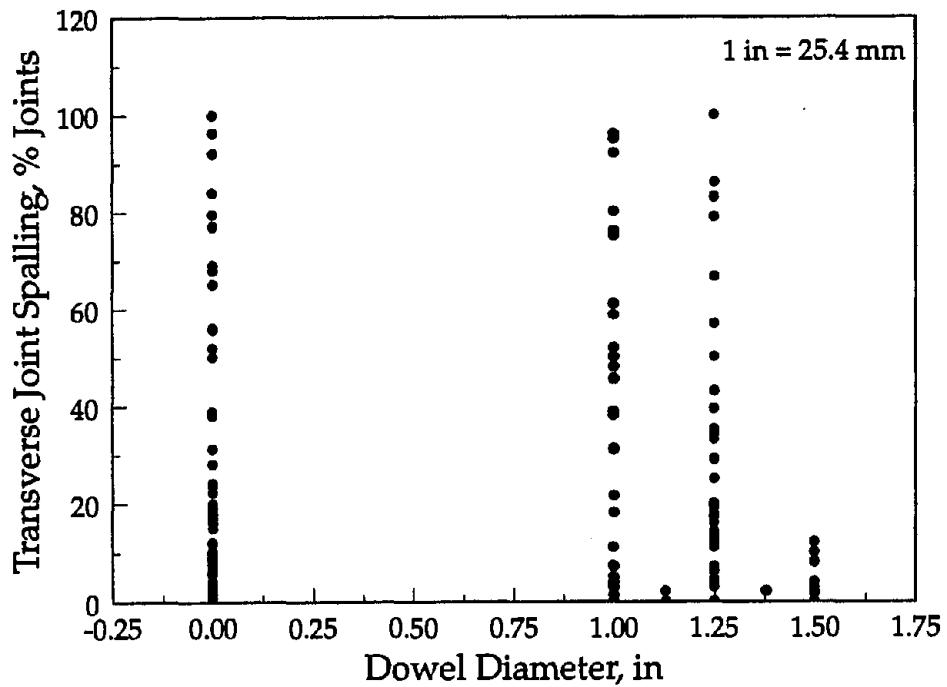


Figure 26. Effect of dowel diameter on transverse joint spalling.

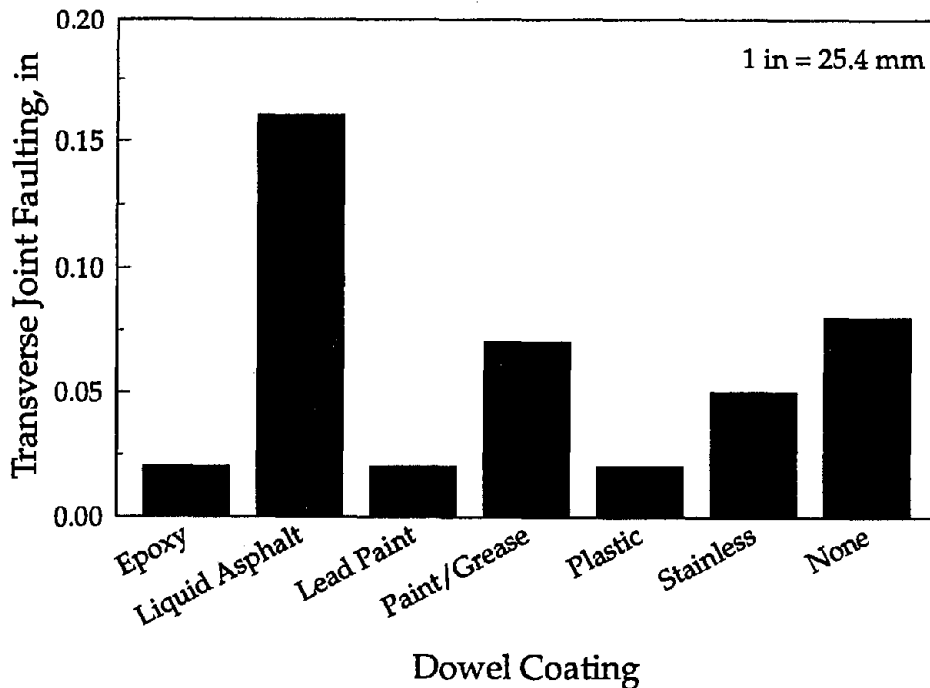


Figure 27. Transverse joint faulting for different dowel bar coatings.

### Joint Sealant

Functional joint sealant (which, in this context, can be defined as sealant that remains in place and retains its durability, resiliency, and adhesive and cohesive properties) is intended to perform several important roles in a concrete pavement. One role is to keep out incompressible matter, such as sand and other large-sized particles. A transverse contraction joint without infiltrated foreign matter is able to function as designed, opening and closing with changes in temperature. A well-sealed and maintained joint also serves a second major function, resisting the infiltration of moisture from surficial sources (rainfall and runoff). Therefore, the likelihood of moisture-related distresses developing in the pavement should be reduced when joints are sealed at construction and kept sealed throughout the pavement's life. Yet another function of the sealant is to keep fine particles from escaping to the surface, thus preventing erosion and loss of support beneath the joint.

Despite the positive functions that sealants are designed to serve, whether to seal transverse joints in concrete pavements is a subject of some debate. The argument against sealing joints is approached from at least three distinct viewpoints: 1) sealants themselves do not perform well for very long, 2) there are enough other sources of moisture available to contribute to pavement deterioration that sealing joints is simply a waste of money, and 3) given the costs associated with sealing and resealing, there are many other needs to which funds used for sealing could be allocated. These three arguments suggest a fourth: the disputed benefits of sealing may be reason enough to not seal joints.

The debate that surrounds joint sealing can be broken down into the following two questions:

- Is joint sealing a cost-effective construction/maintenance/rehabilitation activity?
- Which materials perform best in this application?

Pavement studies designed to examine these issues look at sealed versus nonsealed pavements for the first case and head-to-head comparisons of different materials in the second case.

A number of projects are available in which joint sealing is a variable. These projects include those where both sealed and nonsealed sections are employed, as well as those where different sealant materials are used. In the following section, the comparative performance of the pavement sections at these sites is examined with respect to sealing versus not sealing and, where different sealant materials are used, an examination of which sealants contribute to the best overall performance is also undertaken. The appropriate performance indicators that are considered include those shown in table 64.

Table 64. Pavement performance indicators related to sealing pavements.

Performance Measure	Represents. . .
Pumping	An indication of how well the sealant is succeeding in keeping moisture from infiltrating through the surface to underlying layers with pumpable material.
Joint Spalling	The effectiveness of sealant in keeping incompressibles out of the joint.
Faulting	An indirect indication of the presence of subsurface moisture, which may be in part a function of surface infiltration (faulting is primarily a function of joint load transfer).
D-cracking	Where susceptible aggregate is used, different ratings will be an indication of how much moisture infiltration is present.
Sealant Condition	Sealant may be present but not performing well. Sealant condition is a rating of how well the sealant is performing.
Overall Pavement Condition	An indication of the effect of joint sealant on the overall performance of the pavement.

Review of Project Data

There are nine projects in this study in which joint sealing is a variable. At six of the projects, a single sealant type is compared to no sealant; at one site, two different

sealants are compared to no sealant; and at two sites, different kinds of sealants are compared without a control (no sealant) section. For all sections included in this study (not just those in which sealing was a variable), the distribution of the number of sections by sealant type is shown in figure 28.

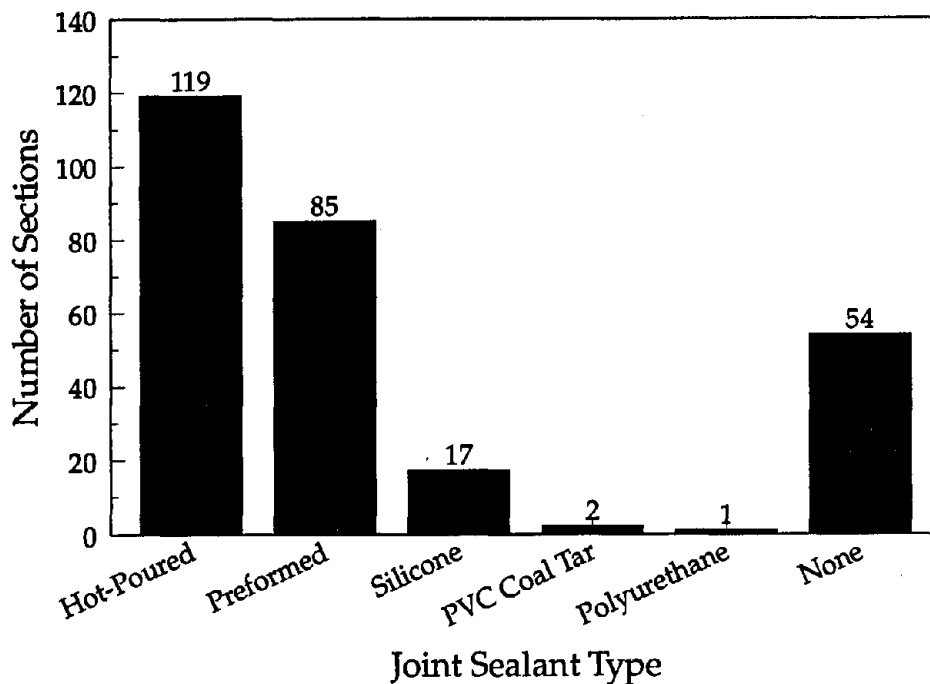


Figure 28. Number of sections sealed with each sealant material (for all sections).

### California 3

In 1975, the California Department of Transportation constructed a project on U.S. 101 near Geyserville to study the effects of shoulder type on pavement performance. In addition to the variation in shoulder type, however, some of the sections were constructed with sealed transverse joints, in contrast with Caltrans' standard practice at that time. All of these sections consist of a 9-in (229-mm) JPCP slab constructed over a 5.4-in (137-mm) CTB and a 6-in (152-mm) aggregate subbase. The nondoweled transverse joints are spaced at intervals of 12-13-19-18 ft (3.7-4.0-5.8-5.5 m).

At this site, six sections were constructed without any transverse joint sealant and four sections were constructed with preformed, neoprene sealant. Appropriate performance indicators for these sections are summarized in table 65. There are several indications from these data that the sealed sections are performing better than the nonsealed sections. Faulting is slightly lower on the sealed sections than on the nonsealed sections, and there are no spalled joints on the sealed sections, whereas the

sections without sealant are exhibiting a small amount of spalling. Nevertheless, after 17 years, the difference in spalling between the sealed and nonsealed joints does not appear to be significant.

Table 65. Summary of effect of joint sealant type for CA 3.

Transverse Joint Sealant Type	Shoulder Type	Shoulder Type							
		Tied PCC		Nontied PCC		AC			
Preformed	Faulting, in	3-1	3-6	3-3	3-8				
		0.09	0.04	0.05	0.10				
		% Joints Spalled	0	0	0			0	
		Pumping	N	N	N			N	
		D-Cracking	N	N	N			N	
		% Damaged Seals	28	11	0			100	
	None	Faulting, in	3-2	3-7	3-5	3-10	3-4	3-9	
			0.09	0.12	0.08	0.09	0.10	0.10	
			% Joints Spalled	3	2	6	2	0	0
			Pumping	N	N	N	N	L	M
			D-Cracking	N	N	N	N	N	N
			% Damaged Seals	n/a	n/a	n/a	n/a	n/a	n/a
IRI, in/mi	167	111	126	121	150	144			

1 in = 25 mm

1 mi = 1.61 km

Age = 17 years, ESAL's = 5.7 million

Common design features: 9-in nondoweled JPCP

12-13-19-18 ft Joints

5.4-in CTB

While there is pumping on only two sections, and these happen to be nonsealed, they are also sections that have AC shoulders, which may contribute to their poorer performance. On the sealed sections, for each shoulder type there is one section that has considerably less sealant damage than its pair, and that section has less than half of the faulting of the other. This suggests that better performing sealant does have a positive effect on pavement performance.

Although no FWD testing was performed on these sections in 1992, some sections were tested in 1987. These results can be used to examine the effect of joint sealant on loss of support. A direct comparison of CA 3-1 (preformed sealant) and 3-2 (no sealant) indicate no difference in performance, as neither section was exhibiting any loss of support. On CA 3-5 (no sealant), 12 percent of the corners were found to have loss of support, although this section had nontied PCC shoulders, which may have contributed to the loss of support.

From an examination of the performance indicators for this site in the WNF zone, it appears that joint sealing has a small positive effect on faulting (when the sealant is performing well) and a small (and perhaps insignificant) positive effect on joint spalling.

California 9

This project, located on I-680 in Milpitas, was constructed in 1974 to evaluate the effect of joint sealing on performance. The site consists of eight selected sections with four different transverse joint sealant materials, as well as control sections in which no sealant is used. The pavement itself is a 9-in (229-mm) nondoweled JPCP constructed on a 5.4-in (137-mm) CTB. Transverse joint spacing is varied in the pattern 12-13-19-18 ft (3.7-4.0-5.8-5.5 m). Subdrainage is only provided at one of the sections.

The sections were surveyed in 1992, after 18 years and approximately 10.5 million ESALs. Selected performance data from that survey are summarized in table 66. There is not a significant difference in performance among these sections, highlighted by the high average faulting of all the pavements. Notable exceptions are the sealant condition, pumping, and loss of support. None of the sealants is in good condition (100 percent damaged sealants) except for the preformed sealant, which has only 2 percent damaged seals.

Table 66. Summary of effect of joint sealing for CA 9.

		Transverse Joint Sealant Type							
		Poly-urethane		Hot-Pour		PVC Coal Tar		Preformed	
No Drains	Faulting, in	9-2	9-1 <sup>†</sup>	9-3	9-4	9-7 <sup>†</sup>	9-5	9-6 <sup>†</sup>	9-10
	% Joints Spalled	0.15	2	0	0.12	0	0.12	0	0.10
	Pumping	H		H	H		H		L
	% Corner Voids	5		30	54		6		75
	D-Cracking	N		N	N		N		N
	% Damaged Seals	100	100	100	100	100	2	0	n/a
	IRI, in/mi	148		154	161		163		153
Drains	Faulting, in								9-8
	% Joints Spalled								0.17
	Pumping								H
	% Corner Voids								20
	D-Cracking								N
	% Damaged Seals								n/a
	IRI, in/mi								212

1 in = 25 mm

1 mi = 1.61 km

†Sections were surveyed by automatic means; no additional data are available.

Common Design Features: 9 in nondoweled JPCP  
 12-13-19-18 ft Joints  
 5.4-in CTB  
 Age = 18 years  
 ESALs = 10.5 million

In terms of pumping, one of the two sections without sealant had a lower pumping rating than any of the sealed sections. On the other hand, this section also exhibited 75 percent corners with voids, more than any other section. The corresponding section with edge drains had voids at 20 percent of the corners tested. The best performing sections in terms of loss of support were those with the polyurethane and preformed sealants. The hot-pour and PVC coal tar sealants had greater loss of support, although still less than the nonsealed section. However, no correlation was observed between the percent of corners with breaks and corner cracking for these 18-year-old sections.

Overall, there is little to differentiate between either the performance of the various sealant materials or the performance of sealed versus nonsealed sites. The four different sealant materials are equally ineffective in reducing pumping or faulting, and the performance indicators in these sealed sections are about the same as those found in the sections that were not sealed. This is also reflected in the spalling results, which were very low throughout this project, on both sealed and nonsealed sections. However, the preformed sealant does stand out as the sole material that is performing well, despite the poor performance of the pavement section. An observation from these sections is that effective sealing alone is clearly not sufficient to reduce or eliminate load-induced distresses such as faulting or pumping; in such cases, dowel bars must be used to obtain good long-term joint performance.

### *Ohio 2*

This experimental project, constructed on S.R. 2 near Vermilion in 1974, was designed to study factors that may affect D-cracking. A total of 104 sections were constructed, covering a wide range of design variables, including those shown below:

- Edge drains and daylighting.
- Joint sealing and sealant type.
- Joint spacing.
- Maximum aggregate size and quality.
- Pavement type.
- Base type.
- Slab thickness.

Unfortunately, most of these sections are extremely short (about 240 ft [73.2 m]) and, depending on the joint spacing, there are not enough joints to provide a good indication of performance. In addition, for the sections of interest in this discussion of the contribution of sealant to performance, with the exception of the 40-ft (12.2-m) JRCP design, there are very few representative sections.

The 1992 performance of selected sections is summarized in table 67, after carrying an estimated 6.5 million ESALs. Looking at the comparative performance of the hot-pour and preformed sealants, direct comparison can be made between sections 2-12 and 2-14, 2-54/57 and 2-58, and 2-11 and 2-9. These pairs of sections

show little difference related to spalling or pumping, with a slight advantage on the preformed sections in terms of loss of support, faulting, and roughness. The preformed sealant shows more medium- and high-severity sealant damage.

A comparison of the performance of sealed and nonsealed sections shows mixed results. For example, OH 2-73 (no sealant) has a higher faulting level and more extensive D-cracking than OH 2-69 (hot-pour sealant), whereas the opposite is true for OH 2-59 (no sealant) and OH 2-54/57 (hot-pour sealant). Similar findings are observed for the comparisons between no sealant and preformed sealants. In terms of loss of support, however, the nonsealed sections have fewer corners with voids compared to the corresponding sections with hot-pour or preformed sealant. The presence of D-cracking was found to have a major impact on joint spalling.

#### *Wisconsin 2/Wisconsin 7*

These two projects are located adjacent to each other on U.S. 18/151 (WI 2 is near Mt. Horeb and WI 7 is near Barneveld). Both sets of sections were constructed in 1988 and share a general pavement design that consists of a 9-in (229-mm) JPCP with variable spaced (12-13-19-18 ft [3.7-4.0-5.8-5.5 m]) and skewed transverse joints. Design variables include 1.25-in (32-mm) epoxy-coated dowels versus none, preformed sealant versus none, base type, and drainage type. Because of the similarity and proximity of the sections, the performance of the two sections is considered together.

The performance of these sections is summarized in table 68, after 4 years and approximately 1.3 million ESALs for all distresses except spalling, which was resurveyed after 9 years of pavement service and approximately 3 million ESALs. An examination of these results suggests some interesting trends, although it must be realized that these sections are not very old and have not been exposed to high traffic volumes. The first item to note is that although there is spalling in both the sealed and nonsealed sections, the nonsealed sections have slightly lower levels of spalling. Faulting levels are fairly low throughout the two projects, but they are higher on the sections without dowels. Faulting on the nondoweled sections is slightly higher on some of the nonsealed sections than on the sealed sections, but the data are not definitive enough to draw any conclusions about the benefits of sealing in terms of reducing faulting. Of the sections examined, only one section is showing any signs of pumping. However, that is the nondrained, nonsealed section (WI 2-4); a similar design with sealant (WI 2-5) shows no signs of pumping. Only two sections show any loss of support (WI 7-1 has preformed sealant and WI 7-2 has no sealant), and both sections are nondoweled sections with an aggregate base. None of the sections show any D-cracking. In terms of roughness, no appreciable difference is noticed between the sealed and nonsealed sections, although it should be remembered that the sections are only 4 years old. Considering that nonsealed joints did not exhibit significantly worse performance than sealed sections but offered significant cost saving, Wisconsin's nonsealed joint design might be considered as a very attractive alternative to the traditional joint design and needs to be investigated in other regions.



Table 67. Summary of effect of joint sealing on OH 2.

Base Type	Sealant Type	Joint Spacing	20-ft JPCP				40-ft JRCP									60-ft JRCP			
			No Drains		Drains		No Drains			Daylighted			Drains			Drains			
			0.5	1.5	0.5	1.5	0.5	1.0	1.5	0.5	1.0	1.5	0.5	1.0	1.5	0.5	1.5		
AGG	None	Faulting, in			<u>2-13</u>			<u>2-73</u>			<u>2-59</u>			<u>2-22</u>					
	% Joints Spalled			0.13			0.05			0.01			0.06						
	Pumping			79			0			14			0						
	% Corner Voids			N			N			N			N						
	D-Cracking			25			0			0			0						
	% Damaged Seals			N			H			N			N						
	IRI, in/mi			n/a			n/a			n/a			n/a						
				157			170			147			136						
	HP	Faulting, in			<u>2-17</u>	<u>2-12</u>	<u>2-75</u>	<u>2-74</u>	<u>2-69</u>	<u>2-55</u>	<u>2-56</u>	<u>2-54</u>	<u>2-57</u>	<u>2-24</u>	<u>2-23</u>	<u>2-20</u>	<u>2-21</u>	<u>2-18</u>	<u>2-11</u>
	% Joints Spalled			0.24	-	0.01	0.03	0.01	0.07	0.02	0.11	0.04	0	0	0.08	0.04	0.17	-	
	Pumping			0	100	14	29	29	0	0	10	29	0	17	57	0	0	100	
	% Corner Voids			N	N	N	N	N	N	N	N	N	N	N	N	N	N	N	
	D-Cracking			100	-	-	0	0	40	10	50	-	10	0	-	20	95	-	
	% Damaged Seals			H	N	L	L	L	M	L	M	L	M	L	H	H	H	H	
	IRI, in/mi			64	0	14	43	28	0	0	14	14	0	17	0	57	15	100	
				239	171	130	140	128	190	114	168	132	161	170	201	180	296	161	
	Pref	Faulting, in			<u>2-14</u>								<u>2-58</u>					<u>2-9</u>	
	% Joints Spalled			0.03									0.02					-	
	Pumping			100									17					100	
	% Corner Voids			N									N					N	
	D-Cracking			67									25					-	
	% Damaged Seals			H									M					H	
	IRI, in/mi			85									67					88	
				183									126					154	

1 in = 25.4 mm; 1 ft = 0.305 m; 1 mi = 1.61 km

All sections except 20-ft JPCP designs contain 1.25-in dowels.

Table 68. Summary of effect of joint sealant for WI 2/WI 7.

			Longitudinal Drains			Trans. Drains	No Drains
			PCTB	PATB	PAGG	AGG	AGG
1.25-in Epoxy-Coated Dowels	Preformed Seals	Faulting, in % Joints Spalled Pumping % Corner Voids D-Cracking % Damaged Seals IRI, in/mi					<u>2-5</u> 0.01 0 N 0 N 2 122
	No Seals	Faulting, in % Joints Spalled Pumping % Corner Voids D-Cracking % Damaged Seals IRI, in/mi	<u>2-1</u> 0.01 0 N 0 N n/a 122	<u>2-2</u> 0.01 3 N 0 N n/a 106	<u>2-3</u> 0.01 3 N 0 N n/a 112	<u>7-10</u> 0.01 0 N - N n/a 113	<u>2-4</u> 0.01 0 M 0 N n/a 121
No Dowels	Preformed Seals	Faulting, in % Joints Spalled Pumping % Corner Voids D-Cracking % Damaged Seals IRI, in/mi	<u>7-3</u> 0.01 6 N 0 N 0 147	<u>7-5</u> 0.01 2 N 0 N 0 86	<u>7-1</u> 0.03 3 N 100 N 0 136		<u>7-8</u> 0.04 3 N 0 N 0 116
	No Seals	Faulting, in % Joints Spalled Pumping % Corner Voids D-Cracking % Damaged Seals IRI, in/mi	<u>7-4</u> 0.04 3 N 0 N n/a 147	<u>7-6</u> 0.02 3 N 0 N n/a 98	<u>7-2</u> 0.03 3 N 100 N n/a 120	<u>7-7</u> 0.02 0 N - N n/a 117	<u>7-9</u> 0.04 0 N 0 N n/a 114

1 in = 25 mm

1 mi = 1.61 km

Age = 4 years, ESALs = 1.3 million (all distresses except spalling)

Age = 9 years, ESALs = 3.0 million (for spalling)

Common Design Features:

9 in JPCP

12-13-19-18 Joints

#### Wisconsin 4

The six sections in WI 4 include five sections in the northbound lanes and one section in the southbound lanes of STH 164 in Waukesha. The pavement was

constructed in 1988, and the primary design features include a 9-in (229-mm) JPCP with tied PCC shoulders placed on an AGG base. The transverse joints are spaced at 20-ft (6.1-m) intervals and are not doweled. Other design variables include sections with and without longitudinal edge drains, sections with and without transverse joint drains, and sections with and without a preformed joint sealant at the transverse joints.

The performance data, available after 9 years and 3.0 million ESALs, show that the nonsealed sections have slightly more spalling than the sealed sections; however, it does not mean that nonsealed joints exhibited significantly worse overall performance. The majority of spalls observed in these sections, including the spalls rated as medium- and high-severity spalls according to SHRP classification were less than 2 ft wide and seemed not to affect pavement ride quality. Although the nonsealed joints were filled by fine incompressibles, it appeared that those incompressibles did not cause any significant damage to the pavement and helped the pavement to keep large incompressibles out of the joints, acting like a natural sealant.

#### *Wisconsin 5*

The WI 5 project is located on STH 50 near Kenosha. Constructed in 1988, the pavement consists of 10-in (254-mm) JPCP on a dense-graded aggregate base. The transverse joints are non-doweled and have a variable spacing of 12-13-19-18 ft (3.7-4.0-5.8-5.5 m). Three different types of drainage are provided: longitudinal fin drains, longitudinal pipe drains, and none (no edge drains). For each drainage type, a sealed and nonsealed section exists; the sealed sections use silicone sealant.

Performance data for these sections are summarized in table 69, after 4 years and 1.4 million ESALs. The results show no substantial contribution to performance from joint sealing. Faulting levels are approximately equal between sealed and nonsealed sections, and there is no evidence of pumping or D-cracking on any of the sections. Likewise, loss of support was observed on only one section (WI 5-1), which contains a silicone joint sealant. Similar results are observed in terms of roughness, as two comparisons show an advantage on the nonsealed sections, whereas another comparison indicates the sealed section has less roughness.

An interesting aspect of the sealed sections is the comparatively high amount of transverse joint spalling and the percent of damaged seals. Less spalling is present on the nonsealed sections than on the sealed sections. In any case, the spalling and sealant damage are not expected in such a new pavement and suggest several possibilities: deficiencies in the sealant material, compatibility problems between the sealant and the pavement, or problems created during installation of the sealant that have contributed to these early distresses. Of these, the latter is perhaps the most likely cause.

Table 69. Summary of effect of joint sealing for WI 5.

		Type of Longitudinal Drain		
		Fin Drain	Pipe Drain	None
Silicone Sealant	Faulting, in	<u>5-1</u> 0.03	<u>5-3</u> 0.06	<u>5-5</u> 0.04
	% Joints Spalled	6	0	3
	Pumping	N	N	N
	% Corner Voids	20	0	0
	D-Cracking	N	N	N
	% Damaged Seals	13	59	0
	IRI, in/mi	138	147	133
No Sealant	Faulting, in	<u>5-2</u> 0.05	<u>5-4</u> 0.06	<u>5-6</u> 0.03
	% Joints Spalled	0	0	3
	Pumping	N	N	N
	% Corner Voids	0	0	0
	D-Cracking	N	N	N
	% Damaged Seals	n/a	n/a	n/a
	IRI, in/mi	132	142	142

1 in = 25 mm

1 mi = 1.61 km

Age = 4 years, ESALs = 1.4 million (all distresses except spalling)

Age = 9 years (spalling)

Common Design Features:

10-in nondoweled JPCP

12-13-19-18-ft Joints

6-in AGG Base

### Wisconsin 6

This project, constructed in 1988, is located on STH 29 near Green Bay. The four sections in this project are all 10-in (254-mm) JPCP with a 12-13-19-18-ft (3.7-4.0-5.8-5.5-m) transverse joint spacing. All sections are constructed on a 4-in (102-mm) permeable aggregate base. Design variables include doweled (1.5-in [38-mm] diameter) and nondoweled joints and sealed (preformed compression sealant) and nonsealed joints.

The 1992 performance of these sections for all distresses except spalling and 1997 performance with respect to joint spalling are summarized in table 70. At the time of 1992 survey, the sections had been subjected to about 4.2 million ESALs. With the exception of IRI, the performance of the doweled sections with and without joint sealant are about the same; the IRI is slightly higher on the nonsealed section. On the nondoweled sections, the sealed section is performing slightly better (in terms of faulting) than the section without sealant. Spalling and roughness also show an advantage on the sealed sections, exhibiting fewer spalled joints and less roughness on the nondoweled sections. The preformed sealant is performing very well, with no damaged seals noted. Not represented in these data is the fact that all of the sections are exhibiting unusually high levels of low-severity spalling (only medium- and high-

severity spalling are presented in the table). The possible cause of this spalling is construction problems during joint sawing.

Table 70. Summary of effect of joint sealing for WI 6.

		1.50-in Dowels	No Dowels
Preformed Compression Sealant	Faulting, in	<u>6-3</u> 0.00	<u>6-2</u> 0.04
	% Joints Spalled	0	2
	Pumping	N	N
	D-Cracking	N	N
	% Damaged Seals	0	0
	IRI, in/mi	81	77
No Sealant	Faulting, in	<u>6-4</u> 0.00	<u>6-1</u> 0.07
	% Joints Spalled	2	18
	Pumping	N	N
	D-Cracking	N	N
	% Damaged Seals	n/a	n/a
	IRI, in/mi	102	88

1 in = 25 mm

1 mi = 1.61 km

Age = 4 years, ESALs = 4.2 million (all distresses except spalling)

Age = 9 years (spalling).

Common Design Features:

10-in JPCP

12-13-19-18-ft Joints

4-in PAGG

For nondoweled sections, there is some evidence to suggest that sealing does reduce joint spalling, but the extensive amount of spalling on that nondoweled, nonsealed section (section 6-1) and the absence of similar levels of spalling on the other sections might suggest a data anomaly; thus, it is possible that other factors (such as snow plows or construction problems during joint sawing) caused the spalling on section 6-1.

### West Virginia 1

Three sections on I-77 near Charleston comprise WV 1. These sections were not constructed as an experiment and, in fact, the pavements were all built at different times. The pavements have in common the following characteristics: 10-in (254-mm) slab, 1.25-in (32-mm) dowels, and an AASHTO A-4 subgrade. Aside from the age and accumulated ESALs, variables include the joint spacing, pavement type, base type, and sealant type.

The 1992 performance of these sections is summarized in table 71. Because of the range of ages and accumulated ESALs of these sections, as well as the different joint spacings of these sections, it is difficult to draw valid conclusions. None of the

sections exhibit pumping or D-cracking, and faulting levels are fairly low considering the age of these sections. There is a large amount of transverse joint spalling, and even more if the low-severity spalling is considered. The two sections with a silicone sealant have loss of support at 100 percent of the joints, compared to no loss of support on the section with a hot-pour sealant. The sealant damage is also quite high, indicating the need for maintenance of these joints. The section with hot-pour sealant has less roughness even though it is older and has been exposed to more ESAL applications; however, it is also the only section constructed on CTB, which may also be contributing to smoother ride. The different ages of the sections make it difficult to draw any meaningful conclusions regarding the relative performance of the two sealant materials.

Table 71. Summary of effect of joint sealing for WV 1.

	JRCP 0.1% steel 40 ft Joints 6-in AGG	JRCP 0.1% steel 40-ft Joints 6-in CTB	JPCP 15-ft Joints 6-in AGG
Year Built	1986	1981	1989
ESALs, millions	6.5	8.9	3.7
Sealant Type	Silicone	Hot-Pour	Silicone
Faulting, in	<u>1-1</u> 0.02	<u>1-2</u> 0.06	<u>1-3*</u> 0.04
% Joints Spalled	35	50	67
Pumping	N	N	N
% Corner Voids	100	0	100
D-Cracking	N	N	N
% Damaged Seals	81	100	84
IRI, in/mi	168	142	168

1 in = 25 mm

1 ft = 0.305 m

1 mi = 1.61 km

Common Design Features: 10-in PCC Slab

1.25-in Dowels

\* Section added as truck climbing lane to existing 60-ft JRCP.

### Overall Evaluation of Joint Sealant

The performance of these sections is quite variable and, in some cases, runs counter to what might be expected. For example, there are a number of projects in which the nonsealed sections are performing better than their sealed counterparts. This result might not be so mysterious if more were known about the construction process. Moreover, under certain conditions, such as premature sealant failure, joint sealing might contribute to poorer pavement performance<sup>(42)</sup>. In addition, many of the nonsealed sections are young or are located in a mild climate. However, a few projects also showed that the sealed sections performed better than the nonsealed sections, the expected result.

The overall effect of sealing on spalling is presented in figure 29. The sections with hot-poured sealant and silicone sealant both have a total of 44 percent of the joints exhibiting spalling, while the sections with preformed sealant and no sealant both exhibit approximately 26 percent spalling. From the limited data, it can be concluded that the preform seals are the best material for limiting spalling, and the silicone sealant is better than the hot-pour sealant. On the other hand, the relatively low percentage of joint spalling of the nonsealed sections suggests that, in some cases, nonsealed joints can perform well. What is not evident from figure 29 are the effects of traffic and climatic forces on sealed (or nonsealed) performance.

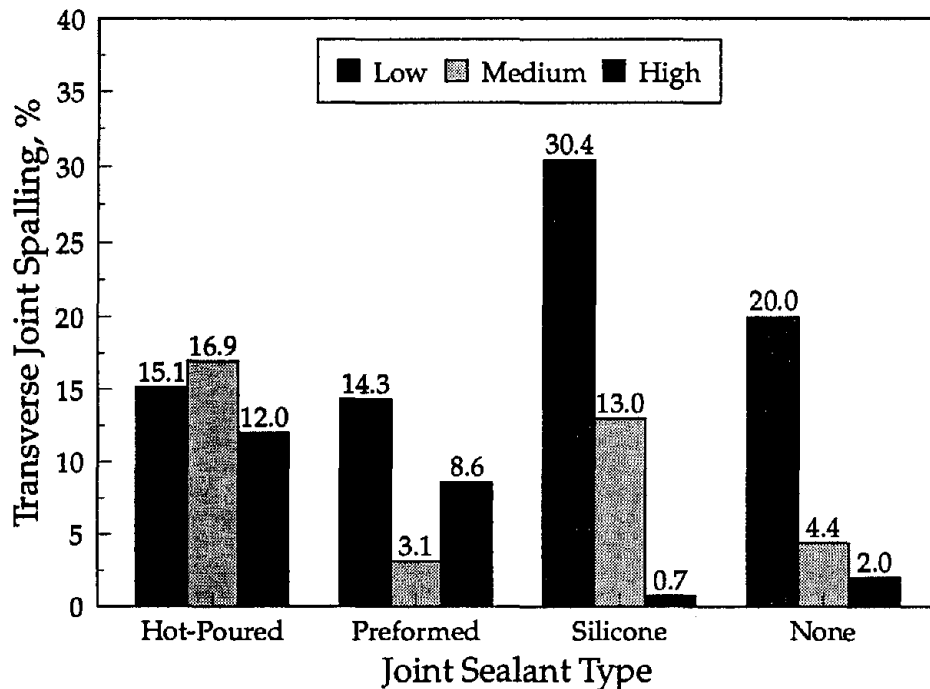


Figure 29. Transverse joint spalling percentage by sealant type for all sections.

The sections in which sealant type is a variable also show inconsistent trends. In OH 2, the limited data show that the hot-pour material performed better than the preformed sealant. However, in CA 9 and WI 6, the preformed material performed very well. The overall performance rating of all of the sealants evaluated in this study is shown in figure 30, with the exception of the two sections that had PVC coal tar sealant and the one section that had polyurethane sealant. The hot-pour materials are the worst, as 49 percent of these materials are showing some damage. The preformed materials and the silicones are performing similarly, with 37.4 and 37.8 percent overall damage, respectively. However, the silicones are showing slightly less medium- and high-severity sealant damage.

Figure 31 illustrates IRI as a function of ESAL applications, broken out by sealant type. This figure does not show any significant trends in terms of the different sealant types. Several sections with a hot-poured sealant are showing considerable roughness, although other sections show little roughness for nearly 20 million ESAL applications. Although not as abundant, the sections with a silicone sealant are not showing as much roughness.

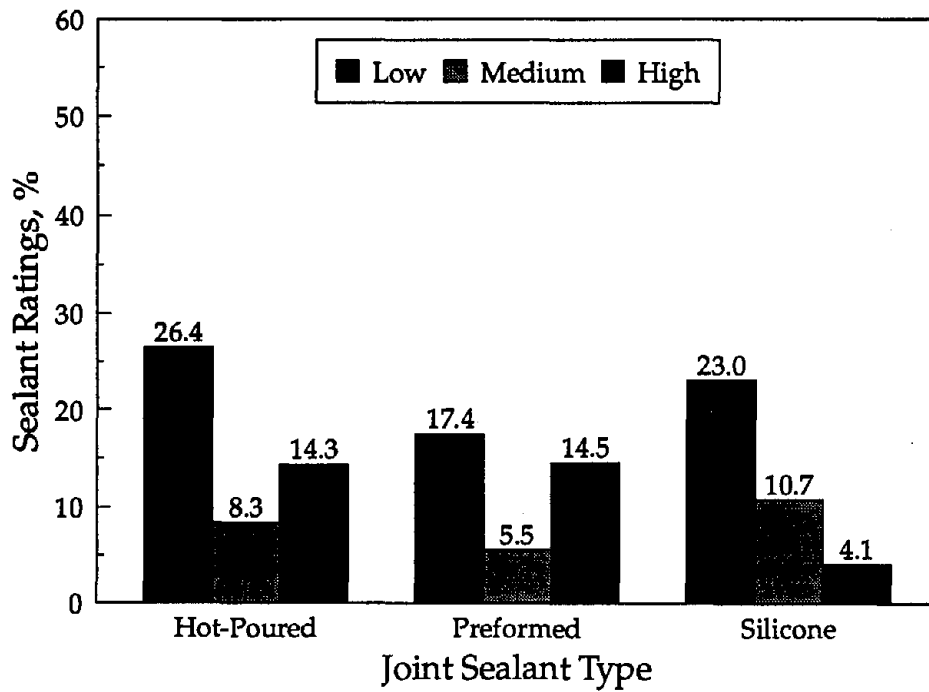


Figure 30. Sealant condition rating by joint sealant type for all sections.

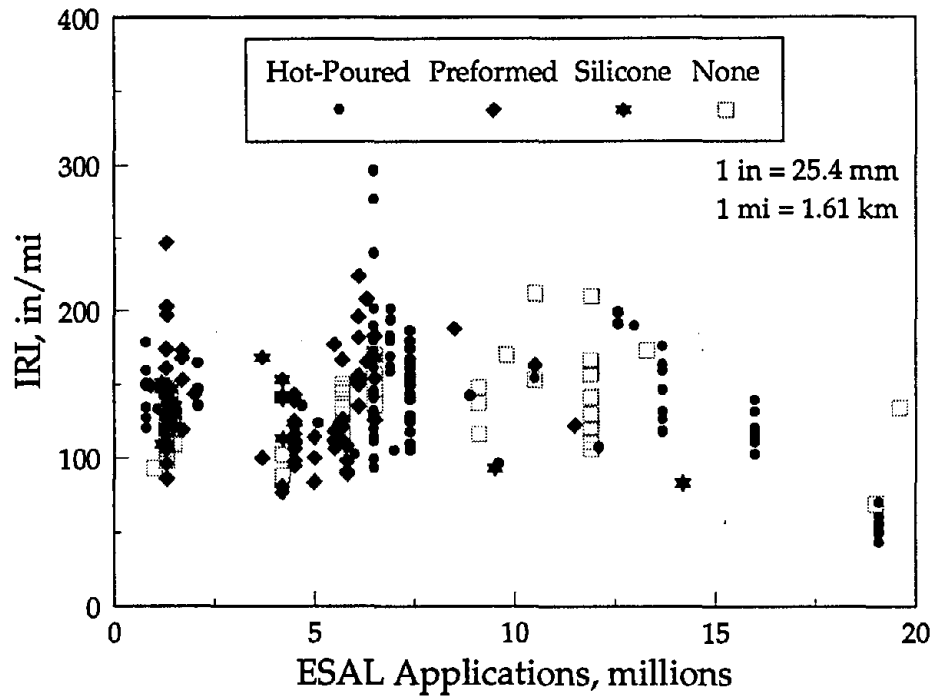


Figure 31. Comparison of IRI for different joint sealant types.



Although joint spalling has traditionally been believed to be influenced by joint sealing, other factors such as concrete durability may also play an important role. Furthermore, the effectiveness of sealing must be better investigated in terms of other distress indicators, such as loss of support, which may have a larger effect on overall pavement performance than joint spalling.

To investigate this, an evaluation of the effect of joint sealant on loss of support was conducted, but mixed results were obtained. For example, CA 9 showed a wide variation in loss of support between the different sealant types and between the sealed and nonsealed sections. The sections with polyurethane and preformed sealants exhibited the least number of corners with voids, the sections with hot-pour and PVC coal tar sealants showed more voids, and the nonsealed sections showed the most corners with voids. The results from OH 2, however, indicate that the nonsealed sections have the same or less potential for loss of support. Although direct comparisons are not available for the nonsealed sections on CA 1, a comparison of the 1987 and 1992 deflection testing results indicate a substantial increase in loss of support, often as many as 40 percent more corners with voids. The lack of joint sealant is a likely contributor to this increase.

Joint sealing costs money. It starts with an initial expense associated with the construction of appropriate sealant reservoirs and the placement of the sealant; in a well-maintained pavement, that initial expense is followed by the additional expense of replacing the sealant at some regular interval. Furthermore, in an otherwise well-designed and good performing pavement, it might be necessary to seal the joints when, at least visually, the pavement is in good condition. Such a strategy is difficult for many agencies to accept. It requires incurring expenses and traffic delays on a pavement that does not appear to need it, and one can always find pavements that are in worse condition that could use maintenance or rehabilitation.

The expense of joint sealing must be justified by demonstrating the contribution of sealed joints to long-term pavement performance. However, benefits may take a long time to be realized. If there is a material problem such as D-cracking, which takes many years to develop, sealant may eventually help to mitigate the effect. Pumping and subsequent faulting may also be lower over time on pavements that are well sealed. Adding sealant as a design feature is not sufficient to address moisture-related problems in a pavement, as these will still occur if steps are not taken to address the moisture that will get into the pavement structure. It has also been seen that sealing a pavement cannot take the place of using load transfer devices where they are needed.

For the benefits of sealant to be realized, the sealant must perform well. In several of these projects there were early sealant failures or higher pavement distresses when sealant was used. Some early sealant material failures may be attributable to one or more of the following construction problems:

- Sawing concrete that is too green.
- Inadequate sealant reservoir preparation.
  - Remaining laitance.
  - Presence of dust or debris.
- Inadequate sealant curing.
- Poor sealant reservoir design.
- Improper material handling.

It is clear that if any benefits are to be derived from sealing, the sealant preparation and placement must be done in a manner that does not contribute to the failure of the pavement. On the other hand, Wisconsin's experience with nonsealed joints which exhibited good overall performance 9 years after traffic opening (Sections WI-2, WI-4, WI-5, WI-6, and WI-7) suggests that Wisconsin's joint design (1/8-in [3-mm] wide, unfilled, and unsealed) is an attractive and cost-effective alternative that needs to be investigated and tested for other climatic regions.

### **Base Type**

The type of base course can influence the performance of PCC pavements, mainly as a result of the support and drainage conditions of the base. A stiffer base course generally provides better support to the PCC slab, which can reduce the potential for faulting. However, a stiffer base can also magnify the effects of curling and warping, thus increasing the potential for transverse cracking.

Because moisture can have such a profound effect on material properties and the overall performance of pavements, a base that improves the drainage of the pavement structure ultimately improves the performance of the pavement. Consequently, many highway agencies have adopted the use of permeable base courses (stabilized and nonstabilized) to provide positive drainage. These base courses contain a relatively large top-size aggregate in conjunction with very few fines, a combination that allows the rapid movement of water through the base. Longitudinal drains located at the edge of the pavement collect the water and transport it away from the pavement structure. A filter layer or separator layer is often placed directly beneath the permeable layer to prevent fines and other debris from clogging the base.

One prominent distress associated with base type is pumping, which ultimately leads to faulting. For pumping to occur, three conditions must be present:

- Repeated heavy loads.
- Presence of moisture in the pavement structure.
- An erodible base material.

This section deals with means of reducing pumping, faulting, and other distress types through different base types and support conditions.

## Review of Project Data

Many projects contain sections in which different base types are incorporated. The following base types are represented:

- Dense-graded aggregate base (AGG).
- Cement-treated base (CTB).
- Lean concrete base (LCB).
- Asphalt-treated base (ATB).
- Asphalt concrete base (AC).
- Soil cement base (SC).
- Sand base (SAND).
- Permeable aggregate base (PAGG).
- Permeable cement-treated base (PCTB).
- Permeable asphalt-treated base (PATB).

Some of the bases were also daylighted. In addition, some slabs were constructed directly on the subgrade. Figure 32 illustrates the distribution of the various base types. Aggregate bases are the most widely used base type, although stabilized bases (ATB, CTB, and LCB) are also well represented. Thirty-six sections were constructed on permeable bases.

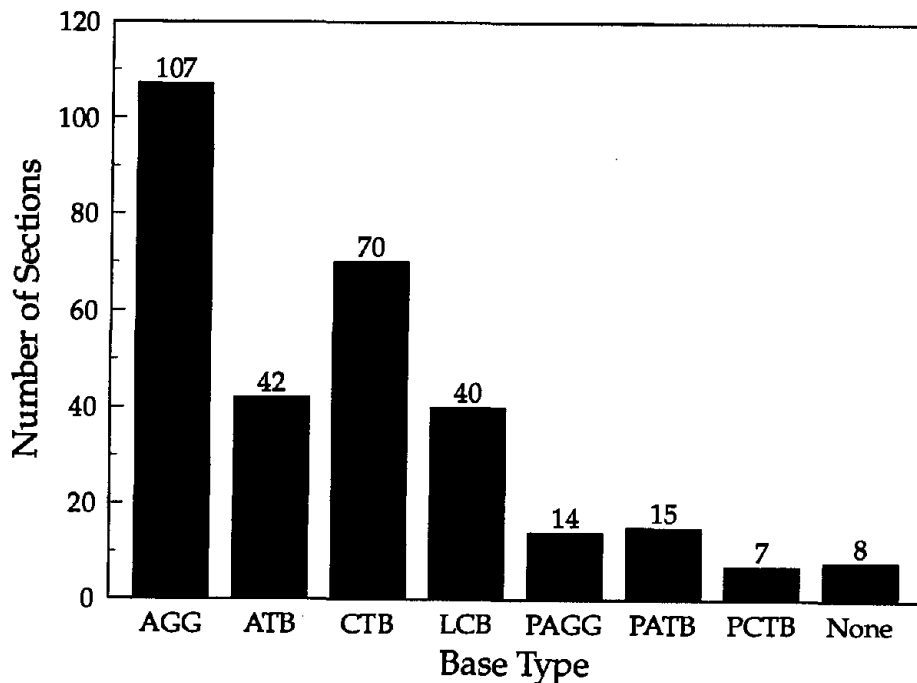


Figure 32. Distribution of different base types.

The base type determines the design factors of interest. For instance, the cement content is a major factor when evaluating CTB. Likewise, the asphalt content and mix type are critical for ATB. For aggregate bases, the percent of fines and the plasticity index are critical factors. These factors are provided when comparing different base types, although they are unavailable in some instances.

### Arizona 1

This project is located on State Route 360 in Phoenix. All sections are nondoweled JPCP with random, skewed transverse joints spaced at 13-15-17-15-ft (4.0-4.6-5.2-4.6-m) intervals. Three sections are examined for the effect of base type. AZ 1-1 is a 9-in (229-mm) JPCP with a 6-in (152-mm) CTB containing 4.3 percent cement and 4-in (102-mm) aggregate subbase. AZ 1-6 is also a 9-in (229-mm) JPCP, but contains a 4-in (102-mm) LCB with 6.9 percent cement and no subbase. AZ 1-5 is an 11-in (279-mm) JPCP with no base. AZ 1-1 has an AC shoulder, whereas the other sections have a tied PCC shoulder. In addition to slab thickness and shoulder type, the comparisons are complicated by differences in age and traffic.

The performance data for the AZ 1 sections are summarized in table 72. Of the different base types—CTB, LCB, and none—the section with a CTB exhibited the worst performance in terms of faulting, longitudinal cracking, and spalling. That section also had the highest edge and corner deflections. Although that section is the oldest of the three sections, the poor performance (especially faulting) is believed to be a result of erosion of the CTB. It is also the only section with an AC shoulder, which may be further contributing to the poor performance. Conversely, the roughness measurements, which are generally well correlated with faulting, indicate that the pavement is smoother than the section with an LCB.

Table 72. Summary of effect of base type for AZ 1.

Section	Design	Year Built	ESALs, millions	Faulting, in	% Slabs Cracked	Long Crk, ft/mi	% Joints Spalled	IRI, in/mi (PSR)
AZ 1-1	9-in JPCP 6-in CTB 4-in AGG AC Shoulder	1972	7.0	0.08	0	278	24	105 (3.9)
AZ 1-6	9-in JPCP 4-in LCB Tied PCC Shld	1981	5.1	0.01	0	0	3	123 (3.5)
AZ 1-5	11-in JPCP No Base Tied PCC Shld	1979	6.0	0.03	0	0	18	102 (3.9)

1 in = 25.4 mm  
1 ft = 0.305 m  
1 mi = 1.61 km

Common Design Features: 13-15-17-15-ft nondoweled joints

The section with no base (AZ 1-5) shows performance similar to that of the section with an LCB. Thus, the 2 in (51 mm) of additional PCC thickness appears to be comparable to the 4-in (102-mm) LCB. However, these sections are located in a mild climate with little rainfall and no freezing conditions. Sections located outside the dry-nonfreeze region would not be expected to perform as well without a base course.

### California 1

This project, located on I-5 near Tracy, provides a direct comparison of CTB and LCB with all other design features held constant. CA 1-3 and 1-4 incorporated a 4-in (102-mm) CTB with 4.0 percent cement, whereas CA 1-7 and 1-8 contain a 4-in (102-mm) LCB with 9.4 percent cement. Each section is an 8.4-in (213-mm) nondoweled JPCP with a 24-in (610-mm) aggregate subbase. The transverse joints are skewed and spaced at 12-13-19-18-ft (3.7-4.0-5.8-5.5-m) intervals.

Table 73 provides a summary of the 1992 performance data for the CA 1 sections. The sections with a LCB exhibit much less faulting, whereas transverse cracking is slightly higher. Both corner and edge deflections are lower on the LCB section. The results indicate that the LCB is more effective at reducing faulting but may contribute to the development of transverse cracking through increased thermal curling stresses, especially on the longer slab lengths of the pattern.

Table 73. Summary of effect of base type for CA 1.

Section	Base Type	ESALs, millions	Joint Faulting, in	% Slabs Cracked	Long Crk, ft/mi	% Joints Spalled	IRI, in/mi (PSR)
CA 1-3	4-in CTB	11.9	0.08	18	812	1	111 (3.3)
CA 1-4	4-in CTB	11.9	0.10	53	0	3	157 (3.3)
CA 1-7	4-in LCB	11.9	0.02	24	210	9	120 (3.1)
CA 1-8	4-in LCB	11.9	0.04	60	85	6	106 (3.5)

1 in = 25.4 mm  
 1 ft = 0.305 m  
 1 mi = 1.61 km

Common Design Features: 8.4-in JPCP  
 12-13-19-18-ft nondoweled joints  
 Built in 1971

### California 2

This project contains two sections on I-210 near Los Angeles, that were specifically designed to evaluate the effect of base type on concrete pavement performance. CA 2-2 contains a PCTB, and CA 2-3 contains a CTB. However, on CA 2-2, a thin AC layer was placed between the slab and the PCTB, rendering the drainage characteristics ineffective. Both sections are 8.4-in (213-mm) JPCP with a random

joint spacing of 12-13-19-18 ft (3.7-4.0-5.8-5.5 m). The transverse joints do not contain dowel bars and are not sealed.

Table 74 shows the performance data for CA 2. The section with the PCTB has a higher faulting level than the section with a CTB. However, faulting on both sections is excessive, which indicates a need for dowel bars. The thin AC layer has reduced the effectiveness of the permeable base, preventing the removal of water and thus increasing the potential for faulting. Conversely, the section with the CTB has considerably more transverse cracking and joint spalling. Most of the cracking occurs on the 18- and 19-ft (5.5- and 5.8-m) slabs. The combination of the long slab and stiff base augments the thermal curling effects, which contributes to the development of transverse cracking. California now employs transverse joints spaced at 12-13-15-14-ft (3.7-4.0-4.6-4.3-m) intervals.

Table 74. Summary of effect of base type for CA 2.

Section	Base Type	ESALs, millions		Joint Faulting, in		% Slabs Cracked		% Joints Spalled		IRI, in/mi (PSR)	
		1987	1992	1987	1992	1987	1992	1987	1992	1987	1992
CA 2-2	AC/PCTB	7.6	11.9	0.11	0.16	0	3	0	3	-(3.8)	137 (4.0)
CA 2-3	CTB	7.6	11.9	0.11	0.13	66	68	0	15	-(4.1)	116 (3.9)

1 in = 25.4 mm  
 1 ft = 0.305 m  
 1 mi = 1.61 km

Common Design Features: 8.4-in JPCP  
 12-13-19-18-ft nondoweled joints  
 Built in 1980

Deflection data from 1987 reveal higher midslab and corner deflections for the CTB section. Although the AC layer diminishes the potential of the permeable base to remove moisture, it appears to provide stable, uniform support to the PCC slab.

A comparison of the performance between 1987 and 1992 indicates that both sections have displayed increases in faulting, transverse cracking, and joint spalling. The most substantial increases are faulting on CA 2-2 and joint spalling on CA 2-3. The serviceability values have remained essentially unchanged since 1987.

### California 6

This project, located on Route 14 near Los Angeles, consists of two separate PCC pavement sections. Both sections are 9-in (229-mm) JPCP without dowels at the transverse joints. CA 6-1 incorporates a 5.4-in (137-mm) CTB with 4 percent cement and a random 12-13-19-18-ft (3.7-4.0-5.8-5.5-m) joint spacing. CA 6-2 has a 4.2-in (107-mm) PATB with 2 percent AR-4000 and a random 12-13-15-14-ft (3.7-4.0-4.6-4.3-m) joint spacing.

A summary of the performance data for the CA 6 sections is provided in table 75. The section with the CTB is exhibiting substantially more faulting than the section with the PATB. The CTB does not appear to be as effective as the PATB at preventing erosion and pumping, which lead to faulting. Although the section with the CTB is 9 years older and has been exposed to 3.5 million more ESAL applications, the section showed similar faulting levels during the 1987 survey. The section with the CTB also has slightly more transverse cracking, joint spalling, and roughness, although these differences may be explained by the age differences.

Table 75. Summary of effect of base type for CA 6.

Section	Year Built	ESALs, millions	Base Type	Joint Faulting, in	% Slabs Cracked	Long Crk, ft/mi	% Joints Spalled	IRI, in/mi (PSR)
CA 6-1	1971	13.3	5.4-in CTB	0.14	4	0	3	173 (3.8)
CA 6-2	1980	9.8	4.2-in PATB	0.05	0	0	0	170 (3.8)

1 in = 25.4 mm  
 1 ft = 0.305 m  
 1 mi = 1.61 km

Common Design Features: 9-in JPCP  
 Nondoweled joints

Based solely on the performance data, CA 6-2 appears to be performing well. However, research conducted by the California Department of Transportation indicates that significant stripping of the PATB has occurred and that the aggregate is in a loose, unbound state.<sup>(43)</sup> Faulting and movement of the unbound aggregate was also noted. This condition is expected to adversely affect the future performance. As a result, California made several design changes: increased the asphalt content of PATB to 3 percent by weight of aggregate, increased the crushing requirement, and upgraded the separation layer to a primed base material to reduce erosion on top of the separator layer. However, a memo issued by the California Department of Transportation (dated 11-8-96) prohibits the use of PATB under JPCP until the stripping problems are further studied and addressed.

#### Florida 4

This experimental project was designed to investigate the feasibility of constructing a two-course pavement system consisting of an LCB bonded to a thin concrete surface wearing course.<sup>(14,15)</sup> It is located in the southbound lanes of U.S. 41 between Punta Gorda and Ft. Myers. All sections in this evaluation are 3-in (76-mm) JPCP bonded to an underlying 9-in (229-mm) LCB. Three different LCBs were used, each containing a different percentage of cement:

- LCB "A"—8.5 percent cement.
- LCB "B"—7.3 percent cement.
- LCB "C"—5.5 percent cement.

The overall analysis is divided into three separate evaluations—one for each specific design. FL 4-2 through 4-6 contain 15-ft (4.6-m) skewed joints without dowels and a 6-in (152-mm) shell-stabilized subgrade (A-3). FL 4-7, 4-8, and 4-9 contain 15-ft nondoweled joints and a 6-in (152-mm) cement-treated subgrade (A-3). Finally, FL 4-10 and 4-11 contain 20-ft (6.1-m) joints with 1-in (25-mm) dowels and a 6-in (152-mm) shell-stabilized subgrade (A-3).

Table 76 presents a summary of the performance data for FL 4. The sections constructed on a higher strength LCB (higher cement content) are performing slightly better than those constructed on a lower strength LCB. This trend is especially noticeable from the joint faulting and serviceability measurements. Transverse cracking and joint spalling are virtually nonexistent on these sections. Two sections exhibit substantial longitudinal cracking, although the reason for this occurrence is not known.

Table 76. Summary of effect of base type for FL 4.

Section	Base Type	Dowel Dia, in	Jt Spc, ft	ESALs, millions	Joint Faulting, in	% Slabs Cracked	Long Crk, ft/mi	% Joints Spalled	IRI, in/mi (PSR)
FL 4-2	LCB "A"	None	15	4.5	0.02	0	0	1	139 (3.8)
FL 4-3	LCB "B"	None	15	4.5	0.04	0	546	0	122 (3.7)
FL 4-4	LCB "B"	None	15	4.5	0.04	0	0	0	98 (3.9)
FL 4-5	LCB "B"	None	15	4.5	0.04	0	0	3	110 (3.6)
FL 4-6	LCB "C"	None	15	4.5	0.05	0	0	0	95 (3.7)
FL 4-7	LCB "A"	None	15	4.5	0.07	0	0	1	110 (3.7)
FL 4-8	LCB "B"	None	15	4.5	0.08	0	0	0	106 (3.6)
FL 4-9	LCB "C"	None	15	4.5	0.11	1	1513	0	125 (3.2)
FL 4-10	LCB "A"	1.00	20	4.5	0.04	0	0	0	112 (3.6)
FL 4-11	LCB "B"	1.00	20	4.5	0.05	0	0	4	116 (3.6)

1 in = 25.4 mm  
 1 ft = 0.305 m  
 1 mi = 1.61 km

Common Design Features: 3-in JPCP bonded to 9-in LCB  
 A-3 subgrade  
 Built in 1978

The sections constructed on shell-stabilized subgrades (FL 4-2 through 4-6) are performing better than those constructed on cement-treated subgrades (FL 4-7, 4-8, and 4-9), although the difference in joint orientation confounds the comparison. The sections with a shell-stabilized subgrade have lower faulting levels and higher serviceability levels than those with cement-treated subgrades.



## Georgia 1

This project is located in the southbound lanes of I-85 near Newnan. The project includes 10 sections using 3 different base types, with and without dowel bars at the transverse joints. Four sections contain a 1-in (25-mm) AC separation layer and a 5-in (127-mm) CTB, two sections contain a 6-in (152-mm) CTB, and four sections contain a 4-in (102-mm) ATB.

The performance data for these sections are provided in table 77. The evaluations are inconclusive because the sections were all diamond ground in 1985, resulting in extremely low faulting and roughness values (diamond grinding due to poor ride quality during initial construction). In addition, little or no transverse cracking, joint spalling, or longitudinal cracking was observed on these sections.

Table 77. Summary of effect of base type for GA 1.

Section	Base Type	Dowel Diameter, in	Joint Faulting, in	% Slabs Cracked	Long Crk, ft/mi	% Joints Spalled	IRI, in/mi (PSR)
GA 1-1	1-in AC (4.5%) 5-in CTB (6%)	1.13	0.01	0	0	0	60 (4.1)
GA 1-3	1-in AC (4.5%) 5-in CTB (6%)	1.13	0.03	0	0	0	54 (4.1)
GA 1-5	6-in CTB (6%)	1.13	0.03	0	0	0	51 (4.0)
GA 1-6	4-in ATB (4.5%)	1.13	0.01	0	0	0	43 (4.1)
GA 1-8	4-in ATB (4.5%)	1.13	0.01	0	0	0	50 (4.1)
GA 1-2	1-in AC (4.5%) 5-in CTB (6%)	0.0	0.04	0	0	0	70 (4.1)
GA 1-4	1-in AC (4.5%) 5-in CTB (6%)	0.0	0.03	0	0	0	51 (4.1)
GA 1-10	6-in CTB (6%)	0.0	0.05	0	0	0	54 (4.0)
GA 1-7	4-in ATB (4.5%)	0.0	0.02	0	0	0	49 (4.0)
GA 1-9	4-in ATB (4.5%)	0.0	0.01	0	0	0	56 (4.1)

1 in = 25.4 mm  
1 ft = 0.305 m  
1 mi = 1.61 km

All sections were diamond ground in 1985.

Common Design Features:

9-in JPCP  
20-ft skewed joints  
Built in 1971  
ESAL's = 19.1 million (since 1971)  
ESAL's = 6.5 million (since 1985)

## Michigan 1

This project, located on U.S. 10 near Clare, contains a comparison of base types with all other factors remaining constant. Three sections contain a 4-in (102-mm)

PATB with 2 to 3 percent of an 85-100 penetration-graded asphalt cement, whereas two sections contain a 4-in ATB with 6 to 8 percent of a 250-300 penetration-grade asphalt cement. All sections are 9-in (229-mm) JPCP with full-depth AC shoulders, a 12-13-19-18-ft (3.7-4.0-5.8-5.5-m) joint spacing, and no dowels at the transverse joints.

A summary of the performance data for MI 1 is shown in table 78. The sections constructed on the PATB are performing much better than those constructed on the ATB. The sections containing an ATB are exhibiting much higher faulting, joint spalling, and roughness values, as well as slightly more transverse cracking. Deflection measurements, on the other hand, indicate that MI 1-4a (PATB) had 14 percent load transfer across the transverse joint, whereas MI 1-10a (ATB) had 61 percent load transfer. However, deflection measurements were taken at temperatures of 41 and 65 °F (5 and 18 °C), respectively.

Table 78. Summary of effect of base type for MI 1.

Section	Base Type	ESALs, millions	Joint Faulting, in	% Slabs Cracked	Long Crk, ft/mi	% Joints Spalled	IRI, in/mi (PSR)
MI 1-4a	4-in PATB	1.3	0.03	0	0	12	106 (3.8)
MI 1-4a10	4-in PATB	1.3	0.02	0	0	6	117 (-)
MI 1-4a12	4-in PATB	1.3	0.02	0	0	0	110 (-)
MI 1-10a	4-in ATB	1.3	0.13	0	0	100	161 (2.0)
MI 1-10a3	4-in ATB	1.3	0.29	15	0	79	203 (-)

1 in = 25.4 mm  
 1 ft = 0.305 m  
 1 mi = 1.61 km

Common Design Features: 9-in JPCP  
 12-13-19-18-ft nondoweled joints  
 Built in 1975

In this evaluation, base type and drainage were shown to significantly affect the performance of the PCC pavement sections. Although the ATB was stiffer, the PATB provided vastly improved drainage, which appears to be directly responsible for the improved performance. The sections with the ATB were bathtub designs (full-depth AC shoulders) that contributed to erosion and joint spalling due to D-cracking.

#### Minnesota 1

This experimental project is located on I-94 near Rothsay. Three different base types are incorporated in the designs: a 6-in (152-mm) aggregate base, a 5-in (127-mm) ATB with 5 percent AC-10, and a 6-in (152-mm) CTB with 5 percent cement. Six sections—two for each base type—are evaluated for four different designs, including sections with varying slab thicknesses and sections with and without dowel bars at the transverse joint.

The performance data for MN 1 are given in table 79. Every section with an ATB exhibited a significant amount of longitudinal cracking, as did many of the sections with a CTB. This longitudinal cracking is believed to be a result of several factors. On the sections with a CTB, cracks occurred immediately after construction and were attributed to reflective cracks from the base.<sup>(21)</sup> In addition, the longitudinal joint between the traffic lanes was formed with a plastic insert, which apparently did not establish an effective weakened plane. As a result, large thermal curling stresses were induced, creating longitudinal cracking in the traffic lanes.

Due to faulting levels in excess of 0.30 in (7.6 mm), the nondoweled sections on both aggregate and cement-treated bases were diamond ground and a tied and doweled edge beam was added in 1984. Thus, the faulting measurements for these sections represent the accumulated faulting from 1984 to 1992. The faulting values on the nondoweled sections are all greater than 0.10 in (2.5 mm), indicating the ineffectiveness of the edge beams in reducing faulting. Faulting on the doweled sections is not as excessive, although some sections have faulting as high as 0.15 in (3.8 mm). In terms of faulting, no base type appears to be showing consistently better performance than another base type.

Transverse cracking and transverse joint spalling are also excessive on many sections, regardless of base type. These distress types are most severe on the sections with an ATB. Obviously, the high levels of distress have resulted in high roughness values and low serviceability levels on nearly every section.

The base type had little influence of the performance of the MN 1 sections; all sections are performing poorly. One exception may be a reduction in transverse cracking on sections with an aggregate base. This poor performance is believed to be a result of the low amount of reinforcing steel, the lack of drainage, and the small diameter of the dowel bars.

### *Missouri 1*

This project, located in the northbound lanes of I-35 near Bethany, contains four different base types: a 4-in (102-mm) aggregate base, a 4-in (102-mm) ATB with 5 to 6 percent of a 60-70 penetration-graded asphalt cement, a 4-in (102-mm) PATB with 3 percent of a 60-70 penetration-graded asphalt cement, and a 4-in (102-mm) CTB with 4.5 percent cement. All sections are 9-in (229-mm) JRCP with 0.10 percent reinforcing steel. The transverse joints are spaced at 61.5-ft (18.7-m) intervals and contain 1.25-in (32-mm) uncoated dowel bars.

Table 80 provides a summary of the performance data for evaluating the effect of base type. The section with a PATB exhibited less transverse cracking and higher serviceability values than the other sections. This occurrence may be due to the ability of the PATB to remove water from the pavement structure, thus preventing ponding and softening of the base course. Pumping was evident on the sections with an aggregate base but not on sections containing a stabilized base. Other distress measurements do not favor one particular base type over another.

Table 79. Summary of effect of base type for MN 1.

Section	Design Features	Base Type	ESALs, millions	Faulting, in	Deter Cracks/mi	Long Crk, ft/mi	% Joints Spalled	IRI, in/mi (PSR)
MN 1-3*	8-in JRPC 0.09% Steel No Dowels	6-in AGG	7.4	0.17	49	350	56	161 (3.4)
MN 1-23*		6-in AGG	7.4	0.15	73	220	28	126 (3.0)
MN 1-5		5-in ATB	7.4	0.19	73	2909	84	186 (3.5)
MN 1-15		5-in ATB	7.4	0.21	106	3724	92	151 (3.0)
MN 1-11*		5-in CTB	7.4	0.16	8	5374	77	125 (3.5)
MN 1-17*		5-in CTB	7.4	0.25	8	130	20	164 (3.2)
MN 1-4	8-in JRPC 0.09% Steel 1-in Dowels	6-in AGG	7.4	0.11	83	0	48	105 (3.3)
MN 1-24		6-in AGG	7.4	0.09	86	383	38	140 (3.2)
MN 1-6		5-in ATB	7.4	0.08	8	3293	96	186 (3.1)
MN 1-16		5-in ATB	7.4	0.14	49	3455	92	149 (3.3)
MN 1-12		5-in CTB	7.4	0.12	81	1255	80	124 (3.5)
MN 1-18		5-in CTB	7.4	0.15	8	0	52	161 (3.2)
MN 1-1*	9-in JRPC 0.08% Steel No Dowels	6-in AGG	7.4	0.13	0	0	68	156 (3.3)
MN 1-21*		6-in AGG	7.4	0.19	0	0	16	152 (3.1)
MN 1-7		5-in ATB	7.4	0.11	16	4164	65	174 (3.6)
MN 1-13		5-in ATB	7.4	0.17	65	5997	92	128 (3.1)
MN 1-9*		5-in CTB	7.4	0.11	0	0	38	155 (3.6)
MN 1-19*		5-in CTB	7.4	0.12	8	722	69	127 (3.5)
MN 1-2	9-in JRPC 0.08% Steel 1-in Dowels	6-in AGG	7.4	0.15	45	0	61	179 (3.5)
MN 1-22		6-in AGG	7.4	0.12	23	0	50	143 (3.2)
MN 1-8		5-in ATB	7.4	0.10	70	5921	96	109 (3.8)
MN 1-14		5-in ATB	7.4	0.08	110	6234	96	166 (3.1)
MN 1-10		5-in CTB	7.4	0.12	18	0	76	117 (3.5)
MN 1-20		5-in CTB	7.4	0.15	39	0	31	167 (3.1)

1 in = 25.4 mm

1 ft = 0.305 m

1 mi = 1.61 km

Common Design Features: 27-ft skewed joints  
Built in 1970

\* Sections were diamond ground and edge beam (tied and doweled) was added in 1984.

Table 80. Summary of effect of base type for MO 1.

Section	Base Type	ESALs, millions	Joint Faulting, in	% Slabs Cracked	Long Crk, ft/mi	% Joints Spalled	IRI, in/mi (PSR)
MO 1-4*	4-in AGG	13.7	0.06	29	0	13	159 (4.0)
MO 1-8	4-in AGG	13.7	0.06	23	367	6	176 (3.9)
MO 1-5*	4-in ATB	13.7	0.05	23	0	6	131 (3.9)
MO 1-6*	4-in PATB	13.7	0.06	6	372	19	163 (4.2)
MO 1-7*	4-in CTB	13.7	0.06	23	269	25	146 (4.0)

1 in = 25.4 mm  
 1 ft = 0.305 m  
 1 mi = 1.61 km  
 \*SHRP test sections

Common Design Features: 9-in JRCF with 0.10% steel  
 61.5-ft joints with 1.25-in dowels  
 Built in 1977

*North Carolina 1*

This project is located on I-95 near Rocky Mount. Four different base types are evaluated for this project:

- 4-in (102-mm) aggregate base.
- 6-in (152-mm) soil cement base containing 8 percent cement.
- 4-in (102-mm) CTB with 6 percent cement.
- 4-in (102-mm) ATB with 4 percent AC-20.

All sections included a 4-in (102-mm) daylighted aggregate base. All sections in this evaluation are 9-in (229-mm) nondoweled JPCP with a 30-ft (9.1-m) transverse joint spacing.

Table 81 presents a summary of the performance data for evaluating the effect of base type. The section with the ATB is exhibiting better performance in every category. The ATB was able to resist faulting better than either of the cementitious bases. In fact, the nondoweled section with the ATB (NC 1-6) had less faulting than the doweled sections with either an aggregate or soil cement base (NC 1-4 and 1-2, not shown in table).

The section with the aggregate base displayed substantial faulting and transverse cracking, whereas the section with a soil cement base exhibited substantial faulting and longitudinal cracking. The section with the CTB contained significant faulting and longitudinal cracking, as well as an extremely low serviceability value.

Table 81. Summary of effect of base type for NC 1.

Section	ESALs, millions		Faulting, in		% Slabs Cracked		Long Crk, ft/mi		IRI, in/mi (PSR)	
	1987	1992	1987	1992	1987	1992	1987	1992	1987	1992
NC 1-8 4-in AGG	9.0	16.0	0.22	0.23	37	77	0	0	-(3.7)	131 (3.3)
NC 1-3 6-in SC	9.0	16.0	0.13	0.14	3	6	3068	4983	-(3.6)	116 (3.4)
NC 1-5 4-in CTB	9.0	16.0	0.16	0.16	0	0	179	372	-(3.2)	139 (2.9)
NC 1-6 4-in ATB	9.0	16.0	0.05	0.03	0	9	0	0	-(3.8)	102 (3.7)

1 in = 25.4 mm  
1 ft = 0.305 m  
1 mi = 1.61 km

Common Design Features: 9-in JPCP  
30-ft nondoweled joints  
Built in 1968

### New Jersey 3

This experimental project, located on I-676 near Camden, includes two sections with different types of permeable bases. NJ 3-1 contains an open-graded aggregate base, and NJ 3-2 contains a PATB with 2.5 percent AC-20. Both sections consist of a 9-in (229-mm) JRCP with 0.16 percent steel, 78.5-ft (23.9-m) transverse joint spacing, and 1.25-in (32-mm) diameter stainless steel-wrapped dowel bars. A filter fabric was placed between the base layer and lime-flyash stabilized subgrade.

The performance data for these sections are presented in table 82. Both sections are performing well after 13 years of service and nearly 13 million ESAL applications, with no appreciable difference for any performance indicator. The high roughness levels are probably a result of the 0.75-in (19-mm) wide expansion joints present at every joint. The joint spalling is also thought to be due to the construction of the expansion joints.

### New York 1

This project is located on Route 23 between Catskill and Cairo. Two different designs are compared using two different base types: a 4-in (102-mm) aggregate base and a 3-in (76-mm) ATB with 2.5 to 4.0 percent of a 60-70 penetration-graded asphalt cement. The first comparison involves a pavement system consisting of a 9-in (229-mm) JPCP with a 20-ft (6.1-m) joint spacing and ACME load transfer devices. The pavement system in the second comparison consists of a 9-in (229-mm) JRCP with 0.20 percent steel, 61-ft (18.6-m) joint spacing, and ACME load transfer devices.

Table 82. Summary of effect of base type for NJ 3.

Section	ESALs, millions		Faulting, in		Deteriorated Cracks/mi		% Joints Spalled		IRI, in/mi (PSR)	
	1987	1992	1987	1992	1987	1992	1987	1992	1987	1992
NJ 3-1 4-in PAGG	4.9	12.6	0.05	0.04	0	0	0	29	- (3.6)	191 (-)
NJ 3-2 4-in PATB	4.9	12.6	0.06	0.03	0	0	43	43	- (3.5)	199 (-)

1 in = 25.4 mm  
 1 ft = 0.305 m  
 1 mi = 1.61 km

Common Design Features: 9-in JRPC with 0.16% steel  
 78.5-ft joints with 1.25-in dowels  
 Built in 1979

The performance data for the JPCP sections are shown in table 83. Both sections are performing well, considering they are 24 years old. NY 1-6 (aggregate base) has more transverse and longitudinal cracking than NY 1-1 (ATB). The longitudinal cracking on NY 1-6 is not believed to be related to the base type, as the traffic lanes were widely separated (0.8 to 3.0 in [20 to 76 mm]) along the centerline joint. The faulting, joint spalling, roughness, and serviceability values are similar for both sections. Some signs of pumping were noticed on both sections.

Table 83. Summary of effect of base type on JPCP for NY 1.

Section	ESALs, millions		Faulting, in		% Slabs Cracked		Long Crk, ft/mi		IRI, in/mi (PSR)	
	1987	1992	1987	1992	1987	1992	1987	1992	1987	1992
NY 1-6 4-in AGG	3.1	5.5	0.03	0.02	10	17	264	475	- (3.9)	118 (3.8)
NY 1-1 3-in ATB	3.1	5.5	0.02	0.02	0	7	0	70	- (4.0)	106 (3.6)

1 in = 25.4 mm  
 1 ft = 0.305 m  
 1 mi = 1.61 km

Common Design Features: 9-in JPCP with 20-ft joints  
 ACME load transfer device  
 Built in 1968

Table 84 presents the performance data for the JRPC sections. These sections exhibited more faulting and roughness than the JPCP sections. Again, the section with the aggregate base has more transverse and longitudinal cracking. The section with an ATB has a much lower IRI value, but also a lower PSR value. Other measurements are about the same. Some signs of pumping were also noticed on these sections.

Table 84. Summary of effect of base type on JRCP for NY 1.

Section	ESALs, millions		Faulting, in		Deteriorated Cracks/mi		Long Crk, ft/mi		IRI, in/mi (PSR)	
	1987	1992	1987	1992	1987	1992	1987	1992	1987	1992
NY 1-4 4-in AGG	3.1	5.5	0.09	0.14	0	9	0	138	- (3.4)	177 (3.4)
NY 1-3 3-in ATB	3.1	5.5	0.14	0.16	0	0	0	35	- (3.6)	117 (3.1)

1 in = 25.4 mm  
 1 ft = 0.305 m  
 1 mi = 1.61 km

Common Design Features: 9-in JRCP with 0.20% steel  
 61-ft joints with ACME transfer device  
 Built in 1968

### Ohio 1

This project, located on U.S. 23 near Chillicothe, compares two different base types: a 7.5-in (190-mm) aggregate base and a 4-in (102-mm) ATB with 5.7 percent AC-20. OH 1-10 (AGG) and 1-3 (ATB) are 9-in (229-mm) JRCP with 0.09 percent reinforcing steel, 21-ft (6.4-m) joint spacing, and 1.25-in (32-mm) dowels. OH 1-1 (AGG), 1-9 (AGG), and 1-4 (ATB) are 9-in (229-mm) JRCP with 0.09 percent reinforcing steel, 40-ft (12.2-m) joint spacing, and 1.25-in (32-mm) dowels.

Table 85 provides a summary of the performance data for OH 1. The faulting measurements were lower in 1992 than in 1987. This reduction in faulting is probably attributable to differences in environmental conditions (moisture and temperature) in which the measurements were taken. The sections with an ATB have less deteriorated transverse cracking and roughness, which may be an indication of the greater resistance of the ATB to moisture and erosion. One of the ATB sections does show some transverse joint spalling.

### Ohio 2

This experimental project, located on State Route 2 near Vermillion, was designed to study the factors that influence the development of D-cracking.<sup>(33)</sup> Two different base types are examined in this evaluation: a 4-in (102-mm) ATB with 4 to 8 percent asphalt cement and a 4-in (102-mm) CTB with 4.5 percent cement. Three sections are included for each base type. All sections are 9-in (229-mm) JRCP with 0.10 percent reinforcing steel. The transverse joints are spaced at 40-ft (12.2-m) intervals and are equipped with 1.25-in (32-mm) dowel bars. OH 2-43 and 2-49 contain no drainage elements, whereas OH 2-49, 2-51, 2-100, and 2-102 contain edge drains. Two 15-in (381-mm) JPCP sections with no base are also included in the evaluation.



Table 85. Summary of effect of base type for OH 1.

	ESALs, millions		Faulting, in		Deter Cracks/mi		% Joints Spalled		IRI, in/mi (PSR)	
	1987	1992	1987	1992	1987	1992	1987	1992	1987	1992
OH 1-10 7.5-in AGG	4.1	6.1	0.10	0.03	0	168	0	0	- (4.2)	182 (-)
OH 1-3 4-in ATB	4.1	6.1	0.06	0.03	0	0	13	13	- (4.2)	152 (-)
OH 1-1 7.5-in AGG	4.1	6.1	0.13	0.02	0	88	0	0	- (4.2)	224 (-)
OH 1-9 7.5-in AGG	4.1	6.1	0.14	0.07	106	251	0	0	- (4.2)	154 (-)
OH 1-4 4-in ATB	4.1	6.1	0.07	0.02	29	132	0	0	- (4.1)	156 (-)

1 in = 25.4 mm  
1 ft = 0.305 m  
1 mi = 1.61 km

Common Design Features: 9-in JRCF with 0.09% steel  
1.25-in dowels  
Built in 1973

Table 86 provides a summary of the performance data for evaluating the effect of base type. The sections with an ATB have less faulting and deteriorated transverse cracks than those with a CTB. The reduced faulting indicates that the ATB is more erosion-resistant and is providing better support at the transverse joints. This conclusion is further supported by the higher deflections obtained on the sections with a CTB. The increased transverse cracking on the sections with a CTB are most likely due to higher thermal curling stresses on the stiffer CTB.

Table 86. Summary of effect of base type for OH 2.

Section	Base Type	ESALs, millions	Joint Faulting, in	Deter Cracks/mi	Long Crk, ft/mi	% Joints Spalled	IRI, in/mi
OH 2-43	4-in ATB	6.5	0.01	22	0	43	276
OH 2-94	4-in CTB	6.5	0.05	110	0	86	153
OH 2-2*	None	6.5	0.08	0	572	52	143
OH 2-3*	None	6.5	0.14	11	148	96	99
OH 2-49	4-in ATB	6.5	0.05	0	0	100	144
OH 2-51†	4-in ATB	6.5	0.06	22	0	0	145
OH 2-100	4-in CTB	6.5	0.06	44	0	43	120
OH 2-102†	4-in CTB	6.5	0.18	88	0	29	166

1 in = 25.4 mm  
1 ft = 0.305 m  
1 mi = 1.61 km

Common Design Features: 9-in JRCF with 0.10% steel  
40-ft joints with 1.25-in dowels  
Built in 1974

\* 15-in JPCF with 20-ft doweled joints.

† Sections contain Sy2 aggregate; others contain Mn3 aggregate.

The joint spalling and roughness values do not provide any conclusive information. For instance, one section with an ATB has 100 percent of the joints spalled, whereas another section has no spalled joints. Longitudinal cracking was not observed on any of the JRC sections. Many of these sections (all but OH 2-51 and 2-102) contained D-cracking susceptible aggregate.

The JPCP sections without a base course show considerably more faulting and longitudinal cracking than the sections on either an ATB or CTB. However, they also show fewer transverse cracks and less roughness.

*Ontario 1*

This experimental project is located on Highway 3N near Windsor. Three sections are compared for evaluating the effect of base types. ONT 1-2 consists of an 8-in (203-mm) JPCP and a 4-in (102-mm) PATB with 2 percent asphalt cement. ONT 1-3 incorporates an 8-in (203-mm) JPCP and a 5-in (127-mm) LCB. ONT 1-1 is a 12-in (305-mm) JPCP with no base. All sections contain subdrainage and skewed joints (no dowel bars) spaced at random 12-13-19-18-ft (3.7-4.0-5.8-5.5-m) intervals.

The performance data for the ONT 1 sections are provided in table 87. The section with the LCB showed the worst performance, exhibiting the highest levels of faulting, transverse cracking, and longitudinal cracking. The stiff base probably resulted in increased thermal stresses in the slab, causing more cracking in the slab.

Table 87. Summary of effect of base type for ONT 1.

	ESALs, millions		Faulting, in		% Slabs Cracked		Long Crk, ft/mi		IRI, in/mi (PSR)	
	1987	1992	1987	1992	1987	1992	1987	1992	1987	1992
ONT 1-2 8-in JPCP 4-in PATB	0.9	2.1	0.05	0.10	0	0	0	105	-(3.8)	135 (3.9)
ONT 1-3 8-in JPCP 5-in LCB	0.9	2.1	0.04	0.14	9	8	490	621	-(3.8)	147 (3.9)
ONT 1-1 12-in JPCP	0.9	2.1	0.05	0.11	0	0	40	40	-(3.8)	146 (3.9)

1 in = 25.4 mm  
 1 ft = 0.305 m  
 1 mi = 1.61 km

Common Design Features: 13-19-18-12-ft nondoweled joints  
 Built in 1982

With the exception of longitudinal cracking, the performance indicators are similar for the section with a PATB and the section without a base. However, the longitudinal cracking on the PATB section is believed to be the result of patches and

not due to the use of the PATB. The use of a thicker slab without a base course did not significantly affect the performance of the section. However, no filter layer was provided beneath the PATB, and the collector system was placed in the dense-graded shoulder (not in contact with the PATB).<sup>(35)</sup> These factors are believed to have detracted from the performance of that section.

For all sections, faulting increased by at least two times from 1987 to 1992, yet the PSR remained about the same. An increase in longitudinal cracking was also observed on the sections with PATB and CTB. Signs of low-severity pumping were observed on all sections.

### *Pennsylvania 1*

This experimental project, located on Routes 66 and 422 near Kittanning, was designed to investigate the performance of alternative base types.<sup>(36)</sup> Five different base types are incorporated in this project:

- 6-in (152-mm) CTB with 6 percent cement.
- 5-in (127-mm) PATB with 2 percent asphalt cement.
- 8-in (203-mm) uniform-graded aggregate base.
- 8-in (203-mm) well-graded aggregate base.
- 13-in (330-mm) dense-graded aggregate base.

All sections are 10-in (254-mm) JRCP with 0.09 percent reinforcing steel. The transverse joints contain 1.25-in (32-mm) epoxy-coated dowel bars and are spaced at 46.5-ft (14.2-m) intervals.

Table 88 provides a summary of the performance data for evaluating the effect of various base types. All sections are exhibiting little distress, having been exposed to only about 1 million ESAL applications. The section with the CTB is the only section that has any deteriorated transverse cracks. This cracking is most likely due to the high curling stresses in the slab caused by the stiffer base.

### *West Virginia 1*

These sections are located on the West Virginia Turnpike (I-77), south of Charleston. WV 1-1 incorporates a 6-in (152-mm) aggregate base, and WV 1-2 has 6-in (152-mm) CTB with 5 percent cement. Both sections are 10-in (254-mm) JRCP with 0.10 percent reinforcing steel, 40-ft (12.2-m) joint spacing, and 1.25-in (32-mm) dowels.

The performance data for these sections are shown in table 89. The section with the CTB has more faulting and joint spalling, although it is 5 years older and has handled more ESAL applications. The section with the aggregate base is only 6 years old but exhibits significant levels of deteriorated transverse cracking, longitudinal cracking, and joint spalling. The large number of deteriorated cracks indicates that the reinforcing steel was not adequate. However, cracking is not as significant on WV 1-2, although it incorporates a stiffer base.

Table 88. Summary of effect of base type for PA 1.

Section	Base Type	ESALs, millions	Faulting, in		Deteriorated Cracks/mi		IRI, in/mi (PSR)	
			1987	1992	1987	1992	1987	1992
PA 1-1	6-in CTB	1.1	0.03	0.05	0	10	- (4.2)	134 (3.9)
PA 1-2	5-in PATB	0.8	0.02	0.01	0	0	- (3.8)	150 (4.2)
PA 1-2a	5-in PATB	0.8	-	0.03	-	0	-	134 (-)
PA 1-3	8-in AGG <sup>a</sup>	0.8	0.03	0.03	0	0	- (3.7)	178 (4.1)
PA 1-3a	8-in AGG <sup>a</sup>	0.8	-	0.03	-	0	-	134 (-)
PA 1-4	8-in AGG <sup>b</sup>	0.8	0.03	0.03	0	0	- (4.0)	159 (4.0)
PA 1-4a	8-in AGG <sup>b</sup>	0.8	-	0.04	-	0	-	159 (-)
PA 1-5	13-in AGG <sup>c</sup>	0.8	0.03	0.02	0	0	- (4.0)	127 (4.3)
PA 1-5a	13-in AGG <sup>c</sup>	0.8	-	0.03	-	0	-	149 (-)

1 in = 25.4 mm

1 ft = 0.305 m

1 mi = 1.61 km

<sup>a</sup> Uniform-graded aggregate

<sup>b</sup> Well-graded aggregate

<sup>c</sup> Dense-graded aggregate

Common Design Features: 10-in JRCP with 0.09% steel  
46.5-ft joints with 1.25-in dowels  
Built in 1980

Table 89. Summary of effect of base type for WV 1.

Section	Base Type	Year Built	ESALs, millions	Faulting, in	Deteriorated Cracks/mi	Long Crk, ft/mi	% Joints Spalled	IRI, in/mi (PSR)
WV 1-1	6-in AGG	1986	6.5	0.02	58	53	35	168 (3.5)
WV 1-2	6-in CTB	1981	8.9	0.06	11	0	50	142 (3.6)

1 in = 25.4 mm

1 ft = 0.305 m

1 mi = 1.61 km

Common Design Features: 10-in JRCP with 0.10% steel  
40-ft joints with 1.25-in dowels

### Wisconsin 1

This project is located in the westbound lanes of I-90 near Stoughton. Although all sections have a PCTB, the cement content does vary. However, these sections were only 2 years old at the time of the survey and had experienced little distress. Therefore, pertinent conclusions could not be obtained from the available data.

### *Wisconsin 2/Wisconsin 7*

These projects are located adjacent to each other on U.S. 18/151 near Mt. Horeb and Barneveld, respectively. Three different base types were investigated in these projects:

- 4-in (102-mm) PCTB with 6 to 8 percent cement.
- 4-in (102-mm) PATB with 2 percent asphalt cement.
- 4-in (102-mm) permeable aggregate base.

All sections are 9-in (229-mm) JPCP with a random 12-13-19-18-ft (3.7-4.0-5.8-5.5-m) joint spacing. All sections also contain longitudinal edge drains. Three different design sections were evaluated:

- WI 2-1, 2-2, and 2-3 have 1.25-in (32-mm) epoxy-coated dowels and no joint sealant.
- WI 7-1, 7-3, and 7-5 have no dowels and preformed joint sealant.
- WI 7-2, 7-4, and 7-6 have no dowels and no joint sealant.

The performance data for these sections are presented in table 90. With the exception of excessive longitudinal cracking on two sections with a PCTB, the sections are performing well. The sections with a PATB show the least roughness, whereas the sections with a PCTB have the highest roughness values. However, these sections were only 4 years old, which makes it difficult to draw any definitive conclusions.

The corner deflection data are also shown in the table. High deflections are noticed on two sections: WI 2-1 (PCTB) and WI 7-1 (PAGG). In addition, WI 7-1 and 7-2, both of which contain PAGG, show 100 corners with voids, whereas all the other sections show no potential for corner voids.

### *Wisconsin 3*

This experimental project is a two-lane highway located on STH 14 near Middleton. WI 3-1 has a 3.5-in (89-mm) PATB with 2 percent asphalt cement, and WI 3-2 has a 6-in (152-mm) aggregate base. Both sections are 8-in (203-mm) nondoweled JPCP with skewed transverse joints spaced at random 12-13-19-18-ft (3.7-4.0-5.8-5.5-m) intervals.

Table 91 provides a summary of the performance for WI 3. Although the sections are only 4 years old, the section with the PATB is performing significantly better in terms of faulting, roughness, and serviceability. The PATB is more effective at removing moisture from the pavement system and is believed to be responsible for the superior performance. These benefits are apparent after only 1.2 million ESALs.

Table 90. Summary of effect of base type for WI 2 & 7.

Section	Design	ESALs, millions	Joint Faulting, in	% Slabs Cracked	Long Crk, ft/mi	% Joints Spalled	IRI, in/mi (PSR)	Corner Def, mils
WI 2-1	4-in PCTB 1.25-in Dowels	1.3	0.01	0	0	5	122 (4.1)	6.7
WI 2-2*	4-in PATB 1.25-in Dowels	1.3	0.01	0	0	3	106 (4.0)	3.2
WI 2-3	4-in PAGG 1.25-in Dowels	1.3	0.01	0	0	3	112 (4.0)	3.9
WI 7-3	4-in PCTB No Dowels	1.3	0.01	0	326	0	147 (4.1)	1.3
WI 7-5	4-in PATB No Dowels	1.3	0.01	0	0	2	86 (4.1)	3.0
WI 7-1	4-in PAGG No Dowels	1.3	0.03	0	0	6	136 (4.3)	6.5
WI 7-4*	4-in PCTB No Dowels	1.3	0.04	0	257	8	147 (4.0)	2.3
WI 7-6*	4-in PATB No Dowels	1.3	0.02	0	0	10	98 (4.0)	1.8
WI 7-2	4-in PAGG No Dowels	1.3	0.03	6	0	8	120 (4.5)	1.7

1 in = 25.4 mm  
 1 ft = 0.305 m  
 1 mi = 1.61 km

\* SHRP test sections.

Common Design Features: 9-in JPCP  
 12-13-19-18-ft skewed joints  
 Built in 1988

Table 91. Summary of effect of base type for WI 3.

Section	Base Type	ESALs, millions	Joint Faulting, in	% Slabs Cracked	Long Crk, ft/mi	% Joints Spalled	IRI, in/mi (PSR)
WI 3-1	3.5-in PATB	1.2	0.03	0	0	2	109 (4.0)
WI 3-2	6-in AGG	1.2	0.13	0	0	3	151 (3.6)

1 in = 25.4 mm  
 1 ft = 0.305 m  
 1 mi = 1.61 km

Common Design Features: 8-in nondoweled JPCP  
 12-13-19-18-ft skewed joints  
 Built in 1988

## Related Research

California has experimented with several different base types. In the 1950s, the use of CTB was adapted to obtain a more erosion-resistant base. Although the rate of faulting was reduced, adequate erosion resistance was still not provided, as faulting and subsequent slab breakup were evident.<sup>(13)</sup> In experimental studies, sections with an LCB (9.4 percent cement) have shown less faulting than corresponding sections with a CTB (4 percent cement).<sup>(13)</sup>

Additional studies have been and are currently being conducted on the use of permeable base layers and their effect on performance. Because of problems with fines being removed from under PCTB, California now recommends that all treated permeable bases be placed on a 4-in (100-mm) aggregate base with a prime coat. Many sections have also exhibited stripping of PATB within as little as 2 years, especially near the transverse joints. An analysis of the PATB sections revealed that sections with lower asphalt contents had more stripping, and California has since increased the asphalt content of PATB from 2.5 to 3.0 percent by weight of aggregate.<sup>(43)</sup>

Another study was conducted to examine the erosion of subbase materials under rigid pavements.<sup>(44)</sup> For cement-treated materials, the cement content is the most important factor for erodibility, with compaction effort and gradation also being important, but to a lesser extent. For asphalt-treated materials, erosion is affected by asphalt content, compaction effort, and environmental factors (wetting and drying have a greater influence on erosion than freezing and thawing). Impervious unstabilized materials were found to always be affected by pumping resulting from surface erosion, mainly due to the buildup of pore water pressure. A series of relationships and curves were developed to predict erosion and to select subbases that will prevent pumping.

Yet another study examined several durability tests (rotational shear device, jetting device, and brush test) and found the tests to be time consuming and not reflective of the mechanical abrasion experienced during Heavy Vehicle Simulator (HVS) testing.<sup>(45)</sup> As a result, a new test method, the Erosion Test, was developed. This test can be conducted relatively quickly (8 days) and compares well with results obtained during HVS testing. Further research is currently being conducted using this test to study the effect of material properties on erodibility.

## Overall Evaluation of Base Type

Direct evaluations between sections with different base types show some common trends. For instance, pumping and faulting were most severe on sections with ATB and CTB, with the use of aggregate bases and no bases also exhibiting substantial faulting. This trend is further illustrated in figure 33, which shows the average faulting of all sections distributed by base type. Sections placed on an LCB or permeable base exhibited considerably less faulting, on average, for both doweled and nondoweled sections. In fact, faulting on nondoweled sections with either an LCB or permeable base was less than faulting on doweled sections with an aggregate or stabilized base. The use of an aggregate or stabilized base was not effective in reducing faulting as compared to the use of no base. Of course, age, traffic, and climate confound these observations.

Another means of examining the effect of base type is through the degree of erodibility of the base. The erodibility class provides a measure of the erosion potential based on the amount of weight loss during the rotary brushing test.<sup>(46)</sup> Materials are divided into five different classes, with each class being five times more erodible than the previous class:

- Class A—Extremely erosion resistant (lean concrete with at least 8 percent cement, bituminous concrete with at least 6 percent bitumen).
- Class B—Erosion resistant (cement-treated granular material with 5 percent cement).
- Class C—Erosion resistant under certain conditions (granular materials treated with 3.5 percent cement or 3 percent bitumen).
- Class D—Fairly erodible (granular material treated in place with 2.5 percent cement, fine soils treated in place, untreated granular materials).
- Class E—Very erodible (contaminated untreated granular material, untreated fine soils).

Figure 34 shows the faulting of doweled and nondoweled sections for each erodibility class (does not include permeable bases). A strong correlation between the erodibility class and the amount of faulting does not exist. However, some classes are only represented by a few sections and may provide unreliable results. In addition, the classes are based solely on the materials and do not account for important factors such as the drainage and climate.

Figure 35 illustrates the degree of spalling at the transverse joints for the different base types. The results are similar to joint faulting, with sections placed on either an LCB or permeable base exhibiting substantially less spalling. The sections with an ATB had considerably more spalling than sections with all other base types.



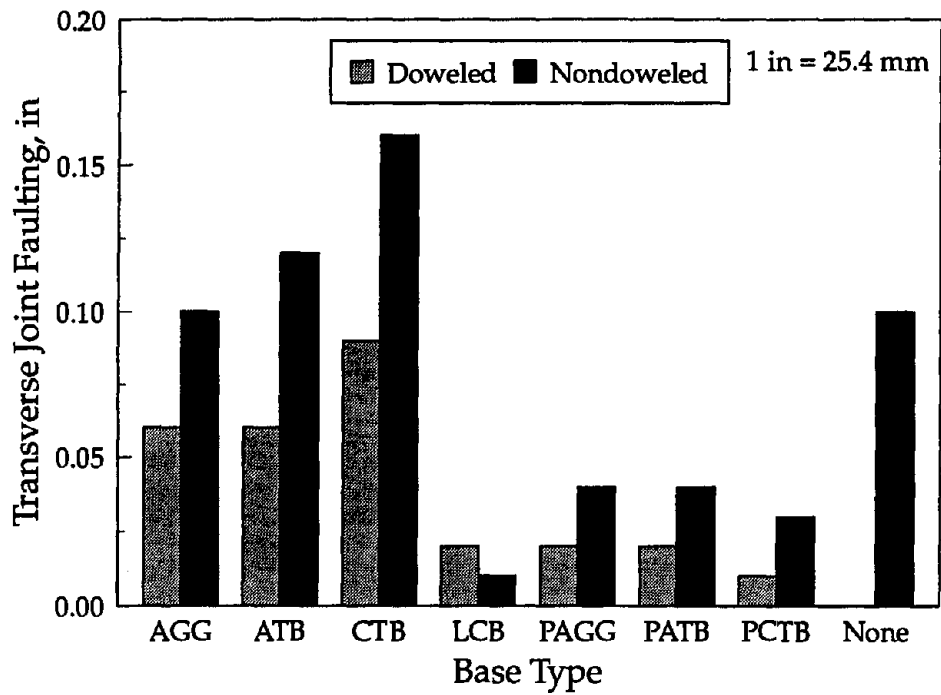


Figure 33. Average transverse joint faulting for each base type.

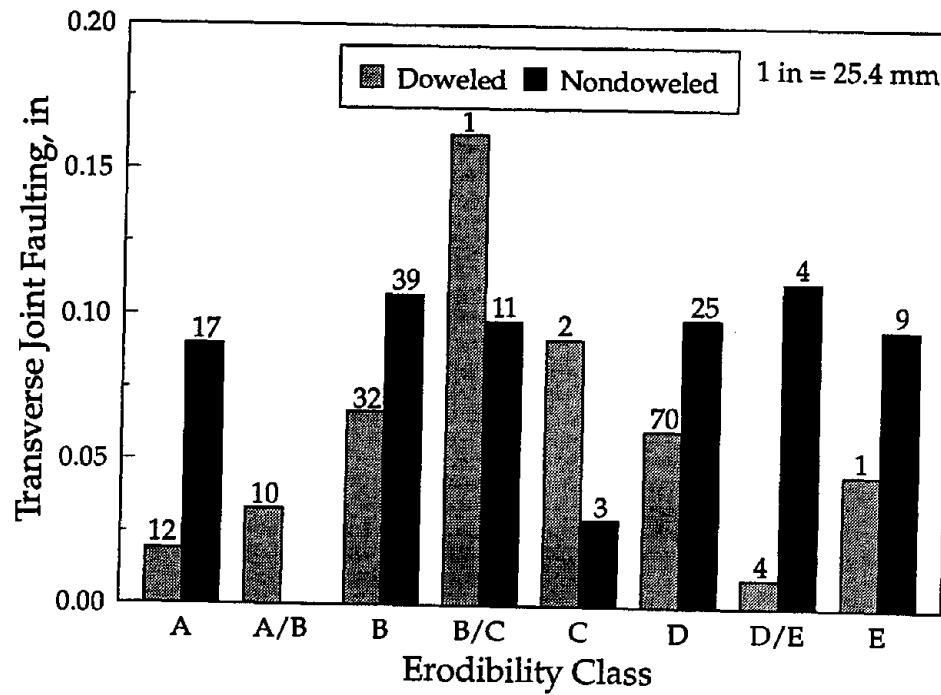


Figure 34. Average transverse joint faulting by erodibility class.

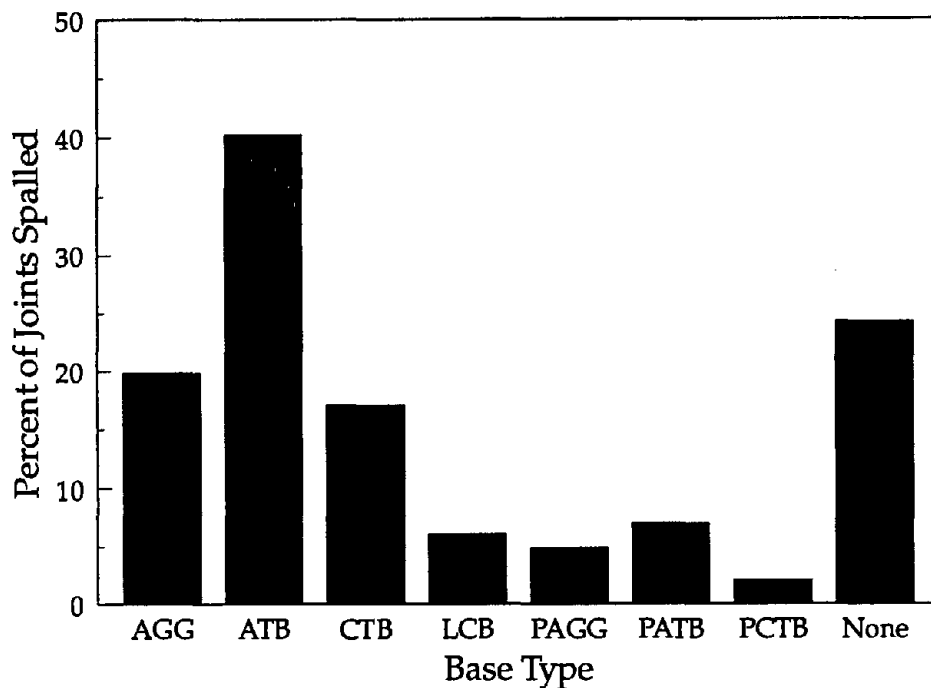


Figure 35. Average joint spalling for each base type.

The evaluation of sections within the same project indicated that for JPCP, transverse cracking was most abundant on sections with a stiff base (CTB or LCB). This occurrence is further supported by figure 36. Sections containing a CTB had transverse cracking on 11 percent of the slabs, whereas sections placed on an LCB had transverse cracking on 18 percent of the slabs. Sections placed on a permeable base exhibited little cracking, although the sections typically are not very old.

Sections placed on an aggregate base show the most transverse cracking for JRCPC sections. Although sections with a CTB had substantial cracking, most cracks were low severity. Sections with an ATB or PAGG exhibited high levels of deteriorated transverse cracks.

Figure 37 illustrates the average deflections for corner, edge, and midslab loading conditions on JPCP separated by base type. Corner deflections are highest on sections with a PAGG or PATB, and only slightly lower for sections with AGG, ATB, or CTB. Corner deflections are lower for sections on an LCB or PCTB, which is expected; the reason for lower deflections on the section without a base may be due to the use of thicker slabs. Less variation in the deflection measurements is observed for the edge and midslab loading conditions.

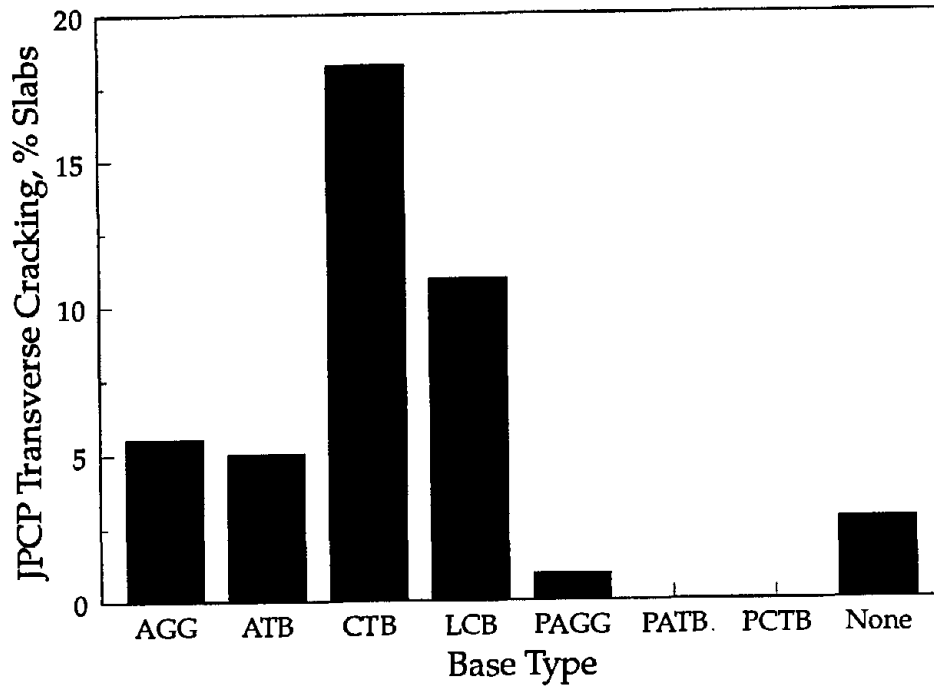


Figure 36. Transverse cracking by base type for JPCP.

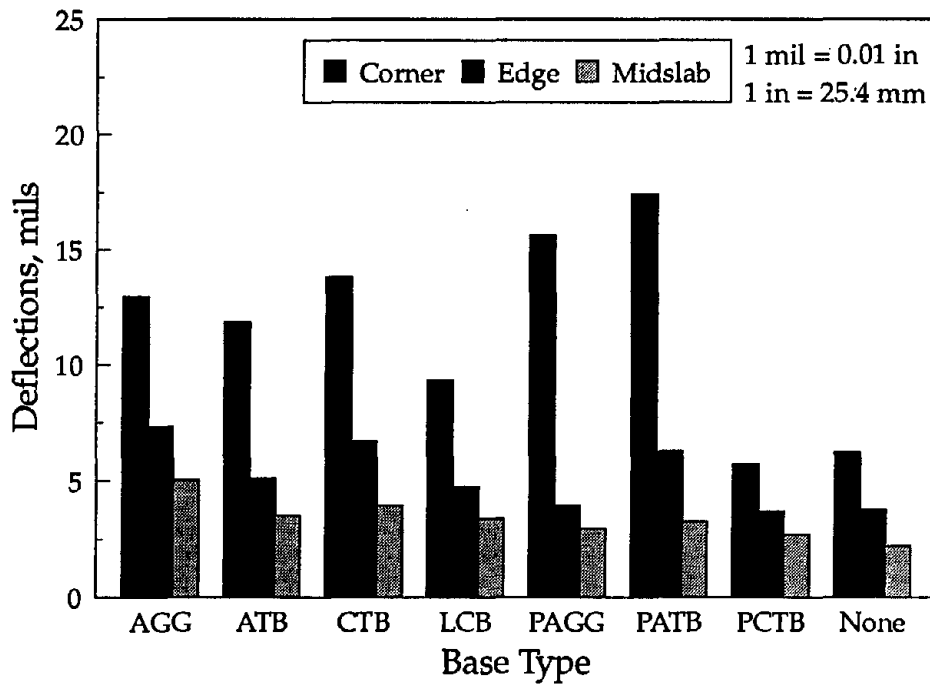


Figure 37. Average deflections for each base type.

For stabilized bases, the amount of stabilizing agent (asphalt or cement) influences the stiffness and strength of the material and the impact of the base layer on performance. Materials with a higher percentage of a stabilizing agent are also more resistant to erosion. Figure 38 shows transverse joint faulting plotted as a function of the percent of cement in the base (does not include permeable bases). Sections incorporating less than 6 percent of cement in the base generally have higher faulting levels and considerably more variability. All sections with more than 6 percent cement in the base have average faulting levels below 0.08 in (2.0 mm), and most have average faulting levels below 0.05 in (1.3 mm). The amount of cement has a greater effect on faulting of the nondoweled sections.

The percentage of cement in the base also appears to be a factor in reducing corner deflections, as shown in figure 39. Again, the critical amount is around 6 percent by weight of the base material. Higher deflections and more variability are associated with sections using base courses less than 6 percent cement. In general, cement contents in the range of 6 to 7 percent represent the difference between CTB and LCB. As with faulting, the nondoweled sections are affected to a greater degree by the cement content.

Similar plots were developed based on the percentage of asphalt cement in the base course. Figures 40 and 41 illustrate the results for transverse joint faulting and corner deflections, respectively (do not include permeable bases). However, an increase in the amount of asphalt cement does not seem to improve the performance of the sections. In fact, the sections with more than 5 percent asphalt cement have more faulting.

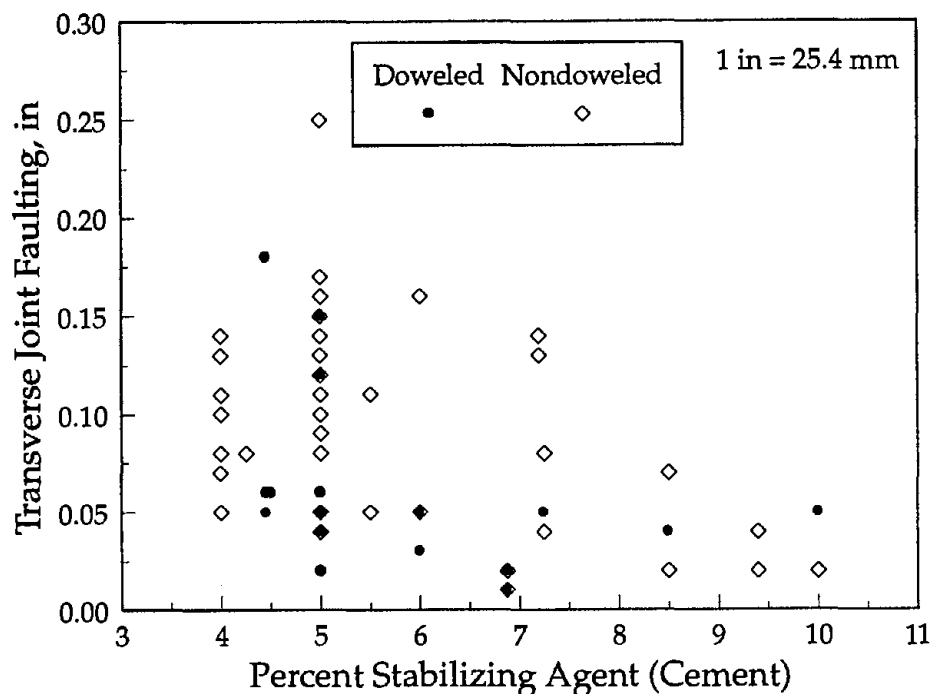


Figure 38. Effect of percentage of cement on transverse joint faulting.

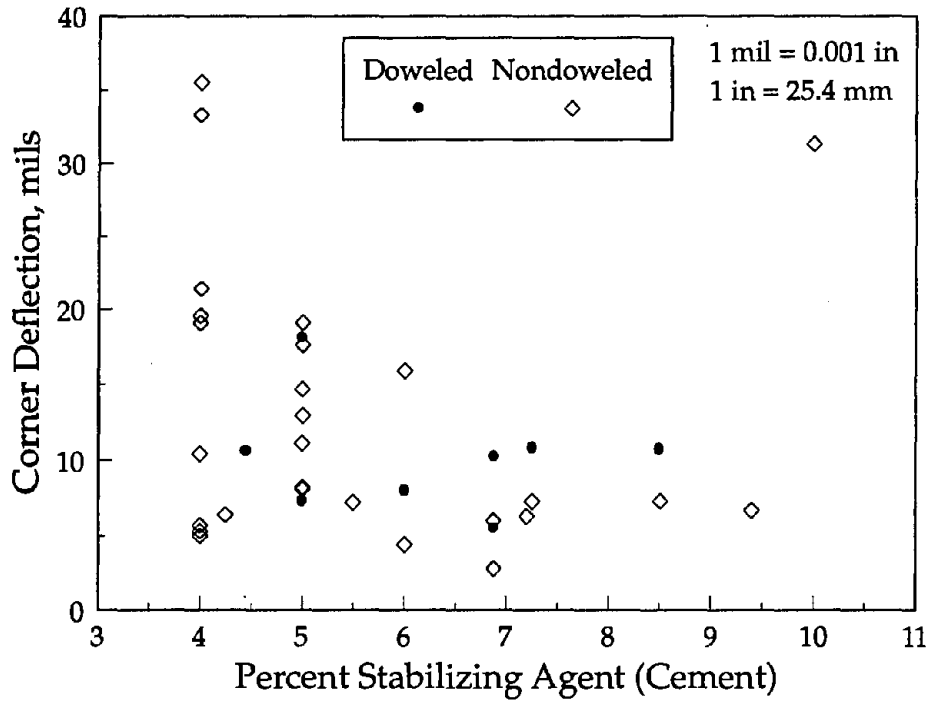


Figure 39. Effect of percentage of cement on corner deflections.

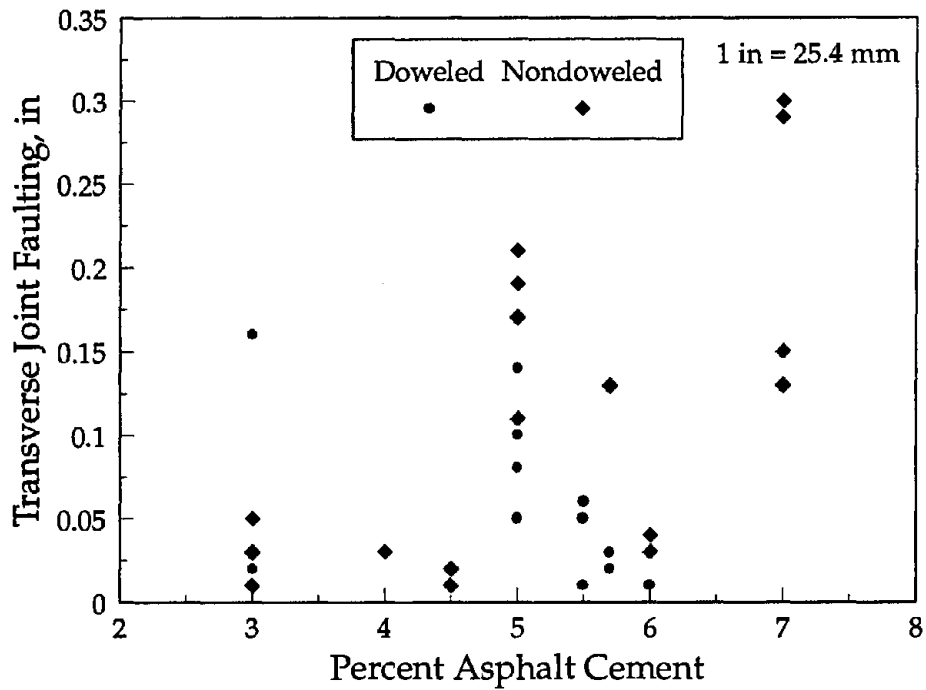


Figure 40. Effect of percentage of asphalt cement on transverse joint faulting.

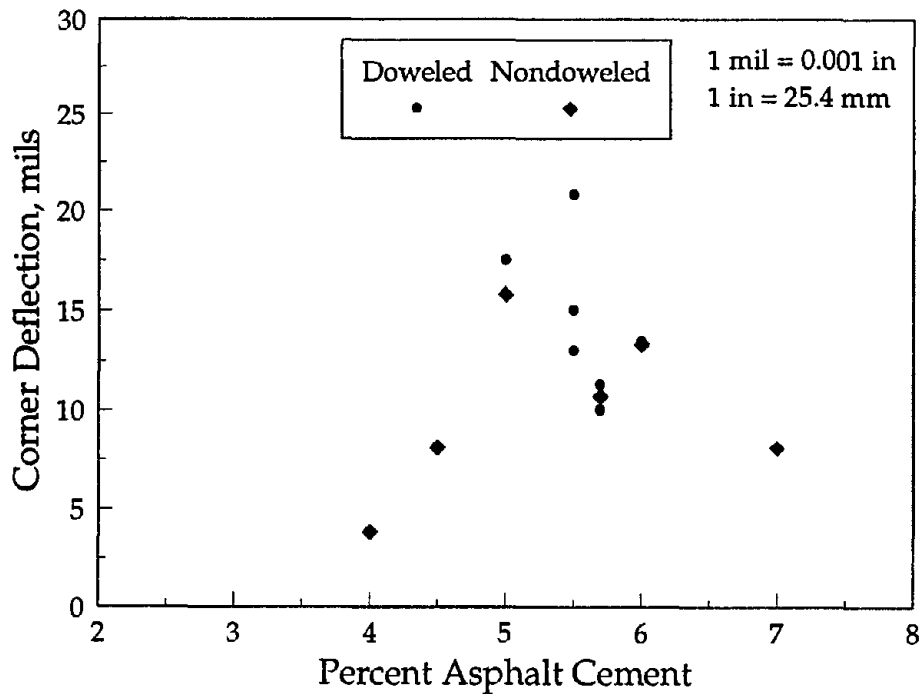


Figure 41. Effect of percentage of asphalt cement on corner deflections.

### Drainage

Moisture has long been recognized as a factor detrimental to the performance of PCC pavements. For example, one of the key elements in the development of faulting is excess moisture. In addition, moisture can soften the underlying support layers, leading to increased deflections and stresses in the PCC slab. Other moisture-related problems include joint spalling, D-cracking, and corrosion of dowels and reinforcement.

The sections evaluated in this study incorporate several different approaches to minimize the effects of moisture on pavement performance. Specifically, the following types of drainage features were used:

- Permeable base layers (PCTB, PATB, PAGG).
- Daylighted base or subbase layers (dense-graded aggregate).
- Longitudinal edge drains.
- Longitudinal fin drains.
- Transverse drains.

These drainage features were used singly and in combination with each other. Figure 42 illustrates the distribution of the various drainage designs. About one-half of the sections incorporate some means of removing moisture from the pavement. Of the different drainage features, edge drains are the most common. Edge drains are used alone and in conjunction with either a permeable base or transverse drains. A daylighted base is used on 35 sections as a means of removing moisture. Figure 43 illustrates a similar plot, with the sections further divided into doweled and nondoweled sections.

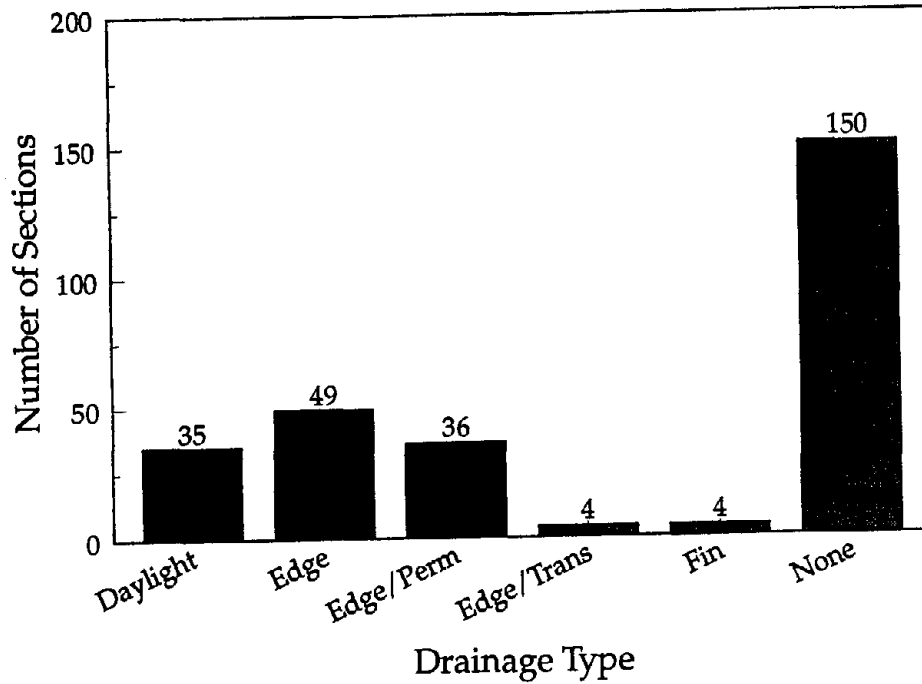


Figure 42. Distribution of drainage designs.

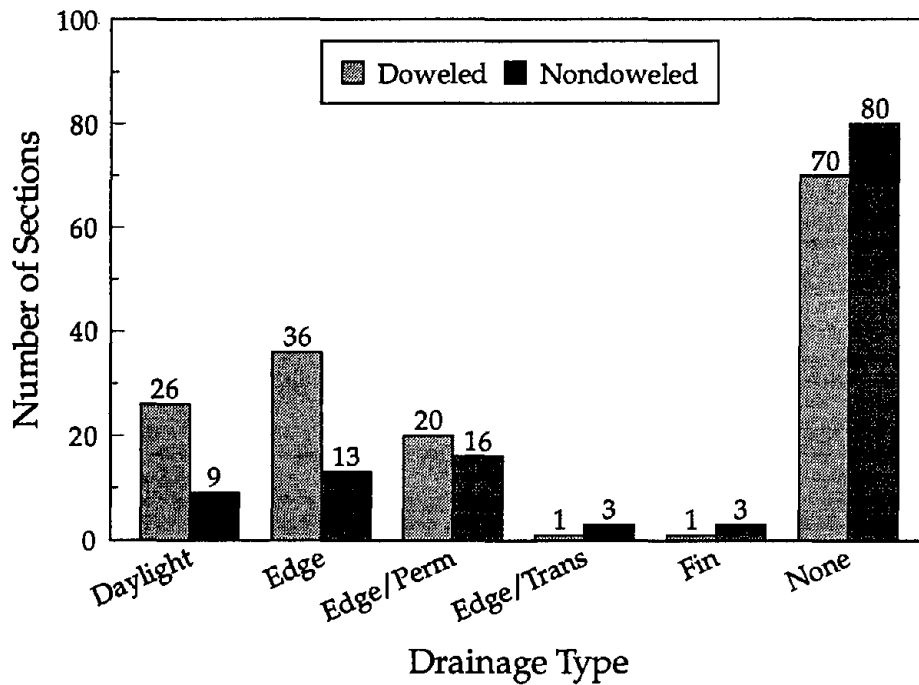


Figure 43. Distribution of drainage designs for doveled and nondoweled pavements.

## Review of Project Data

This section provides comparisons of similar sections that incorporate different drainage features. These comparisons include the use of different base types and different types of drains, as well as various  $C_d$  values and permeabilities. Sections in which no drainage elements were incorporated are also included in the comparisons when available.

### *Arizona 1*

This project, located on State Route 360 in Phoenix, provides a comparison of a section with no drainage elements (AZ 1-6) and a section with longitudinal edge drains (AZ 1-7). Both sections consist of a 9-in (229-mm) JPCP and a 4-in (102-mm) LCB with 6.9 percent cement. The transverse joints are nondoweled and spaced at random 13-15-17-15-ft (4.0-4.6-5.2-4.6-m) intervals.

Table 92 provides a summary of the performance data for AZ 1-6 and 1-7. Both sections are performing very well, especially considering that dowel bars are not provided. The edge drains do not appear to provide any substantial benefit in terms of performance. This result is likely related to the climatic conditions of the Phoenix area, which receives little moisture (average annual precipitation of 8 in [200 mm]) and no freezing conditions.

Table 92. Summary of effect of drainage for AZ 1.

Section	ESAL's, millions		Faulting, in		% Slabs Cracked		% Joints Spalled		IRI, in/mi (PSR)	
	1987	1992	1987	1992	1987	1992	1987	1992	1987	1992
AZ 1-6 No Drainage	2.0	5.1	0.01	0.01	0	0	1	3	-(3.5)	123 (3.5)
AZ 1-7 Edge Drains	1.5	4.7	0.02	0.02	0	0	0	8	-(3.8)	135 (3.6)

1 in = 25.4 mm  
1 ft = 0.305 m  
1 mi = 1.61 km

Common Design Features: 9-in nondoweled JPCP  
13-15-17-15-ft joint spacing  
4-in LCB (6.9% cement)  
Built in 1981

### *California 2*

This project, located on I-210 near Los Angeles, includes two sections with completely different drainage designs. CA 2-2 contains a PCTB (6-8 percent cement) and longitudinal edge drains. CA 2-3, however, does not contain any provisions for drainage (CTB with 5 percent cement). However, a thin layer of asphalt concrete was placed between the slab and the PCTB, altering the drainage capabilities of the PCTB.



Both sections are 8.4-in (213-mm) nondoweled JPCP with transverse joints spaced at 12-13-19-18-ft (3.7-4.0-5.8-5.5-m) intervals. The pavements are exposed to an average annual precipitation of 9.7 in (250 mm) but are not exposed to freezing conditions.

A summary of the performance data for CA 2 is provided in table 93. Both sections are exhibiting excessive faulting levels, although faulting is more severe on the section with AC/PCTB. Apparently, the thin AC layer has reduced the effectiveness of the PCTB, thus increasing the potential for faulting. This incident illustrates the importance of proper design and construction of the drainage system. However, significantly more transverse cracking and spalling has occurred on the section with no drainage elements.

Table 93. Summary of effect of drainage for CA 2.

Section	ESAL's, millions		Faulting, in		% Slabs Cracked		% Joints Spalled		IRI, in/mi (PSR)	
	1987	1992	1987	1992	1987	1992	1987	1992	1987	1992
CA 2-2 AC/PCTB Edge Drains	4.4	9.1	0.11	0.16	0	3	0	3	-(3.8)	137 (4.0)
CA 2-3 CTB No Drainage	4.4	9.1	0.11	0.13	66	68	0	15	-(4.1)	116 (3.9)

1 in = 25.4 mm  
1 ft = 0.305 m  
1 mi = 1.61 km

Common Design Features: 8.4-in nondoweled JPCP  
12-13-19-18-ft joint spacing  
Built in 1980

### California 6

This project, located on Route 14 near Los Angeles, consists of two separate sections with different drainage designs. Both sections are 9-in (229-mm) JPCP with no dowel bars at the transverse joints. CA 6-1 contains a 5.4-in (137-mm) CTB with 4 percent cement, a 12-13-19-18-ft (3.7-4.0-5.8-5.5-m) joint spacing, and no drainage elements. CA 6-2 contains a 12-13-15-14-ft (3.7-4.0-4.6-4.3-m) joint spacing, a 4.2-in (107-mm) PATB with 2 percent AR-4000, and longitudinal edge drains.

Table 94 presents a summary of the performance data for these two sections. The section with a permeable base and edge drains is performing better, especially in terms of faulting and serviceability. The higher faulting level cannot be explained by the higher number of ESAL applications alone; it is probably more associated with the superior drainage capabilities of the section.

Table 94. Summary of effect of drainage for CA 6.

Section	ESAL's, millions	Joint Faulting, in	% Slabs Cracked	Long Crk, ft/mi	% Joints Spalled	IRI, in/mi (PSR)
CA 6-1 5.4-in CTB No Drainage	13.3	0.14	4	0	3	173 (3.5)
CA 6-2 4.2-in PATB Edge Drains	9.8	0.05	0	0	0	170 (3.8)

1 in = 25.4 mm  
1 ft = 0.305 m  
1 mi = 1.61 km

Common Design Features: 9-in nondoweled JPCP  
CA 6-1 built in 1971  
CA 6-2 built in 1980

Research conducted by the California Department of Transportation has shown significant stripping of the PATB, resulting in loss of bond between the aggregate particles.<sup>(43)</sup> This condition may lead to adverse performance and contamination of the surrounding soil. The addition of lime or other anti-stripping agents may help prevent (or at least delay) stripping of the asphalt cement. However, stabilization of permeable bases is generally considered a construction expedient and should not be relied on for long-term structural support.

### California 9

This experimental project, located on I-680 in Milpitas, contains two sections with different drainage designs. CA 9-8 incorporates longitudinal edge drains, whereas CA 9-10 does not include any drainage elements. Both sections consist of a 9-in (229-mm) JPCP and a 5.4-in (137-mm) CTB with 5 percent cement. The transverse joints are spaced at 12-13-19-18-ft (3.7-4.0-5.8-5.5-m) intervals and do not contain any load transfer devices or joint sealant.

Table 95 shows the performance data for CA 9. The section containing edge drains has more faulting and roughness than the nondrained section. However, the drainage outlets were reportedly damaged by landscaping crews about 3 years after construction and were never repaired.<sup>(12)</sup> It seems logical to assume that the damaged outlets resulted in moisture being trapped in the pavement system and directly lead to the poor performance. However, transverse and longitudinal cracking were significantly higher on the section without drainage elements.

### Michigan 1

This experimental project, located on U.S. 10 near Clare, contains several sections in which the effect of drainage on performance can be evaluated. Many different design features are also employed, including various pavement types, joint spacings, and base types.

Table 95. Summary of effect of drainage for CA 9.

Section	ESAL's, millions	Joint Faulting, in	% Slabs Cracked	Long Crk, ft/mi	% Joints Spalled	IRI, in/mi (PSR)
CA 9-8 Edge Drains	10.5	0.17	3	0	0	212 (3.3)
CA 9-10 No Drainage	10.5	0.10	67	96	2	153 (2.9)

1 in = 25.4 mm  
 1 ft = 0.305 m  
 1 mi = 1.61 km

Common Design Features: 9-in JPCP, 5.4-in CTB  
 12-13-19-18-ft nondoweled joints  
 Built in 1974

Table 96 presents a summary of the JPCP performance data for different drainage designs. The first four sections have a 4-in (102-mm) aggregate base, a random 12-13-17-16-ft (3.7-4.0-5.2-4.9-m) joint spacing, and 1.25-in (32-mm) dowel bars. The latter four sections have a 4-in (102-mm) ATB (bathtub design), a 12-13-19-18-ft (3.7-4.0-5.8-5.5-m) joint spacing, and no load transfer devices. For both designs, sections with and without drainage are compared. The sections with drainage contain retrofitted longitudinal edge drains consisting of an aggregate (French) drain directly beneath the lane-shoulder interface (retrofitted in 1981).

For the same design, the distress and roughness levels are about the same regardless of the drainage conditions. This result indicates that the inclusion of the retrofitted French drains without a permeable base layer did not improve the performance. The first four sections have performed better than the latter four sections, although it is uncertain whether the addition of dowel bars, the use of an aggregate base, or the combination of the two resulted in the improved performance.

The performance data for the JRCP sections are presented in table 97. These sections are all 9-in (229-mm) JRCP with 0.15 percent reinforcing steel and a 4-in (102-mm) aggregate base. The transverse joints are spaced at 71.2-ft (21.7-m) intervals and contain 1.25-in (32-mm) dowel bars. MI 1-1a and 1-1a2 contain retrofitted French drains, and MI 1-1b and 1-1b2 contain no provisions for drainage.

The sections with retrofitted french drains have slightly less faulting and spalling than the sections without edge drains. However, they also have more deteriorated cracks and roughness. At this point, it is difficult to determine whether the retrofitted French drains were effective at improving performance.

Table 96. Summary of effect of drainage on JPCP for MI 1.

Section	ESAL's, millions	Joint Faulting, in	% Slabs Cracked	Long Crk, ft/mi	% Joints Spalled	IRI, in/mi (PSR)
MI 1-7a French Drains* AGG Base 1.25-in Dowels	1.3	0.05	0	0	18	121 (3.0)
MI 1-7a5 French Drains* AGG Base 1.25-in Dowels	1.3	0.05	0	0	0	130 (-)
MI 1-7b No Drainage AGG Base 1.25-in Dowels	1.3	0.03	0	0	11	120 (3.1)
MI 1-7b5 No Drainage AGG Base 1.25-in Dowels	1.3	0.06	0	0	20	121 (-)
MI 1-10a French Drains* ATB No Dowels	1.3	0.13	0	0	100	161 (2.0)
MI 1-10a3 French Drains* ATB No Dowels	1.3	0.29	15	0	79	203 (-)
MI 1-10b No Drainage ATB No Dowels	1.3	0.15	5	0	100	197 (2.1)
MI 1-25 No Drainage ATB No Dowels	1.3	0.30	13	0	100	247 (2.3)

1 in = 25.4 mm  
 1 ft = 0.305 m  
 1 mi = 1.61 km

Common Design Features: 9-in JPCP  
 Built in 1975

\* French drains were retrofit in 1981.

Table 97. Summary of effect of drainage on JRCP for MI 1.

Section	ESAL's, millions	Joint Faulting, in	Deter Cracks/mi	Long Crk, ft/mi	% Joints Spalled	IRI, in/mi (PSR)
MI 1-1a French Drains*	1.3	0.06	0	0	11	141 (3.5)
MI 1-1a2 French Drains*	1.3	0.03	32	0	0	174 (-)
MI 1-1b No Drainage	1.3	0.10	5	0	20	135 (2.9)
MI 1-1b2 No Drainage	1.3	0.06	0	0	33	136 (-)

1 in = 25.4 mm

1 ft = 0.305 m

1 mi = 1.61 km

\* French drains were retrofit in 1981.

Common Design Features: 9-in JRCP with 0.15% steel  
71.2-ft joints with 1.25-in dowels  
Built in 1975

### *New Jersey 3*

This experimental project, located on I-676 near Camden, contains two sections with longitudinal edge drains but varying base types. NJ 3-1 contains a 4-in (102-mm) permeable aggregate base, and NJ 3-2 contains a 4-in (102-mm) PATB with 2.5 percent AC-20. Both sections have 9-in (229-mm) JRCP slabs with 0.16 percent reinforcing steel, 78.5-ft (23.9-m) expansion joint spacings, and 1.25-in (32-mm) stainless steel-wrapped dowel bars. On both sections, longitudinal edge drains are provided and a filter fabric is placed between the permeable base and the lime-flyash stabilized subgrade.

Table 98 presents a summary of the performance data for NJ 3. Both sections are performing well after 13 years of service and nearly 13 million ESAL applications. No appreciable difference in the performance indicators was noticed between 1987 and 1992. The high roughness levels are believed to be a result of the 0.75-in (19-mm) wide expansion joints. The joint spalling is also thought to be due to improper construction of the expansion joints.

### *Ohio 2*

This experimental project is located on State Route 2 near Vermillion. The sections analyzed in the evaluation of drainage are all 9-in (229-mm) JRCP with 0.10 percent reinforcing steel, 40-ft (12.2-m) transverse joint spacing, and 1.25-in (32-mm) dowel bars. The sections include designs with longitudinal edge drains, with a daylighted dense-graded aggregate base, and with no provisions for drainage.

Table 98. Summary of effect of drainage for NJ 3.

	ESAL's, millions		Faulting, in		% Slabs Cracked		% Joints Spalled		IRI, in/mi (PSR)	
	1987	1992	1987	1992	1987	1992	1987	1992	1987	1992
NJ 3-1 Edge Drains 4-in PAGG	4.9	12.6	0.05	0.04	0	0	0	29	- (3.6)	191 (-)
NJ 3-2 Edge Drains 4-in PATB	4.9	12.6	0.06	0.03	0	0	43	43	- (3.5)	199 (-)

1 in = 25.4 mm  
1 ft = 0.305 m  
1 mi = 1.61 km

Common Design Features: 9-in JRCF with 0.16% steel  
78.5-ft joints with 1.25-in dowels  
Built in 1979

Table 99 provides the performance data for the sections used for evaluating the effect of drainage. Three separate evaluations can be made using this data. The first group of sections have a maximum aggregate size of 0.5 in (13 mm), the second group has a maximum aggregate size of 1.0 in (25 mm), and the third group has a maximum aggregate size of 1.5 in (38 mm). OH 2-21, 2-54, and 2-72 contain Sy2 coarse aggregate (source known to produce durable material); the other sections contain Mn3 coarse aggregate (source commonly associated with D-cracking).

The results of the evaluations are mixed. The sections with a maximum aggregate size of 0.5 and 1.0 in (13 and 25 mm) indicate a reduction in faulting but no benefit in terms of distress measurements by using either a daylighted base or longitudinal edge drains. The sections with a maximum aggregate size of 1.5 in (38 mm) show improved performance in terms of transverse cracking using a daylighted base or edge drains (for sections containing durable aggregate). However, faulting levels are higher on the sections in which positive drainage features are incorporated. For sections containing durable aggregate, a reduction in faulting is noticed for the section with edge drains compared to the section with a daylighted base. Overall, little to no structural benefit was noticed from the use of these drainage elements, although the daylighted base was effective in delaying the onset of D-cracking.

Table 100 also provides performance data for OH 2. The major design change for these sections is the base type. OH 2-43 and 2-49 have a 4-in (102-mm) ATB with 4 to 8 percent asphalt cement, whereas OH 2-94, 2-100, and 2-102 contain a 4-in (102-mm) CTB with 4.5 percent cement. The sections with longitudinal edge drains have less deteriorated transverse cracks and less roughness, although they also have higher faulting levels. Again, the use of longitudinal edge drains does not appear to offer any benefit in terms of performance.

Table 99. Summary of effect of drainage for OH 2 (aggregate base).

Section	Design	ESAL's, millions	Joint Faulting, in	Deter Cracks/mi	Long Crk, ft/mi	% Joints Spalled	IRL, in/mi
OH 2-75	None 0.5-in Agg.	6.5	0.01	110	0	14	130
OH 2-55	Daylight 0.5-in Agg.	6.5	0.07	198	0	0	190
OH 2-24	Edge Drains 0.5-in Agg.	6.5	0.00	154	0	0	161
OH 2-74	None 1.0-in Agg.	6.5	0.03	66	0	29	140
OH 2-56	Daylight 1.0-in Agg.	6.5	0.02	132	0	0	114
OH 2-23	Edge Drains 1.0-in Agg.	6.5	0.00	132	0	17	172
OH 2-69	None 1.5-in Agg.	6.5	0.01	132	0	29	128
OH 2-72*	None 1.5-in Agg.	6.5	-	254	0	0	-
OH 2-57	Daylight 1.5-in Agg.	6.5	0.04	132	0	29	132
OH 2-54*	Daylight 1.5-in Agg.	6.5	0.11	176	0	0	168
OH 2-20	Edge Drains 1.5-in Agg.	6.5	0.08	132	0	17	172
OH 2-21*	Edge Drains 1.5-in Agg.	6.5	0.04	132	0	0	180

1 in = 25.4 mm

1 ft = 0.305 m

1 mi = 1.61 km

\* Sections contain Sy2 coarse aggregate;  
others contain Mn3 coarse aggregate.

Common Design Features: 9-in JRPC with 0.10% steel  
40-ft joint spacing  
1.25-in dowels  
Built in 1974

### Ontario 1

This project, located on Highway 3N near Windsor, compares two sections with longitudinal edge drains but different base types. ONT 1-2 contains a 4-in (102-mm) PATB with 2 percent asphalt cement, and ONT 1-3 contains a 5-in (127-mm) LCB with 7.2 percent cement. Both sections are 8-in (203-mm) nondoweled JPCP with transverse joints spaced at 12-13-19-18-ft (3.7-4.0-5.8-5.5-m) intervals.

Table 100. Summary of effect of drainage for OH 2 (stabilized base).

Section	Design	ESAL's, millions	Joint Faulting, in	Deter Cracks/mi	Long Crk, ft/mi	% Joints Spalled	IRI, in/mi
OH 2-43	None ATB (4-8%)	6.5	0.01	22	0	43	276
OH 2-49	Edge Drains ATB (4-8%)	6.5	0.05	0	0	100	144
OH 2-94	None CTB (4.5%)	6.5	0.05	110	0	86	153
OH 2-100	Edge Drains CTB (4.5%)	6.5	0.06	44	0	43	120
OH 2-102*	Edge Drains CTB (4.5%)	6.5	0.18	88	0	29	166

1 in = 25.4 mm

1 ft = 0.305 m

1 mi = 1.61 km

\* Sections contain Sy2 coarse aggregate; others contain Mn3 coarse aggregate.

Common Design Features:

9-in JRCP with 0.10% steel

40-ft joint spacing

1.25-in dowels

Built in 1974

A summary of the performance data for these sections is provided in table 101. The section with the PATB is performing better than the section constructed on an LCB. The lower faulting and roughness levels are believed to be a result of the improved drainage provided by the PATB. The transverse cracking on ONT 1-3 is likely a result of the increased thermal stresses caused by the stiff LCB.

Although the performance was improved, an even greater improvement would be expected had the drainage system been designed better. A separator layer was not provided beneath the PATB, and the bottom of the PATB was contaminated with fines and showing signs of stripping, with AC contents of 2.0 percent at the bottom compared to 2.7 percent at the top.<sup>(35)</sup> Cores taken at faulted transverse joints revealed that the base was stripped and heavily contaminated with subgrade grading, with asphalt contents as low as 1.1 percent.<sup>(35)</sup> In addition, the edge drain was placed in the dense-graded shoulder base, thus reducing the movement of moisture to the edge drains.

### *Pennsylvania 1*

This experimental project, located on Routes 66 and 422 near Kittanning, contains sections with longitudinal edge drains and varying base types. All sections are 10-in (229-mm) JRCP with 0.09 percent reinforcing steel. The transverse joints are spaced at 46.5-ft (14.2-m) intervals and contain 1.25-in (32-mm) epoxy-coated dowel bars. PA 1-1 contains a 6-in (152-mm) CTB with 6 percent cement, PA 1-2 contains a 5-in (127-mm) PATB with 2 percent asphalt, and the other sections contain an aggregate base varying in thickness from 8 to 13 in (203 to 330 mm).



Table 101. Summary of effect of drainage for ONT 1.

Section	ESAL's, millions		Faulting, in		% Slabs Cracked		Long Crk, ft/mi		IRI, in/mi (PSR)	
	1987	1992	1987	1992	1987	1992	1987	1992	1987	1992
ONT 1-2 4-in PATB Edge Drains	0.9	2.1	0.05	0.10	0	0	0	105	- (3.8)	135 (3.9)
ONT 1-3 5-in LCB Edge Drains	0.9	2.1	0.04	0.14	9	8	490	621	- (3.8)	147 (3.9)

1 in = 25.4 mm  
1 ft = 0.305 m  
1 mi = 1.61 km

Common Design Features: 8-in nondoweled JPCP  
13-19-18-12-ft joint spacing  
Built in 1982

Table 102 presents a summary of the performance data for PA 1. All sections exhibited little distress, but they have only been exposed to about one million ESAL applications. The section with the CTB exhibited the most faulting and was the only section in which deteriorated cracks were observed. Based on the limited amount of distress on these sections, it is difficult to determine the effect of the base type and longitudinal edge drains on PCC pavement performance.

Table 102. Summary of effect of drainage for PA 1.

Section	Drainage	ESAL's, millions	Joint Faulting, in	Deter Cracks/mi	Long Crk, ft/mi	% Joints Spalled	IRI, in/mi (PSR)
PA 1-1	6-in CTB Edge Drains	1.1	0.05	10	0	0	134 (3.9)
PA 1-2	5-in PATB Edge Drains	0.8	0.01	0	0	4	150 (4.2)
PA 1-3	8-in AGG <sup>a</sup> Edge Drains	0.8	0.03	0	0	0	178 (4.1)
PA 1-4	8-in AGG <sup>b</sup> Edge Drains	0.8	0.03	0	0	0	159 (4.0)
PA 1-5	13-in AGG <sup>c</sup> Edge Drains	0.8	0.02	0	0	0	127 (4.3)

1 in = 25.4 mm  
1 ft = 0.305 m  
1 mi = 1.61 km

Common Design Features: 10-in JRCP with 0.09% steel  
46.5-ft joint spacing with 1.25-in dowels  
Built in 1980

<sup>a</sup> Uniform-graded aggregate  
<sup>b</sup> Well-graded aggregate  
<sup>c</sup> Dense-graded aggregate

### *Wisconsin 2/Wisconsin 7*

These projects are located adjacent to each other on U.S. 18/151 near Mt. Horeb and Barneveld, respectively. The projects include sections with longitudinal edge drains, with both transverse and longitudinal drains, and with no drains, as well as various base types. Three different groups of sections are shown in table 103. The first group (five sections) has 1.25-in (32-mm) epoxy-coated dowel bars and no joint sealant. The second group (four sections) has no dowel bars and a preformed joint sealant. The last group (five sections) has no dowel bars and no joint sealant. All sections are 9-in (229-mm) JPCP with skewed transverse joints spaced at 12-13-19-18-ft (3.7-4.0-5.8-5.5-m) intervals.

Although it is difficult to evaluate these sections after only 4 years of service and 1.3 million ESAL applications, some trends in the data were noticed. For instance, two of the three sections with a PCTB exhibited high levels of longitudinal cracking, whereas no other section exhibited any longitudinal cracking. The stiff base and the 14-ft (4.3-m) outer lane result in increased thermal stresses in the slab. The ineffectiveness of the plastic inserts used to form the joints may also be responsible for the cracking.

Joint spalling is a problem on some of the sections, although it is fairly consistent regardless of base type and drainage conditions. Transverse cracking was observed on only one section (PAGG) and only on 6 percent of the slabs. For each evaluation, roughness values are lowest on the section with the PATB.

### *Wisconsin 3*

This experimental project, located on STH 14 near Middleton, contains sections with different base types and drainage conditions. WI 3-1 contains longitudinal fin drains and a 3.5-in (89-mm) PATB with 2 percent asphalt cement. WI 3-2 contains longitudinal fin drains and a 6-in (152-mm) aggregate base. WI 3-3 contains a 6-in (152-mm) aggregate base but no drainage elements. All sections are 8-in (203-mm) nondoweled JPCP with skewed transverse joints spaced at 12-13-19-18-ft (3.7-4.0-5.8-5.5-m) intervals.

Table 104 presents the performance data for evaluating the effect of drainage on PCC pavement performance. The combination of longitudinal fin drains and a PATB has resulted in substantially improved performance over the other designs, especially in terms of faulting and roughness. Apparently, the section with the PATB is more effective at removing moisture from the pavement structure. For WI 3-2, the data are insufficient to determine whether the aggregate base is ineffective at moving moisture to the fin drains or the fin drains are ineffective. No provisions for drainage were incorporated in WI 3-3 and consequently, the performance has suffered.

Table 103. Summary of effect of drainage for WI 2 & 7.

Section	Design	ESAL's, millions	Joint Faulting, in	% Slabs Cracked	Long Crk, ft/mi	% Joints Spalled	IRI, in/mi (PSR)
WI 2-1	Edge Drains 4-in PCTB	1.3	0.01	0	0	5	122 (4.1)
WI 2-2	Edge Drains 4-in PATB	1.3	0.01	0	0	3	106 (4.0)
WI 2-3	Edge Drains 4-in PAGG	1.3	0.01	0	0	3	112 (4.0)
WI 7-10	Trans. Drains Edge Drains 6-in AGG	1.3	0.01	0	0	3	113 (4.2)
WI 2-4	No Drainage 6-in AGG	1.3	0.01	0	0	6	115 (4.1)
WI 7-3	Edge Drains 4-in PCTB	1.3	0.01	0	326	0	147 (4.1)
WI 7-5	Edge Drains 4-in PATB	1.3	0.01	0	0	2	86 (4.1)
WI 7-1	Edge Drains 4-in PAGG	1.3	0.03	0	0	6	136 (4.3)
WI 7-8	No Drainage 6-in AGG	1.3	0.04	0	0	3	116 (3.9)
WI 7-4	Edge Drains 4-in PCTB	1.3	0.04	0	257	8	147 (4.0)
WI 7-6	Edge Drains 4-in PATB	1.3	0.02	0	0	10	98 (4.0)
WI 7-2	Edge Drains 4-in PAGG	1.3	0.03	6	0	8	120 (4.5)
WI 7-7	Trans. Drains Edge Drains 6-in AGG	1.3	0.02	0	0	3	117 (4.3)
WI 7-9	No Drainage 6-in AGG	1.3	0.04	0	0	8	114 (3.9)

1 in = 25.4 mm

1 ft = 0.305 m

1 mi = 1.61 km

Common Design Features: 9-in JPCP

12-13-19-18-ft joint spacing (skewed)

Built in 1988

Note: Sections 7-1, 7-3, 7-5, and 7-8 contain a preformed joint sealant; others contain no joint seal.

Sections 2-1, 2-2, 2-3, 2-4, and 7-10 contain 1.25-in epoxy-coated dowels; others contain no dowels.

Table 104. Summary of effect of drainage for WI 3.

Section	Design	ESAL's, millions	Joint Faulting, in	% Slabs Cracked	Long Crk, ft/mi	% Joints Spalled	IRI, in/mi (PSR)
WI 3-1	Fin Drains 3.5-in PATB	1.2	0.03	0	0	2	109 (4.0)
WI 3-2	Fin Drains 6-in AGG	1.2	0.13	0	0	3	151 (3.6)
WI 3-3	No Drainage 6-in AGG	1.2	0.15	0	0	2	147 (3.5)

1 in = 25.4 mm  
1 ft = 0.305 m  
1 mi = 1.61 km

Common Design Features: 8-in nondoweled JPCP  
12-13-19-18-ft skewed joints  
Built in 1988

### Wisconsin 5

This experimental project, constructed on STH 50 near Kenosha, includes sections with longitudinal fin drains, with longitudinal pipe drains, and with no drains. All sections are 10-in (254-mm) JPCP with a 14-ft (4.3-m) outer lane, AC shoulders, and a 6-in (102-mm) dense-graded aggregate base. Transverse joints are spaced at 12-13-19-18-ft (3.7-4.0-5.8-5.5-m) intervals and do not contain any load transfer devices. The joints of WI 5-1, 5-3, and 5-5 are sealed using a silicone sealant. The joints are not sealed on WI 5-2, 5-4, and 5-6. The longitudinal centerline joints were formed using plastic inserts.

The performance data for WI 5 is provided in table 105. The sections with longitudinal pipe drains exhibited the most faulting and spalling of the pavement sections. In addition, transverse cracking occurred on only one section, which contains longitudinal pipe drains. With the exception of longitudinal cracking, the sections with longitudinal fin drains and without drains showed similar performance. One section without drains exhibited significant longitudinal cracking. Overall, the short life of the pavements (4 years) makes it difficult to draw definitive conclusions.

### Related Research

A good source of design and construction information for pavement drainage systems is available in the form of Demonstration Project No. 87, *Drainable Pavement Systems*.<sup>(47)</sup> The purpose of this demonstration project is to provide State highway engineers with current state-of-the-art drainage guidance on the design and construction permeable bases and edge drains for PCC pavements.<sup>(47)</sup> Guidance is also provided for retrofit edge drains and maintenance of the drainage system.

Table 105. Summary of effect of drainage for WI 5.

Section	Design	ESAL's, millions	Joint Faulting, in	% Slabs Cracked	Long Crk, ft/mi	% Joints Spalled	IRI, in/mi (PSR)
WI 5-1*	Fin Drains	1.4	0.03	0	0	8	138 (3.8)
WI 5-3*	Pipe Drains	1.4	0.06	0	0	12	147 (3.8)
WI 5-5*	No Drainage	1.4	0.04	0	545	6	133 (3.8)
WI 5-2	Fin Drains	1.4	0.05	0	0	3	132 (3.7)
WI 5-4	Pipe Drains	1.4	0.06	3	0	9	142 (3.9)
WI 5-6	No Drainage	1.4	0.03	0	0	8	142 (3.7)

1 in = 25.4 mm

1 ft = 0.305 m

1 mi = 1.61 km

\*Sections contain silicone joint sealant; others contain no sealant.

Common Design Features:

10-in nondoweled JPCP

6-in aggregate base

12-13-19-18-ft skewed joints

Built in 1988

Based on case studies of pavement sections from nine states, Cedegren concluded that rapidly drained sections are vastly superior to poorly drained sections and will suffer considerably less damage.<sup>(48)</sup> Guidelines for the design and construction of subsurface drainage systems are given for greatly reducing the effects of moisture damage. Based on cost studies, Cedegren indicated that effective subsurface drainage systems usually are economically and technically feasible under prevailing environmental conditions within the United States.<sup>(48)</sup>

Research at the University of Illinois was conducted in order to develop a complete pavement system that incorporated an open-graded drainage layer to effectively remove infiltrated water.<sup>(49)</sup> Based on the results of the study, the following design provisions were recommended:

- The open graded drainage layer should be placed immediately below the surface course.
- A filter layer should be placed below the open graded layer to prevent intrusion of fines from the underlying layer.
- Lateral drainage provisions (e.g., longitudinal edge drains) must be included to remove the infiltrated water from the pavement structure.
- For optimal performance, open graded permeable materials should have permeabilities exceeding 1000 ft/day (305 m/day), a coefficient of uniformity ( $C_u$ ) less than 3.5, and a coefficient of curvature ( $C_z$ ) between 0.9 and 4.0.
- If construction traffic will be applied directly on the permeable layer, stabilization is required. Portland cement contents of 6 percent or more and

asphalt cement contents of 2.5 percent or more by weight of aggregate are required for adequate strength.

The New Jersey Department of Transportation conducted an extensive investigation (field and laboratory) of the need for subsurface drainage systems in 1983.<sup>(50)</sup> Field surveys revealed a definite need to provide better drainage systems, as extensive moisture-related distress was observed on PCC pavements and to a lesser extent on AC pavements. An extensive literature search and testing program resulted in the following conclusions and design recommendations:

- An asphalt-treated open-graded material was considered most appropriate for AC pavements, whereas a nonstabilized open-graded was best for PCC pavements.
- For the nonstabilized open-graded material, a 50/50 blend of NJDOT #57 and #9 stones was found to be optimal for permeability, stability, and filtration.
- The optimum asphalt-treated open-graded material was found to be a slightly modified NJDOT #8 stone containing 2 percent asphalt cement and an anti-stripping agent.
- The open-graded drainage layers were found to have little effect on frost penetration under pavements in New Jersey.
- The use of a 4-in (102-mm) open-graded drainage layer, in conjunction with longitudinal edge drains, was recommended.
- The gradation specification alone cannot always secure adequate base, subbase, and embankment materials.
- Subsurface drainage should not be designed as a separate entity, but rather in conjunction with other elements within the entire pavement system.

#### Overall Evaluation of Drainage

An investigation of different drainage designs for the individual projects provided some interesting conclusions. The most prominent conclusion was the lack of benefit provided by the use of longitudinal edge drains when not accompanied by a permeable base layer. This result was not an isolated event, as it was seen on numerous sections (AZ 1, MI 1, OH 2, ONT 1, and WI 5). Some possible explanations for this lack of benefit are improper placement of the edge drains or an inability to move moisture to the edge drains. The time it takes to remove the moisture from the base is likely longer than the time between rainfalls. Therefore, moisture is continuously trapped within the dense-graded base and the adverse effects of moisture are constantly at work.

Conversely, inclusion of a permeable base layer with edge drains resulted in

improved performance, especially in terms of joint faulting and spalling. The permeable base layer allows free movement of moisture through the base to the edge drains. By removing this moisture from the base, the adverse effects of moisture can be prevented.

Parallel to this result, sections with a daylighted base did not outperform equivalent sections with a conventional base. In fact, the performance was actually worse in some cases. Again, if moisture cannot effectively move through the base and out of the pavement structure, then one cannot expect any benefit. In addition, daylighted bases often become clogged at the outlet from grass and debris. When the system gets clogged, the base becomes fully saturated. In this case, the daylighted base has provided a condition that is more detrimental to the pavement than if no drainage was provide.

Just as proper maintenance is required to keep the system operating properly, proper design of the drainage system is equally important. The drainage system should be designed to maximize the potential of removing moisture from the pavement, especially at the critical areas such as along the transverse and longitudinal joints. Improper design can result in ineffective drainage and poor performance. For instance, CA 2-2 was provided with a PCTB and longitudinal edge drains. However, a thin AC layer was placed between the nondoweled PCC slab and the PCTB and infiltrated water was not able to reach the PCTB. Consequently, excessive faulting (0.16 in [4.1 mm]) occurred at the transverse joints.

An important design feature for sections with a permeable base is a filter or separation layer between the base and the underlying layer (subbase or subgrade). This layer keeps fines from migrating into the permeable base layer and reducing the permeability. A few sections with a permeable base were not provided with a filter or separation layer, resulting in high faulting levels.

An overall examination of the sections was conducted to investigate the effect of other design features and variables that could not be evaluated through individual projects. Each drainage system was evaluated as to the effect on distress and roughness measurements. In addition, other design variables; such as the AASHTO drainage coefficient ( $C_d$ ), annual precipitation, and coefficient of uniformity ( $C_u$ ) were also investigated.

Transverse joint faulting is the most common distress directly associated with the drainage conditions. Figure 44 illustrates the faulting of doweled and nondoweled sections distributed by drainage design. The sections with a daylighted base have the most faulting, followed by the sections with edge drains and no permeable base. Both designs have faulting levels exceeding those in which no drainage was provided. The sections that are effective at moving water to the edge drains, such as those with either a permeable base or transverse drains, have significantly less faulting. In fact, nondoweled sections with a permeable base or transverse drains have less faulting than doweled sections with ineffective drainage.

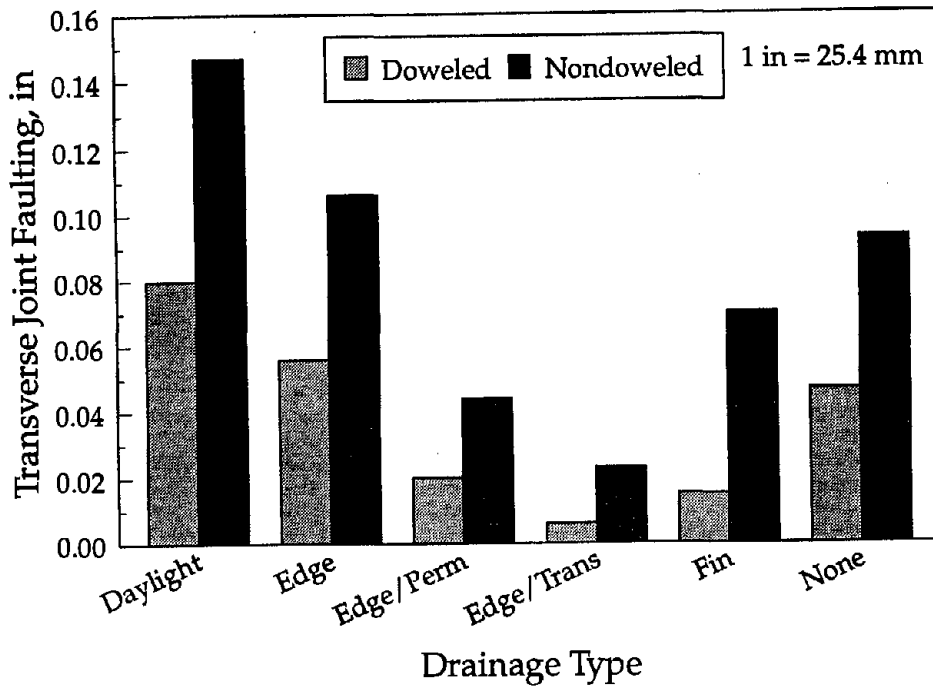


Figure 44. Transverse joint faulting for each drainage design.

With a few exceptions, similar trends were observed for transverse joint spalling and transverse cracking. The results are illustrated in figures 45 and 46, respectively. The joint spalling chart is almost identical to the faulting chart (although not as much differentiation between doweled and nondoweled sections), with sections containing daylighted bases or edge drains performing poorly. Transverse cracking also shows similar trends. The sections containing daylighted bases or edge drains are exhibiting more cracking than sections without drainage provisions.

The use of permeable bases is still somewhat of an experimental design in that long-term performance data are not available. Thus, these sections have not been exposed to the climatic effects and load applications of the more conventional designs. Figure 47 shows the average age for each drainage design. The drainage designs that exhibited better performance are also the youngest sections.

However, the improved performance is not thought to be entirely due to the age differences. To prove this theory, 1987 faulting data from the sections with edge drains were compared with 1992 faulting data from the sections with edge drains and a permeable base, at which point the average age of both designs was about 8 years. The nondoweled sections with edge drains had an average faulting level of 0.06 in (1.5 mm), and the nondoweled sections with edge drains and a permeable base had an average faulting level of 0.03 in (0.76 mm). In addition, the MI 1 sections with a



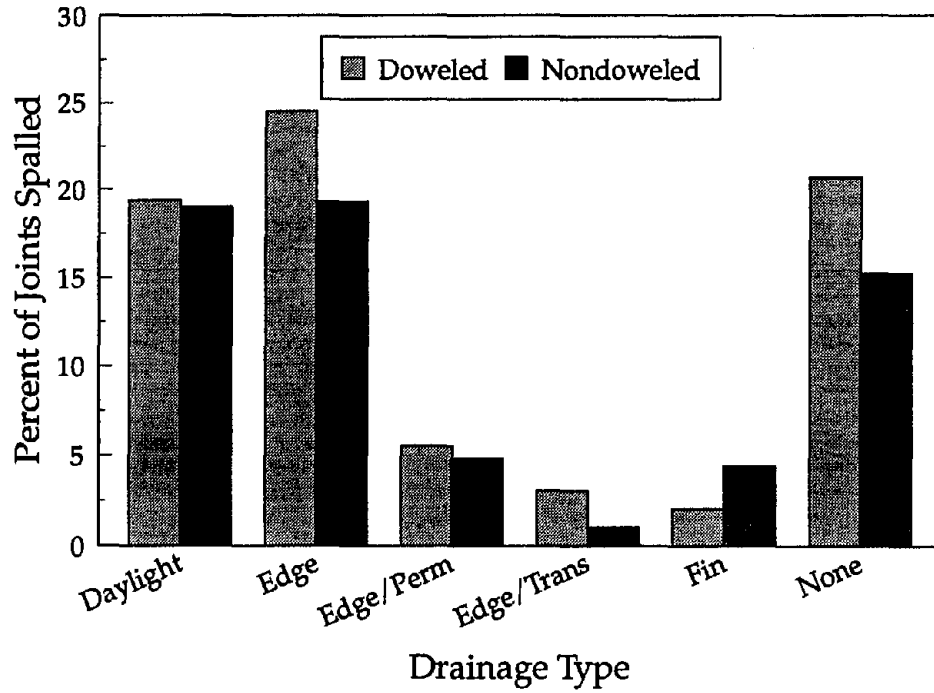


Figure 45. Transverse joint spalling for each drainage design.

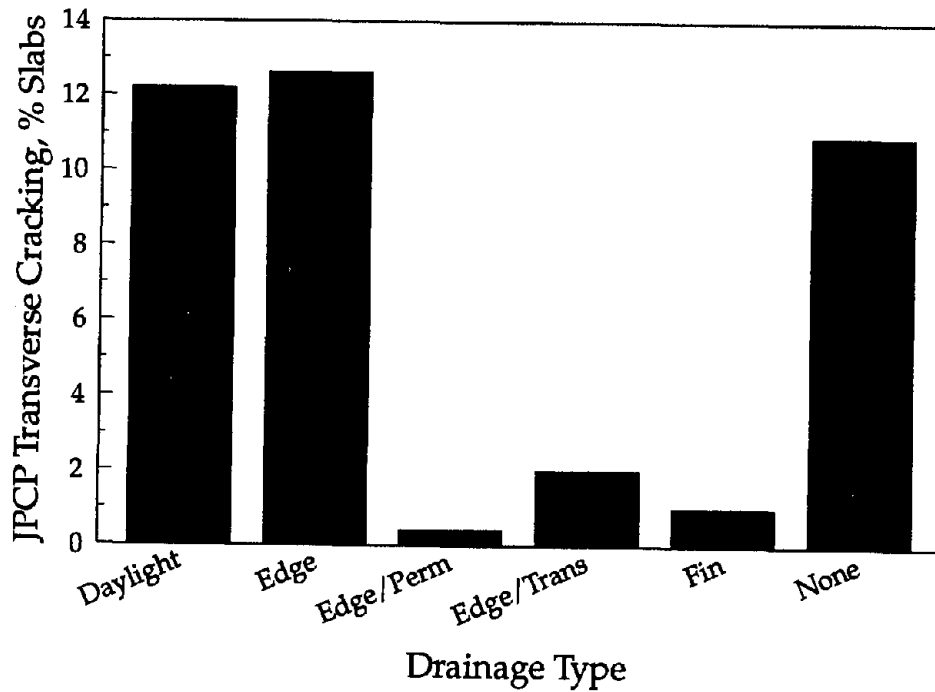


Figure 46. Transverse cracking for each drainage design.

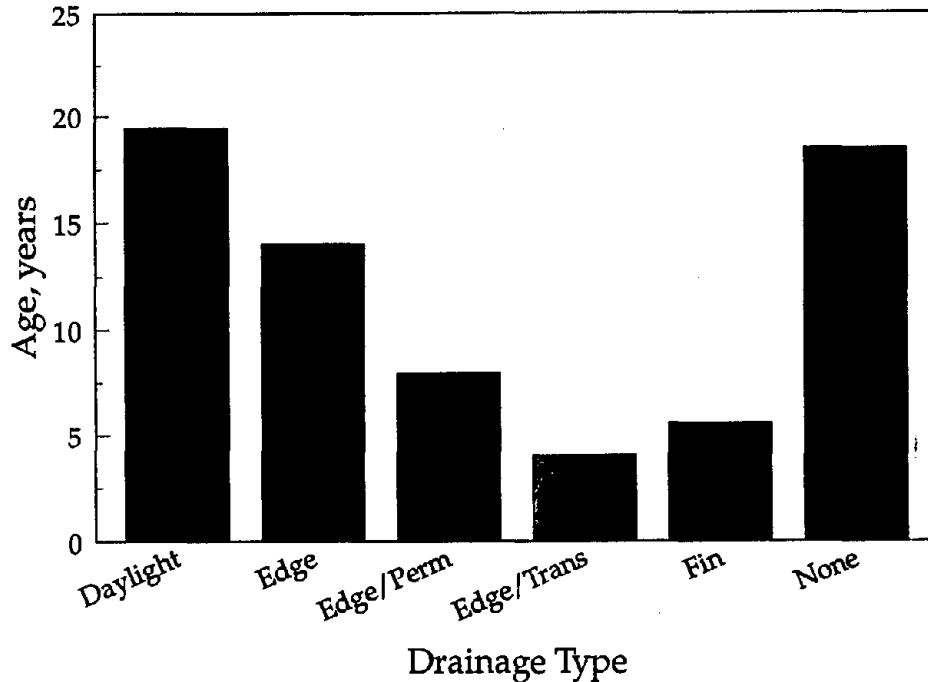


Figure 47. Average age for each drainage design.

permeable base are 17 years old, and all have faulting of 0.03 in (0.8 mm) or less. The only badly faulted section is CA 2-2, in which an AC layer was placed between the PCC slab and the PCTB.

An important measure of the overall drainage characteristics of a pavement is the AASHTO drainage coefficient ( $C_d$ ). This coefficient provides a means of considering the effect of drainage on performance. It is based on the quality of the drainage and the percent of time the pavement structure is exposed to moisture levels approaching saturation. A drainage coefficient of 1.0 represents drainage conditions similar to sections at the AASHTO Road Test (no drains and daylighted granular base).

The  $C_d$  value appears to be a significant variable in terms of predicting the amount of faulting, as illustrated in figure 48. For each incremental increase in  $C_d$ , the average faulting levels are reduced for both doweled and nondoweled sections.

In the AASHTO design procedure, higher  $C_d$  values indicate better drainage and a reduction in design thickness for the same ESAL applications. However, most researchers believe that drainage should not be used as a tradeoff for design thickness, but rather as a means of extending pavement life.

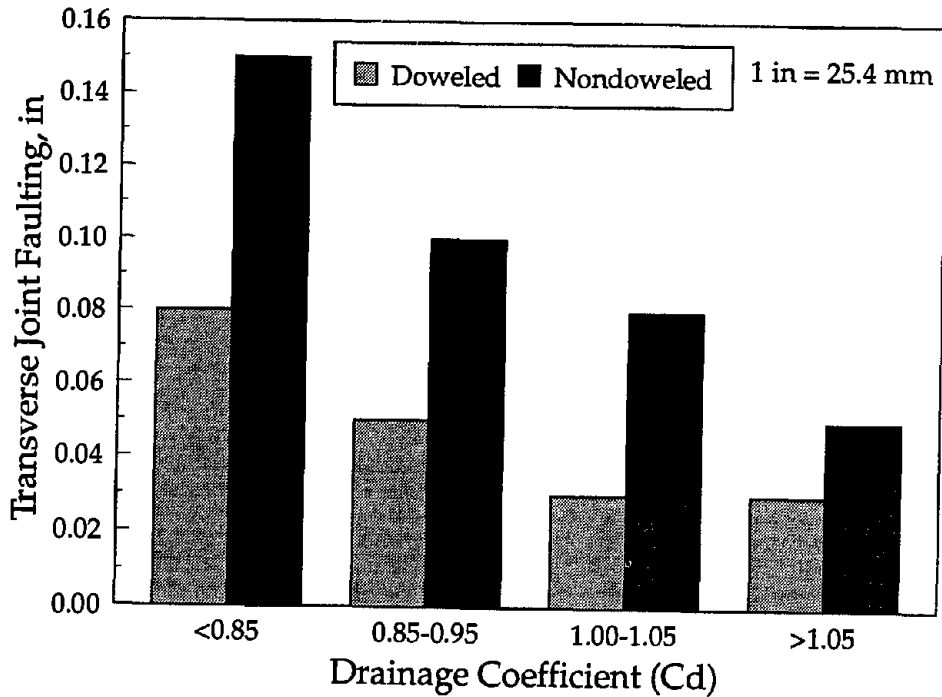


Figure 48. Transverse joint faulting for various drainage coefficients.

For aggregate bases, two parameters that provide an indication of the degree of permeability are the percent of material passing the No. 200 (0.075 mm) sieve ( $P_{200}$ ) and the coefficient of uniformity ( $C_u$ ).  $P_{200}$  represents the amount of fines in the material, with a higher amount of fines indicating less permeability. Figure 49 shows the effect of this variable on faulting for sections with a nonstabilized aggregate base. A strong correlation between the variables cannot be seen. However, all sections with  $P_{200}$  less than 5 percent have faulting levels below 0.05 in (1.3 mm).

The coefficient of uniformity indicates the spread of particle sizes. A material in which all particles were equal size spheres would have a  $C_u$  of one.  $C_u$  can be computed from the following relationship:

$$C_u = \frac{D_{60}}{D_{10}} \quad (2)$$

where:

- $C_u$  = Coefficient of uniformity.
- $D_{60}$  = Particle size in which 60 percent of the material is smaller, mm.
- $D_{10}$  = Particle size in which 10 percent of the material is smaller, mm.

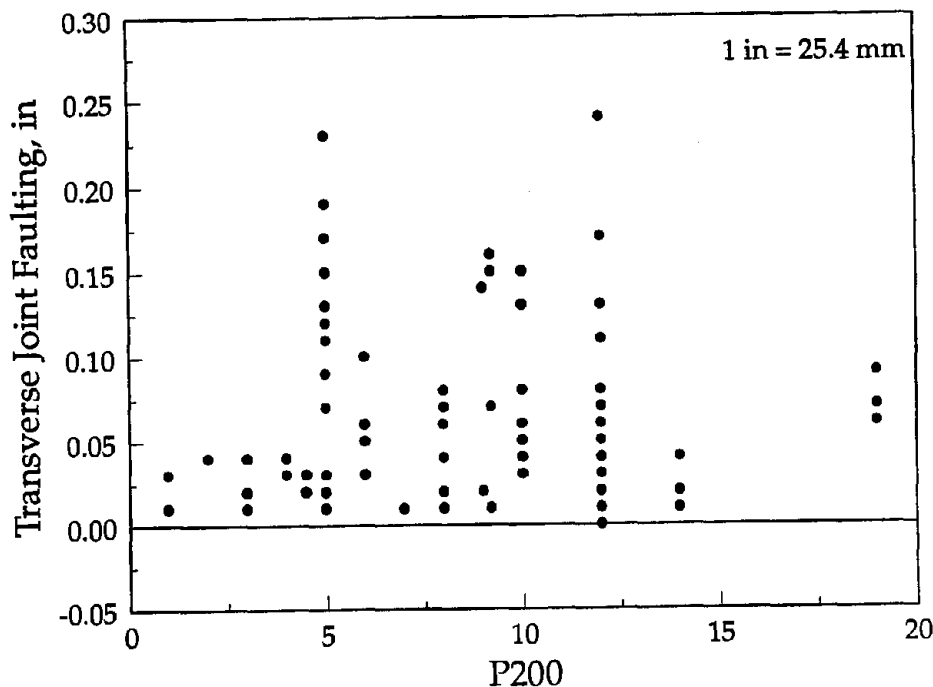


Figure 49. Effect of  $P_{200}$  on transverse joint faulting.

Open-graded materials have a  $C_U$  in the range of 2 to 6, whereas dense-graded materials are in the range of 20 to 50.<sup>(47)</sup> Aggregate bases in which  $C_U$  is less than 6 generally have lower faulting levels, as shown in figure 50. Aggregate bases with  $C_U$  greater than 10 show a wide range of faulting levels.

### Subgrade Type

Although considered more of a site condition than a design variable, subgrade type can play a key role in the performance of PCC pavements. Coarse-grained soils are generally considered to provide better performance due to the increased strength and drainage capabilities. Because fine-grained soils retain more moisture and consist of smaller particles, they are more prone to pumping and loss of support.

NCHRP Report 372, *Support Under Portland Cement Concrete Pavements*, found that support provided by the base and subgrade have a significant effect on the performance of PCC pavements.<sup>(51)</sup> The same study found that the concept of a composite k-value (measured at the top of the base course), which is commonly used in design, to be invalid. The appropriate k-value for design is that measured on top of the finished subgrade.<sup>(52)</sup> Other deficiencies relating to subgrade support were found in the AASHTO design procedure, including the use of a seasonally adjusted k-value and the use of a loss of support adjustment factor.

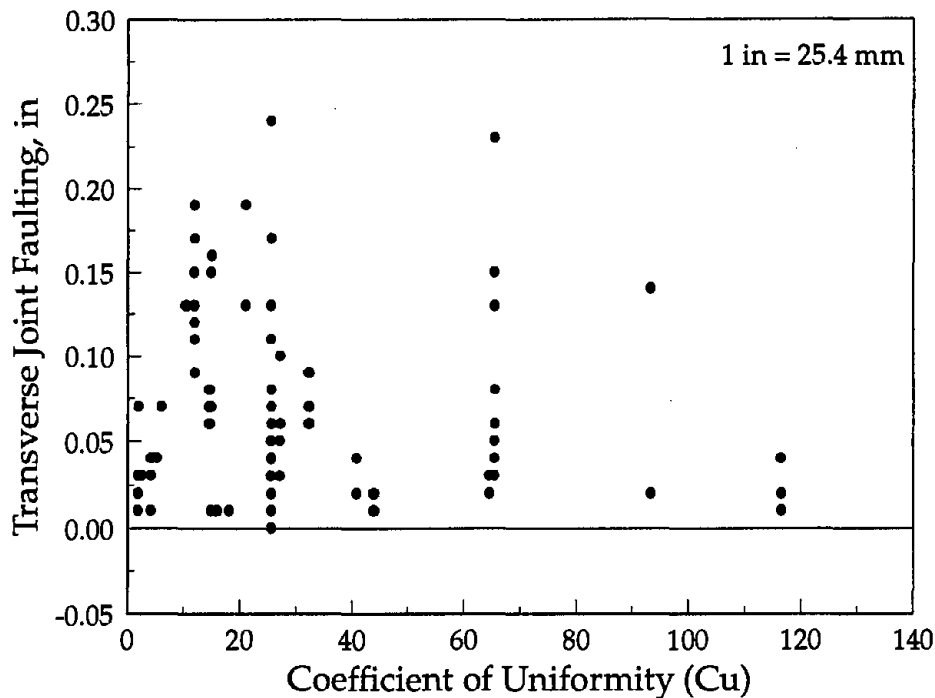


Figure 50. Effect of  $C_U$  on transverse joint faulting.

Because the sections within a given project are located within close proximity and therefore do not provide variations in subgrade type, direct comparisons of subgrade type were not available. However, more global comparisons using all data were conducted to provide some general insight into the effect of subgrade type. These comparisons should be taken only as general trends, as variations in other design variables make it difficult to ascertain the true effect of subgrade type.

The overall distribution of subgrade types using the AASHTO classification is illustrated in figure 51. With the exception of the A-5 classification, each soil class is well represented. The classifications can be broadly classified as coarse-grained soils (A-1, A-2, and A-3) and fine-grained soils (A-4, A-5, A-6, and A-7), with the division represented by 35 percent of the particles passing the No. 200 (0.075 mm) sieve.

Figure 52 illustrates the effect of subgrade type and ESAL applications on transverse joint faulting of doweled concrete pavements. The AASHTO classifications are divided into fine-grained soils and coarse-grained soils. For both soil types, faulting is affected by the number of ESAL applications. However, it appears that the coarse-grained soils are better able to withstand the effects of traffic, especially on heavily traversed sections. The sections constructed on fine-grained soils have a

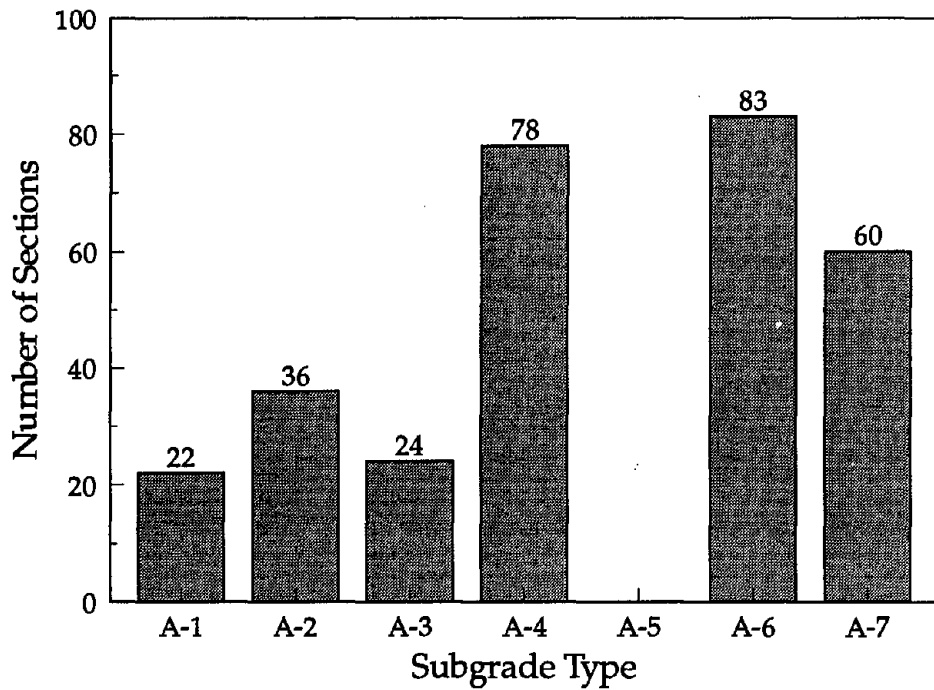


Figure 51. Distribution of subgrade types.

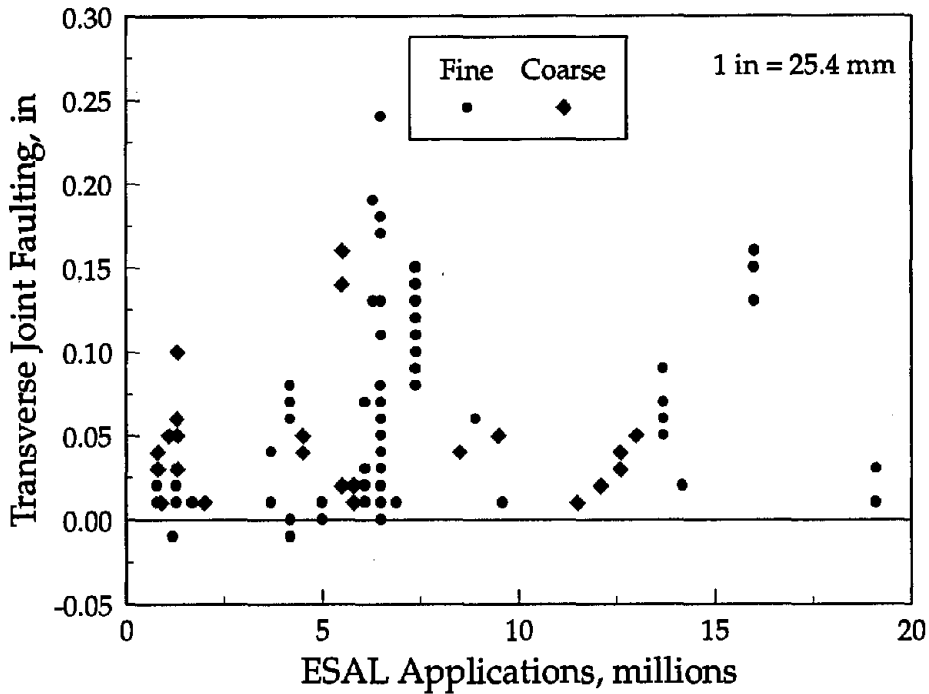


Figure 52. Effect of subgrade type on transverse joint faulting of doweled pavements.

higher percentage of sections exhibiting critical faulting levels (greater than 0.10 in [2.5 mm]).

A similar plot is shown in figure 53 for the nondoweled concrete pavement sections. Similar results can be seen in this figure, although the overall faulting levels are higher than on the doweled sections, as expected. The fine-grained soils have more sections at the higher faulting levels, indicating their increased susceptibility to pumping and loss of support.

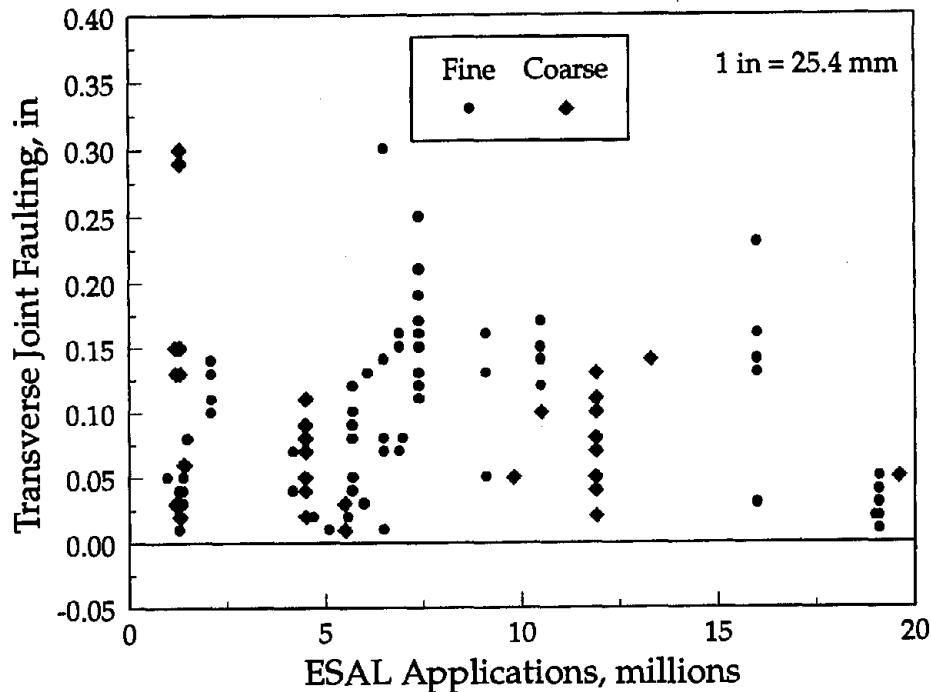


Figure 53. Effect of subgrade type on transverse faulting of nondoweled pavements.

An evaluation of the subgrade type was also conducted for other performance indicators, such as transverse cracking and roughness. However, no clear correlations between subgrade type and these performance indicators could be found. This finding is not meant to imply that subgrade type does not affect these performance indicators, but only that the effects may have been confounded by variations in other design variables.

### Shoulder Type

In concrete pavements, critical stresses develop when a free edge or corner of the slab is subjected to a wheel load. These stresses are much larger in magnitude than stresses due to interior loading conditions and, when combined with stresses due to thermal curling or moisture warping, can lead to transverse cracking (for the edge loading condition) and corner breaks (for the corner loading condition).

One way of reducing the magnitude of these critical stresses is the provision of lateral edge support to the slab. For example, a concrete shoulder tied to the mainline pavement slab transfers a portion of the load from the mainline slab to the shoulder, effectively reducing both edge deflections and edge stresses. However, several means of providing edge support are available, including the following:

- Concrete shoulder (both tied and nontied).
- Tied concrete curb and gutter.
- Concrete edge beam (narrow strip of concrete, generally about 2 ft [0.6 m] wide, placed adjacent to mainline pavement).
- Adjacent lane.

Asphalt or aggregate shoulders provide little or no lateral edge support to the mainline pavement; therefore, edge and corner loading on pavements with these shoulder types are "free edge" loading conditions. An inadequate tie bar design may also result in little benefit from tied concrete shoulders.

### Review of Project Data

This section provides a review of the performance data from the projects in which different shoulder types are used. The ideal comparison is one in which all design features, with the exception of edge support, are the same. Thus, sections that differ only in the edge support condition will be compared whenever possible. However, most comparisons involve sections with different shoulder types, as well as variations in other design features. Therefore, determining the direct effect of different shoulder types on concrete pavement performance is often difficult with the available data.

#### *Arizona 1*

The effect of different shoulders on performance can be examined from the AZ 1 project, located on State Route 360 in Phoenix, Arizona. Comparisons can be made between AZ 1-2 and 1-4 and between AZ 1-1 and 1-6. Although the type of shoulder does not vary between AZ 1-2 and AZ 1-4, the average thickness of the concrete shoulder does vary. The other design features are similar for each section. AZ 1-4 contains a 13-in (330-mm) concrete shoulder, which is the same thickness as the traffic lane. AZ 1-2, on the other hand, has a tapered shoulder, which is 13 in (330 mm) thick at the pavement edge and 6 in (150 mm) thick at the free outer edge. The concrete shoulders on these sections were paved separately from the mainline pavement.

Table 106 summarizes the performance data for these sections. AZ 1-2 has more cracking and spalling, although it is also 4 years older than AZ 1-4. The higher degree of cracking and spalling is probably not a result of the tapered PCC shoulder, as both sections are the same thickness at the lane-shoulder joint.



Table 106. Summary of effect of shoulder type for AZ 1.

Section & Shoulder Type	Year Built	ESAL's, millions		Joint Faulting, in		% Slabs Cracked		% Joints Spalled		IRI, in/mi (PSR)	
		1987	1992	1987	1992	1987	1992	1987	1992	1987	1992
AZ 1-2* 13-6 in PCC	1975	3.4	6.5	0.01	0.01	0	18	1	12	- (3.8)	111 (4.2)
AZ 1-4* 13 in PCC	1979	2.4	5.6	0.01	0.02	0	0	0	3	- (3.6)	122 (3.8)
AZ 1-1** 3 in AC	1972	4.0	7.0	0.08	0.08	0	0	22	24	- (3.4)	105 (3.9)
AZ 1-6** 9 in PCC	1981	2.0	5.1	0.01	0.01	0	0	1	3	- (3.5)	123 (3.5)

1 in = 25.4 mm  
1 ft = 0.305 m  
1 mi = 1.61 km

Common Design Feature: 13-15-17-15-ft nondoweled joints  
\* 13-in JPCP without base.  
\*\* 9-in JPCP on 6-in CTB (AZ 1-1) or on 4-in LCB (AZ 1-6).

The effect of shoulder type on pavement performance can be examined by comparing AZ 1-1 and AZ 1-6. Both sections are 9.0-in (230-mm) JPCP with similar design features and different shoulder types. AZ 1-1 has a 3-in (76-mm) AC shoulder, and AZ 1-6 has a 9.0-in (230-mm) tied PCC shoulder. However, a direct comparison is complicated by the use of different support conditions for the traffic lanes. AZ 1-1 contains a 6.0-in (150-mm) CTB over a 4.0-in (100-mm) aggregate subbase and an A-4 subgrade, whereas AZ 1-6 contains a 4.0-in (100-mm) LCB placed on an A-6 subgrade.

Section AZ 1-1 (AC shoulder) has considerably more faulting and spalling than AZ 1-6 (PCC shoulder), as shown in table 106. As previously mentioned, tied PCC shoulders provide a much higher degree of load transfer, which could account for the reduction in faulting and spalling. In fact, AZ 1-6 has a load transfer value approaching 100 percent, which indicates that the load transfer system is still performing well. However, AZ 1-1 is 9 years older and has been exposed to about 2 million more ESAL's, which also explains some of the differences in performance.

### California 3

The CA 3 project, located on U.S. 101 near Geyserville, was constructed as an experimental project to study the effects of shoulder type on pavement performance (Reference 21). The sections investigated include those with tied PCC shoulders, nontied PCC shoulders, and AC shoulders. The sections with tied PCC shoulders (paved separately from mainline pavement) are tied using 22 in (560 mm) long, No. 4 (13-mm) bars at 30-in (760-mm) centers. Some sections contain preformed joint sealants, whereas others contain no joint sealant. All sections are 9-in (229-mm) JPCP

with a 12-13-19-18-ft (3.7-4.0-5.8-5.5-m) random joint spacing and skewed joints.

The performance data for the sections with preformed sealant at the transverse joints are shown in table 107. Two sections—one in the northbound lane and one in the southbound lane—are available for both shoulder types. The sections with tied PCC shoulders are exhibiting less cracking (both transverse and longitudinal) as compared to the sections with nontied PCC shoulders. Faulting and spalling are about the same for each shoulder type.

Table 107. Effect of shoulder type for CA 3 sections (preformed sealant).

Section	Shoulder Type	Joint Faulting, in	% Slabs Cracked	Long Crk, ft/mi	% Joints Spalled	IRI, in/mi (PSR)
CA 3-1 (NB)	Tied PCC	0.09	10	0	0	167 (3.4)
CA 3-6 (SB)	Tied PCC	0.04	3	0	0	111 (3.7)
CA 3-3 (NB)	Nontied PCC	0.05	34	25	0	126 (3.7)
CA 3-8 (SB)	Nontied PCC	0.10	12	0	0	121 (3.4)

1 in = 25.4 mm  
 1 ft = 0.305 m  
 1 mi = 1.61 km

Common Design Features: 9 in nondoweled JPCP  
 12-13-19-18 ft joints  
 Built in 1975  
 1992 ESAL's = 5.7 million

The sections with more cracking are not necessarily the sections with lower roughness values (IRI or PSR). However, the roughness values do correspond with the faulting measurements. Although cracking provides a good indication of the structural capacity of the pavement, it does not drastically affect the functional capacity until the cracks become deteriorated.

Table 108 illustrates the performance data for the sections with no joint sealant at the transverse joints. Each shoulder type is represented in two sections—one in the northbound lane and one in the southbound lane. As with the sections with preformed sealant, the use of different shoulder types does not appear to affect the faulting measurements or consequently, the roughness values. However, the sections with tied PCC shoulders have experienced considerably less transverse cracking than the other sections. Likewise, the sections with tied PCC shoulders have less spalling and longitudinal cracking than the sections with nontied PCC shoulders. The additional support provided by the tied PCC shoulder apparently is effective in reducing the edge stress, and consequently the amount of slab cracking.

Deflection measurements taken during the 1987 survey indicate that the load transfer across the shoulder for CA 3-2 (tied PCC shoulder) is 85 percent, whereas CA 3-5 (nontied PCC shoulder) has a load transfer of 55 percent. The reduced edge support is likely responsible for the increased transverse cracking.

Table 108. Effect of shoulder type for CA 3 sections (no sealant).

Section	Shoulder Type	Joint Faulting, in	% Slabs Cracked	Long Crk, ft/mi	% Joints Spalled	IRI, in/mi (PSR)
CA 3-2 (NB)	Tied PCC	0.09	5	0	3	129 (3.5)
CA 3-7 (SB)	Tied PCC	0.12	7	0	2	147 (3.5)
CA 3-5 (NB)	PCC	0.10	34	34	6	134 (3.5)
CA 3-10 (SB)	PCC	0.09	47	0	2	116 (3.5)
CA 3-4 (NB)	AC	0.10	0	0	0	150 (3.8)
CA 3-9 (SB)	AC	0.10	26	0	0	144 (3.0)

1 in = 25.4 mm  
 1 ft = 0.305 m  
 1 mi = 1.61 km

Common Design Features: 9 in nondoweled JPCP  
 12-13-19-18 ft joints  
 Built in 1975  
 1992 ESAL's = 5.7 million

Curiously, the sections with AC shoulders exhibited fewer transverse cracks than the sections with nontied PCC shoulders, although still more transverse cracks than the sections with tied PCC shoulders. The following conclusions can be drawn from the investigation of these sections:

- The sections with AC shoulders are performing better than the sections with nontied PCC shoulders.
- The beneficial aspects of a PCC shoulder are only recognized when the shoulder is tied to the mainline pavement.
- A more effective tie bar design might provide improved performance. In fact, based on the results of recent studies, California now uses 30 in (760 mm) long, No. 5 (16-mm), epoxy-coated bars at 30-in (760-mm) centers.

#### Florida 4

The FL 4 project is located in the southbound lanes of U.S. 41 between Punta Gorda and Ft. Myers. This experimental project was designed to determine the feasibility of constructing a two-course pavement system of a lean concrete base and a thin concrete wearing course. Three sections—FL 4-3, 4-4, and 4-5—have the same design features with the exception of the shoulder type. FL 4-3 contains an AC shoulder, whereas FL 4-4 and 4-5 incorporate a tied lean concrete shoulder using No. 4 (13-mm) bars spaced 5 ft (1.5 m) apart.

The shoulder type does not appear to significantly affect the performance of the FL 4 sections, as shown in table 109. With the exception of longitudinal cracking, the

data indicate that the sections are performing similarly. The section with an AC shoulder has 546 ft/mi (104 m/km) of longitudinal cracking, compared to none for the sections with a tied lean concrete shoulder. However, the high degree of longitudinal cracking is more likely due to factors unrelated to the use of AC shoulders (e.g., improper bonding of layers). In addition, although the sections with PCC shoulders are performing well, the 5-ft (1.5-m) tie bar spacing is probably excessive.

Table 109. Effect of shoulder type for FL 4 sections.

Section	Edge Support	Joint Faulting, in	% Slabs Cracked	Long Crk, ft/mi	% Joints Spalled	IRI, in/mi (PSR)
FL 4-3	AC	0.04	0	546	0	122 (3.7)
FL 4-4	Tied PCC	0.04	0	0	0	98 (3.9)
FL 4-5	Tied PCC	0.04	0	0	3	110 (3.6)

1 in = 25.4 mm  
 1 ft = 0.305 m  
 1 mi = 1.61 km

Common Design Features: 3 in JPCP bonded to 9 in LCB  
 15 ft nondoweled joints  
 Built in 1978  
 1992 ESAL's = 4.5 million

These sections do not receive many heavy traffic loadings, as indicated by the 4.5 million ESAL applications after 14 years of service (320,000 ESAL's/year). Consequently, the tied PCC shoulders may not provide as much benefit as compared to a section with more heavily-loaded vehicles.

### Michigan 1

Michigan 1 is an experimental project constructed on U.S. 10 near Clare in which the effect of edge support can be examined. Section MI 1-10b contains a full-depth AC shoulder, and section MI 1-25 contains a tied PCC acceleration ramp. The ramp is tied to the mainline pavement using 30-in (760-mm) long No. 5 (16-mm) deformed tie bars spaced at 40 in (1020 mm). Both sections consist of a 9-in (30-in) JPCP constructed on a dense-graded ATB. The transverse joints are nondoweled, skewed, and spaced at random intervals.

Table 110 shows a summary of the performance data for sections MI 1-10b and MI 1-25. The 1987 data indicate that the sections are performing similarly, as the distress quantities are about the same. However, by 1992, section MI 1-25 had developed considerably more faulting and transverse cracking.

On this project, the tie bars failed shortly after initial construction. Expansion anchors were provided in the tie bar system, which allow wider joint openings and likely contributed to the failures. In addition, the excessive 40-in (1020-mm) tie bar spacing is believed to be partially responsible for the failure. In addition, the joint

Table 110. Summary of effect of shoulder type for MI 1.

Section	Shoulder Type	Joint Faulting, in		% Slabs Cracked		% Joints Spalled		IRI, in/mi (PSR)	
		1987	1992	1987	1992	1987	1992	1987	1992
MI 1-10b	AC	0.19	0.15	6	5	63	100	- (2.8)	197 (2.1)
MI 1-25	Tied PCC	0.20	0.30	8	13	75	100	- (2.9)	247 (2.3)

1 in = 25.4 mm  
 1 ft = 0.305 m  
 1 mi = 1.61 km

Common Design Features: 9 in nondoweled JPCP  
 12-13-19-18 ft skewed joints  
 Dense-graded ATB  
 Built in 1975  
 1992 ESAL's = 1.3 million

between the outer lane and acceleration ramp was not sealed, allowing moisture and debris to enter the pavement structure. As a result, the potential beneficial aspects of the tied PCC ramp were negated. Consequently, the performance was comparable or inferior to the section with an AC shoulder.

#### Michigan 4

This project, located on I-69 near Charlotte, was specifically designed to evaluate the performance of JRPC sections with different shoulder types. MI 4-1 contains a tied PCC shoulder (paved separately from mainline pavement) using 0.56-in (14-mm) hook bolts spaced 40 in (1020 mm) apart. The transverse shoulder joints were sawed at the third points (i.e., three shoulder slabs per each mainline slab). MI 4-2 contains a standard AC shoulder. Both sections are 9-in (230-mm) JRPC with a 71.2-ft (22-m) joint spacing.

Table 111 shows the performance data from the 1987 and 1992 surveys. Overall, these sections are performing about the same, with the section with a tied PCC shoulder exhibiting slightly more deteriorated cracks and greater joint faulting than the section with an AC shoulder. The number of deteriorated cracks for both sections corresponds to about three deteriorated cracks on each slab.

Deflection measurements obtained in 1987 indicate that the section with a tied PCC shoulder had smaller corner deflections and fewer corners with loss of support. However, the load transfer across the traffic lane and the tied PCC shoulder was only 35 percent, indicating the minimal effect of the PCC shoulder. Consequently, the PCC shoulder did not improve the performance. However, it should also be noted that a rubber washer was added to the tie bar to allow differential movement between the slab and the shoulder.

Table 111. Summary of effect of shoulder type for MI 4.

Section	Shoulder Type	Joint Faulting, in		Deteriorated Cracks/mi		% Joints Spalled		IRI, in/mi (PSR)	
		1987	1992	1987	1992	1987	1992	1987	1992
MI 4-1	Tied PCC	0.12	0.19	227	222	0	0	- (2.4)	208 (2.2)
MI 4-2	AC	0.03	0.13	183	198	6	6	- (2.4)	165 (2.2)

1 in = 25.4 mm  
 1 ft = 0.305 m  
 1 mi = 1.61 km

Common Design Features: 9 in JRCP with 0.15% steel  
 71.2 ft doweled joints  
 Built in 1972  
 1992 ESAL's = 6.3 million

The fact that the tied PCC shoulder did not improve the performance of the mainline pavement implies that other mechanisms may be controlling the performance. Some possible explanations are an inadequate tie design system and differences in drainability or support between the sections. For example, MI 1-25 contain tie bars (expansion anchors) spaced at 40-in (1020-mm) centers, which reportedly failed shortly after construction. More than likely, the combination of these factors has resulted in the performance differences.

#### Minnesota 2

This project, located on I-90 near Albert Lea, is an experimental project designed to study the effect of tied PCC shoulders and widened traffic lanes.<sup>(16,17)</sup> Two sections were constructed with PCC shoulders (paved separately from mainline pavement) and two sections were constructed with AC shoulders. However, the sections cannot be directly compared because the pavement type differs—the sections with tied concrete shoulders are JPCP and the sections with AC shoulders are JRCP. All sections have a 15-ft (4.6-m) widened inside traffic lane and are constructed on an aggregate base. With the exception of the inside lanes of the sections with PCC shoulders, all sections contain 1-in (25-mm) dowel bars.

The performance of the MN 2 sections is summarized in table 112. The section with a tied PCC shoulder has less transverse cracking. Faulting and roughness values are about the same for all sections. The sections with tied PCC shoulders have considerably more longitudinal cracking. One reason may be a result of tying the widened inside traffic lane, outside traffic lane, and outer shoulder (total tied width of 37-ft [11-m]), although the shoulders were paved separately. Another explanation may be late sawing or inadequate depth of the centerline joint.

The tied PCC shoulders are in better overall condition than the AC shoulders, which are exhibiting some alligator cracking and lane-shoulder dropoff. The load transfer across the tied PCC shoulder was very high in 1987, although the corner deflections were lower on the sections with AC shoulders (JRCP design).

Table 112. Summary of effect of shoulder type for MN 2.

Section	Shoulder Type	Joint Faulting, in		Deteriorated Cracks/mi		Long. Cracks, ft/mi		IRI, in/mi (PSR)	
		1987	1992	1987	1992	1987	1992	1987	1992
MN 2-1	Tied PCC	0.06	0.08	0	0	746	932	- (3.8)	140 (4.0)
MN 2-3	AC	0.05	0.06	0	10	0	142	- (4.0)	113 (4.0)
MN 2-4	AC	0.06	0.07	5	5	0	0	- (4.0)	153 (3.9)

1 in = 25.4 mm  
 1 ft = 0.305 m  
 1 mi = 1.61 km

Common Design Features: 1.25-in doweled joints  
 Built in 1972  
 1992 ESAL's = 4.2 million

*New York 2*

This project is located on I-88 near Otego and contains both tied PCC shoulders and AC shoulders. However, the pavement design varies from JPCP to JRCP, so a direct comparison is not possible. The tied PCC shoulders (paved separately from mainline pavement) are only 6-in (152-mm) thick and contain tie bars spaced at 40-in (1020-mm) intervals. Both sections contain 1-in (25-mm) I-beams at the transverse joints for load transfer and a 4-in (102-mm) aggregate base.

Table 113 summarizes the performance data for NY 2-3 and 2-15. Both sections have little faulting and roughness. NY 2-3 has some deteriorated transverse cracks and NY 2-15 has no transverse cracking; this might indicate that the tied PCC shoulder design is ineffective. A New York State Department of Transportation study indicated that additional stress was induced into the PCC slab as a result of frost heave caused by a thin PCC shoulder and a bathtub design.<sup>(28)</sup>

Table 113. Summary of effect of shoulder type for NY 2.

Section	Pavement Design	Joint Faulting, in		Deteriorated Cracks/mi		Longitudinal Cracks, ft/mi		IRI, in/mi (PSR)	
		1987	1992	1987	1992	1987	1992	1987	1992
NY 2-3	Tied PCC Shoulder 9-in JPCP	0.01	0.01	35	55	0	0	- (4.2)	108 (-)
NY 2-15	AC Shoulder 9-in JRCP	0.02	0.02	0	0	234	284	- (4.0)	89 (4.3)

1 in = 25.4 mm  
 1 ft = 0.305 m  
 1 mi = 1.61 km

Common Design Features: 1-in I-beam load transfer design  
 4-in AGG base  
 Built in 1975  
 1992 ESAL's = 5.8 million

Deflection measurements from 1987 indicate that the section with tied PCC shoulders has more corners with voids and consequently, significantly higher corner deflections. However, the load transfer across the shoulder is 65 percent according to 1987 deflection data.

In summary, the poor performance of the tied PCC shoulders is believed to be related to a combination of factors:

- 6-in (152-mm) thick PCC shoulders.
- Bathtub design.
- 40-in (1020-mm) tie bar spacing.

### Ohio 1

This experimental project was constructed in 1973 on U.S. 23 near Chillicothe. Although no section contains a tied PCC shoulder, OH 1-1 is tied to an adjacent lane. OH 1-9 has the same design characteristics and an AC shoulder. Both sections are 9-in (229-mm) JRCP with a 40-ft (12.2-m) joint spacing.

The performance data for these sections is outlined in table 114. The most noticeable information is the apparent reduction in faulting over time. This peculiar trend may be attributable to measurements taken under different environmental conditions. OH 1-9 has higher faulting measurements and considerably more deteriorated cracks, although the IRI value indicates less roughness. The 1987 deflection data indicate that OH 1-9 has higher corner deflections and more corners with voids. Thus, the tied adjacent lane appears to be contributing to improved performance.

Table 114. Summary of effect of shoulder type for OH 1.

Section	Edge Support	Joint Faulting, in		Deteriorated Cracks/mi		Longitudinal Cracks, ft/mi		IRI, in/mi (PSR)	
		1987	1992	1987	1992	1987	1992	1987	1992
OH 1-1	Adjacent Lane	0.13	0.02	0	88	0	0	-(4.2)	224 (-)
OH 1-9	AC Shoulder	0.14	0.07	106	251	0	0	-(4.2)	154 (-)

1 in = 25.4 mm  
 1 ft = 0.305 m  
 1 mi = 1.61 km

Common Design Features: 9-in JRCP (0.09% steel)  
 40-ft doweled joints  
 Built in 1973  
 1992 ESAL's = 6.1 million



## Ohio 2

This project, located on S.R. 2 near Vermillion, can also be used to examine the effect of shoulder type on pavement performance. Two separate comparisons can be made from this project:

- OH 2-1 (tied PCC shoulder) and OH 2-4 (AC shoulder)—both sections have a maximum aggregate size of 0.5 in (13 mm).
- OH 2-2 (tied PCC shoulder) and OH 2-3 (AC shoulder)—both sections have a maximum aggregate size of 1.5 in (38 mm).

All sections contain coarse aggregate from the same source, Mn3, which is commonly associated with D-cracking where 1.0 and 1.5 in (25 and 38 mm) maximum coarse aggregate are used. All sections are 15-in (380-mm) JPCP with a 20-ft (6.1-m) joint spacing and skewed joints. The sections do not contain dowel bars or a base course. Table 115 illustrates the performance data from the 1992 survey.

Some common trends are apparent from both comparisons. For instance, the sections with tied PCC shoulders have less faulting and joint spalling, which indicates better performance. On the other hand, they are also exhibiting more longitudinal cracking and roughness. Deteriorated transverse cracks are virtually nonexistent on all sections.

Table 115. Effect of shoulder type for OH 2 sections.

Section	Edge Support	Joint Faulting, in	Deteriorated Cracks/mi	Longitudinal Cracks, ft/mi	% Joints Spalled	IRI, in/mi
OH 2-1	Tied PCC	0.07	0	158	0	131
OH 2-4	AC	0.30	0	0	0	93
OH 2-2	Tied PCC	0.08	0	572	52	143
OH 2-3	AC	0.14	11	148	96	99

1 in = 25.4 mm  
 1 ft = 0.305 m  
 1 mi = 1.61 km

Common Design Features: 15-in JPCP  
 20-ft nondoweled joints  
 Built in 1978  
 1992 ESAL's = 4.5 million

The most noticeable aspect is the poor correlation between IRI and faulting. For example, OH 2-4 has an average faulting of 0.30 in (7.6 m), yet it also has an IRI value of 93 in/mi (1500 mm/km). It is difficult to imagine that a pavement with such high faulting measurements could be so smooth. OH 2-3 shows the same trend.

## Ontario 2

This project is located on Highway 3N near Windsor, Ontario. ONT 1-2 has an AC shoulder, and ONT 1-3 has a tied PCC shoulder. However, the comparison is confounded by the base type, as ONT 1-2 has a PATB, and ONT 1-3 has an LCB. All sections are 8-in (203-mm) JPCP with a 13-18-19-12-ft (4.0-5.8-5.5-3.7-m) random joint spacing and longitudinal edge drains.

The performance data are shown in table 116. The section with a tied PCC shoulder has more faulting, transverse cracking, and longitudinal cracking, although the roughness values are about the same. Based on these results, the tied PCC shoulder does not offer any benefit in terms of improved performance. However, the sections are also constructed on different base types, which may also be a factor contributing to distress. Although different designs were used, other sections with a tied PCC shoulder are high exhibiting high levels of distress.

Table 116. Summary of effect of shoulder type for ONT 1.

Section	Shoulder Type	Joint Faulting, in		% Slabs Cracked		Longitudinal Cracks, ft/mi		IRI, in/mi (PSR)	
		1987	1992	1987	1992	1987	1992	1987	1992
ONT 1-2	AC	0.05	0.10	0	0	0	105	- (3.8)	135 (3.9)
ONT 1-3	Tied PCC	0.04	0.14	9	8	490	621	- (3.8)	147 (3.9)

1 in = 25.4 mm  
 1 ft = 0.305 m  
 1 mi = 1.61 km

Common Design Features: 8-in nondoweled JPCP  
 13-18-19-12-ft joint spacing  
 Built in 1982  
 1992 ESAL's = 2.1 million

### Overall Evaluation of Edge Support

Judging the effectiveness of different edge support conditions is difficult, as the results are mixed. Some sections with edge support exhibited better performance, whereas others exhibited poorer performance. However, some general trends were apparent from the evaluation.

Overall, PCC shoulders were structurally in better condition than AC shoulders. The AC shoulders typically exhibited extensive deterioration and lane-shoulder dropoff, whereas with the exception of the 6-in (152-mm) thick PCC shoulder in NY, the PCC shoulders exhibited little or no deterioration. Although the shoulder condition is important, a more extensive analysis was conducted on the effect of edge support on the performance of the mainline pavement.

In general, sections that were tied to an adjacent PCC structure—traffic lane, shoulder, edge beam, or curb—exhibited about the same or slightly less distress than sections with an AC shoulder. The results for transverse cracking and faulting are inconclusive. Corner deflections and the percent corners with voids were usually reduced for tied sections. Longitudinal cracking, on the other hand, was generally greater on sections with tied PCC shoulders. Most sections with a tied structure exhibited high levels of load transfer across the longitudinal joint. However, it should be noted that some FWD testing was conducted at high temperatures.

In contrast, sections with nontied PCC shoulders appeared to offer no benefits to performance when compared to sections with AC shoulders. In fact, the performance was considerably worse in some cases. Similarly, sections that were inadequately tied did not provide any substantial improvement. Generally, sections that were tied using anything smaller than No. 5 (16-mm) bars, or tie bars spaced farther than 36 in (914 mm) apart, were found to be inadequate. Some States, such as California, have since altered their tie bar design system.

Another common trend was the effect of shoulder thickness on performance. Tied PCC shoulders that were thinner than mainline pavement did not perform as well as full-depth PCC shoulders. Both the mainline pavement and the shoulder exhibited higher distress levels than corresponding sections with thicker shoulders. Transverse joints in the tied PCC shoulder, where not matched with joints in the mainline, were also found to induce cracking in the mainline pavement.

Another factor for tied PCC shoulders is whether the shoulders are constructed monolithically with the mainline pavement or added separately. However, this effect could not be evaluated in this study, as none of the shoulders are known to have been constructed monolithically with the mainline pavement.

Several plots were developed to compare the effect of edge support on pavement performance. Figure 54 compares the average edge deflection for sections with AC and tied PCC shoulders (sections with nontied PCC shoulders and tied edge beams are not included because only a few sections are available). The sections with tied PCC shoulders show lower deflections than the sections with AC shoulders, which should translate to better performance. Similar results are shown in figures 55 and 56, which illustrate faulting and transverse cracking, respectively. Relatively speaking, only a few sections with tied PCC shoulders exhibit significant faulting or transverse cracking.

Based on the analysis, PCC shoulders can improve the performance of PCC pavements if properly constructed. Some of the key design factors for PCC shoulders are as follows:

- The shoulders should be tied to the mainline pavement. Sections that were not tied to the mainline pavement exhibited the same, and often times, worse performance than sections with AC shoulders.

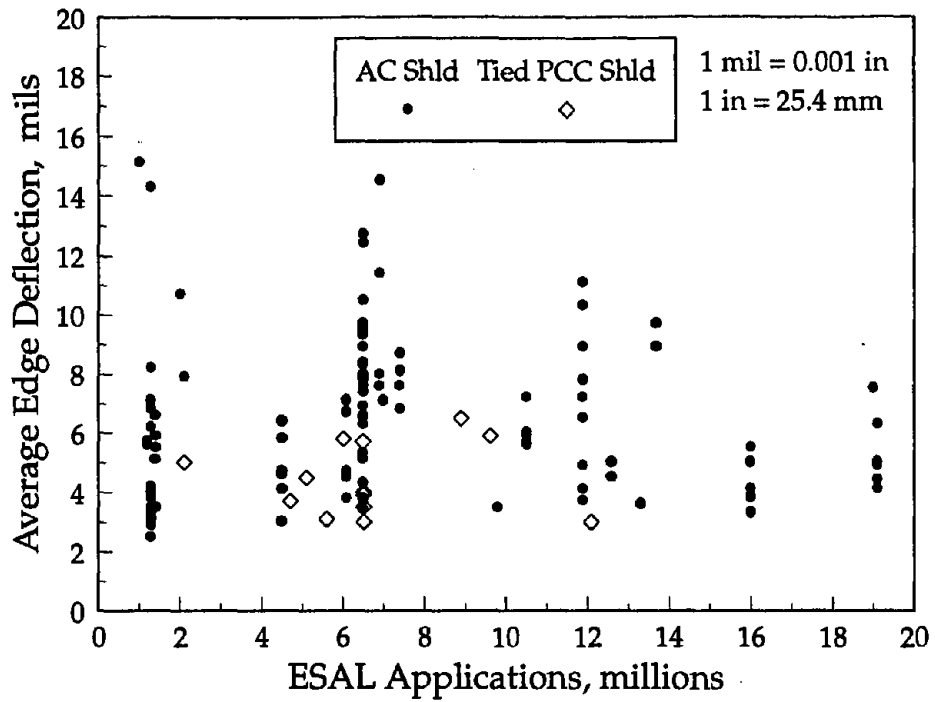


Figure 54. Effect of edge support on edge deflection.

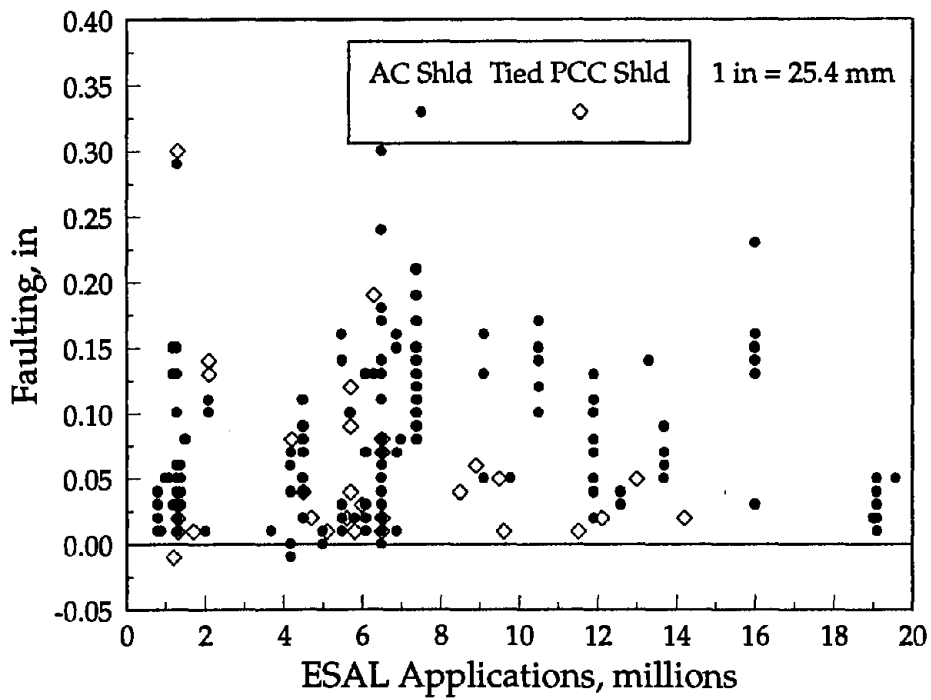


Figure 55. Effect of edge support on transverse joint faulting.

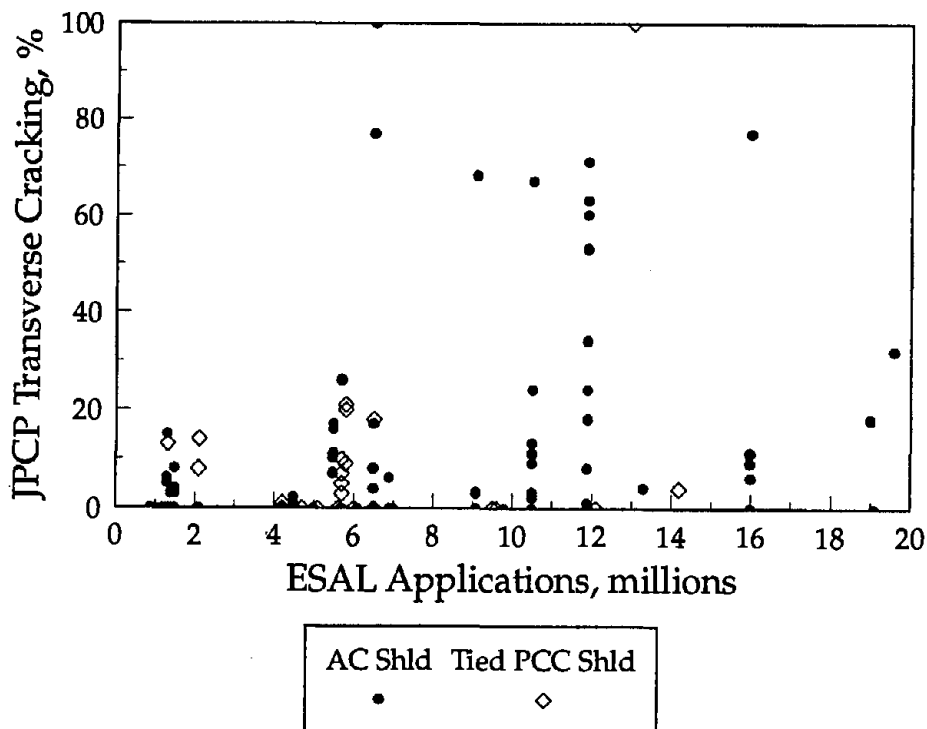


Figure 56. Effect of edge support on JPCP transverse cracking.

- Table 117 illustrates the recommended tie bar spacing and tie bar diameters. The maximum recommended spacing is 48 in (1220 mm), although many spacings are in the range of 30 in (760 mm). Many sections evaluated in this study had spacings greater than those recommended, and consequently did not perform as well. Caution should be exercised when selecting No. 4 (13-mm) tie bars, as they were found to be inadequate in many cases.
- The thickness of the PCC shoulder should be the same thickness as the mainline pavement. Sections with shoulders that were not constructed with the same thickness resulted in more deterioration in the mainline pavement and the shoulder itself.
- Bathtub designs must be eliminated.

Several studies have shown that the use of tied PCC shoulders can reduce pavement responses, thus improving performance. Table 118 shows the ratio of pavement responses at the tied shoulder joint to those at the free edge based on two projects in Minnesota and on a theoretical analysis using a finite element program. The results indicate that each pavement response at the tied shoulder joint is about 65 to 85 percent of the value at the free edge.<sup>(53)</sup> The same study also concluded that, based on AASHTO load equivalency factors (LEF) and design procedures, the use of tied concrete shoulders will reduce the thickness of the mainline pavement by approximately 1 in (25 mm) for the same traffic levels.<sup>(53)</sup> However, this study only

Table 117. Maximum recommended tie bar spacings.<sup>(51)</sup>

Bar Size		#4 Bar										#5 Bar									
Grade Steel		Grade 40					Grade 60					Grade 40					Grade 60				
Distance to Free Edge, ft		10	12	16	22	24	10	12	16	22	24	10	12	16	22	24	10	12	16	22	24
Pvmt Depth, in	Type of Joint																				
9	Warp	37	31	23	17	16	56	74	35	25	23	59	49	36	26	24	88	73	55	40	36
	Butt	26	22	16	12	11	40	34	25	18	16	42	35	26	19	17	63	52	39	29	26
10	Warp	34	28	22	16	14	51	42	32	23	20	53	44	33	24	22	79	66	49	36	32
	Butt	24	20	16	11	10	36	30	23	16	14	38	31	24	17	16	56	47	35	26	23
11	Warp	31	25	20	15	13	47	38	29	21	19	48	40	30	22	20	72	60	44	32	30
	Butt	22	18	14	11	9	34	27	21	15	14	34	29	21	16	14	51	43	31	23	21
12	Warp	28	23	18	13	12	42	35	27	19	18	44	36	28	20	18	66	55	41	30	28
	Butt	20	16	13	9	9	30	25	19	14	13	31	26	20	14	13	47	39	29	21	20

Table 118. Improvement in pavement responses.<sup>(53)</sup>

Response	Ratio of Response at Tied Shoulder Joint to Free Edge, %				
	Measured		Calculated		
	Project 1	Project 2	LTE=80%	LTE=60%	LTE=50%
Edge Deflection	75-90	—	65	70	75
Corner Deflection	70-87	58-80	65	79	75
Edge Stress	80-85	94-97	80	85	90

considered stresses due to traffic loads; thermal curling and moisture warping stresses are not considered.

Another study was conducted on experimental concrete pavement sections on I-70 in Colorado.<sup>(54)</sup> This study, which considered both load and curling stresses, also found the effective contribution of tied PCC shoulders to be equivalent to about 1 in (25 mm) of slab thickness. However, the study also found that for the tied PCC shoulder to provide significant structural benefit, high load transfer efficiency (greater than 80 percent) across the lane-shoulder joint must be achieved. The use of No. 5 (16-mm) tie bars spaced 30 in (760 mm) apart should be sufficient to achieve this high load transfer efficiency.

### Widened Lanes

Another means of reducing edge stresses is through the use of a widened traffic lane. Although this is a fairly recent concept in the United States (has been used since 1970's in Europe), many agencies believe that widening the traffic lane (thus providing a more interior loading condition) will lead to better performance. However, care must be taken not to widen the lane excessively, as longitudinal cracking can result. Typical lane widenings are 1.5 to 3.0 ft (0.5 to 0.9 m).

The effect of widened lanes on PCC pavement performance will be investigated in this section. Eleven projects (34 sections) contained sections with a widened outside traffic lane. Table 119 illustrates the average performance data from these projects. In addition, MN 2 contained a widened inside lane.

Based on the performance data, the sections are in good overall condition, exhibiting little distress and roughness. The only distress that is prevalent to any significant degree is spalling, which is not affected by widened lanes but by the joint characteristics. Some longitudinal cracking is also apparent on a few projects, although it is not excessive.

Table 119. Summary of performance data for sections with widened lanes.

Project	Lane Width	Age, Years	ESAL's, millions	Faulting, in	Deter Cracks/mi	Longitudinal Cracks, ft/mi	% Joints Spalled	IRI, in/mi (PSR)
CA 8	14	9	9.1	0.05	0	0	17	148 (4.0)
FL 2	14	6	9.5	0.05	0	0	7	93 (3.7)
MN 3	14	8	3.7	0.01	0	0	0	100 (4.2)
MN 4	14	6	0.9	0.01	0	0	1	149 (4.4)
MN 6	14	9	2.0	0.01	5	0	3	143 (4.2)
WI 1	14	2	5.0	0.01	0	0	0	99 (3.8)
WI 2	14	4	1.3	0.01	0	0	3	117 (4.0)
WI 5	14	4	1.4	0.05	2	91	8	139 (3.8)
WI 6	14	4	4.2	0.03	0	0	6	87 (3.9)
WI 7	14	4	1.3	0.03	2	58	5	119 (4.1)
WV 1	15	1	3.7	0.04	10	0	67	168 (3.4)

1 in = 25.4 mm  
 1 ft = 0.305 m  
 1 mi = 1.61 km

Although these sections are performing well so far, they are all less than 10 years, and many are less than 5 years old. Therefore, the long-term performance of widened lanes cannot be analyzed. However, the indications are favorable at this point that widened outside lanes will improve the long-term performance of PCC pavements.

The effect of widened outer lanes on pavement performance has also been analyzed by other researchers. Sehr investigated the maximum edge stress as a function of the distance from the slab edge; these results are illustrated in figure 57.<sup>(55)</sup> Likewise, pavement deflections can be reduced by 27, 40, and 46 percent for widening of 1, 2, and 3 ft (0.3, 0.6, and 0.9 m), respectively.<sup>(55)</sup> For a PCC pavement that is widened 18 to 24 in (460 to 610 mm), the reduction in pavement responses can lead to a 20 to 30 percent increase in pavement fatigue life.<sup>(55)</sup>

Another study, which was conducted on I-80 in Colorado, found that widened lanes can significantly improve the fatigue life of PCC pavements, being equivalent to approximately 1 in (25 mm) of slab thickness.<sup>(54)</sup> The study recommended lane widenings of 2 ft (0.6 m), which is wide enough to significantly reduce stresses and improve performance, yet not so wide as to create excessive curling stresses in the transverse direction.



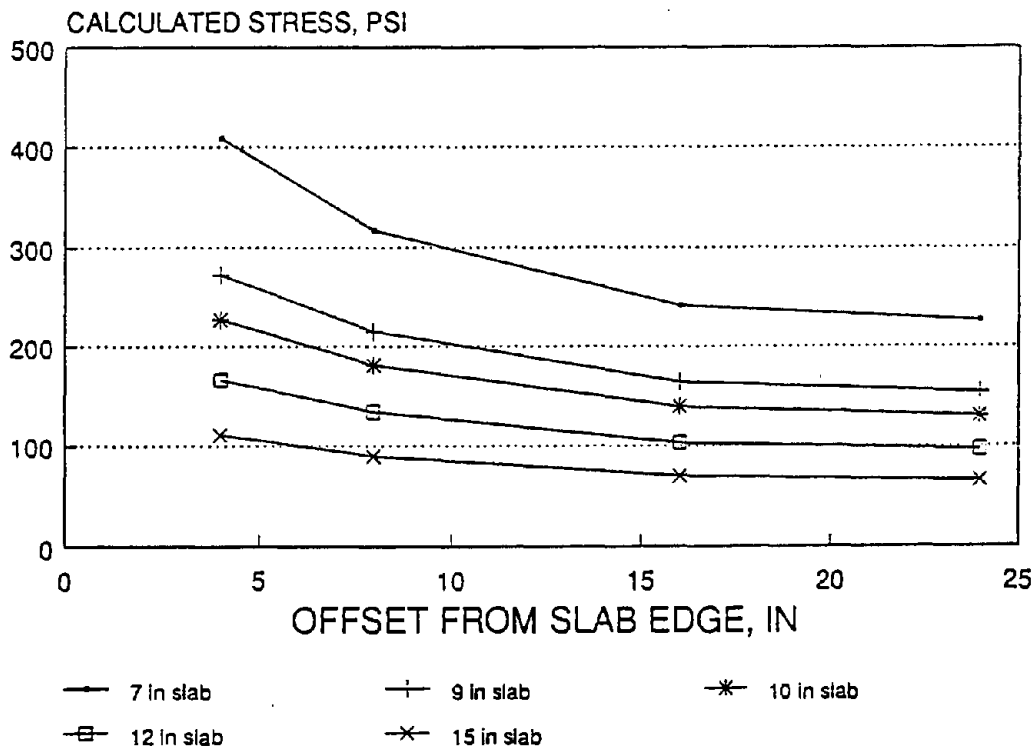


Figure 57. Effect of load offset on calculated stress.

## Reinforcement

Steel reinforcement is placed in JRCP and CRCP to keep transverse cracks from opening and deteriorating. Due to high curling and shrinkage stresses in the long jointed JRCP and in the nonjointed CRCP, cracking occurs at regular intervals in both pavement types. The reinforcement is designed to keep cracks tight and to prevent spalling and faulting of cracks. For CRCP, the amount of steel is also selected to force the pavement to crack at intervals between 3 and 8 ft (0.9 and 2.5 m). However, determining the amount of reinforcement required to accomplish these goals is often difficult, as little guidance has been provided on this subject.

Traditionally, the *AASHTO Guide for Design Pavement Structures* has been used, although many researchers believe that it does not fully simulate field conditions.<sup>(56,57)</sup> The reinforcement procedure for JRCP is based on the subgrade drag theory, whereas the procedure for CRCP is empirical. Other procedures have also been developed for JRCP reinforcement design.<sup>(58)</sup> The steel content is generally expressed as the percent of the steel cross-sectional area to the slab cross-sectional area.

## Review of Project Data

This sections provides a review of projects for JRCP and CRCP sections and the effect of the amount and type of reinforcing steel on PCC pavement performance. Few projects are available in which the amount of reinforcement changes between

sections. Thus, direct comparisons are limited. However, an overall evaluation of the projects should provide additional insight into the effects of reinforcement.

### California 1

This experimental project, located on I-5 near Tracy, contains six CRCP sections, all with 0.56 percent reinforcing steel. However, two sections are provided with transverse reinforcement, and two sections contain deformed welded wire fabric (WWF) for reinforcement. All sections are 8.4 in (213 mm) thick and are placed on a 5.4-in (137-mm) CTB with 4 percent cement.

Table 120 provides a summary of the performance data for the CRCP sections. With the exception of CA 1-15, which exhibited deteriorated transverse cracking and pavement failures, all sections are performing well. CA 1-15 contains deformed WWF (1-C) in the form of mats with D-19 longitudinal wires spaced at 4 in (102 mm) welded to D-6 transverse wires spaced at 16 in (406 mm). The longitudinal deformed bars appear to more effective at holding cracks tight than the deformed WWF. Also, the addition of transverse bars did not result in significantly improved performance.

Table 120. Summary of effect of reinforcement for CA 1.

Section	Reinf. Design	ESAL's, millions	Det. Trans. Cracks/mi	Long. Cracks, ft/mi	Failures per mile	IRI, in/mi	PSR
CA 1-11	Long. Bars	11.9	0	0	0	99	3.4
CA 1-12	Long. Bars	11.9	0	0	0	119	3.3
CA 1-13	Long. and Trans. Bars	11.9	0	0	0	94	3.4
CA 1-14	Long. and Trans. Bars	11.9	0	0	0	93	3.6
CA 1-15	WWF	11.9	111	0	48	141	3.5
CA 1-16	WWF	11.9	0	0	0	94	3.8

1 in = 25.4 mm  
 1 ft = 0.305 m  
 1 mi = 1.61 km

Common Design Features: 8.4-in CRCP with 0.56% reinforcement  
 4-in CTB with 4% cement  
 Built in 1971

### Illinois 1

This project is located on U.S. 50 near Carlyle and includes both JRCP and CRCP sections. The three CRCP sections are 7, 8, and 9 in (178, 203, and 229 mm) thick, with longitudinal steel contents of 0.70, 0.73, and 0.72 percent, respectively. All three CRCP sections contain a 4-in (102-mm) LCB, longitudinal edge drains, no joint seal, and tied PCC shoulders.

The CRCP sections are all performing quite well and the steel contents are not sufficiently different that different levels of performance are expected. None of the sections have experienced any deteriorated transverse cracking, longitudinal cracking, or pavement failures (punchouts). The sections are six years old and have sustained 1.6 million ESAL applications.

The four JRCP sections are 8.5 in (216 mm) thick and are constructed on a 4-in (102-mm) LCB. One section is a conventional JRCP design, and the other three are hinge joint JRCP designs. All sections contain conventional doweled joints with 1.5-in (38-mm) dowel bars at 40-ft (12.2-m) intervals. The hinge joint designs also have one or two intermediate joints that are sawed between the conventional joints. These joints contain 36 in (914 mm) long, epoxy-coated, No. 6 (19-mm) deformed bars spaced at 18-in (457-mm) centers. The conventional JRCP design contains 0.13 percent reinforcing steel, whereas the hinge joint design contains 0.29 percent reinforcing steel.

Table 121 shows a summary of the performance data for IL 1. None of the hinge joint design sections experienced any deteriorated transverse cracks, whereas the conventional JRCP exhibited extensive medium- and high-severity transverse cracks. These deteriorated cracks were also faulted (average faulting of 0.11 in [2.8 mm]). These results indicate that the hinge joint design is more effective at preventing transverse cracking. The performance data do not reveal any advantage from the number of intermediate hinge joints and or the use of wire mesh.

Table 121. Summary of effect of reinforcement for IL 1.

Section	Reinf. Design	ESAL's, millions	Faulting, in	Det. Trans. Cracks/mi	Long. Cracks, ft/mi	% Joints Spalled	IRI, in/mi
IL 1-13 20-ft Hinge	0.29% Steel No Mesh	1.7	0.01	0	0	4	153
IL 1-14 20-ft Hinge	0.29% Steel Wire Mesh	1.7	0.01	0	132	10	173
IL 1-15 13.3-ft Hinge	0.29% Steel No Mesh	1.7	0.01	0	236	3	168
IL 1-16 No Hinge	0.13% Steel Wire Mesh	1.7	0.01	129	1072	8	119

1 in = 25.4 mm  
1 ft = 0.305 m  
1 mi = 1.61 km

Common Design Features:

8.5-in JRCP with tied PCC shoulders  
1.50-in dowels  
4-in LCB and no subbase  
Built in 1986

Illinois 2

This project, located on U.S. 20 near Freeport, includes four JRCP sections. The sections are similar to those constructed for IL 1, except the slabs are 10-in (254-mm) thick. One section is a conventional JRCP design, and the other three are hinge joint JRCP designs. The conventional JRCP design contains 0.11 percent reinforcing steel, whereas the hinge joint design contains 0.25 percent reinforcing steel.

A summary of the performance data for IL 2 is provided in table 122. Again, deteriorated transverse cracking is only found on the conventional JRCP design. The sections have no longitudinal cracking and a minimal amount of faulting and spalling. The effect of the number of hinge joints and the use of wire mesh cannot be established from these data.

Table 122. Summary of effect of reinforcement for IL 2.

Section	Reinf. Design	ESAL's, millions	Faulting, in	Det. Trans. Cracks/mi	Long. Cracks, ft/mi	% Joints Spalled	IRI, in/mi
IL 2-5 20-ft Hinge	0.25% Steel No Mesh	1.3	0.01	0	0	2	121
IL 2-6 20-ft Hinge	0.25% Steel Wire Mesh	1.3	0.02	0	0	12	127
IL 2-7 13.3-ft Hinge	0.25% Steel No Mesh	1.3	0.03	0	0	3	96
IL 2-8 No Hinge	0.11% Steel Wire Mesh	1.3	0.00	42	0	8	131

1 in = 25.4 mm  
 1 ft = 0.305 m  
 1 mi = 1.61 km

Common Design Features: 10-in JRCP with tied PCC shoulders  
 1.50-in dowels  
 4-in LCB and no subbase  
 Built in 1986

Overall Evaluation of Reinforcement

*Jointed Reinforced Concrete Pavements (JRCP)*

Few direct comparisons were available for analyzing the effects of reinforcement on PCC pavement performance. The two projects from Illinois indicated that a hinge joint design, in which a greater amount of reinforcement is concentrated at a controlled crack, provides superior performance compared to the conventional design, in which the reinforcement is distributed through the entire length of the slab. This type of design is not currently common practice but its current performance should merit future consideration.

An overall evaluation of the JRCP sections indicates that the sections with higher steel percentages are performing better, especially in terms of the number of deteriorated transverse cracks. The six hinge joint design sections from Illinois, which contain from 0.25 to 0.29 percent reinforcing steel at the controlled crack, did not exhibit any deteriorated transverse cracking. The three sections from New York contain 0.20 percent reinforcing steel. Of these, two sections contain no deteriorated transverse cracks after 17 and 25 years of service, and the other section contains only nine deteriorated transverse cracks per mile (5.6/km) after 25 years. Likewise, the only JRCP from North Carolina contains 0.17 percent reinforcing steel and has no deteriorated transverse cracks after 25 years of service and 16 million ESAL's.

On the other hand, sections with less than 0.10 percent reinforcing steel have a much higher risk of the transverse cracks becoming deteriorated. For example, the seven sections from OH 1, which have 0.09 percent reinforcing steel, have an average of 163 deteriorated transverse cracks per mile (101/km) after 19 years of service and 6.1 million ESAL's. Of the 24 JRCP sections from MN 1, 21 have some deteriorated transverse cracks, with an average of 43 deteriorated cracks per mile (27/km).

These results are further evidenced through figure 58. With a few exceptions, the sections with greater than 0.10 percent reinforcing steel do not have an overabundance of deteriorated transverse cracks. Of these sections, the three sections with the most cracking are all from Michigan, although the reason for the increased number of deteriorated cracks is not apparent. The sections with lower steel percentages have a large variation in performance, with some sections having many deteriorated transverse cracks and others having very few.

Overall, it appears that the ideal steel percentage is somewhere in the range of 0.10 to 0.20 percent reinforcing steel. Based on research results, Kunt and McCullough found that the steel percentages obtained from the AASHTO Guide are inadequate and should be more in the range of 0.20 to 0.30 percent.<sup>(58)</sup> Likewise, Snyder and Raja conducted laboratory tests (fatigue loading across reinforced cracks) on large-scale test specimens and found that the 0.17 percent steel content commonly used in Michigan is inadequate for loading conditions encountered in the field.<sup>(59)</sup>

This same study also revealed improved performance of JRCP sections containing deformed wire mesh compared with those containing smooth wire mesh.<sup>(59)</sup> Sections using the "hinge joint" design (0.27 percent steel at the crack) showed excellent performance after several million repetitions of a critical load.<sup>(59)</sup> Texas experienced poor performance on pavements with welded wire fabric, and currently uses only deformed reinforcing bars.

Japan has also conducted experimental studies using combined load and curling stresses.<sup>(60)</sup> The critical edge stress was reduced by providing additional 0.5-in (13-mm) deformed bars along the longitudinal edge, which proved to be effective not only at minimizing cracks but also at reducing crack widths.<sup>(60)</sup> Performance studies indicate that JRCP with wire mesh, the most common pavement type in Japan (about 70 percent of all pavements), have exhibited excellent performance on sections

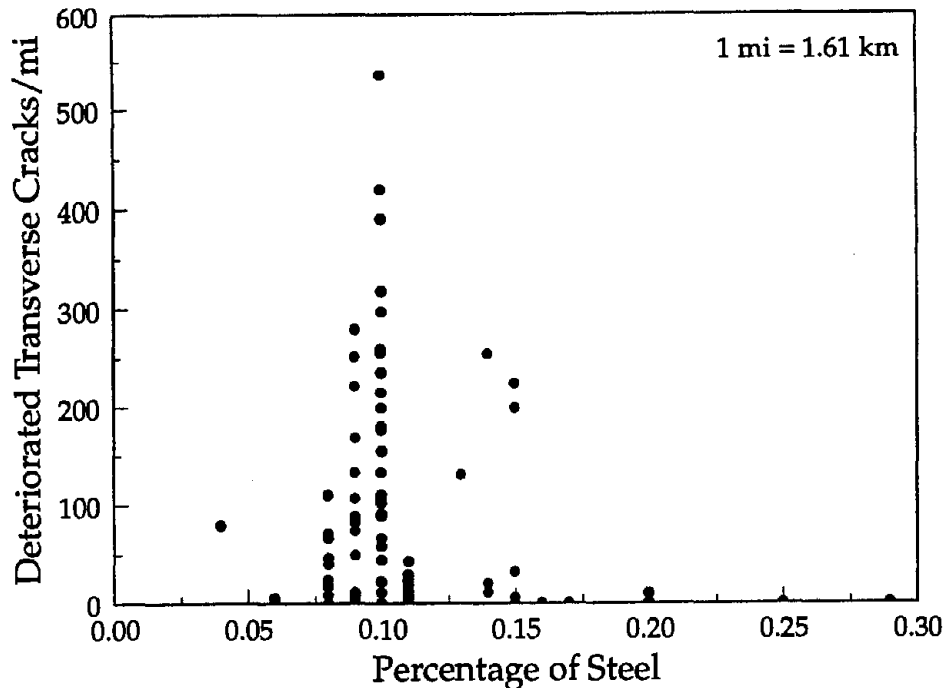


Figure 58. Effect of steel percentage on deteriorated transverse cracking.

constructed as early as 1971.<sup>(61)</sup> The use of a 1-in (25-mm) AC interlayer was also found to significantly increase pavement durability.<sup>(61)</sup>

#### *Continuously Reinforced Concrete Pavements (CRCP)*

CRCP sections from four states—California, Illinois, North Carolina, and Ohio—were included in this study. The only direct comparison came from California, which included sections with and without transverse steel and sections with WWF. One section with WWF (CA 1-15) exhibited extensive deteriorated transverse cracking and pavement failures (punchouts), whereas performance on the sections with deformed reinforcing bars was much better. The sections without transverse steel had similar performance as the sections with transverse steel.

The performance data for all CRCP sections from this study are provided in table 123. Every OH 2 section is severely cracked, with an average of 289 deteriorated transverse cracks per mile (180/km). These sections have 0.61 percent reinforcing steel and have sustained 6.5 million ESAL's over 18 years. D-cracking was prevalent on these sections and is believed to be a major factor in the deterioration of the transverse cracks.

With the exception of the sections mentioned, the CRCP sections are performing quite well. No other sections have deteriorated transverse cracks or pavement failures. The crack spacings are between 2.5 to 4.3 ft (0.76 to 1.3 m). In contrast to initial beliefs, recent findings indicate that shorter crack spacings, somewhere in the

Table 123. Overall performance of CRCP sections

Section	Slab Thick, in	Base Type	% Steel	Age	ESAL's, millions	Crack Spacing, ft	Crack Width, in	Det. Trans. Cracks/mi	Failures per mile	IRI, in/mi
CA 1-11	8.4	CTB	0.56	21	11.9	4.0	0.036	0	0	99
CA 1-12	8.4	CTB	0.56	21	11.9	4.0	0.042	0	0	119
CA 1-13	8.4	CTB	0.56	21	11.9	3.1	0.052	0	0	94
CA 1-14	8.4	CTB	0.56	21	11.9	3.1	0.042	0	0	93
CA 1-15	8.4	CTB	0.56	21	11.9	3.4	0.050	111	48	141
CA 1-16	8.4	CTB	0.56	21	11.9	2.5	0.040	0	0	94
IL 1-1	9.0	LCB	0.72	6	1.7	3.4	—	0	0	103
IL 1-2	8.0	LCB	0.73	6	1.7	3.0	—	0	0	114
IL 1-9	7.0	LCB	0.70	6	1.7	3.5	—	0	0	123
NC 1-9	8.0	AGG	0.60	25	16.0	4.3	0.045	0	0	—
OH 2-47	9.0	ATB	0.61	18	6.5	3.1	0.056	238*	0	197
OH 2-48	9.0	ATB	0.61	18	6.5	4.1	0.058	106*	0	144
OH 2-98	9.0	CTB	0.61	18	6.5	4.1	0.030	792*	0	123
OH 2-99	9.0	CTB	0.61	18	6.5	6.1	0.030	449*	0	86
OH 2-CRC	9.0	AGG	0.61	18	6.5	3.2	0.030	145*	13	150
OH 2-Sa	9.0	AGG	0.61	18	6.5	3.0	0.030	211*	0	172
OH 2-Sb	9.0	AGG	0.61	18	6.5	3.4	0.030	79*	0	143

1 in = 25.4 mm  
 1 ft = 0.305 m  
 1 mi = 1.61 km

\* D-cracking has caused crack spalling on these sections.

range of 2 to 4 ft (0.6 to 1.2 m), can perform well. The surface crack widths range from 0.30 to 0.58 in (7.6 to 14.7 mm). Recent studies have found that the AASHTO design crack width of 0.04 in (1.0 mm) may be excessive, with a crack width of 0.02 (0.5 mm) considered more appropriate (commonly used in Europe).

CRCP sections from Belgium, which contain 0.85 percent reinforcement, have an average crack spacing less than 2 ft (0.6 m). These sections have continued to perform well after 15 years of service, with no fragmentation or deterioration of the cracks.<sup>(62)</sup> Spain, which has a legal axle load limit of 28,600 lb (13 tons) for single axles and 46,300 lb (21 tons) for tandem axles, has also experienced good performance of CRCP with 0.73 and 0.85 percent reinforcement.<sup>(63)</sup>

These findings raise questions about current CRCP design practices in the United States. A higher steel content, resulting in a shorter crack spacing and smaller crack

width, may be more appropriate for long-term performance. A higher steel content may be more desirable in high-traffic urban areas, where no maintenance and long life are critical.

### **Maximum Coarse Aggregate Size**

In concrete mix design, the maximum coarse aggregate size refers to the smallest sieve opening through which a selected aggregate sample passes. The maximum coarse aggregate size not only affects the concrete mix design, but also influences the structural and durability characteristics of the concrete. For example, larger maximum coarse aggregate sizes can lead to increases in concrete strength, but concrete containing larger aggregates that are susceptible to D-cracking exhibit more severe deterioration than concrete containing a smaller size of that same D-cracking susceptible aggregate. Also, larger coarse aggregate sizes have a beneficial effect on the load transfer capabilities of abutting joint or crack faces, particularly in the absence of positive load transfer devices.

### Review of Project Data

While the projects evaluated under this study included concrete mixes with maximum coarse aggregate sizes ranging from 0.5 to 2 in (13 to 51 mm), only two projects included in the study provide direct comparisons between concrete pavements containing different maximum coarse aggregate sizes: MO 1 and OH 2. These projects are described in the following sections.

#### *Missouri 1*

This project consists of concrete pavements with three different maximum coarse aggregate sizes: 2 in (51 mm), 1 in (25 mm), and 0.75 in (19 mm). All sections for which the maximum coarse aggregate size varied are 9-in (229-mm) JRCP with 0.10 percent steel placed on a dense-graded aggregate base course. Transverse joints are spaced at 61.5-ft (18.7-m) intervals and contain 1.25-in (32-mm) dowel bars. With the exception of the 2-in (51 mm) top size aggregate, all aggregate used in the construction of the concrete was mildly susceptible to D-cracking.<sup>(25)</sup>

Table 124 provides a summary of the performance of the MO 1 sections as influenced by coarse aggregate type. Since the joints are doweled, the primary distress to be affected by the coarse aggregate size is the amount of deteriorated transverse cracking. As expected, the section with the largest coarse aggregate size (MO 1-1) shows the least amount of deteriorated transverse cracking. However, the sections with the smallest maximum coarse aggregate size (MO 1-2 and MO 1-3) actually display less deteriorated transverse cracking than the sections with the intermediate size coarse aggregate (MO 1-4 and MO 1-8). It is possible that the difference in size between the 0.75 and 1.0 maximum coarse aggregates is small enough that it has no discernible effect on pavement performance. However, greater extremes in the amount of deteriorated crack faulting were observed on the sections containing the 0.75-in (19-mm) coarse aggregate (up to 0.25 in [6.4 mm] in one case).



Table 124. Summary of effect of maximum coarse aggregate size for MO 1.

Section	Coarse Agg. Size, in	ESAL's, millions	Joint Faulting, in	Det. Cracks/mi	% Joints Spalled	IRI, in/mi	D-Cracking
MO 1-1	2.0	13.7	0.09	0	19	117	None
MO 1-4	1.0	13.7	0.06	29	13	159	Low
MO 1-8*	1.0	13.7	0.06	23	6	176	None
MO 1-2*	0.75	13.7	0.07	11	12	118	Low
MO 1-3	0.75	13.7	0.07	17	6	126	Low

\* Contains polyethylene moisture barrier.

1 in = 25.4 mm  
 1 ft = 0.305 m  
 1 mi = 1.61 km

Common Design Features: 9-in JRPC with 0.10% Steel  
 61.5 ft joints with 1.25 in dowels  
 4 in aggregate base  
 Built in 1977

Although one objective of this pavement project was to evaluate the effect of coarse aggregate size on the development of D-cracking, the performance results do not show any clear trends. The section with the largest top size aggregate displayed no signs of D-cracking, but recall that it was not a D-cracking susceptible material. Of the two sections with the next largest maximum coarse aggregate size, one shows signs of low-severity D-cracking and one shows no signs of D-cracking, while the two sections with the smallest coarse aggregate size exhibit low severity D-cracking.

### Ohio 2

This major experimental project on SR 2 near Vermilion contains a wide range of design features, including pavement type, joint spacing, base type, drainage, joint sealant, and maximum coarse aggregate size. The project was constructed primarily to evaluate the effects of aggregate durability on pavement performance, with maximum coarse aggregate sizes of 0.5, 1.0, and 1.5 in (13, 25, and 38 mm) included in the study.<sup>(33)</sup>

Table 125 provides a summary of the effect of maximum coarse aggregate size for those sections constructed on a dense-graded aggregate base. An examination of this table shows that for the 20-ft (6.1-m) JPCP design and the 60-ft (18.3-m) JRPC sections, the larger coarse aggregate does appear to have a significant reduction in the amount of deteriorated transverse cracks. However, these trends are not as strong for the 40-ft (12.2-m) JRPC sections, particularly for the nondrained sections in which the sections with the largest coarse aggregate display the most deteriorated transverse cracking. Although there is also some variability in the amount of deteriorated cracking for the replicate sections, it still appears that the general trend is toward less deteriorated cracking for sections containing larger coarse aggregate.

Unfortunately, faulting data were unavailable for one of the nondoweled JPCP designs so the effect of coarse aggregate size on nondoweled joint faulting could not be examined.

Table 125. Summary of effect of maximum coarse aggregate size for OH 2 sections constructed on aggregate base.

			20-ft JPCP		40-ft JRCP			60-ft JRCP		
			0.5-in Agg.	1.5-in Agg.	0.5-in Agg.	1.0-in Agg.	1.5-in Agg.	0.5-in Agg.	1.5-in Agg.	
ESAL's, millions			6.5	6.5	6.5	6.5	6.5	6.5	6.5	
AGG BASE	No Drains	Faulting, in Det. Tr. Crks/mi % Joints Spalled IRI, in/mi D-Cracking			2-75* 0.01 110 14 130 Low	2-74* 0.03 66 29 140 High	2-69* 0.01 132 29 128 Medium	2-72 — 254 0 — n/a		
	Daylighted	Faulting, in Det. Tr. Crks/mi % Joints Spalled IRI, in/mi D-Cracking			2-55* 0.07 198 0 190 Low	2-56* 0.02 132 0 114 Low	2-57* 0.04 132 29 132 Low	2-54 0.11 176 0 168 None		
	Edge Drains	Faulting, in Det. Tr. Crks/mi % Joints Spalled IRI, in/mi D-Cracking	2-17* 0.24 317 0 239 None	2-12* 0 100 171 High	2-24* 0 154 0 161 None	2-23* 0 132 17 172 None	2-20* 0.08 132 57 201 High	2-21 0.04 132 0 180 None	2-18* 0.17 418 0 296 None	2-11* 88 100 161 High

\* Contains D-cracking susceptible aggregate.

1 in = 25.4 mm  
1 ft = 0.305 m  
1 mi = 1.61 km

Common Design Features: 9 in slabs  
1.25-in dowels (no dowels on 2-12 and 2-17)  
Built in 1974

The effect of coarse aggregate size on the development of D-cracking is also apparent from table 125. For those sections containing aggregate susceptible to D-cracking, there is an incidence of higher severity D-cracking on those sections with larger coarse aggregate size.

The summary of the effect of maximum coarse aggregate size for sections constructed on no base, ATB, and CTB is provided in table 126. The results from this table are more conclusive in showing that sections with larger maximum coarse aggregate size display less deteriorated transverse cracking than those sections with smaller coarse aggregate sizes, particularly for the JRCP designs. The effect of coarse aggregate size on the cracking of the JPCP designs is not apparent, probably due to these sections being thickened pavement structures (15-in [381-mm] slabs).

As before, the effect of aggregate size on the development of D-cracking also observed in table 126. Again, there is a clear trend that sections with larger coarse aggregate (and containing the D-cracking susceptible aggregate) show higher

severities of D-cracking than those sections with smaller coarse aggregate.

Table 126. Summary of effect of maximum coarse aggregate size for OH 2 sections constructed on no base, ATB, and CTB.

		15 in JPCP, 20-ft Joints				9 in JRCP, 40-ft Joints					
		No Base				ATB (4-8% AC)			CTB (4.5% Cement)		
		0.5-in Aggregate		1.5-in Aggregate		0.5-in Agg	1.5-in Aggregate		0.5-in Agg	1.5-in Aggregate	
ESAL's, millions		6.5		6.5		6.5	6.5		6.5	6.5	
No Drains	Faulting, in	<u>2-1*</u> 0.07	<u>2-4*</u> 0.30	<u>2-2*</u> 0.08	<u>2-3*</u> 0.14	<u>2-44*</u> —	<u>2-43*</u> 0.01	<u>2-45*</u> —	<u>2-95*</u> —	<u>2-94*</u> 0.05	<u>2-96*</u> —
	Det. Tr. Crks/mi	0	0	0	11	234	22	44	535	110	179
	% Joints Spalled	0	0	52	96	0	43	0	33	86	34
	IRI, in/mi	131	93	143	99	—	276	—	—	153	—
		None	None	High	High	n/a	Medium	n/a	n/a	High	n/a
Drains	Faulting, in					<u>2-50*</u> —	<u>2-49*</u> 0.05	<u>2-51</u> 0.06	<u>2-101*</u> —	<u>2-100*</u> 0.06	<u>2-102</u> 0.18
	Det. Tr. Crks/mi					258	0	22	389	44	88
	% Joints Spalled					11	100	0	0	43	29
	IRI, in/mi					—	144	145	—	120	166
						n/a	Medium	None	n/a	Medium	None

\* Contains D-cracking susceptible aggregate

1 in = 25.4 mm  
1 ft = 0.305 m  
1 mi = 1.61 km

Common Design Features: 1.25-in dowels (except 2-1 through 2-4)  
Built in 1974

On the entire OH 2 project, field observations of the cracking patterns in sections containing the smaller coarse aggregate show very straight cracks across the pavement. Cores retrieved across these cracks also show very straight vertical cracks. Because of the smaller aggregate size, the cracks do not meander substantially, either through or across the concrete slab, a phenomenon that detracts from the ability for aggregate interlock load transfer to exist across the crack. While load transfer was not measured across these cracks, crack faulting measurements of 0.2 in (5 mm) or more was not uncommon for sections containing smaller coarse aggregate.

Because the JPCP designs shown in table 126 are not doweled, it is expected that coarse aggregate size may have an effect on the faulting of these joints. When considering average joint faulting of the replicate sections, there is observed to be some effect of the larger maximum coarse aggregate size on reducing faulting.

### Overall Evaluation of Maximum Coarse Aggregate Size

Two projects were included in the study that allow direct comparisons on the effect of maximum coarse aggregate size on pavement performance. While there was some variability in the results, generally the sections with the larger maximum coarse aggregate size show less deteriorated cracking than those sections with a smaller maximum coarse aggregate size. There is also some evidence that shows faulting of

cracks and joints is less for sections containing larger maximum coarse aggregate sizes.

Cracks that develop in pavement slabs with very small maximum coarse aggregate size (say, 0.5-in [13-mm]) tend to be very straight, both across the pavement and through the depth of the slab. This is due to the small size aggregate, and this type of crack formation detracts from the load transfer capabilities of the aggregate at joints and cracks.

For D-cracking susceptible aggregate, the maximum coarse aggregate size was also determined to have an effect on the development of D-cracking. Pavements containing larger maximum coarse aggregate size (1.5 in [38 mm]) display higher levels of D-cracking (in the form of more severe joint and corner spalling) than those sections with smaller maximum coarse aggregate size (0.5 in [13 mm]). In fact, a reduction to a maximum coarse aggregate size of 0.5 in (13 mm) eliminated the development of D-cracking in many instances.

### **Pavement Type**

In the preceding sections, the effect of various design features on the performance of PCC pavements is examined. Evaluations are performed by looking at sections within projects in which these design features are varied as well as by considering general comparisons across projects in which many other variables (such as climate, loading, and support) also vary. The results of these evaluations are used later to develop or refine guidance on the use or application of these design features.

One feature of pavement design not yet considered is pavement type (which, in the context of this analysis, refers to JPCP, JRCP, and CRCP). Strictly speaking, pavement type is not a design feature; design features are those elements of a design that are determined once the pavement type is decided upon. However, a number of the projects included test sections of more than one pavement type. Because of the existence of these sections side by side at a number of sites around the country, it is possible to consider a comparative relationship between pavement type and pavement performance.

There are two major caveats associated with the evaluation of the relative performance of the different pavement types. Generally, an evaluation of pavement type as a design feature will, by default, introduce many more variables (or confounding factors) than are present when other variables are examined. In other words, comparing one pavement type to another is not as straightforward even as comparing reinforced slabs to nonreinforced slabs, doweled to nondoweled joints, or short to long slabs; changing from one type to another will involve the change of several of these variables. For example, JPCP is characterized by short-jointed slabs with or without doweled transverse joints; JRCP typically includes much longer jointed slabs, the transverse joints are doweled, and the slabs are lightly reinforced. When CRCP is considered, these comparisons become more problematic, as continuously reinforced concrete pavements do not have transverse contraction joints

(and their associated potential for faulting, corner breaks, and spalling) and contain considerably more steel reinforcement than do JRCP.

The other caveat is that these different pavement types perform differently. That is, there are fundamental and major differences in the way that these pavements respond to applied loads. For example, JPCP are not expected to develop transverse cracks, and typical load-associated deterioration includes faulting, corner breaks, and spalling. JRCP are expected to develop transverse cracking. Load associated failures include deteriorated transverse cracks, faulting, spalling, and corner breaks. CRCP will have transverse cracks, and load-associated deterioration will include deteriorated transverse cracks, ruptured steel, and punchouts. A comparison of pavement types, in order to be "fair," must not consider modes of failure that are specific to any one or two types.

With a good deal of long-term performance data available, the ideal comparison of different pavement types would consider life-cycle costs or some sort of cost/benefit analysis, in which the benefit might be the overall quality of the ride, safety, user costs, and so on. In the absence of this type of definitive data for each of the pavement types, the overall rideability (PSR, IRI) of the pavements is really the only performance parameter that can be compared. Considering rideability alone has the advantage of eliminating from the evaluation process elements of performance that are intrinsic to each pavement type, while still permitting comparisons of an engineering nature.

In the following section, the performance of test sites in which more than one rigid pavement type was constructed is considered. The section begins with the test sites at which all three rigid pavement types were constructed, and continues with the sites at which two different pavement types were constructed. The primary basis for the comparisons that are made is the rideability, as represented by the PSR and IRI. However, for each rigid pavement type, other key performance indicators are discussed when appropriate.

### Comparisons of all Three Pavement Types

Two test sites included sections of all three pavement types, North Carolina 1 (Rocky Mount) and Ohio 2 (Vermilion). The comparative performance by pavement type at these sites is discussed below.

#### *North Carolina 1*

This project, on I-95 near Rocky Mount, is located in the WNF zone and includes seven JPCP sections, one JRCP section, and one CRCP section. Variables at this test site include base type, doweled and nondoweled transverse joints, and joint orientation. Both the JRCP and CRCP sections were 8 in (203 mm) thick; the JRCP has 0.17 percent longitudinal reinforcement and the CRCP has 0.60 percent. The JPCP sections are all 9 in (229 mm) thick. All sections include a daylighted aggregate base that extends from the outer lane-shoulder joint to the outer ditch line.

Table 127 compares the performance of the three pavement types in 1992, 25 years after construction. Of the JPCP sections, the best performing pavement is constructed on ATB. This section has the least faulting, the highest PSR, and the lowest IRI of all of the JPCP sections at the Rocky Mount site. Interestingly, the sections with an aggregate base appear to be exhibiting less pumping than those with stabilized bases.

Table 127. Performance data summary for NC 1.

Type	Section	Thickness, in	Base	Load Transfer	PSR	IRI	Faulting, in
JPCP	NC 1-1*	9	4-in AGG	No	3.3	111	0.13
	NC 1-2	9	6-in SC	Yes	3.3	114	0.16
	NC 1-3	9	6-in SC	No	3.4	116	0.14
	NC 1-4*	9	4-in AGG	Yes	3.2	110	0.13
	NC 1-5	9	4-in CTB	No	2.9	139	0.16
	NC 1-6	9	4-in ATB	No	3.7	102	0.05
	NC 1-8*	9	4-in AGG	No	3.3	131	0.22
JRCP	NC 1-7*	8	4-in AGG	Yes	3.2	120	0.15
CRCP	NC 1-9*	8	4-in AGG	n/a	3.7	—	n/a

1 in = 25.4 mm

1 ft = 0.305 m

1 mi = 1.61 km

\* Sections share a common base type and are more appropriate for direct comparisons.

Common Design Features:

30-ft joint spacing

Built in 1967

1992 ESAL's = 16.0 million

Considering only the performance of sections with an aggregate base, the CRCP section appears to be performing better than the others. The PSR is 3.7, equal to the best-performing JPCP section. The average crack spacing of this design is 4.3 ft (1.3 m), which is good, but the crack width is 0.045 in (1.14 mm), which is considered high. There is little to distinguish between either the JPCP or JRCP sections. They have similar average PSR values, IRI values, and faulting levels.

## Ohio 2

This test site is located on State Route 2 near Vermilion and includes 104 different short sections that were constructed in 1974. As part of this study, a total of 43 JRCP, 4 JPCP, and 7 CRCP sections were evaluated, although complete performance data are not available for all of these sections. The JRCP sections consist of 9-in (229-mm) doweled slabs on three different base types (AGG, CTB, and ATB), while the JPCP sections consist 15-in (381-mm) nondoweled slabs on grade and 9-in (229-mm) doweled slabs on an AGG base. Three different slab lengths are used on the JRCP

sections, 40 ft, 20 ft, and 60 ft (12.2, 6.1, and 18.3 m); all of the JPCP sections have 20-ft (6.1-m) transverse joint spacing. All of the JRCP sections have 0.10 percent longitudinal reinforcement. Distinguishing features of the CRCP designs include 8-in (203-mm) thick slabs, 0.61 percent longitudinal reinforcement, and sections on different base types (AGG, CTB, and ATB).

Table 128 summarizes available average performance data for some of these sections (those for which IRI data were available). None of the jointed pavement sections have PSR data because of the extremely short sections (and the associated inability to distinguish between sections when driving at highway speeds). The CRCP sections exhibit the best overall performance, followed by the JPCP sections, and then the JRCP sections. The performance of the JRCP sections, however, was adversely affected by severe D-cracking.

Table 128. Performance data summary for OH 2.

Type	Number of Sections	Joint Spacing, ft	Base Type	Avg IRI, in/mi	Avg. Faulting, in
JRCP	15	40	AGG	153	0.04
	3	60	AGG	204	0.17
	3	40	CTB	146	0.10
	3	40	ATB	188	0.04
JPCP	4	20	None	117	0.15
	4	20	AGG	189	0.13
CRCP	2	n/a	CTB	105	n/a
	2	n/a	ATB	171	n/a
	3	n/a	AGG	155	n/a

1 in = 25.4 mm  
 1 ft = 0.305  
 1 mi = 1.61 km

Built in 1974  
 1992 ESAL's = 6.5 million  
 JRCP designs are doweled; JPCP are not

Within subcategories in each pavement type, the best performing cross section was the CRCP with a CTB, followed in order by the full-depth JPCP, the JRCP with a CTB, the JRCP with the aggregate base, and the JPCP with the aggregate base. There are performance measurements for the CRCP sections, however, that are cause for concern. While the crack spacing in all of the sections is good (average of 3.9 ft [1.2 m]), the average crack width (0.038 in [1 mm]) is near the upper limit of what is considered acceptable, and all of the sections show a very high number of deteriorated cracks per mile (1.6 km). Nonetheless, only one of the CRCP sections,

on an aggregate base, shows any punchouts (13/mi [21/km]).

### Comparisons Between JPCP and JRCP

#### *Michigan 1*

At this WF test site, located on U.S. 10 near Clare, four of the sections studied were JRCP and 11 were JPCP. The pavements were constructed in 1975, and by the time of their 1992 evaluation had carried an estimated 1.3 million ESAL's. All of the JRCP sections consisted of a doweled 9-in (229-mm) slab (with 0.15 percent longitudinal reinforcement) on an aggregate base. Transverse joint spacing in these reinforced sections was 71.2 ft (21.7 m). The JPCP sections included both doweled and nondoweled sections, two different joint spacing patterns, and three different base types (PATB, AGG, and ATB). Some design information and selected performance data are summarized in table 129.

Overall, the JPCP sections are performing better than the JRCP sections. This observation is especially true if the sections consisting of JPCP on an ATB are removed from consideration; as discussed previously, at this location this cross section acted as a bathtub and did not perform well. Without those sections, the average IRI for the nondoweled JPCP on PATB was 115 in/mi (1815 mm/km) and for the doweled JPCP on an aggregate base was 123 in/mi (1941 mm/km). In contrast, the average IRI for the JRCP sections was 147 in/mi (2320 mm/km).

#### *West Virginia 1*

This project, located on I-77 south of Charleston, consists of three sections—two JRCP and one JPCP. All slabs are doweled and 10 in (254 mm) thick. The JRCP sections contain 0.10 percent longitudinal reinforcement and have 40-ft (12.2-m) joint spacing. The JPCP section, which has a 15-ft (4.6-m) joint spacing, was added as a truck climbing lane adjacent to an existing 60-ft (18.3-m) JRCP. Table 130 summarizes key design and performance data for these three sections. As can be seen, these sections all have different construction dates, so direct comparisons of performance are not possible. It is interesting to note, however, that the performance of these three different designs was similar. Considering only the PSR and IRI, the oldest section—JRCP on a CTB—exhibited the best performance, and the JRCP are performing better than the JPCP.



Table 129. Performance data summary for MI 1.

Type	Section	Joint Spacing, ft	Base Type	Load Transfer	PSR	IRI, in/mi	Faulting, in
JRCP	MI 1-1a	71.2	AGG	Yes	3.5	141	0.06
	MI 1-1a2	71.2	AGG	Yes	-	174	0.03
	MI 1-1b2	71.2	AGG	Yes	-	136	0.06
	MI 1-1b	71.2	AGG	Yes	2.9	135	0.10
JPCP	MI 1-4a	13-19-18-12	PATB	No	3.8	106	0.03
	MI 1-4a10	13-19-18-12	PATB	No	-	117	0.02
	MI 1-4a12	13-19-18-12	PATB	No	-	121	0.02
	MI 1-7a5	13-17-16-12	AGG	Yes	-	130	0.05
	MI 1-7b5	13-17-16-12	AGG	Yes	-	121	0.06
	MI 1-7a	13-17-16-12	AGG	Yes	3.0	121	0.05
	MI 1-7b	13-17-16-12	AGG	Yes	3.1	120	0.03
	MI 1-10a3	13-19-18-12	ATB	No	-	203	0.29
	MI 1-25	13-19-18-12	ATB	No	2.3	247	0.30
	MI 1-10a	13-19-18-12	ATB	No	2.0	161	0.13
	MI 1-10b	13-19-18-12	ATB	No	2.1	197	0.15

1 in = 25.4 mm

1 ft = 0.305 m

1 mi = 1.61 km

Sections with "a" in their ID have positive subdrainage.

Built in 1975

1992 ESAL's = 1.3 million

Table 130. Performance data summary for WV 1.

Type	Section	Year Built	1992 ESAL's, million	Base Type	PSR	IRI, in/mi	Faulting, in	Det. Cracks/mi	% Cracked
JRCP	WV 1-1	1986	6.5	AGG	3.5	168	0.02	58	100
	WV 1-2	1981	8.9	CTB	3.6	142	0.06	11	16
JPCP*	WV 1-3	1989	3.7	AGG	3.4	168	0.04	10	3

1 in = 25.4 mm

1 ft = 0.305 m

1 mi = 1.61 km

All joints are doweled.

\* Section added as a truck climbing lane to existing 60-ft JRCP

*New York 1*

New York 1, constructed in 1968 and located on US 23 near Catskill, consists of six JPCP sections and two JRCP sections. All of the slabs are 9 in (229 mm) thick. Transverse joint spacing is 20 ft (6.1 m) for the JPCP and 60.8 ft (18.5 m) for the JRCP. There is 0.20 percent longitudinal steel reinforcement in the JRCP sections. As can be seen from table 131, this project includes sections on soil cement bases, aggregate bases, and ATB. For those sections that had load transfer, it was provided for by ACME devices, two-part, malleable iron devices, which are known to contribute to performance problems.

Table 131. Performance data summary for NY 1.

Type	Section	Load Transfer Device	Base Type	PSR	IRI, in/mi	Faulting, in	Det. Cracks/mi	% Cracked
JPCP	NY 1-5a	None	SC	-	-	-	20	11
	NY 1-5b	ACME	SC	-	-	-	51	16
	NY 1-6	ACME	AGG	3.8	118	0.02	44	17
	NY 1-8a	None	ATB	4.2	112	0.01	26	10
	NY 1-8b	None	ATB	3.9	111	0.03	18	7
	NY 1-1	ACME	ATB	3.7	106	0.02	18	7
JRCP	NY 1-3	ACME	ATB	3.1	117	0.16	0	50
	NY 1-4	ACME	AGG	3.4	177	0.14	9	30

1 in = 25.4 mm  
 1 ft = 0.305 m  
 1 mi = 1.61 km

Built in 1968  
 1992 ESAL's = 5.5 million

Overall, the performance of the JPCP sections was better than that of the JRCP sections. The average PSR was 3.9 compared to 3.3, and the average IRI was 112 in/mi (1768 mm/km) compared to 147 in/mi (2320 mm/km). Looking at some of the other measures of performance, the JPCP performed much better in terms of faulting (0.02 in [0.5 mm] versus 0.15 in [3.8 mm]) and percent of cracked slabs (11 percent versus 40 percent).

*New York 2*

The four sections of NY 2 that were evaluated include three JPCP sections and one JRCP. This project is located on I-88 near Otego and was constructed in 1975. All of the sections are 9 in (229 mm) thick, contain an aggregate base, and have 1-in

(25-mm) thick I-beams for load transfer devices. There are two different joint spacings for the JPCP, two different base thicknesses, and sections 2-3 and 2-15 had aggregate subbases as well. The three JPCP have PCC shoulders, while the JRCP section has an AC shoulder. The JRCP has 0.20 percent longitudinal reinforcing steel. Performance data for these four sections are summarized in table 132.

Table 132. Performance data summary for NY 2.

Type	Section	Joint Spacing, ft	PSR	IRI, in/mi	Faulting, in	Det. Cracks/mi	% Cracked
JPCP	NY 2-11	26.7	4.1	98	0.01	40	20
	NY 2-3	20	-	108	0.01	55	21
	NY 2-9	20	3.9	91	0.01	25	9
JRCP	NY 2-15	63.5	4.3	89	0.02	0	12

1 in = 25.4 mm  
 1 ft = 0.305 m  
 1 mi = 1.61 km

All sections contain 1-in I-beams  
 Built in 1975  
 1992 ESAL's = 5.8 million

The performance of the JRCP section is marginally better than that of the JPCP sections. Its average PSR and IRI are both better (4.3 to 4.0 and 99 in/mi [1562 mm/km] to 89 in/mi [1404 mm/km]) and the transverse cracking is less severe on that section. Faulting levels on both pavement types are similar and quite low. Overall, both designs are performing well.

### Ohio 1

Ohio 1, located on U.S. 23 near Chillicothe, includes seven JRCP sections and one JPCP section. All of the slabs are 9 in (229 mm) thick. For the JRCP, the design variables include joint spacing (21 and 40 ft [6.4 and 12.2 m]), base type (7.5 in [191 mm] of aggregate and 4 in [102 mm] ATB), and dowel coatings (standard and plastic coated). All sections have 0.09 percent longitudinal reinforcement. The JPCP section has 17-ft (5.2-m) transverse joint spacing, contains an ATB, and does not have dowels at the transverse joints.

The overall performance of these eight sections is presented in table 133. Because of the rather large number of variables in this limited number of sections, there is a fair amount of confounding of the results. The following is a breakdown of average IRI values of various combinations of these sections:

- All JRCP = 171 in/mi (2698 mm/km).
- All JRCP with aggregate base = 178 in/mi (2808 mm/km).
- All JRCP with ATB = 154 in/mi (2430 mm/km).

Table 133. Performance data summary for OH 1.

Type	Section	Dowel Type	Joint Spacing, ft	Base Type	IRI, in/mi	Faulting, in	Det. Cracks/mi	% Cracked
JRCP	OH 1-1	Std	40	AGG	224	0.02	88	100
	OH 1-7	Plastic Coat.	40	AGG	135	0.01	279	100
	OH 1-9	Std	40	AGG	154	0.07	251	100
	OH 1-10	Std	21	AGG	182	0.03	168	89
	OH 1-3	Std	21	ATB	152	0.03	0	0
	OH 1-4	Std	40	ATB	156	0.02	132	100
	OH 1-6	Plastic Coat.	21	AGG	196	0.01	220	100
JPCP	OH 1-5	None	17	ATB	150	0.13	0	0

1 in = 25.4 mm  
 1 ft = 0.305 m  
 1 mi = 1.61 km

Built in 1973  
 1992 ESAL's = 6.1 million

- All 40-ft (12.2-m) JRCP = 167 in/mi (2635 mm/km).
- All 21-ft (6.4-m) JRCP = 177 in/mi (2792 mm/km).
- All 17-ft (5.2-m) JPCP = 150 in/mi (2366 mm/km).

Looking at the IRI, the only JRCP sections that distinguish themselves from the others are the sections on the ATB (OH 1-3 and OH 1-4). Their average IRI is very similar to that of the best-performing section, the long-jointed JPCP on an ATB. The JPCP section had a fairly high level of faulting, which would normally indicate that it is nearing a point where it needs rehabilitation. Also, of the two JRCP sections on ATB, the section with the shorter joint spacing (21 ft [6.4 m] versus 40 ft [12.2 m]) has no cracking and would appear to have better long-term performance potential.

### Minnesota 2

Minnesota 2, located on I-90 between Albert Lea and Blue Earth, consists of two JPCP and two JRCP constructed in 1977. Three sections have 9-in (229-mm) thick slabs and one has an 8-in (203-mm) slab; all have 1-in (25-mm) diameter dowels at the transverse joints. All sections are also constructed on an aggregate base of either 5 or 6 in (127 or 152 mm). The JPCP have a tied PCC shoulder while the JRCP do not. The JRCP sections contain 0.09 percent longitudinal reinforcement.

The performance of these sections is summarized in table 134. As can be seen, there is little to distinguish between the performance of the two pavement types. The

PSR values are identical, the faulting is very similar, and only a slight difference in the amount and severity of cracking exists. The average IRI is higher for the JPCP sections, but the difference is not considered significant (141 to 133 in/mi [2225 to 2099 mm/km]).

Table 134. Performance data summary for MN 2.

Type	Section	Joint Spacing, ft	PSR	IRI, in/mi	Faulting, in	Det. Cracks/mi	% Cracked
JPCP	MN 2-1	13-16-14-19	4.0	140	0.08	0	0
	MN 2-2	13-16-14-19	3.9	142	0.08	5	1
JRCP	MN 2-3	27	4.0	113	0.06	10	5
	MN 2-4	27	3.9	153	0.07	5	3

1 in = 25.4 mm  
 1 ft = 0.305 m  
 1 mi = 1.61 km

All sections contain 1.00-in diameter dowels  
 Built in 1977  
 1992 ESAL's = 4.2 million

### Comparison Between JPCP and CRCP

#### *California 1*

CA 1, constructed in 1971 on I-5 near Tracy, includes ten nondoweled JPCP sections and six CRCP sections. Every slab is 8.4 in (213 mm) thick except for 1-5 and 1-6, which are 11.4 in (290 mm) thick. Primary variables in the JPCP design include joint spacing, slab thickness, and base type. The CRCP sections are all on a CTB, and have 0.56 percent longitudinal reinforcement. The primary variable within these sections is the type of reinforcing steel. Several design and performance variables are summarized in table 135.

On this project, the CRCP sections have performed much better than JPCP. Only one CRCP has any deteriorated transverse cracks, whereas all but one JPCP section exhibits deteriorated transverse cracks. The average PSR for the CRCP sections is 3.5 and the average IRI is 107 in/mi (1689 mm/km). These averages are about the same as the PSR and IRI of the best-performing JPCP section, CA 1-8. Overall, the average PSR and IRI for the short-jointed JPCP sections are 3.0 and 169 in/mi (2667 mm/km), and for the longer-jointed JPCP sections they are 3.2 and 143 in/mi (2256 mm/km). The average crack spacing for the CRCP is 3.2 ft (1 m), which is a little short, and the average crack width is 0.041 in (1 mm), which is at the high end of normal (especially for such short crack spacing). Among the CRCP sections, the section with the deformed welded wire fabric is performing the worst; there is no consistent basis for differentiating between the performance of the other two CRCP sections.

Table 135. Performance data summary for CA 1.

Type	Section	Slab Thick, in	Joint Spacing, ft	Base Type	Deter. Cracks/mi	PSR	IRI, in/mi
JPCP	CA 1-1	8.4	8-11-7-5	CTB	5	3.3	129
	CA 1-2	8.4	8-11-7-5	CTB	56	2.7	210
	CA 1-3	8.4	12-13-19-18	CTB	60	3.3	111
	CA 1-4	8.4	12-13-19-18	CTB	240	3.3	157
	CA 1-5	11.4	12-13-19-18	CTB	0	3.2	141
	CA 1-6	11.4	12-13-19-18	CTB	135	3.5	166
	CA 1-7	8.4	12-13-19-18	LCB	85	3.1	120
	CA 1-8	8.4	12-13-19-18	LCB	255	3.5	106
	CA 1-9	8.4	12-13-19-18	CTB	271	3.1	130
	CA 1-10	8.4	12-13-19-18	CTB	321	2.7	210
CRCP	CA 1-11	8.4	n/a	CTB	0	3.4	99
	CA 1-12	8.4	n/a	CTB	0	3.3	119
	CA 1-13§	8.4	n/a	CTB	0	3.4	94
	CA 1-14§	8.4	n/a	CTB	0	3.6	93
	CA 1-15‡	8.4	n/a	CTB	111	3.5	141
	CA 1-16‡	8.4	n/a	CTB	0	3.8	94

1 in = 25.4 mm  
 1 ft = 0.305 m  
 1 mi = 1.61 km

Built in 1971; ESAL's = 11.9 million  
 § longitudinal and transverse steel  
 ‡ deformed welded wire fabric reinforcement

### Comparisons Between JRCP and CRCP

#### *Illinois 1*

This project, located on U.S. 50 near Carlyle, compared JRCP sections to CRCP (although JPCP sections were constructed as part of the project, they were not evaluated in this study). These sections are in the WF zone and were constructed in 1986. The four JRCP sections are all 8.5 in (216 mm) thick, doveled, have 40-ft (12.2-m) transverse joint spacing, and are on an LCB. The design variable in these sections is the inclusion and spacing of warping joints (and the associated reinforcement). The three CRCP sections include different slab thicknesses and percent longitudinal reinforcement. They are also all constructed over an LCB.

The key design variables and IRI for these sections are shown in table 136. No PSR data are available for these sections. As can be seen, the average ride of the CRCP sections is better than that of the JRCP sections (113 in/mi [1783 mm/km] as opposed to 153 in/mi [2415 mm/km]). The IRI of only one of the JRCP sections, IL 1-16, is close to that of the CRCP sections, but that section (which does not have the steel reinforced warping joint) is exhibiting the most cracking of all of the JRCP sections (deteriorated cracks also exhibiting faulting). The average crack spacing of the CRCP sections is 3.3 ft (1 m); no average crack width was recorded.

Table 136. Performance data summary for IL 1.

Type	Section	Slab Thick, in	Warp Joint Spacing, ft	Effective Reinf, %	IRI, in/mi	Deter. Cracks/mi	% Cracked
JRCP	IL 1-13	8.5	20	0.29	153	0	0
	IL 1-14	8.5	20	0.29	173	0	20
	IL 1-15	8.5	13.3	0.29	168	0	0
	IL 1-16	8.5	None	0.13	119	129	100
CRCP	IL 1-1	9	n/a	0.72	103	0	n/a
	IL 1-2	8	n/a	0.73	114	0	n/a
	IL 1-9	7	n/a	0.70	123	0	n/a

1 in = 25.4 mm  
 1 ft = 0.305 m  
 1 mi = 1.61 km

Built in 1986  
 1992 ESAL's = 1.7 million

### Overall Summary

The preceding discussion has presented information about a number of test sections in which the relative performance of different types of concrete pavements can be compared. The comparisons that are made are summarized in table 137. The first two sites had all three concrete pavement types. At both of these locations, the JPCP and CRCP showed similar performance, followed by the JRCP. The CRCP designs had about the same amount of reinforcement (0.60 and 0.61 percent), but the JRCP at NC 1 had 0.17 percent reinforcement compared to 0.10 percent at OH 2. These values are at the lower end of the acceptable limit, and might be especially problematic in the WF climatic zone. At OH 2, one of the major deterioration modes was D-cracking, which commonly initiates at the joints (where moisture can enter pavement structure). Thus, there are more critical locations for D-cracking on short jointed pavements (more joints). On the other hand, the severity may be greater on long jointed pavements, which experience more movement at the transverse joints and thus allow more moisture into the pavement structure to accelerate the break-up.

Table 137. Comparison of performance by pavement type.

Location	Pavement Types Evaluated	Age, years	ESAL's, millions	Order of Performance
NC 1	CRCP JRCP JPCP	24	16.0	CRCP JPCP JRCP
OH 2	CRCP JRCP JPCP	18	6.5	CRCP JPCP JRCP
MI 1	JPCP JRCP	17	1.3	JPCP JRCP
WV 1	JPCP JRCP	3 to 11	3.7 to 8.9	JRCP JPCP
NY 1	JPCP JRCP	24	5.5	JPCP JRCP
NY 2	JPCP JRCP	17	5.8	JRCP JPCP
OH 1	JPCP JRCP	19	x.x	JPCP JRCP
MN 2	JPCP JRCP	15	14.2	JRCP JPCP
CA 1	JPCP CRCP	21	11.9	CRCP JPCP
IL 1	JRCP CRCP	6	1.7	CRCP JRCP

Six sites had both JPCP and JRCP. An examination of the comparative performance of these two pavement types at these six sites shows no definitive trend. The rideability of the JPCP was better than that of the JRCP at four out of the six sites, but at the two sites where JRCP were performing better there was not that much difference between the overall performance of both. There is no clearer trend if the data are broken out by either climatic zone, pavement age, or ESAL's.

At one site, CA 1, CRCP performance is compared to that of JPCP. At this site, the CRCP was the better pavement type. The JPCP sections did not have dowels and experienced a significant amount of faulting after 21 years and 11.9 million ESAL's. The CRCP sections had 0.56 percent longitudinal reinforcement, which may have proven to be sufficient in this relatively mild environment.

There is also one site at which the comparison of JRCP to CRCP is made. At IL 1, the CRCP sections also performed better than the JRCP sections. While the site has



only been open since 1986, there is already a clear difference between the performance of the CRCP sections, even of the thinner slabs, in comparison to the hinged joint designs of the JRCP.

### Related Research

In recognition of the fact that only a limited number of pavement sections was examined to assess the role of pavement type on performance, a brief review of the literature was undertaken to evaluate what others have reported regarding the relative performance of the different types of rigid pavements. Findings from other comparative studies follow.

Several "road tests" have considered the issue of pavement type, with perhaps the most notable being the Bates Road Test (1920 to 1923) and the AASHO Road Test (1958-1960). At the Bates Road Test, excessively long JPCP and JRCP slabs were constructed; while they both cracked, the steel mesh held the JRCP together and its performance was reported by Bradbury to be superior to that of the JPCP.<sup>(64)</sup> However, the types of test pavements that were constructed in the 1920's are hardly comparable to today's pavements and these findings are not applicable now.

A study of reinforced pavements in Indiana, initiated in 1938, was reported by Cashell and Teske over 15 years later.<sup>(65)</sup> With the broad range of joint spacings, percent longitudinal reinforcement, and types of reinforcement used in this field test, the findings can be evaluated in terms of the relative performance of JRCP and CRCP. Their general finding is that "sections of any length within the range studied (20 to 1,310 ft [6 to 400 m]) can be reinforced longitudinally to give satisfactory performance without failure of the steel or adverse effects on the concrete." Regarding jointed sections, it was noted that "all percentages of longitudinal steel of 0.17 and greater had been able to maintain in a closed condition all cracks in their respective group of sections." The continuously reinforced sections that were adequately reinforced also performed well, although no corresponding guidance on the percent reinforcement was given.

One of the best documented studies in which pavement type is a variable is the AASHO Road Test. Fordyce and Teske studied data from the Road Test and concluded that the JPCP showed equal or slightly better performance than the reinforced slab design.<sup>(66)</sup> Specifically, they noted that with thinner slabs, the JPCP performed better than JRCP; when the slabs were thicker, their performance was the same.

McCullough et al. report on the performance of JRCP and CRCP in Texas.<sup>(67)</sup> While this study evaluated both these pavement types, they were not constructed at the same time and no conclusions were drawn as to the relative superiority of one design over the other.

In 1977, Blum and Solberg reported on the analytical process undertaken by Wisconsin DOT to arrive at the selection of a JPCP as the type of pavement to be

constructed.<sup>(68)</sup> The authors report that the original pavement type was the (at that time) typical 9-in (229-mm) JRCP. Prior to construction, this design was supplanted by an 8-in (203-mm) CRCP. Because of the high cost of this design, a third alternative, an 11-in (280-mm) JPCP was introduced. For these three designs, the initial construction costs were calculated based on the prevailing material costs. Then the performance of a JPCP and JRCP on a different highway were studied, and the conclusion was reached that they performed similarly, although the reinforced pavement required more repairs. Based on the results of this analysis and the lower initial construction costs of the JPCP, the DOT selected the JPCP as the rigid pavement type to construct.

Darter et al., in their development of the COPES system and data base, evaluated JPCP and JRCP in six States.<sup>(69)</sup> Performance prediction models were developed for both pavement types, and used to compare the predicted performance of JPCP and JRCP using typical data from a wet-freeze, midwestern United States climate. Considering cracking, joint deterioration, faulting, pumping, and PSR, the following were concluded:

*The predicted serviceability and pumping of these two types of pavements are approximately the same. However, the JRCP exhibits a greater amount of cracking throughout most of the 30 years. The JRCP also has significantly more joint deterioration, resulting in a need for joint repairs after about 15 to 20 years. Faulting is also greater for the JRCP, except that the impact is less due to the greater joint spacing. Thus this specific JRCP design (which is a common design) does not perform as well as the JPCP.*

### Overall Evaluation of Pavement Type

Pavement type is not, strictly speaking, a design feature. Treating it as such obscures the importance of the different design elements that are unique to each pavement, such as long joints in JRCP or no joints in CRCP. In the earlier analyses and discussion of other design features, the concept of confounding, in which more than one variable is changed (making the determination of the effect of that one variable on pavement performance moot), is often raised. In this consideration of pavement type, confounding is the norm. Furthermore, many of these pavements include non-standard features, such as the hinge joints in the JRCP at IL 1 or the thicker JPCP slabs on grade at OH 2. This makes comparisons between pavement types problematic. Furthermore, as discussed earlier, the different concrete pavement types do perform differently. In order to make comparisons that remove from consideration these performance differences, for this analysis only the PSR and IRI are considered. However, there are a number of sections where the other performance data are important, such as is the case where the IRI may be low but faulting or cracking are excessively high and may be a portent of future problems.

Overall, the CRCP generally performed better than the other two pavement types at the sites when comparisons could be made, although the JPCP showed comparable performance. Overall, the JRCP sections appear to show worse performance when

compared to the other pavement types. To a certain extent, this also summarizes findings from the literature. But this does not mean that a CRCP is the best type of rigid pavement to construct. Each of these pavement types has different costs and different lives. The best pavement type is the one with the lowest life-cycle costs, taking into account initial construction costs, service life, and maintenance and rehabilitation costs. All of these are not yet known for these sections, so definitive conclusions may not be made. There are also problems with many of these sections that were built, such as insufficient reinforcement, lack of subdrainage, or excessive joint spacing, that adversely affected performance. A better comparison could be made between the "best" design of each of these types.

What would be needed to make a definitive comparison? Additional perspective on the problem of pavement type can be gleaned by considering the evolution of these three different types of rigid pavements. The earliest concrete pavements were nonreinforced slabs, essentially without joints. The intermediate cracking and subsequent breakup that inevitably developed led to two trends: the construction of shorter slabs and the introduction of wire reinforcement in longer slabs to keep the cracks together. Many studies were undertaken to determine the best joint spacing for nonreinforced JPCP and the required amount of reinforcement for JRCP. As the effects of slab length on the movement at cracks and joints became understood, CRCP was introduced and studies of the appropriate amount of reinforcement of these pavements were undertaken.

The pavements studied in this research do not, unfortunately, provide as sound a basis for considering pavement type. Many of the pavements are not representative of "good" design practices. In order to draw legitimate and valid conclusions about the relative performance of pavement types, those pavements that are constructed for head to head performance comparisons must reflect sound design (and construction) practices.

Although it is difficult to draw conclusions about the effect of pavement type, the information assembled in this study can be used to assist an agency in the pavement type selection process. The process is started by developing an acceptable design for each rigid pavement type. Guidance on joint spacing, slab thickness, percent reinforcement, drainage, and so on would be used to develop designs that could reasonably be expected to perform well. For a fixed number of ESAL's, performance models may then be used to project to a PSR or IRI that reflects the time at which that pavement would require rehabilitation (that level would be based on the type of facility, such as urban, rural, and so on). Depending upon the analysis period, rehabilitation(s) would be added at the age/ESAL's dictated by the performance models. In order to complete this analysis, performance of the different types would be carried out until costs for the entire analysis period were estimated. Life-cycle costs could then be computed, based on the initial costs, assumptions made about maintenance, and the costs of the required rehabilitations (plus salvage value if used by the agency).

The expected result of this analysis is that there would not be one best pavement type. The models will undoubtedly have different pavements carrying different levels of ESAL's before reaching the same level of deterioration. Costs will also vary, from pavement type to pavement type and from region to region. Maintenance costs will vary as well, although if high quality PCC of any of these types is constructed, maintenance costs should be extremely low.

## 4. EXAMINATION OF BACKCALCULATION RESULTS

### Introduction

Most of the concrete pavement sections included in this study were subjected to deflection testing using the Falling Weight Deflectometer. This testing was conducted in both 1987 and 1992 for the purposes of characterizing the elastic modulus ( $E$ ) of the concrete slab, the modulus of subgrade reaction ( $k$ ), and the transverse load transfer efficiency (LTE) of each section. The procedures for the determination of these values from deflection data are described in volume I and, for both the 1987 and 1992 backcalculation analyses, were founded upon AREA-based concepts.

Although the AREA-based methodology employed in the original backcalculation effort is theoretically sound and has enjoyed widespread use, there is sufficient variation in the results that an additional evaluation appeared warranted. In addition, further evaluation of the data was needed to account for the effects of bonding conditions between the slab and base.

To verify the results of the backcalculation effort, a new interpretation scheme was used. This procedure is based on a theoretically rigorous approach utilizing the closed form solution for the plate on a Winkler foundation (as proposed by Korenev) and effective plate concepts (as presented by Ioannides, et. al., and by Ioannides and Khazanovich).<sup>(70,71,72)</sup>

The backcalculation method finds a pavement system elastic parameters that provide the least discrepancy between the calculated and measured deflection basins. The new methodology also permits the evaluation of two layer systems, and this evaluation methodology is also discussed in this chapter. This ability is particularly valuable because the bonding condition between the slab and base can have a significant effect on the backcalculation results (as well as on the performance of the pavement). The procedure allows for the identification of bonded and nonbonded structures, which results in a more accurate representation of the pavement structure.

This chapter describes the methodology of that new backcalculation procedure and the steps taken to verify and further refine the backcalculation results. The chapter begins with a presentation of the theoretical background of the new procedure, followed by a discussion of the validation results. Finally, the evaluation of bonding conditions between the slab and base are evaluated. This ability to distinguish between bonded and nonbonded systems gives rise to the "equivalent thickness" concept, which is also described in this chapter.

## Fundamental Concept

This section describes the theoretical basis for the new backcalculation procedure. First, the analytical solution for the interior loading of the single layer plate resting on the Winkler foundation is presented. This solution was developed by Russian researcher Korenev in 1954, but was relatively unknown in the West. Although the alternative solutions obtained by Losberg and Ioannides often produce similar results, the presented solution is more simple, more general, and better suited for the development of an efficient backcalculation algorithm.<sup>(73,74)</sup> The new backcalculation procedure for a single layer plate, which utilizes this solution, will also be presented. Finally, this procedure will be generalized for the case of a two-layered plate.

### Interior Loading of the Slab-on-Grade

Consider a plate consisting of a linear elastic, homogeneous and isotropic material, resting on a dense liquid foundation. Under a load distributed uniformly over a circular area of radius,  $a$ , the distribution of deflections,  $w(s)$ , may be written as:<sup>(73)</sup>

$$w(r) = \frac{p}{k} [1 - C_1(a_l) \text{ber } s - C_2(a_l) \text{bei } s] \quad \text{for } 0 < r \leq a \quad (3)$$

$$w(r) = \frac{p}{k} [C_3(a_l) \text{ker } s + C_4(a_l) \text{kei } s] \quad \text{for } r \geq a \quad (4)$$

where:

- $a_l = (a/l)$   
= dimensionless radius of the applied load
- $r$  = radial distance measured from the center of the load
- $s = (r/l)$   
= normalized radial distance
- $l = (D/k)^{1/4}$   
= radius of relative stiffness of plate-subgrade system for the dense liquid foundation
- $D = Eh^3/12(1-\mu^2)$   
= flexural rigidity of the plate
- $E$  = plate elastic modulus
- $\mu$  = plate Poisson's ratio
- $h$  = plate thickness
- $k$  = modulus of subgrade reaction
- $p$  = applied load intensity (pressure) =  $P/(\pi a^2)$
- $P$  = total applied load

Note that ber, bei, ker, kei are Kelvin Bessel functions, which may be evaluated using appropriate series expressions available in the literature.<sup>(75)</sup>

A method for determining the constants  $C_1$  through  $C_4$  have been proposed by Ioannides.<sup>(74)</sup> However, that method is tedious and is valid only for relatively small radius of the applied load. A more general and simple solution has been proposed by Korenev, who suggests that these constants have the following form for any value of the radius of the applied load:<sup>(70)</sup>

$$C_1 = - a_l \ker' a_l \quad (5)$$

$$C_2 = a_l \text{kei}' a_l \quad (6)$$

$$C_3 = - a_l \text{ber}' a_l \quad (7)$$

$$C_4 = - a_l \text{bei}' a_l \quad (8)$$

Analysis of equations 3 to 8 shows that for a given magnitude and radius of the applied load and for a given distance from the center of the applied load, the deflection is a function of the radius of relative stiffness,  $\ell$ , and modulus of subgrade reaction,  $k$ . In order to determine them, measurements at least two locations should be available.

In the conventional U.S. practice, four or seven sensors are usually employed. It is desirable to use in backcalculation all information available to reduce the effect of measurement errors and to obtain the most reliable solution. Hoffman and Thompson proposed to use the area of the deflection basin for interpreting measured deflection profile.<sup>(76)</sup> They introduced a parameter AREA, which combines the effect of several measured deflections in the basin and may be defined as follows:

$$AREA = \frac{1}{2W_0} \left[ W_0 r_1 + \left( \sum_{i=1}^{n-1} W_i (r_{i+1} - r_i) \right) + W_n (r_n - r_{n-1}) \right] \quad (9)$$

where:

- $W_i$  = measured deflections ( $i = 0, n$ ).
- $n$  = number of sensors used minus one.
- $r_i$  = distances between the center of the plate and sensors.

Ioannides identified the unique relationship between AREA and radius of relative stiffness.<sup>(74)</sup> Hall obtained a simple approximation for this relationship for different sensors configurations.<sup>(77)</sup> The relationship for a conventional spacing configuration (0, 12, 24, 36 in [0, 305, 610, and 914 mm]) is as follows:

$$\ell = \left[ \frac{\ln \left( \frac{36 - AREA_4}{1812.279133} \right)}{-2.559340} \right]^{4.387009} \quad (10)$$

Similarly, the following relationship was developed for SHRP spacing configuration (0, 8, 12, 18, 24, 36, 60 in [0, 203, 305, 457, 610, 914, and 1524 mm]):

$$\ell = \left[ \frac{\ln \left( \frac{60 - AREA_{SHRP}}{289.708} \right)}{-0.698} \right]^{2.566} \quad (11)$$

The advantage of the AREA approach is that it leads to a simple backcalculation procedure that utilizes all measured deflections. This, however, does not necessarily mean that the AREA-based procedure provides the best possible interpretation of the deflection measurements. A more rigorous alternative approach has been developed and is presented below.

### The "Best Fit" Backcalculation Procedure

The objective of the backcalculation procedure for concrete pavements is to find a set of modulus of elasticity of concrete and modulus of subgrade reaction whose calculated deflection profile closely matches the measured profile. The problem can be formulated as minimization of the error function,  $F$ , defined as follows:

$$F(E, k) = \sum_{i=0}^n \alpha_i (w(r_i) - W_i)^2 \quad (12)$$

where  $\alpha_i$  represents the weighing factors. The weighing factors might be set equal to 1, or  $(1/W_i)^2$ , or any other numbers.



Analysis of equations 3 and 4 shows that the deflections at the sensor locations can be rewritten in the following form:

$$w(r_i) = \frac{1}{k} f_i(\ell) \quad (13)$$

where:

$$f_0(\ell) = \frac{p}{k} [1 - C_1(a_1)] \quad \text{for } i = 0 \quad (14)$$

$$f_i(\ell) = \frac{p}{k} [C_3(a_i) \ker s_i + C_4(a_i) \kei s_i] \quad \text{for } i = 1, \dots, n \quad (15)$$

$$s_i = \frac{r_i}{\ell} \quad (16)$$

It is assumed that the first sensor is located at the center of the load, and the rest sensors are placed beyond the area of load application.

The function F can be presented in the following form:

$$F(E, k) \equiv F(\ell, k) = \sum_{i=0}^n \alpha_i \left( \frac{p}{k} f_i(\ell) - W_i \right)^2 \quad (17)$$

To provide the minimum of the function F, the following conditions should be satisfied:

$$\frac{\partial F}{\partial k} = 0 \quad (18)$$

$$\frac{\partial F}{\partial \ell} = 0 \quad (19)$$

Substitution of equation 17 into equation 18 leads to the following equation for the modulus of subgrade reaction:

$$k = p \frac{\sum_{i=0}^n \alpha_i (f_i(\ell))^2}{\sum_{i=0}^n \alpha_i W_i f_i(\ell)} \quad (20)$$

Substitution of equation 17 into equation 19 and accounting for equation 20 leads to the following equation for the radius of relative stiffness:

$$\frac{\sum_{i=0}^n \alpha_i f_i(\ell) f_{i'}(\ell)}{\sum_{i=0}^n \alpha_i (f_i(\ell))^2} = \frac{\sum_{i=0}^n \alpha_i W_i f_{i'}(\ell)}{\sum_{i=0}^n \alpha_i W_i f_i(\ell)} \quad (21)$$

The solution of equation 21 does not causes any difficulties, as a short computer program has been coded. The execution time per backcalculation on a PC is trivial (a fraction of a second).

With the development of equations 20 and 21, the following procedure can be proposed for backcalculating the pavement parameters:

1. Assign weighting factors. In this study they were set equal to 1.
2. Determine the radius of relative stiffness that satisfies equation 21.
3. Using equation 20 determine the modulus of subgrade reaction.
4. With  $\ell$  and  $k$  known, determine modulus of elasticity of the slab:

$$E = \frac{12 (1 - \mu^2) \ell^4 k}{h^3} \quad (22)$$

### Justification of Using the New Approach

In this study, the following requirements were formulated for the backcalculation procedure:

- The procedure should be reliable. This means that the procedure should produce reasonable results for each project to be considered.
- The procedure should be efficient. The large amount of data to be analyzed and limited time called for selection of a computational efficient procedure.

- For this study it was important that the procedure be capable of handling data from both 1987 and 1992. The FWD testing performed in 1987 and 1992 had a different number of sensors and sensor configurations. In 1987 an equal spacing configuration with six sensors located at (0, 12, 24, 36, 48, 60 in [0, 305, 610, 914, 1219, and 1524 mm]) from the center of the applied load was used. In 1992 the SHRP spacing configuration (0, 8, 12, 18, 24, 36, 60 in [0, 203, 305, 457, 610, 914, and 1524 mm]) from the center of applied load was used.

A sensor configuration may significantly affect the results of backcalculation. Hall reported that the modulus of elasticity of concrete backcalculated using the SHRP sensor configuration may be up to 34 percent higher than that backcalculated from the standard sensor configuration.<sup>(77)</sup> Therefore, it is preferable to use the same sensor configuration for every project in backcalculation.

The "best fit" procedure, which uses sensors located at 0, 12, 24 and 36 in (0, 305, 610, and 914 mm), was found to satisfy all these requirements. The 1992 data set was used to compare this procedure with the AREA-based procedure developed by Hall for the SHRP sensor configuration.<sup>(77)</sup> The results of this comparison are presented in figure 59. One can observe that although the "best fit" backcalculation procedure uses fewer sensors, it produces results similar with AREA-based procedure the employs 7 sensors. It proves the robustness of the proposed algorithms. On the other hand, since this procedure can be applied for both data sets, it make it preferable to the 7 sensor AREA-based procedure and it has been used in this study.

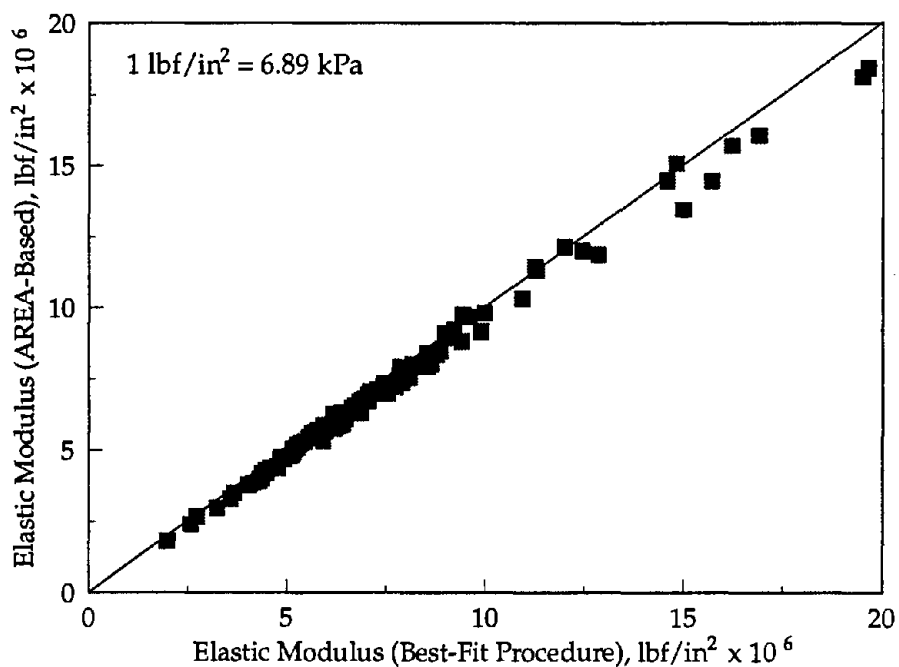


Figure 59. Comparison between the "best fit" and AREA-based backcalculation procedures.

## Backcalculation Procedure for Two-Layered Slab

Concrete pavements are generally analyzed as slab-on-grade structures, with no structural contributions given to the underlying base or subbase layers. However, it is known that these underlying layers can have a significant effect on the structural performance of the pavement, particularly if bonding between the slab and base occurs. If such bonding develops, the effective pavement structure is now greater and the manner in which the pavement reacts to loading is altered. Because multi-layered concrete pavements are quite common, the ability to evaluate these structures as multi-layered systems is quite valuable to both new and rehabilitation design activities.

The approach for the backcalculation of two-layered slab-on-grade is given below, based on methodology proposed by Ioannides and Khazanovich.<sup>(72)</sup> The two constructed layers may be bonded or unbonded, and are assumed to act as plates. Thus, no through-the-thickness compression is assumed. The backcalculation procedure described below represents an adaptation of the forward calculation approach for such pavement systems, which was presented by Ioannides, et al.<sup>(71)</sup> The resulting scheme was combined in a computer program with the "best fit" procedure described above.

### Unbonded Case

In accordance with the derivations presented by Ioannides, et al., two distinct cases may be recognized, depending on the interface condition between the two constructed layers.<sup>(71)</sup> The case of two unbonded plates is considered first. Such plates will act independently, although their respective deflected shapes will of necessity remain identical, if there is to be no separation between them. Under these conditions, it has been shown that:<sup>(71)</sup>

$$D_e = D_1 + D_2 \quad (23)$$

where:

- $D_1$  = the flexural stiffness of the upper plates
- $D_2$  = the flexural stiffness of the lower plate
- $D_e$  = the corresponding stiffness of a fictitious "effective," composite, homogeneous plate, which deforms in an identical manner to the actual two-plate system.

In one sense, slab-on-grade backcalculation schemes may be thought of as producing an estimate of  $D_e$  when applied to a three-layer PCC pavement system. The apparent task that remains, therefore, is to subdivide  $D_e$  into its component parts,

namely  $D_1$  and  $D_2$ . This cannot be accomplished merely by reference to the field measurements of the deflection profile, but an additional input parameter is needed. This requirement is akin to the need to provide seed moduli for conventional multi-layered AC pavement system backcalculation. In this case, it is convenient to introduce the modular ratio,  $\beta$ , of the two plates as the additional input parameter. Furthermore, it may be assumed with no loss of generality that the thickness of the "effective" plate,  $h_e$ , is equal to the thickness of the upper plate,  $h_1$ . As a result, the backcalculated E-value from a slab-on-grade analysis is  $E_e$ , such that:

$$\frac{E_e h_e^3}{12 (1-\mu_e^2)} = D_e \quad (24)$$

It is convenient at this point to introduce the additional assumption that:

$$\mu_1 = \mu_2 = \mu_e \quad (25)$$

Thus, it follows that:

$$E_e h_e^3 = E_e h_1^3 = E_1 h_1^3 + E_2 h_2^3 \quad (26)$$

where:

- $E_1$  = modulus of upper plate
- $E_2$  = modulus of lower plate
- $h_2$  = thickness of lower plate

Therefore,

$$E_1 = \frac{h_1^3}{h_1^3 + \beta h_2^3} E_e \quad (27)$$

and

$$E_2 = \frac{\beta h_1^3}{h_1^3 + \beta h_2^3} E_e \quad (28)$$

where:

$$\beta = \frac{E_2}{E_1} \quad (29)$$

Given values for  $\beta$  and for the real plate thicknesses  $h_1$  and  $h_2$ , Equations 27 and 28 may be used with the  $E_e$ -value backcalculated from slab-on-grade analysis (assuming  $h_e=h_1$ ), to yield  $E_1$  and  $E_2$  for the two plates.

### Bonded Case

For the case of two bonded plates, the flexural stiffness of the fictitious "effective," homogeneous, composite plate is no longer a linear sum of the two actual plate stiffness, but may be derived using the parallel axes theorem.<sup>(71)</sup> Thus:

$$\frac{E_e h_e^3}{12} = \frac{E_1 h_1^3}{12} + E_1 h_1 \left( x - \frac{h_1}{2} \right)^2 + \frac{E_2 h_2^3}{12} + E_2 h_2 \left( h_1 - x + \frac{h_2}{2} \right)^2 \quad (30)$$

where:

$$x = \frac{\frac{h_1^2}{2} + \beta h_2 \left( h_1 + \frac{h_2}{2} \right)}{h_1 + \beta h_2} \quad (31)$$

Proceeding as for the unbonded plates, it may be assumed that  $h_e=h$ , which makes the backcalculated E-value from slab-on-grade analysis to be  $E_e$ . Therefore:

$$E_1 = \frac{h_1^3}{h_1^3 + \beta h_2^3 + 12 h_1 \left(x - \frac{h_1}{2}\right)^2 + 12 \beta h_2 \left(h_1 - x + \frac{h_2}{2}\right)^2} E_e \quad (32)$$

$$E_2 = \frac{\beta h_1^3}{h_1^3 + \beta h_2^3 + 12 h_1 \left(x - \frac{h_1}{2}\right)^2 + 12 \beta h_2 \left(h_1 - x + \frac{h_2}{2}\right)^2} E_e \quad (33)$$

Equations 36 and 37 for the bonded plates correspond to equations 31 and 32 for the unbonded plates, and may be used in a manner analogous to the latter in backcalculating  $E_1$  and  $E_2$  for the two plates.

#### Effect of the Moduli Ratio

The backcalculation procedure presented above requires the modular ratio as an input parameter. This ratio should be assigned based on engineering judgment. It is assumed that if the ratio is assigned within the reasonable limits the results of backcalculation are insensitive to the ratio.

To verify this assumption, two sets of the ratios between the moduli of elasticity of base materials and PCC were assigned. Table 138 presents the modular ratios for each type of a base layer. The 1992 deflection data were used for backcalculation. Figures 60 and 61 present comparison of backcalculated moduli of PCC slab using two data sets for unbonded and bonded interface conditions, respectively. One can observe that an influence of the moduli ratio is not significant in the vast majority of the projects. The set A was selected for further investigation.

#### Data Screening

Using 1987 and 1992 data sets, the moduli of elasticity of PCC slab and base and modulus of subgrade reaction were backcalculated for every station and for every load level. Using these results, the representative values of these parameters were determined for each section using both bonded and unbonded assumptions for the interface condition. For some sections, a large scatter of backcalculated parameters resulted, which cannot be explained solely by variation in material properties. The scatter can be referred to the variation in the pavement conditions (presence or absence of cracks), pavement layer thicknesses, interface conditions, and so on. To determine the most representative values for the elastic parameters, the following data screening procedure was applied for each section:

Table 138. Two sets of the moduli ratios,  $E_{pcc}/E_{base}$

Base Type	Set A	Set B
Cement Treated	4.5	5.0
Lean Concrete	2.25	2.0
Lean Concrete A	1.5	2.0
Lean Concrete B	1.75	3.0
Lean Concrete C	2.5	3.0
Permeable Cement Treated	5.6	10
Permeable Asphalt Treated	15	20
Asphalt Treated	10	15
Aggregate	150	100
Permeable Aggregate	225	200
Soil Cement	35	40
Sand Gravel	200	200

- Step 1. Using the backcalculation results for all stations and load levels, the mean values and standard deviations of the elastic parameters were calculated.
- Step 2. The backcalculation results from each individual measurement were compared with the mean values. If at least one parameter was greater than two standard deviations away from the mean value, the results from that measurement were dropped.
- Step 3. If at least one measurement was dropped in step 2, new mean values and standard deviations of the elastic parameters were calculated and step 2 repeated; otherwise the mean values were accepted as the final results for the section.



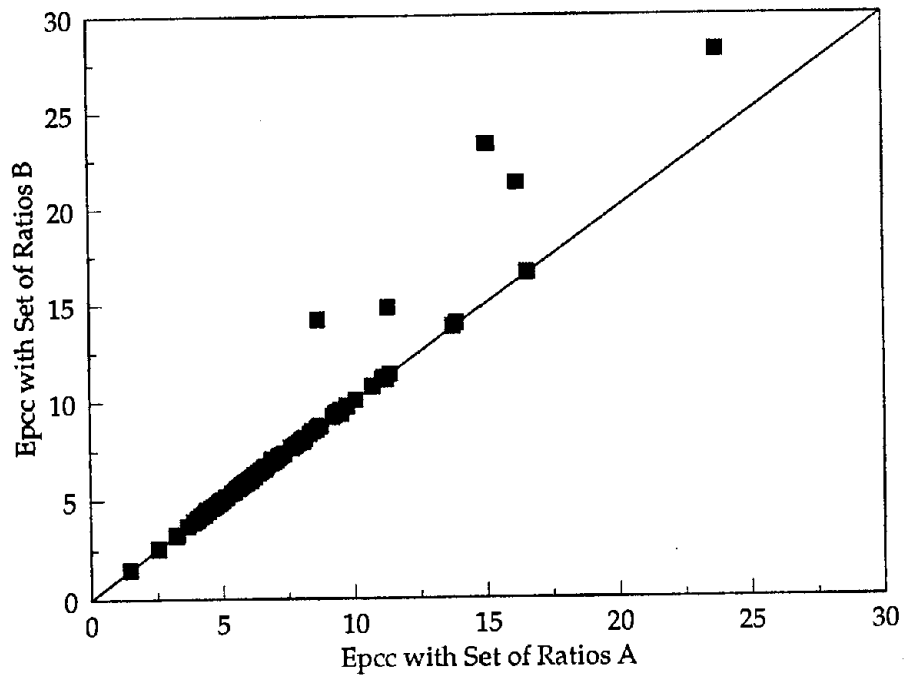


Figure 60. Comparison of backcalculated PCC moduli for two sets of modular ratio. Unbonded interface between PCC plate and base.

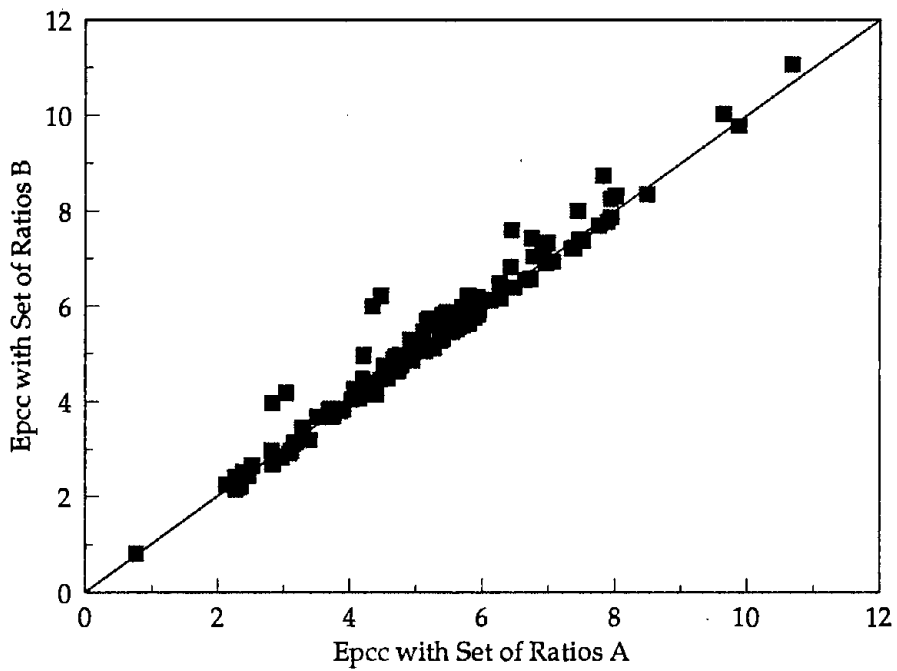


Figure 61. Comparison of backcalculated PCC moduli for two sets of modular ratio. Bonded interface between PCC plate and base.

Figure 62 shows the percentage of sections as a function of the percentage of kept data. One can observe that only three sections exhibit a large percentage of data that were dropped. These section are:

- AZ 1-7: 41.7 percent of data were kept.
- CA 11: 50 percent of data were kept.
- MN 7-16: 50 percent of data were kept.

The results of backcalculated moduli of elasticity of concrete and modulus of subgrade reaction for these sections are presented in table 139. This table presents backcalculated values before and after data screening. One can observe that data screening significantly reduces variability in data and leads to more realistic and representative mean values.

Figures 63 and 64 compare the mean values of backcalculated  $E_{pcc}$  and  $k$ , respectively, for the 1992 data set obtained before and after screening. One can observe that for most cases these values are very close. Just for few cases is the difference significant, and in those cases the corrected values are more realistic.

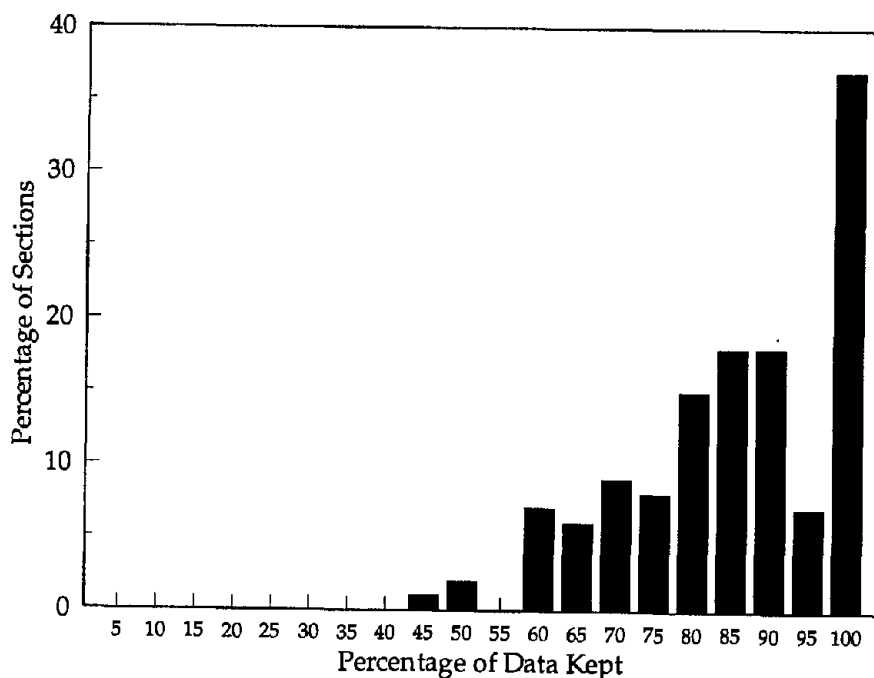


Figure 62. Percentage of sections versus percentage of data kept.

Table 139. Results of backcalculation for sections with a high percentage of dropped data.

Section	Statistical Parameter	Uncorr. $E_{pcc}$ , Million lb/in <sup>2</sup>	Uncorr. $k$ , lb/in <sup>2</sup> /in	$E_{pcc}$ , Million lb/in <sup>2</sup>	$k$ , lb/in <sup>2</sup> /in
AZ1-7	mean	5.75	410	6.20	443
	max	9.42	762	6.60	532
	min	2.39	170	5.88	332
	std. dev	1.75	160	0.21	69
	coef. var	0.304	0.391	0.034	0.155
CA-11	mean	3.04	0.391	3.09	250
	max	6.12	192	3.64	287
	min	0.18	287	2.53	215
	std. dev	1.66	87	0.33	21.2
	coef. var	0.552	0.453	0.107	0.085
MN7-16	mean	5.39	75.7	4.42	63.2
	max	8.72	42.4	5.33	58.5
	min	3.57	126.7	3.61	67.0
	std. dev	1.38	24.3	0.63	3.1
	coef. var	0.255	0.320	0.142	0.048

### Determination of In-Place Material Properties

This section illustrates the application of the procedures described above to the deflection data collected under this study. Using those procedures, an approach is presented that accounts for the boundary conditions between the slab and base. The structural contributions of all layers above the subgrade are expressed in terms of an effective thickness.

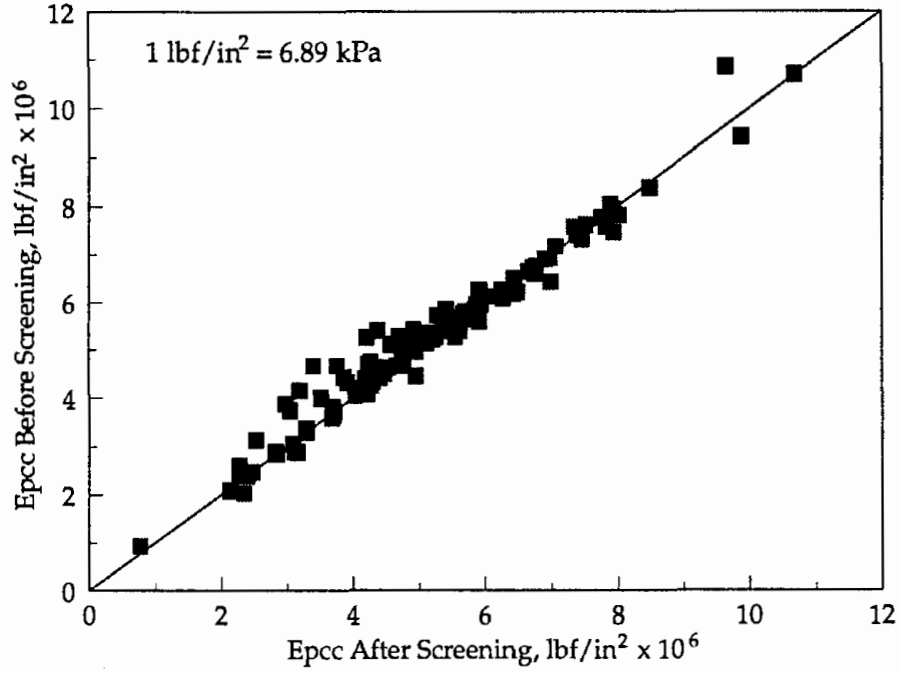


Figure 63. Comparison between backcalculated  $E_{pcc}$  before and after screening.

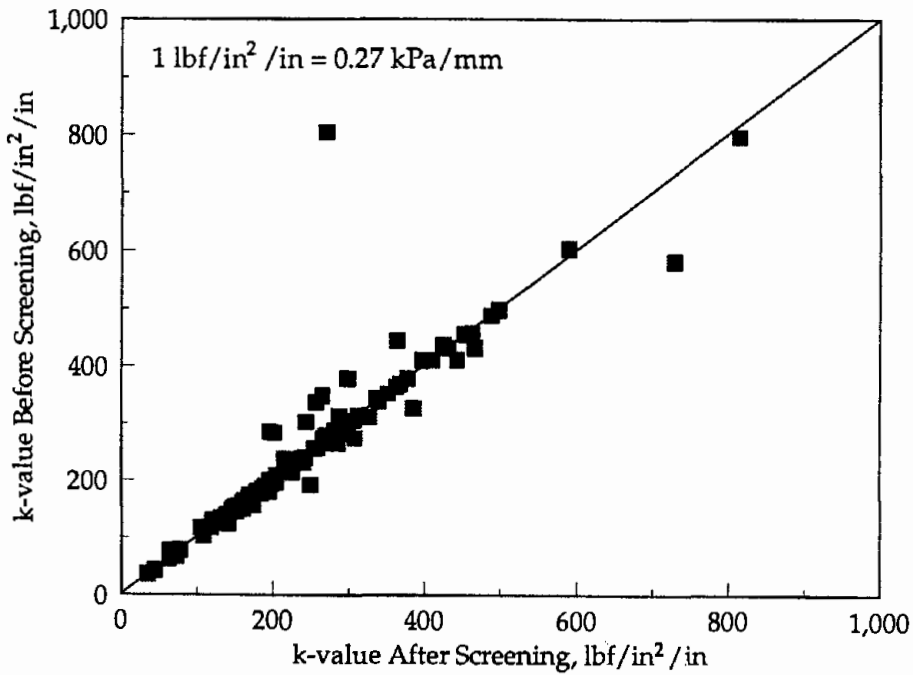


Figure 64. Comparison between backcalculated  $k$  before and after screening.

## Treatment of Variabilities

Variabilities exist in all materials, and dealing with those variabilities is a normal part of any design or evaluation process. In determining the in-place material properties by backcalculation, the major difficulty is distinguishing the actual material variability from the apparent variability arising from the errors introduced in the calculation. The source of these errors is the deviations in the actual pavement structure at the FWD testing points from the model used in the backcalculation.

Because slab thickness and the interface condition between the pavement layers (for stabilized base sections) have such a strong influence on pavement deflection, even small variations in these features can dramatically affect backcalculation results. These variations in the pavement structure, however, are usually ignored in performing backcalculation. The apparent variabilities resulting from these calculation errors can completely overshadow the actual material variability and give erroneous results.

### *Effects of Backcalculation Errors on Performance Evaluation*

Any errors introduced during the determination of the in-place material properties become amplified when the backcalculated material properties are used in the analysis. The difficulties in obtaining accurate values of PCC modulus of elasticity,  $E$ , by backcalculation and the importance of minimizing the errors associated with  $E$  are best explained by examining how  $E$  is determined.

The pavement parameters that can be directly obtained from backcalculation are the modulus of subgrade reaction,  $k$ , and the radius of relative stiffness,  $\ell$ . For the analysis purposes, the material properties of interest are  $k$  and  $E$ . The  $k$  is obtained directly from backcalculation; therefore, the only variability associated with the backcalculated  $k$  is the normal material variability, and no special consideration is required to address the variabilities in  $k$ . The PCC modulus, however, has to be determined using a theoretical relationship from  $\ell$  (equation 22). The equation for  $\ell$  is given below:

$$\ell = \left( \frac{Eh^3}{12 (1 - \mu^2) k} \right)^{\frac{1}{4}} \quad (34)$$

It is important to note that backcalculation results do not provide any information regarding how  $\ell$  should be resolved into its components.

From equation 22 it can be seen that the backcalculated  $E$  is very sensitive to the slab thickness,  $h$ , since  $\ell$  is a function of  $h^3$ , and that the calculated  $E$  may be excessively high or low, depending on whether the thickness used in the calculation is less or greater than the actual slab thickness at the testing point. If accurate values of slab thickness at the FWD testing points are available,  $E$  can be determined accurately from  $\ell$ ; however, this much information is usually not available.

When the backcalculated  $E$  is used in the forward analysis, any errors introduced in determining  $E$  are amplified. A low estimate of the in-place slab thickness results in excessively high estimate of  $E$ . In forward calculation, both the high  $E$  and the low  $h$  leads to excessively high calculated stress. On the other hand, if the assumed slab thickness is too high, the calculated  $E$  will be excessively low, and both the high  $h$  and low  $E$  contribute to produce unconservatively low calculated stress. Hence, the efforts to minimize backcalculation errors are important to the accurate evaluation of in-place pavement performance.

#### *Handling of the Pavement Structure Variability*

In this project, efforts were made to isolate and remove the apparent variability in backcalculated PCC modulus of elasticity,  $E$ , taking into consideration the typical variabilities associated with slab thickness and concrete modulus of elasticity. The actual variability of  $E$  in any given project is much less than the large variabilities typically reported on backcalculation results.

The typical coefficient of variation for compressive strength of concrete is 10 to 15 percent.<sup>(78)</sup> Since the empirical relationship for  $E$  is a function of the square root of compressive strength, the coefficient of variation for  $E$  may be expected to be less than 4 percent. The typical variability in slab thickness is 0.5 in (13 mm) and that of aggregate bases range from 0.75 to 1.5 in (19 to 38 mm). The penetration of the PCC material into the base (particularly on permeable bases) can also lead to greater variability of the effective thickness of the PCC slabs. The composite action between the slab and the base (stabilized bases) also gives greater effective thickness of the pavement structure. The failure to consider these variabilities in pavement structure will lead to large apparent variabilities in backcalculated  $E$ .

One way to account for the variabilities in pavement structure is to use the backcalculation results to determine the effective slab thickness using an estimated  $E$ , rather than using a fixed value of  $h$  and determine  $E$ . Similar approach was proposed by Uzan, Briggs, and Scullion.<sup>(79)</sup> Given that the typical variability of  $E$  is small and that a minor variation in pavement structure can have significant effect on backcalculated  $E$ , more accurate results can be obtained by treating the effective slab thickness as the unknown rather than  $E$ . Equation 22 can be rearranged as follows to obtain  $h$  from  $\ell$ :

$$h_e = \left( \frac{12 (1 - \mu^2) \ell^4 k}{E} \right)^{\frac{1}{3}} \quad (35)$$

where  $h_e$  is the effective pavement thickness in inches. Since  $\ell$  is the actual measured value, the effective slab thickness,  $h_e$ , obtained using equation 35 accounts for the structural contribution of both the PCC slab, the base, and any interaction between the two layers. The  $h_e$  represents the thickness of a single PCC layer (bonded) that is structurally equivalent to the capacity of all pavement layers above the subgrade.

For this project, the PCC modulus was estimated from the results of normal backcalculation, using either the design thickness or the core thickness (when available) and equation 22. First, the PCC modulus for each section was determined normally. Then, based on the assumption that the E is fairly uniform for any given project, the average project E was determined, discarding any values that are outside of reasonable range. The project average E was then used to determine  $h_e$  as described above.

The procedure used in this project for determining the project average E is adequate, but more accurate results could be obtained using core testing results. Although the dependence on core testing means that some destructive testing is involved, given the relative ease with which the cores can be retrieved and tested, the additional information provided by the core testing is well worth the effort to improve the accuracy of the evaluation. The cores can provide not only the strength and modulus information, but also the layer thicknesses and bond condition.

In the following discussion, the procedure used to determine the project average E and the effective slab thickness are described in more detail.

### Project Average PCC Modulus

In an attempt to minimize the errors associated with backcalculation, the project average, rather than the section average, PCC moduli were used in this project. The rationale for the use of the project average E was discussed earlier. The use of the project average helps to minimize the calculation errors introduced in the backcalculation results that arise from the variabilities in the pavement structure.

The assumption that the principal source of large variability in the backcalculated E is the calculation errors and not the actual material variability is implicit in using the project average E. This is a reasonable assumption, given the sensitivity of the backcalculated E to the slab thickness used in the calculation and the low coefficient of variation of actual, measured concrete properties in any given project. Assuming that any large deviations in the backcalculated E (from the average) may be attributed to the calculation error, the average project E was determined after

dropping extreme E values.

In determining the project average E, the section E was first determined for all sections that were tested using the new backcalculation procedure described in this section. All sections having a base were analyzed as a two-layered system using the modular ratios given in table 138. The FWD data from the original RIPPER study were also reanalyzed using the new procedure.

The project average E was determined iteratively, dropping the E values that were considered outside the reasonable range after each iteration and recalculating the average. The following criteria were used to identify the E values that are outside the reasonable range:

- The E values greater than 8,000 kips/in<sup>2</sup> (55 GPa) were dropped.
- The E values that are not within one standard deviation of the interim project average were dropped.

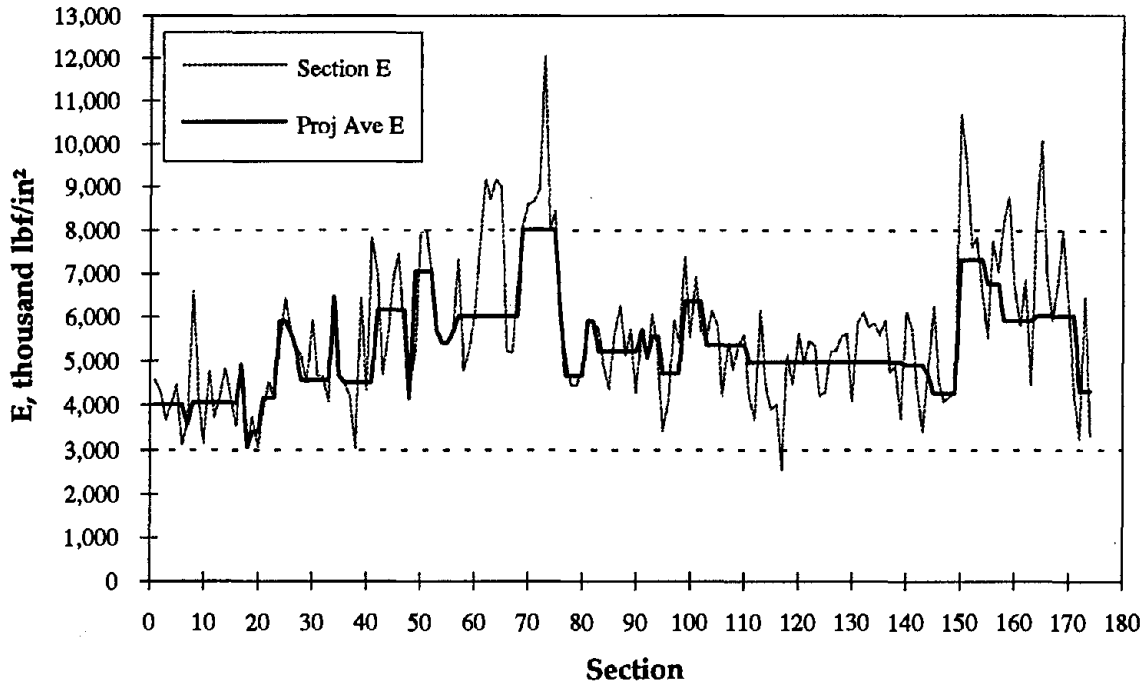
The project average E was recalculated after dropping the E values falling outside the reasonable range. This process was repeated until all E values were within the allowable range.

The backcalculation results for the PCC modulus values and the subgrade modulus of reaction are shown in figures 65 and 66. The horizontal axis on these figures are dummy values that simply indicate individual sections. As shown in figure 65, the project average E is representative of the average of the individual section E values. Also evident in this figure is the effects of imposing absolute maximum value of E (8,000 kips/in<sup>2</sup> [55 GPa]) and eliminating the values that deviate significantly from the project average.

The backcalculated k values are shown in figure 66. The k values for all sections were within a reasonable range (between 100 and 500 lb/in<sup>2</sup>/in [27 to 136 KPa/mm]) except in a few cases. The backcalculated k values were very high (well above 500 lb/in<sup>2</sup>/in [136 KPa/mm]) for few sections and very low (well below 100 lb/in<sup>2</sup>/in [27 KPa/mm]) for few sections. Very high k values were determined for CA 2-2, CA 10, WV 1-3, and PA 1-2. All these sections exhibiting high k values are in a deep cut area of a mountainous region. Similar results were obtained in 1987, and the reason for the very high k values is likely to be the close proximity to the bedrock of these deep-cut pavement sections. Most of the sections exhibiting a very low k values were sections provided with a gravel or sand/gravel base. Again, similar results were obtained in 1987.

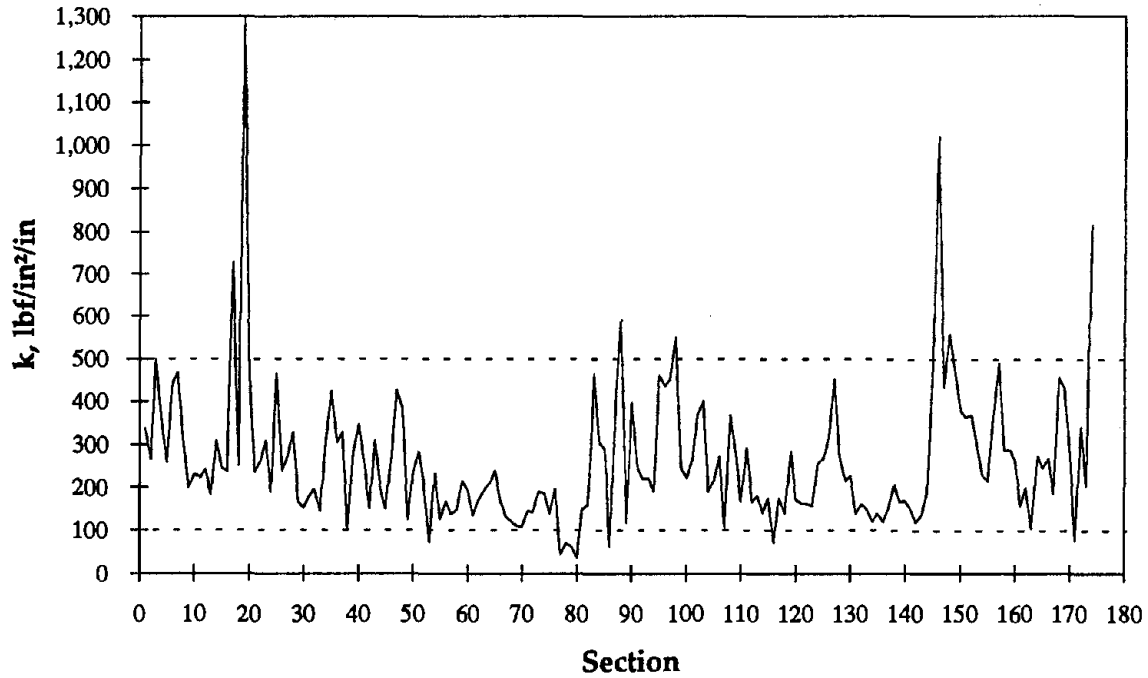
The comparison of k values determined in the original RIPPER study and the current study are shown in figure 67. In general, the k values determined using the new data and the new backcalculation procedure were slightly lower than the 1987 values, but the same trend in k values were obtained among different sections.





1 thousand lbf/in<sup>2</sup> = 6.89 MPa

Figure 65. Backcalculated project average PCC moduli values.



1 lbf/in<sup>2</sup>/in = 0.27 kPa/mm

Figure 66. Backcalculated subgrade modulus of reaction, k, values.

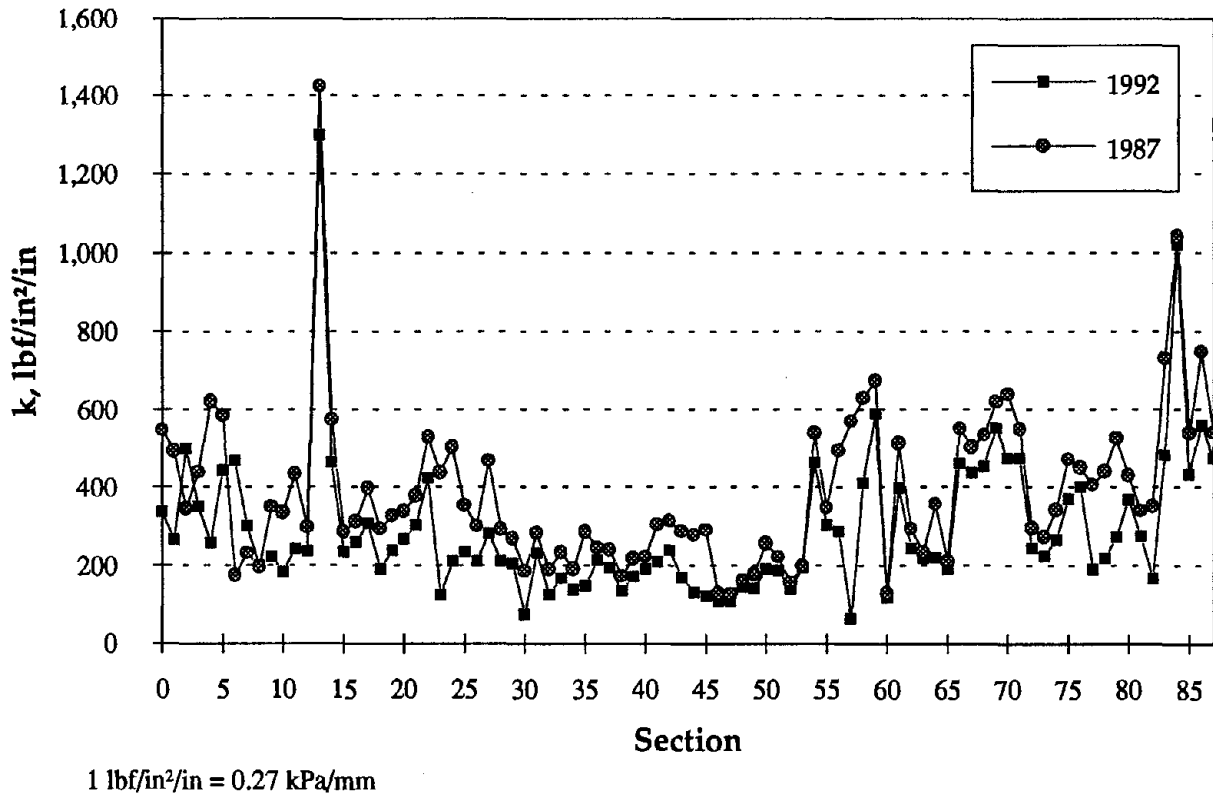


Figure 67. Comparison of k values determined in 1987 and 1992.

Effective Slab Thickness

The concept of effective slab thickness was used in this project to account for the variabilities in the pavement structure and the structural contribution of the stabilized bases. The effective slab thickness  $h_e$  is determined from the backcalculated  $l$  using equation 35 and the project average E values. The  $h_e$  is representative of the structural capacity of all pavement layers above the subgrade and the value determined using equation 35 accounts for the effects of different bond conditions between the pavement layers.

The theoretical value of  $h_e$ , assuming a fully bonded interface, is given by equation 30. This equation was used to determine the  $h_e$  for the sections that were not tested using FWD. The  $h_e$  determined for all stabilized pavement sections are shown in figure 68. This figure shows that there is a considerable variability in the effective slab thickness, and that the structural contribution of a stabilized base can be significant.

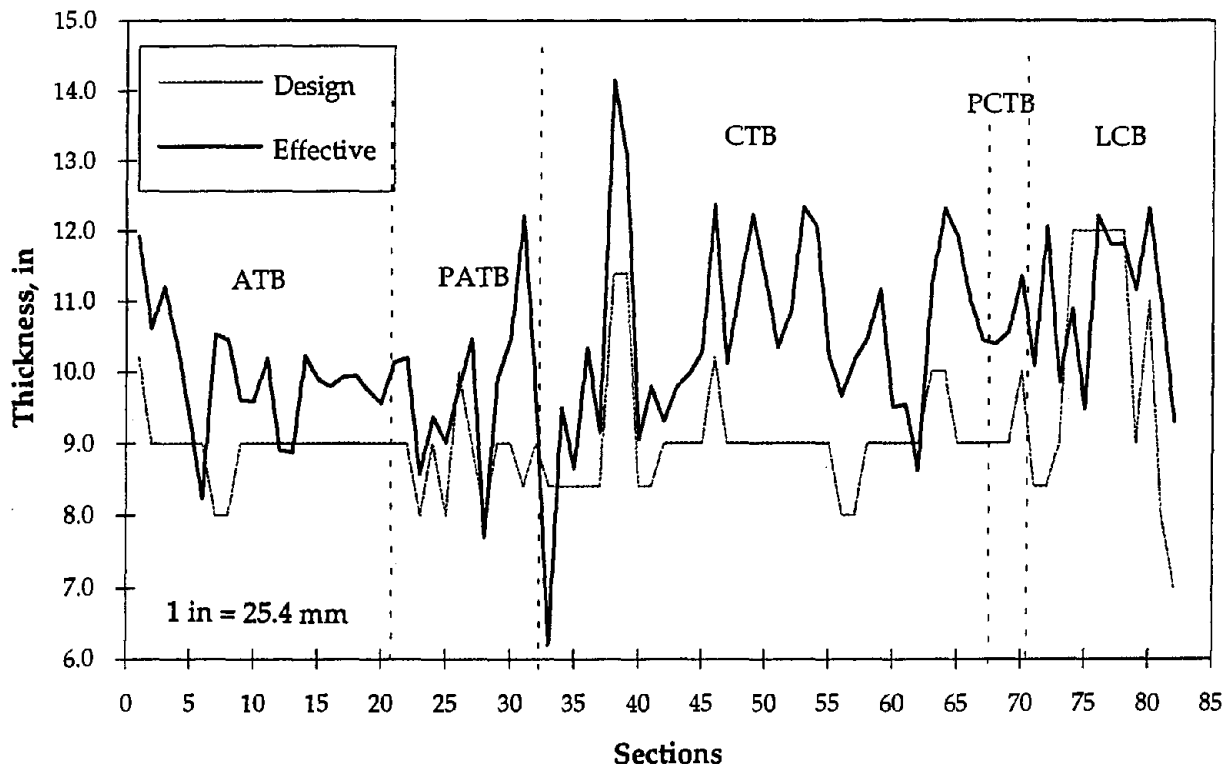


Figure 68. Effective slab thickness of stabilized base sections.

In the NCHRP report *Support Under Portland Cement Concrete Pavements*, the structural contribution of the base layer was modeled considering friction between the PCC slab and the base using a 3-D finite analysis program.<sup>(51)</sup> This model gives thicknesses that are somewhere between the slab-only and bonded thickness. The analysis of the cracking data showed that the level of interaction between the slab and the base can be highly variable, ranging from fully bonded to unbonded. The use of the interface friction gives greater flexibility in the ability to model the interaction between the two pavement layers, but further research is needed to apply this model to backcalculation procedures.

For the nonstabilized base sections, the design thickness was taken as the  $h_e$ . Although the variability typical of normal construction was observed in the variation of slab thicknesses in these sections, design thicknesses were used in the analysis because of lack of adequate data. While  $h_e$  for the nonstabilized base sections could be determined from the backcalculated  $l$  for those sections that were tested, no data are available for determining the  $h_e$  for the sections that were not tested. Since the thickness variations are random, the use of statistical methods to assign  $h_e$  for performance evaluations is not appropriate. Hence, design thicknesses were used on all nonstabilized base sections for consistency. Since the design thickness is representative of the average thickness and the project average  $E$  is a good estimate

of the in-place PCC modulus, the use of the design thickness in the forward calculation for nonstabilized base sections is expected to give reasonable results.

### Effects of Base Stiffness on Critical Stresses and Deflections

#### *Critical Stress*

The difference between the effective slab thickness,  $h_e$ , and the design slab thickness,  $h$ , represents the additional structural capacity provided by the base. On stabilized base sections,  $h_e$  is greater than  $h$ ; however, the critical stress location remains at the bottom of the PCC slab, because the PCC modulus is significantly greater than that of any base layer. The stress at the bottom of the PCC slab is given by the following equation:<sup>(71)</sup>

$$\sigma = \sigma_e \frac{2(h - x)}{h_e} \quad (36)$$

where:

- $\sigma$  = stress at the bottom of PCC slab.
- $\sigma_e$  = stress at the bottom of effective slab ( $h_e$ ).
- $h_e$  = effective slab thickness.
- $x$  = neutral axes location (equation 31).

#### *Critical Deflection*

The  $h_e$  discussed in this section are determined based on the FWD testing data obtained at the center locations, where strong interaction between the slab and the base are typically observed. At the slab corners, where the critical deflections occur, the bond between the pavement layers is usually not as strong as the center locations because of large movements. If the interaction between the base and the slab is not sufficient to provide bonded response, the structural contribution of the base layer is insignificant. Hence, for the determination of maximum deflections, only the actual slab thickness should be used.

## 5. SUMMARY OF EUROPEAN AND CHILEAN CONCRETE PAVEMENT PERFORMANCE

### Introduction

The investigation into the performance of concrete pavements conducted in the United States coincides with similar efforts conducted in other countries. Several European countries—France, Italy, the United Kingdom, Belgium, and Switzerland—have collectively conducted evaluations on 96 concrete pavements. More evaluations are expected in these countries, as well in Germany. Chile has also been involved in monitoring of concrete and asphalt pavements within their country.

The data from these sections are being analyzed as part of this study in hopes of providing additional information on the effect of different design variables on concrete pavement performance. Moreover, the effects of design variables that are not common in the United States, but are widely used in other countries, can be examined. The effect of higher legal axle loading in Europe can also be examined, as 44 of the 96 European sections (46 percent) have carried more than 20 million ESAL applications, compared to only 4 of 303 sections (1 percent) in the United States. An evaluation of these sections should prove most beneficial to this study.

### Evaluation of European Concrete Pavement Performance

Under the auspices of the Technical Committee on Concrete Roads of the Permanent International Association of Road Congresses (PIARC), several European countries have been monitoring the performance and behavior of their concrete pavements. The ultimate purpose of this monitoring is to obtain information on how well the concrete pavements perform so that continual improvements can be made to the design, construction, and maintenance of these pavements. PIARC's interest in monitoring the performance of highway pavements parallels a similar interest that has developed in the United States over the last 15 years.

This section provides a summary of the report, *An Evaluation of European Concrete Pavements*, which is provided in appendix B of volume IV. This section explains the objectives and scope of the European COPES program and provides an evaluation of the performance of concrete pavements for each country and for the European community as a whole. The effect of various design features on performance was investigated, and performance prediction models were developed for those countries with sufficient sections.

### Monitoring Program

The monitoring of European concrete pavements undertaken by PIARC was conducted in accordance with the COPES procedures. It included involvement with and cooperation from both FHWA and University of Illinois researchers. The

following sections describe the participation in this study and the content of the available data.

### *Participating Countries*

The countries involved in this cooperative study include France, Italy, the United Kingdom, Belgium, Switzerland, and Germany. Currently, however, only five countries—France, Italy, the United Kingdom, Belgium, and Switzerland—have contributed to the study. These countries have collectively contributed 96 sections to the study, distributed as shown in table 140.

Table 140. Distribution of sections by country and pavement type.

Country	JPCP	JRCP	CRCP	Total
France	28	1	0	29
Italy	4	2	0	6
United Kingdom	16	1	0	17
Belgium	14	0	11	25
Switzerland	2	17	0	19

These sections represent pavements with a range of design features, including widened lanes, trapezoidal cross sections, and nonerodible bases. Roughly one-half of the sections are more than 10 years old, and many are subjected to very heavy traffic loadings. The majority of the pavement sections are jointed plain concrete pavements (JPCP), although some jointed reinforced concrete pavement (JRCP) and continuously reinforced concrete pavement (CRCP) sections are included.

### *Data Collection*

The data collection activities followed the procedures in the original COPES report.<sup>(69)</sup> The data collected for each of the pavement sections may be broadly classified into the following categories:

- Section identification data (e.g., highway number, location, and length).
- Pavement design data (e.g., pavement type, slab thickness, and base type).
- Distress data (e.g., type and amount of pavement distresses).
- Roughness data (e.g., PSR and IRI).
- Patching data (e.g., type and amount of pavement patching).
- Environmental data (e.g., ambient temperatures and precipitation).
- Traffic data (e.g., traffic volumes, truck volumes, and axle weight data).

Data collection sheets similar to those presented in the original COPES report were used to collect this information.<sup>(69)</sup> The data were first collected by the participating countries using the International System of Units (SI) and European terminology. Once the data were prepared for entry into an electronic data base, the units were converted to English equivalencies and American terminology to be compatible with the COPES format.

### European COPES Analysis

The data collected under the European COPES program was submitted on magnetic media data files. In addition to those files, hard copies of the data entry sheets were available for roughly half of the sections. Summary tables documenting the design, construction, and performance of the European COPES concrete pavement sections were developed from the data contained in the magnetic media data files.

#### *Traffic Data*

One data item not included in the original European COPES summary tables is the estimated number of (18-kip) 80-kN ESAL applications that the pavement sections had sustained at the time of pavement survey. This factor is determined by expressing the damage done by every vehicle type in terms of the equivalent amount of damage done by a standard axle. The basis for the conversion of mixed traffic loads to the equivalent number of standard axle load applications is the load equivalency factors (LEF) developed from data collected at the AASHO Road Test.<sup>(80)</sup> Through the use of the LEF's, the average amount of damage inflicted on the pavement by each truck (expressed in 18-kip [80-kN] ESAL applications per truck) can be computed; this value is termed the truck factor (TF).

The basic equation for the computation of the number of ESAL applications on a given highway for *one* year is shown below:

$$ESAL = ADT \times TKS \times DD \times LD \times TF \times 365 \quad (37)$$

where:

- ESAL = Number of 18-kip (80-kN) ESAL applications per lane for 1 year.
- ADT = Initial two-way average daily traffic, vehicles per day.
- TKS = Percent of ADT that is heavy trucks (FHWA class 5 or greater).
- DD = Directional distribution of truck traffic (decimal, not percent).
- LD = Lane distribution of trucks in design lane (decimal, not percent).
- TF = Average truck factor for all trucks, ESAL's/truck.

The European COPES data base contained information on traffic volumes (ADT), truck volumes (percent trucks), and truck factors. Although this traffic information was not as complete as desired (for example, traffic data were not available for every year since construction), it served as the basis for the calculation of the cumulative ESAL applications. In doing so, several assumptions were made, such as assuming an average 4 percent growth rate in traffic volumes and truck factors (for years when no data were available). The ESAL estimates for many of the European COPES sections are much higher than those typically encountered in the United States, with values ranging from 1 to 106 million. This can be attributed to the higher axle loads present in many European countries.<sup>(63)</sup>

### *Climatic Information*

The climatic conditions can play a critical role in the performance of the concrete pavement sections. Because the sections are located in different countries and represent a range of climatic conditions, they must be considered in the evaluation. Two important indicators of climatic effects are the average annual precipitation and the freezing index (FI). Both of these parameters have been shown to influence concrete pavement performance.

The average annual precipitation provides an indication of the amount of free moisture to which the pavement is exposed. Although the amount of precipitation is not by itself an indicator of severe moisture conditions (one must also consider the relative evapotranspiration and the drainage characteristics of the pavement), it can be used to provide some insight into the prevailing moisture conditions.<sup>(61)</sup> Average annual precipitation values of greater than 15 in (380 mm) may be considered significant.

The freezing index indicates the amount of time throughout the year that the pavement is subjected to temperatures below freezing. It is the summation of the number of degrees that the average daily temperature is below freezing for each day throughout a year.<sup>(61)</sup> Values greater than 100 may be considered significant.

### *Modernity Elements*

In the initial evaluation of the European COPES data, Christory described the development of the modernity coefficient.<sup>(62)</sup> The modernity coefficient is a number from 0 to 4 that indicates the number of specific design features present in a pavement section that are expected to contribute to the overall performance of that pavement.<sup>(62)</sup> The design features that are expected to contribute to the performance of a pavement are classified in the following four categories:

- Nonerodible base course (specifically, lean concrete base).
- Positive pavement drainage.
- Strengthened structure (thickened slab, dowel bars, or CRCP).
- Optimization of the use of materials with respect to loading (widened traffic lanes and trapezoidal cross sections).



A pavement incorporating design elements from each of the above categories is assigned a modernity coefficient of 4. A pavement containing only dowel bars and positive drainage is assigned a modernity coefficient of 2.

The number of modernity elements in a pavement section is a useful way of categorizing the pavement sections in terms of its inclusion of desirable design elements. It is also very useful in assessing the performance of the concrete pavement sections.

### *Data Analysis*

An initial evaluation of data from 53 sections has been conducted and the results presented at the 19th World Road Congress held in Marrakech in 1991.<sup>(82)</sup> In this analysis, Christory noticed some interesting trends using indicators such as the product of age and traffic and the number of modernity elements incorporated in a pavement. Since that time, more sections have been incorporated in the European COPES data base, and a more detailed analysis of the performance data is now desired.

Complete performance data are not available for all of the 96 pavement sections included in the evaluation. For example, transverse joint faulting, an important measure of concrete pavement performance, is available for only a few sections. Likewise, transverse slab cracking, an important indicator of fatigue in jointed plain concrete pavements, is not available for many pavement sections. However, the present serviceability rating (PSR) is provided for nearly every section and can be used to compare the relative performance of the pavement sections. Unfortunately, one drawback of the PSR is that the effect of certain design features (e.g., dowel bars) on pavement performance cannot be directly measured; rather, their effect can only be surmised based on whether the design feature reduced any pavement distress that would have otherwise detracted from the serviceability of the pavement.

Another factor complicating the comparison of the performance of the various pavement sections is that they were not constructed as experimental sections with the sole purpose of evaluating design features. While many of the sections within a country are located on the same highway, they are often constructed in different years and with similar (if not the same) design features. This means that direct performance comparisons are not only infrequent but, when possible, they are difficult because of differences in traffic loadings and aging/climatic effects.

Models predicting the PSR of the pavement sections were developed for France, the United Kingdom, Belgium, and Switzerland; the number of sections was insufficient for developing models for Italy. A faulting model was also developed for Switzerland. The models are based on a limited number of sections and design variables; they were developed only as a means for evaluating the effect of the various design features on pavement performance. In addition, the models are only accurate within the range of variable incorporated in the section in which they were developed. Therefore, the prediction models should not be used for design purposes.

Because of the absence of complete performance data, and because of the difficulty in making direct comparisons between different pavement sections, a more general evaluation of the performance of the European COPES sections was conducted. The purpose of this type of evaluation is to identify general performance trends. Three different types of plots were used to examine the European section:

- PSR vs. Age.
- PSR vs. ESAL's.
- PSR vs. (Age\*ESAL's).

By plotting the PSR as a function of age, the effects of both climate and traffic on pavement performance can be indirectly quantified. The PSR vs. ESAL's plot directly considers the effect of traffic loadings, although it does not directly consider climatic and aging effects. In the initial evaluation of the European COPES sections, an analysis was done by plotting the PSR as a function of the product of age and traffic.<sup>(82)</sup> In this way, both traffic and aging effects are considered in evaluating the performance of the pavement sections.

### Evaluation of Pavement Performance for Each European Country

Table 141 provides detailed design and construction information for each of the 96 concrete pavement sections for European COPES. As can be seen from the tables, the sections (except Switzerland) are assigned a seven digit code:

ABCDE\_FG

where:

- AB = Country code (55 = France; 56 = Italy; 57 = United Kingdom; 58 = Belgium).
- CDE = Project number (not highway number) within each country (for example, 001 = project no. 1).
- FG = Section number within each project.

For the purposes of this report, a *section* refers to an individual segment of pavement with a unique design. A *project* refers to a group of sections located on the same roadway. For example, the first project shown in table 141 is located on Highway A6 and consists of four sections: 55001\_01, 55001\_02, 55001\_03, and 55001\_04. The second project is located on Highway 85 and consists of two sections: 55002\_01 and 55002\_02. The performance data for the Swiss projects represent the average measurements of several sections.

### France

France has contributed 29 concrete pavement sections to the study. These 29 sections represent 10 different projects and a variety of different design features and traffic loadings. A summary of the design and performance of the French section are described in the following sections.

Table 141. Summary of design features and performance data.

Country	Project ID/ Highway	Year Built	Slab Design	Lane Width	Joint Spacing	Dowels	Base Type	Reinf Steel	Drainage	Shldr Type	Age	ESAL's, x 10 <sup>6</sup>	PSR
France	55001_01 Highway A6	1981	280 mm JPCP (11.0 in)	3.75 m (12.3 ft)	5.0 m (16.4 ft)	None	150 mm LCB (5.9 in)	None	Longitudinal Edge Drain	AGG	5	26.5	3.5
	55001_02 Highway A6	1986	280 mm JPCP (11.0 in)	3.75 m (12.3 ft)	5.0 m (16.4 ft)	20 mm (0.79 in)	200 mm PCTB (7.9 in)	None	Longitudinal Edge Drain	AGG	3	29.3	2.0
	55001_03 Highway A6	1980	280 mm JPCP (11.0 in)	3.75 m (12.3 ft)	5.0 m (16.4 ft)	None	150 mm LCB (5.9 in)	None	Longitudinal Edge Drain	AGG	9	52.3	4.0
	55001_04 Highway A6	1983	250 mm JPCP (9.8 in)	3.75 m (12.3 ft)	5.0 m (16.4 ft)	None	200 mm LCB (7.9 in)	None	None	AGG	6	52.4	4.5
	55002_01 Highway 85	1986	200 mm JPCP (7.9 in)	3.5 m (11.5 ft)	4.8 m (15.7 ft)	None	120 mm ATB (4.7 in)	None	Porous AGG Drainage Trench	Surface Treat.	3	1.5	3.5
	55002_02 Highway 85	1986	230 mm JPCP (9.1 in)	3.5 m (11.5 ft)	4.8 m (15.7 ft)	None	220 mm ATB (8.7 in)	None	Porous AGG Drainage Trench	Surface Treat.	3	2.8	3.5
	55003_01 Highway N6	1985	200 mm JPCP (7.9 in)	3.5 m (11.5 ft)	4.8 m (15.7 ft)	None	150 mm ATB (5.9 in)	None	Porous AGG Drainage Trench	AGG	4	2.2	3.0
	55003_02 Highway N6	1985	200 mm JPCP (7.9 in)	3.5 m (11.5 ft)	4.0 m (13.1 ft)	None	150 mm ATB (5.9 in)	None	Porous AGG Drainage Trench	AGG	4	2.2	3.0
	55003_03 Highway N6	1985	200 mm JPCP (7.9 in)	3.5 m (11.5 ft)	4.8 m (15.7 ft)	None	250 mm ATB (9.8 in)	None	Porous AGG Drainage Trench	AGG	4	2.2	4.0
	55004_01 Highway N57	1987	370 mm JPCP (14.6 in)	3.5 m (11.5 ft)	10.0 m (32.8 ft)	None	500 mm AGG (19.7 in)	None	Porous PCC Drainage Trench	AGG	2	0.9	3.5
	55004_02 Highway N57	1987	220 mm JPCP (8.7 in)	3.5 m (11.5 ft)	5.0 m (16.4 ft)	25 mm (0.98 in)	150 mm LCB (5.9 in)	None	Porous PCC Drainage Trench	AGG	2	0.9	3.5
	55005_01 Highway A42	1983	260 mm JPCP (10.2 in)	3.5 m (11.5 ft)	5.0 m (16.4 ft)	None	150 mm LCB (5.9 in)	None	Porous PCC Drainage Trench	AC	6	5.9	3.3
	55006_01 Highway A1	1977	280 mm JPCP (11.0 in)	3.5 m (11.5 ft)	5.0 m (16.4 ft)	None	200 mm LCB (7.9 in)	None	Porous PCC Drainage Trench	AC	9	15.2	3.5
	55006_02 Highway A1	1977	470-510 mm JPCP* (18.5-20.1 in)	3.5 m (11.5 ft)	5.0 m (16.4 ft)	None	None	None	Porous PCC Drainage Trench	AC	11	43.1	3.5
	55006_03 Highway A1	1964	270-280 mm JPCP* (10.6-11.0 in)	3.5 m (11.5 ft)	5.0 m (16.4 ft)	None	180-220 mm CTB (7.1-8.7 in)	None	None	AC	22	24.6	2.5
	55006_04 Highway A1	1976	275-290 mm JPCP* (10.8-11.4 in)	3.5 m (11.5 ft)	5.0 m (16.4 ft)	None	195-220 mm CTB (7.7-8.7 in)	None	None	AC	10	36.3	3.5
	55007_01 Highway A6a	1960	260 mm JRCP (10.2 in)	3.5 m (11.5 ft)	5.0 m (16.4 ft)	25 mm (0.98 in)	100 mm SC (3.9 in)	0.06%	Transverse Drains	AC	26	21.2	1.5
	55008_01 Highway 26	1983	370 mm JPCP (14.6 in)	3.5 m (11.5 ft)	4.5 m (14.8 ft)	None	250 mm AGG (9.9 in)	None	Longitudinal Edge Drain	AC	6	9.2	4.0
	55008_02 Highway 26	1983	370 mm JPCP (14.6 in)	3.5 m (11.5 ft)	4.5 m (14.8 ft)	None	250 mm AGG (9.9 in)	None	Longitudinal Edge Drain	AC	7	5.6	5.0
	55008_03 Highway 26	1981	370 mm JPCP (14.6 in)	3.5 m (11.5 ft)	4.5 m (14.8 ft)	None	250 mm AGG (9.9 in)	None	Longitudinal Edge Drain	AC	9	9.0	4.0

Table 141. Summary of design features and performance data (continued).

Country	Project ID/ Highway	Year Built	Slab Design	Lane Width	Joint Spacing	Dowels	Base Type	Reinf Steel	Drainage	Shldr Type	Age	ESAL's, x 10 <sup>6</sup>	PSR
France	55008_04 Highway 26	1981	370 mm JPCP (14.6 in)	3.5 m (11.5 ft)	4.5 m (14.8 ft)	None	250 mm AGG (9.9 in)	None	Longitudinal Edge Drain	PCC	9	9.2	5.0
	55008_05 Highway 26	1982	370 mm JPCP (14.6 in)	3.5 m (11.5 ft)	4.5 m (14.8 ft)	None	250 mm AGG (9.9 in)	None	Longitudinal Edge Drain	AC	8	8.4	4.0
	55008_06 Highway 26	1982	370 mm JPCP (14.6 in)	3.5 m (11.5 ft)	4.5 m (14.8 ft)	None	250 mm AGG (9.9 in)	None	Longitudinal Edge Drain	AC	8	8.4	4.0
	55008_07 Highway 26	1985?	370 mm JPCP (14.6 in)	3.5 m (11.5 ft)	4.5 m (14.8 ft)	None	250 mm AGG (9.9 in)	None	Longitudinal Edge Drain	AC	8	4.2	4.0
	55008_08 Highway 26	1985	370 mm JPCP (14.6 in)	3.5 m (11.5 ft)	4.5 m (14.8 ft)	None	250 mm AGG (9.9 in)	None	Yes	AC	5	6.8	4.0
	55008_09 Highway 26	1985	370 mm JPCP (14.6 in)	3.5 m (11.5 ft)	4.5 m (14.8 ft)	None	250 mm SC (9.9 in)	None	Yes	??	5	6.8	??
	55009_01 Highway 4	1976	290 mm JPCP (11.4 in)	3.5 m (11.5 ft)	5.0 m (16.4 ft)	None	150 mm CTB (5.9 in)	None	No	AC	10	3.3	3.5
	55009_02 Highway 4	1976	220 mm JPCP (8.7 in)	3.5 m (11.5 ft)	5.0 m (16.4 ft)	None	150 mm CTB (5.9 in)	None	No	AC	10	3.3	3.5
	55010_01 Highway A13	1966	250 mm JPCP (9.8 in)	3.5 m (11.5 ft)	5.0 m (16.4 ft)	None	250 mm CTB (9.8 in)	None	No	AC	20	22.5	2.5
Italy	56001_01 Highway SS7	1958	220 mm JRCP (8.7 in)	5.25 m (17.2 ft)	12.3 m (40.3 ft)	28 mm (1.10 in)	250 mm Pozzolan (9.8 in)	0.06%	No	AC	31	62.3	2.5
	56001_02 Highway SS7	1958	220 mm JRCP (8.7 in)	5.25 m (17.2 ft)	12.3 m (40.3 ft)	28 mm (1.10 in)	250 mm Pozzolan (9.8 in)	0.06%	No	AC	31	62.3	2.5
	56002_01 Highway E45	1985	260 mm JPCP (10.2 in)	3.5 m (11.5 ft)	5.0 m (16.4 ft)	30 mm (1.18 in)	150 mm LCB (5.9 in)	None	Longitudinal Edge Drain	Porous PCC	4	7.8	2.8
	56002_02 Highway E45	1985	250 mm JPCP (9.8 in)	3.5 m (11.5 ft)	5.0 m (16.4 ft)	30 mm (1.18 in)	200 mm CTB (7.9 in)	None	Longitudinal Edge Drain	Porous PCC	4	8.0	2.8
	56002_03 Highway E45	1985	260 mm JPCP (10.2 in)	3.5 m (11.5 ft)	5.0 m (16.4 ft)	30 mm (1.18 in)	150 mm CTB (5.9 in)	None	Longitudinal Edge Drain	Porous PCC	4	8.0	2.4
	56003_01 Highway 21	1971	240 mm JPCP (9.5 in)	3.75 m (12.3 ft)	5.0 m (15.7 ft)	None	160 mm CTB (6.3 in)	None	None	AC	18	33.5	1.0
United Kingdom	57001_01 Highway M20	1972	275 mm JPCP (10.8 in)	3.65 m (12.0 ft)	6.0 m (19.7 ft)	20 mm (0.79 in)	150 mm AGG (5.9 in)	None	Longitudinal Edge Drain	AC	16	52.2	2.5
	57001_02 Highway M20	1972	275 mm JPCP (10.8 in)	3.65 m (12.0 ft)	6.0 m (19.7 ft)	20 mm (0.79 in)	150 mm AGG (5.9 in)	None	Longitudinal Edge Drain	AC	16	52.2	2.5
	57002_01 Highway M25	1979	305 mm JPCP (12.0 in)	3.65 m (12.0 ft)	5.0 m (16.4 ft)	20 mm (0.79 in)	225 mm AGG (8.9 in)	None	Longitudinal Edge Drain	PCC	9	55.7	2.5
	57002_02 Highway M25	1979	305 mm JPCP (12.0 in)	3.65 m (12.0 ft)	5.0 m (16.4 ft)	20 mm (0.79 in)	225 mm AGG (8.9 in)	None	Longitudinal Edge Drain	PCC	9	55.7	2.5
	57003_01 Highway A2	1973	250 mm JPCP (9.8 in)	3.65 m (12.0 ft)	6.0 m (19.7 ft)	20 mm (0.79 in)	150 mm CTB (5.9 in)	None	Longitudinal Edge Drain	AGG	14	40.4	1.5

Table 141. Summary of design features and performance data (continued).

Country	Project ID/ Highway	Year Built	Slab Design	Lane Width	Joint Spacing	Dowels	Base Type	Reinf. Steel	Drainage	Shldr Type	Age	ESAL's, x 10 <sup>6</sup>	PSR
United Kingdom	57003_02 Highway A2	1973	250 mm JPCP (9.8 in)	3.65 m (12.0 ft)	6.0 m (19.7 ft)	20 mm (0.79 in)	150 mm CTB (5.9 in)	None	Longitudinal Edge Drain	AGG	14	40.3	1.5
	57004_01 Highway A12	1987	280 mm JPCP (11.0 in)	3.65 m (12.0 ft)	5.0 m (16.4 ft)	20 mm (0.79 in)	130 mm CTB (5.1 in)	None	Longitudinal Edge Drain	PCC	2	10.8	4.5
	57005_01 Highway M25	1976	275 mm JPCP (10.8 in)	3.65 m (12.0 ft)	5.0 m (16.4 ft)	25 mm (0.98 in)	150 mm AGG (5.9 in)	None	Longitudinal Edge Drain	PCC	12	106.4	1.5
	57005_02 Highway M25	1976	275 mm JPCP (10.8 in)	3.65 m (12.0 ft)	5.0 m (16.4 ft)	25 mm (0.98 in)	75 mm AGG (3.0 in)	None	Longitudinal Edge Drain	PCC	12	106.4	1.5
	57006_01 Highway M1	1981	300 mm JPCP (11.8 in)	3.65 m (12.0 ft)	5.0 m (16.4 ft)	20 mm (0.79 in)	225 mm LCB (8.9 in)	None	Longitudinal Edge Drain	PCC	7	27.3	3.5
	57006_02 Highway M1	1982	300 mm JPCP (11.8 in)	3.65 m (12.0 ft)	5.0 m (16.4 ft)	20 mm (0.79 in)	150 mm LCB (5.9 in)	None	Longitudinal Edge Drain	PCC	6	24.2	3.5
	57007_01 Highway M11	1975	275 mm JPCP (10.8 in)	3.65 m (12.0 ft)	5.0 m (16.4 ft)	25 mm (0.98 in)	150 mm CTB (5.9 in)	None	Longitudinal Edge Drain	AC	14	39.7	2.5
	57008_01 Highway A12	1971	250 mm JPCP (9.8 in)	3.65 m (12.0 ft)	5.0 m (16.4 ft)	25 mm (0.98 in)	150 mm CTB (5.9 in)	None	Longitudinal Edge Drain	??	18	39.5	3.5
	57008_02 Highway A12	1971	250 mm JPCP (9.8 in)	3.65 m (12.0 ft)	5.0 m (16.4 ft)	25 mm (0.98 in)	150 mm CTB (5.9 in)	None	Longitudinal Edge Drain	??	18	39.5	1.5
	57008_03 Highway A12	1969	250 mm JPCP (9.8 in)	3.65 m (12.0 ft)	6.0 m (19.7 ft)	30 mm (1.18 in)	150 mm LCB (5.9 in)	None	Longitudinal Edge Drain	??	20	47.8	3.5
	57008_04 Highway A12	1965	200 mm JPCP (7.9 in)	3.65 m (12.0 ft)	25.0 m (82.0 ft)	30 mm (1.18 in)	150 mm LCB (5.9 in)	0.12%	Longitudinal Edge Drain	??	24	62.0	3.5
	57009_01 Highway A120	1982	250 mm JPCP (9.8 in)	3.65 m (12.0 ft)	5.0 m (16.4 ft)	25 mm (0.98 in)	230 mm CTB (9.8 in)	None	Longitudinal Edge Drain	??	7	8.3	??
Belgium	58001_01 Highway 411	1979	200 mm CRCP (7.9 in)	3.75 m (12.3 ft)	n/a	n/a	150 mm LCB (5.9 in)	0.85%	Longitudinal Edge Drain	AC	11	29.5	3.5
	58001_02 Highway 411	1979	200 mm CRCP (7.9 in)	3.75 m (12.3 ft)	n/a	n/a	200 mm LCB (7.9 in)	0.85%	Longitudinal Edge Drain	AC	11	29.5	3.5
	58001_03 Highway 411	1973	200 mm CRCP (7.9 in)	3.75 m (12.3 ft)	n/a	n/a	200 mm LCB (7.9 in)	0.85%	Longitudinal Edge Drain	AC	17	37.6	3.5
	58001_04 Highway 411	1978	200 mm CRCP (7.9 in)	3.75 m (12.3 ft)	n/a	n/a	200 mm LCB (7.9 in)	0.67%	Longitudinal Edge Drain	AC	12	17.9	3.5
	58001_05 Highway 411	1987	200 mm CRCP (7.9 in)	3.75 m (12.3 ft)	n/a	n/a	200 mm LCB (7.9 in)	0.67%	Longitudinal Edge Drain	AC	3	6.2	4.5
	58001_06 Highway 411	1988	200 mm CRCP (7.9 in)	3.75 m (12.3 ft)	n/a	n/a	200 mm CTB (7.9 in)	0.67%	Longitudinal Edge Drain	AC	2	3.6	4.5
	58002_01 Highway 4	1979	230 mm JPCP (9.1 in)	3.75 m (12.3 ft)	5.0 m (16.4 ft)	None?	150 mm CTB (5.9 in)	None	Longitudinal Edge Drain	AC	10	30.8	3.0
	58002_02 Highway 4	1979	230 mm JPCP (9.1 in)	3.75 m (12.3 ft)	5.0 m (16.4 ft)	None	150 mm CTB (5.9 in)	None	??	AC	10	30.8	3.0

Table 141. Summary of design features and performance data (continued).

Country	Project ID/ Highway	Year Built	Slab Design	Lane Width	Joint Spacing	Dowels	Base Type	Reinf. Steel	Drainage	Shldr Type	Age	ESAL's, x 10 <sup>6</sup>	PSR	
Belgium	58002_03 Highway 4	1979	200 mm JPCP (7.9 in)	3.75 m (12.3 ft)	5.0 m (16.4 ft)	25 mm (0.98 in)	150 mm CTB (5.9 in)	None	Longitudinal Edge Drain	AC	10	30.8	3.0	
	58002_04 Highway 4	1979	200 mm JPCP (7.9 in)	3.75 m (12.3 ft)	5.0 m (16.4 ft)	25 mm (0.98 in)	150 mm CTB (5.9 in)	None	Longitudinal Edge Drain	AC	10	30.8	3.0	
	58002_05 Highway 4	1979	200 mm JPCP (7.9 in)	3.75 m (12.3 ft)	5.0 m (16.4 ft)	25 mm (0.98 in)	150 mm CTB (5.9 in)	None	Longitudinal Edge Drain	AC	10	30.8	3.0	
	58002_06 Highway 4	1979	200 mm JPCP (7.9 in)	3.75 m (12.3 ft)	5.0 m (16.4 ft)	25 mm (0.98 in)	150 mm CTB (5.9 in)	None	Longitudinal Edge Drain	AGG	10	30.8	3.0	
	58002_07 Highway 4	1979	200 mm JPCP (7.9 in)	5.0 m (16.4 ft)	5.0 m (16.4 ft)	25 mm (0.98 in)	150 mm CTB (5.9 in)	None	Transverse Drains	AC	10	30.8	3.0	
	58002_08 Highway 4	1979	200 mm JPCP (7.9 in)	4.0 m (13.1 ft)	5.0 m (16.4 ft)	25 mm (0.98 in)	150 mm CTB (5.9 in)	None	??	AC	10	30.8	3.5	
	58002_09 Highway 4	1979	230 mm JPCP (9.1 in)	4.0 m (13.1 ft)	5.0 m (16.4 ft)	None	150 mm CTB (5.9 in)	None	??	AC	10	30.8	3.0	
	58002_10 Highway 4	1979	230 mm JPCP (9.1 in)	4.0 m (13.1 ft)	5.0 m (16.4 ft)	None	150 mm CTB (5.9 in)	None	??	AC	10	30.8	3.0	
	58002_11 Highway 4	1979	230 mm JPCP (9.1 in)	4.0 m (13.1 ft)	3.5 m (11.5 ft)	None	150 mm CTB (5.9 in)	None	Longitudinal Edge Drain	AC	10	30.8	3.0	
	58002_12 Highway 4	1979	200 mm JPCP (7.9 in)	4.0 m (13.1 ft)	5.5 m (18.0 ft)	25 mm (0.98 in)	150 mm CTB (5.9 in)	None	??	AC	10	30.8	3.0	
	58002_13 Highway 4	1983	200 mm CRCP (7.9 in)	3.75 m (12.3 ft)	n/a	n/a	150 mm CTB (5.9 in)	0.63%	Longitudinal Edge Drain	AC	6	21.3	4.0	
	58002_14 Highway 4	1979	200 mm CRCP (7.9 in)	3.75 m (12.3 ft)	n/a	n/a	150 mm CTB (5.9 in)	0.63%	??	AC	10	30.8	3.5	
	58002_15 Highway 4	1985	200 mm JPCP (7.9 in)	3.5 m (11.5 ft)	5.0 m (16.4 ft)	25 mm (0.98 in)	150 mm CTB (5.9 in)	None	Longitudinal Edge Drain	AC	5	3.8	4.0	
	58002_16 Highway 4	1984	230 mm JPCP (9.1 in)	3.5 m (11.5 ft)	5.0 m (16.4 ft)	None	150 mm CTB (5.9 in)	None	Longitudinal Edge Drain	AC	6	4.4	4.5	
	Switzer- land	58003_01 Highway 97	1984	200 mm CRCP (7.9 in)	3.75 m (12.3 m)	n/a	n/a	150 mm CTB (5.9 in)	0.85%	Longitudinal Edge Drain	Turf	5	2.9	4.5
		58003_02 Highway 97	1975	200 mm CRCP (7.9 in)	3.5 m (11.5 m)	n/a	n/a	150 mm CTB (5.9 in)	0.85%	Longitudinal Edge Drain	Turf	14	8.0	2.5
58003_03 Highway 97		1983	200 mm CRCP (7.9 in)	3.75 m (12.3 m)	n/a	n/a	250 mm CTB (9.9 in)	0.85%	Longitudinal Edge Drain	Turf	6	4.5	4.5	
Bern W. - Gurbru	1981	200-230 mm JPCP (7.9-9.1 in)	??	5.0 m (16.4 ft)	22 mm (0.87 in)	200 mm (7.9 in) CTB or 500 mm (19.7 in) AGG or 170 mm (6.7 in) CTB + 230 mm (9.1 in) AGG	??	Longitudinal and Transverse Drains	AC	12	0.4	4.3		
Lenzburg - Rothrist	1966 1967	50 + 150 mm JRCP (2.0-5.9 in)	??	6-8 m (20-26 ft)	22 mm (0.87 in)	600 mm (23.6 in) AGG	??	Longitudinal Edge Drain	AC	27	19.6	4.1*		
Erstfeld - Amsteg	1977 1978	50 + 150 mm JRCP (2.0 + 5.9 in)	??	6.0 m (19.7 ft)	22 mm (0.87 in)	110 mm (4.3 in) ATB or 450 mm (17.8 in) AGG	??	Longitudinal Edge Drain	AC	2	0.7	4.1		

Table 141. Summary of design features and performance data (continued).

Country	Project ID/ Highway	Year Built	Slab Design	Lane Width	Joint Spacing	Dowels	Base Type	Reinf. Steel	Drainage	Shldr Type	Age	ESAL's, x 10 <sup>6</sup>	PSR
Switzer- land	Flums - Mels	1970 1973	220 mm JRCP (8.7 in)	??	6-8 m (20-26 ft)	22 mm (0.87 in)	400 mm (15.7 in) AGG or 250 mm (9.9 in) CTB or 600 mm (23.6 in) AGG	??	Longitudinal and Transverse Drains	AC	12	3.4	4.0
	Walenstadt - Flums	1985	200-220 mm JPCP (7.9-5.7 in)	??	5.0 (16.4 ft)	22 mm (0.87 in)	80 mm (3.1 in) ATB + 800 mm (31.5 in) AGG	??	Longitudinal and Transverse Drains	AC	??	??	??
	Wil - Gossau - St. Gallen	1968 1969	50 + 150 mm JRCP (2.0 + 5.9 in)	??	8.0 m (26.2 ft)	22 mm (0.87 in)	800-1000 mm (31.5- 39.4 in) AGG	??	??	PCC	18	5.4	4.2
	Muri - Kiesen	1970 1971	50 + 150 mm JRCP (2.0 + 5.9 in)	??	6.0 m (19.7 ft)	22 mm (0.87 in)	?? AGG	??	??	AC	7	1.0	3.6
	Haag - Trubbach	1979	210 mm JRCP (8.3 in)	??	5.0 (16.4 ft)	22 mm (0.87 in)	100 mm (3.9 in) ATB + 500 mm (19.7 in) AGG	??	Longitudinal and Transverse Drains	Soil	4	2.6	4.2
	Cadenazzo - Riviera	1965	50 + 130 mm JRCP (2.0 + 5.1 in)	??	8.0 m (26.2 ft)	20 mm (0.79 in)	200 mm (7.9 in) ATB	??	??	Soil	29	5.3	3.7*
	Lukmanier- pass	1959 1965	50 + 130 mm JRCP (2.0 + 5.1 in)	??	7.5 m (24.6 ft)	16 mm (0.63 in)	600-1000 mm (23.9-39.4 in) AGG	??	??	Soil	35	0.6	3.4*
	Altmarkt - Bad Bubendorf	1954	50 + 130 mm JRCP (2.0 + 5.1 in)	??	8.0 m (26.2 ft)	20 mm (0.79 in)	250-350 mm (9.9-13.8 in) AGG	??	Longitudinal Edge Drain	??	32	5.7	3.4
	Selzach - Grenchen	1954	50 + 130 mm JRCP (2.0 + 5.1 in)	??	10.0 m (32.8 ft)	20 mm (0.79 in)	60-200 mm (2.4-7.9 in) AGG	??	Longitudinal Edge Drain	Soil	32	7.8	3.1
	Melano - Capolago	1953	50 + 120 mm JRCP (2.0 + 4.7 in)	??	8.0 m (26.2 ft)	20 mm (0.79 in)	150 mm (5.9 in) AGG	??	??	??	41	3.5	3.3*
	Piotta - Faido - Pollegio	1956	50 + 130 mm JRCP (2.0 + 5.1 in)	??	8.0 m (26.2 ft)	20 mm (0.79 in)	80-200 mm (3.1-7.9 in) AGG	??	Longitudinal and Transverse Drains	??	38	8.0	3.0*
	Gordola - Riazzino	1957	50 + 130 mm JRCP (2.0 + 5.1 in)	??	11.5 m (37.7 ft)	20 mm (0.79 in)	300-500 mm (11.8-19.7 in) AGG	??	Longitudinal and Transverse Drains	??	37	8.2	3.8*
	Buckten - Rumlingen	1960	50 + 150 mm JRCP (2.0 + 5.9 in)	??	10 m (32.8 ft)	22 mm (0.87 in)	50 mm (2.0 in) ATB + 330 mm (13.0 in) AGG	??	??	??	26	2.1	4.1
	Pratteln - Liestal	1960	50 + 150 mm JRCP (2.0 + 5.9 in)	??	8.0 m (26.2 ft)	22 mm (0.87 in)	450 mm (17.7 in) AGG	??	??	??	26	12.1	3.8
	Cama - Soazza	1957 1958	50 + 120 mm JRCP (2.0 + 4.7 in)	??	8.0 m (26.2 ft)	20 mm (0.79 in)	??	??	??	PCC	37	3.6	3.6*
Gotthardpass	1967	50 + 150 mm JRCP (2.0 + 5.9 in)	??	??	??	700 mm (27.6 in) AGG	??	Longitudinal and Transverse Drains	Soil	27	0.4	4.2*	

\* Rideability measured by "ARAN" and given PSR value is the result of correlation.

Key: PSR = Present Serviceability Rating (0 to 5 scale)	CTB = Cement-Treated Base
JPCP = Jointed Plain Concrete Pavement	ATB = Asphalt-Treated Base
JRCP = Jointed Reinforced Concrete Pavement	LCB = Lean Concrete Base
AC = Asphalt Concrete	AGG = Aggregate
CRCP = Continuously Reinforced Concrete Pavement	SC = Sand Cement
PCC = Portland Cement Concrete	PCTB = Permeable Cement-Treated Base

### *Design Features*

The COPES sections in France consist of a variety of pavement designs, ages, and features. Of the 29 pavement sections, all but one are JPCP designs. The one reinforced pavement, section 55007\_01 on Highway A6a, is a JRCP that contains 0.06 percent longitudinal reinforcing steel (expressed as a percentage of the cross-sectional area). The following design features and conditions are representative of the French sections:

- The French sections range from 2 to 26 years old, with an average age of 8.1 years. Most of the sections are less than 10 years old, although four sections are over 20 years old. These ages represent the time from when the sections were opened to traffic until they were surveyed under the European COPES program.
- The slab thicknesses range from less than 8 in (200 mm) to more than 16 in (400 mm); the majority of the sections are either between 10 and 12 in (250 and 300 mm) or between 14 and 16 in (350 and 400 mm). At least three pavement sections contain trapezoidal cross sections (in which the outside edge of the slab is thicker than the inside edge), and it is suspected that several other sections also contain this design feature.
- A variety of base types are represented in the French European COPES section, distributed as follows: aggregate base (9 sections), lean concrete base (6 sections), cement-treated base (5 sections), asphalt-treated base (5 sections), sand cement (2 sections), permeable cement-treated base (1 section), and no base (1 section).
- Several of the French sections include an aggregate subbase beneath the treated base course, especially when the subgrade is a fine-grained soil. For example, Highway 85, N6, and N57 have aggregate subbases ranging from 7.9 to 19.7 in (200 to 500 mm) between a treated base and an A-4 subgrade.
- Most of the French sections have joint spacings of either 14.8 ft (4.5 m) or 16.4 ft (5.0 m). One section has a joint spacing of 13.1 ft (4.0 m), and one section has a spacing of 32.8 ft (10.0 m). The lone JRCP section (55007\_01) has a joint spacing of only 16.4 ft (5.0 m).
- Most of the sections contain some drainage, either through the use of longitudinal edge drains or through the placement of a longitudinal drainage trench of porous aggregate. One section contains transverse drains and six sections contain no drainage.
- Most of the European COPES sections from France include either asphalt concrete (AC) or aggregate shoulders; only one section contains a tied concrete shoulder.



- Three pavement sections contain dowel bars, with diameters ranging from 0.79 to 0.98 in (20 to 25 mm). The other sections do not contain any type of load transfer device.
- The predominant joint sealant type is asphalt-rubber, although a few sections are sealed with silicone or preformed joint seals.
- Lane widths are either 11.5 ft (3.5 m) or 12.3 ft (3.75 m).
- About one-half of the sections contain two modernity elements. Five sections contain three modernity elements, seven sections contain one modernity element, and two sections do not contain any modernity elements.

### *Climatic Information*

The average annual precipitation ranges from 23.6 in (600 mm) to 42.1 in (1070 mm) for the sections in France. This indicates, most likely, conditions in which the pavement would be exposed to significant levels of excess moisture. The freezing index has a smaller variation, ranging from 288 to 468 degree-days (with degrees measured in Fahrenheit). Based on the climatic data provided, it appears that the prevailing climatic conditions in France may be comparable to those in central Illinois.

### *Traffic Data*

Although truck and traffic volumes for the French sections were available for 2 years, only one truck factor value (representing a single year) was available. Thus, some assumptions had to be made in growth rates of both traffic volumes and truck factors to develop the ESAL estimates. Based on the available data and necessary assumptions, the number of ESAL applications to the time of the survey was estimated.

Nineteen of the 29 sections have sustained fewer than 10 million ESAL applications. Six sections have sustained between 15 and 30 million ESAL's, and the remaining four sections have been subjected to more than 35 million ESAL applications. The large number of ESAL applications is mainly a result of the heavy axle loads experienced in France. For example, 25 percent of the single axles are greater than 20,000 lb (9.1 tons), the legal limit for single axles in the United States. Similarly, 70 percent of all tandem axles are greater than 34,000 lb (15.4 tons), the legal limit for tandem axles in the United States. The legal limit for single axles in France is 28,600 lb (13 tons); legal limits for tandem axles in France is 46,200 lb (21 tons).<sup>(63)</sup>

### *Pavement Performance*

The performance data for the outer traffic lane (heaviest traveled lane) of the French sections are summarized in appendix B of volume IV. As previously mentioned, the only performance indicator consistently provided for each pavement section is the

PSR. However, it is somewhat informative to examine the performance data that are available. For example, section 55001\_02 displays a significant number of corner breaks (36), as well as some transverse (184 ft [56 m]) and longitudinal (16 ft [6 m]) cracking. These distresses are reflected in the PSR value of 2.0, which indicates a pavement in poor condition.

Section 55006\_03 represents one of the few sections for which transverse faulting is available. This nondoweled pavement (trapezoidal thickness of 10.6 to 11.0 in [270 to 280 mm]) is exhibiting a significant level of faulting (0.20 in [5 mm]) and is also displaying some corner breaks (5), pumping (low severity), and joint spalling (23 spalled joints of low severity) after 22 years and 24.6 million ESAL applications. These distresses appear to be reflected in the PSR value of 2.5 (fair condition).

Section 55007\_01 is another section for which faulting data are available. This 10.2-in (260-mm) JRCP, which contains 0.98-in (25-mm) dowel bars, is exhibiting an extremely high level of faulting (0.39 in [10 mm]) after 26 years and approximately 21.2 million ESAL's. It is also exhibiting transverse cracking (23 ft [7 m] of low severity, 49 m [161 ft] of medium severity), longitudinal cracking (7 ft [2 m] of low severity, 13 ft [4 m] of medium severity), and joint spalling (10 joints of low severity). Again, these distresses appear to be reflected in the PSR value of 1.5 (poor condition).

Finally, section 55010\_01 (9.8 in [250 mm] nondoweled JPCP) displays a significant level of faulting (0.16 in [4 mm]), as well as some longitudinal cracking (65 ft [5 m] of low severity, 98 ft [30 m] of medium severity) and joint spalling (40 spalled joints of medium severity) after 20 years and 22.5 million ESAL applications. This appears to be consistent with the PSR rating of 2.5 (fair condition).

On the other hand, some sections are performing quite well after many years of service and high traffic levels. For instance, section 55006\_02 is 11 years old and has been exposed to 43 million ESAL applications, yet it has a PSR of 3.5. This section has a trapezoidal cross-section with a slab thickness ranging from 18.5 in (470 mm) at the center to 20.1 in (510 mm) at the edge.

Likewise, sections 55001\_03 and 55001\_04 have been exposed to over 50 million ESAL applications and have PSR values of 4.0 and 4.5, respectively. The slabs are 11.0 and 9.8 in (280 and 250 mm) thick and are placed over an LCB, which is believed to be attributing to the performance.

The plot of PSR vs. age shows a general trend of a reduction in PSR with increasing age, although some scatter exists in the data (particularly in the 5-to-10 year age group). The plot of PSR as a function of ESAL's also shows a considerable amount of scatter in the data. Several points are outside of the expected trend line, many of which represent the most heavily-trafficked sections. For example, two sections that have been subjected to more than 50 million ESAL applications have PSR values of 4.0 or greater. These two sections both have a lean concrete base, which may contribute to their performance. The PSR vs. (Age \* ESAL's) plot shows a better trend than the previous plots. The few outliers are believed to be due to the wide

range of designs, design features, and characteristics of the various pavement sections.

### *Prediction Model*

The JRCPC sections and the sections with dowel bars were not included in the development of the PSR prediction model. Thus, the model is only applicable for JPCPC sections without dowel bars. In addition, the model is limited to the range of design features and conditions for the French sections (e.g. less than 20 years old and 50 million ESAL's). Based on the available data, the following model was developed utilizing the least-square regression:

$$PSR = 3.0803 - 0.00043AGE^2ESAL^{0.5} + 0.00159THICK + 0.4945DRAIN \quad (38)$$

$$\begin{aligned} R^2 &= 0.75 \\ R^2_{adj} &= 0.71 \\ SEE &= 0.28 \\ N &= 24 \end{aligned}$$

where:

- PSR = Present serviceability rating.
- AGE = Time since construction, years.
- ESAL = Estimated 18-kip (80-kN) ESAL's, millions.
- THICK = PCC slab thickness, mm.
- DRAIN = Dummy variable for drainage design (1 if longitudinal edge drains are used, 0 if not).

The model is sensitive to both age and ESAL's, especially after about 15 years. Edge drains increase the PSR by about 0.5 regardless of the conditions (as evident by the coefficient on the drainage variable). The model is not overly sensitive to changes in PCC thickness. Other variables (e.g., base type, subgrade type, and joint spacing) were also introduced into the model but were shown to be insignificant.

### *Examination of Design Features*

Based on a sensitivity analysis of the PSR prediction model, the most significant variables are pavement age, ESAL's, and drainage. A comparison of the various design features was also conducted using the plot of PSR as a function of the product of age and ESAL's. Again, some benefit in pavement performance is gained by providing drainage to the pavement. It appears, however, that these benefits may not be immediately evident, as there are some nondrained pavement sections that are showing good performance. However, as age and ESAL loadings increase, the loss in pavement performance occurs at a more rapid rate for the nondrained sections than for the drained sections.

Other design features were also shown to have an effect on pavement performance. For instance, the sections constructed on an LCB performed better than sections constructed on other base types. This trend is especially evident as the product of age and ESAL's reaches higher levels (> 100).

Likewise, slab thickness appeared to have an effect on pavement performance. To analyze this effect, slab thickness was isolated as a design feature using three levels: less than 9.8 in (250 mm), between 9.8 and 13.8 in (250 and 350 mm), and more than 13.8 in (350 mm). Again, although some scatter exists in the data, the thicker slabs appear to exhibit better performance than the thinner slabs. In addition, the thicker slabs appear to exhibit a slower rate of deterioration than the thinner slabs.

A final evaluation of pavement performance was conducted using the number of modernity elements. The sections with three modernity elements appear to deteriorate more slowly than those with two or fewer. Again, some exceptions to this trend can be found in the data.

## Italy

Italy has contributed six concrete pavement sections to the European COPES program. These sections represent two projects located on three different highways. The following sections describe the design and performance of these sections.

### *Design Features*

The COPES sections from Italy represent a variety of pavement designs, ages, and features. The data consist of four JPCP sections and two JRCP sections with 0.06 percent longitudinal reinforcing steel (expressed as a percentage of the cross-sectional area). The following characteristics are representative of the Italian sections:

- The sections range from 4 to 31 years old, with an average age of 15.3 years. Three of the sections are 4 years old, one is 18 years old, and two are 31 years old.
- The slab thicknesses range from 8.7 to 10.2 in (220 to 260 mm).
- The pavement sections contain three different base types: pozzolan, LCB, and CTB. One pavement section contains an LCB with a thickness of 5.9 in (150 mm), two sections contain a pozzolan base with a thickness of 9.8 in (250 mm), and three sections contain a CTB with thicknesses ranging from 5.9 to 7.9 in (150 to 200 mm).
- All pavement sections with available data are constructed on an AASHTO A-6 subgrade.
- All but one section has dowel bars at the transverse joints.

- The slab widths range from 11.5 to 17.2 ft (3.5 to 5.25 m)
- The joint spacings are 15.7 ft (5.0 m) for the JPCP sections and 40.3 (12.3 m) for the JRCP sections. Every section contains an asphalt-rubber joint sealant.
- The pavement sections also contain different shoulder types. Three sections contain AC shoulders and three contain porous PCC shoulders.
- Three sections have longitudinal edge drains and three have no drainage system.
- The number of modernity elements ranges from 0 to 3. The modernity elements in these sections consist of drainage (longitudinal edge drains), strengthened structure (dowels), edge support (porous PCC shoulders), and a nonerodible base (LCB).

### *Climatic Information*

The only climatic information available is the annual precipitation, which ranges from 9.8 to 24.1 in (248 to 611 mm). The freezing index is not available for any of the sections, but it is likely to be close to zero based on the generally mild Italian climate.

### *Traffic Data*

For the Italian pavement sections, only 1 year of traffic data (traffic volumes, truck volumes, and truck factors) was available for most sections. Thus, several assumptions were made regarding the growth of traffic volumes and truck factors. Based on these traffic estimates, the number of ESAL applications ranges from 1 to 62 million. Three sections have sustained fewer than 10 million ESAL's, one section has sustained between 30 and 35 million ESAL's, and the remaining two sections have sustained more than 60 million ESAL's.

In Italy, the legal load limit is 26,500 lb (12 tons) for single axles and 41,900 lb (19 tons) for tandem axles, compared to the U.S. legal load limits of 20,000 and 34,000 lb (9.1 and 15.4 tons).<sup>(63)</sup> Therefore, pavements in Italy can experience considerably more ESAL applications at the same traffic volumes. Approximately 30 percent of the axles are over the legal limit in the United States. However, only 8 percent are over the legal load limit in Italy.

### *Pavement Performance*

Section 56003\_01 has been exposed to 33 million ESAL applications and has a PSR of 1.0. This section is the only section without dowels and, consequently, the only section with faulting at the transverse joints, which can cause a drastic decrease in PSR. In fact, this section contains no modernity elements, which may also contribute to this low PSR value.

Sections 56001\_01 and 56001\_02 have considerably more transverse cracking than the other sections. However, these sections are both JRCP sections, which are designed to crack. These cracks relieve the curling stresses in the pavement, yet they do not affect pavement performance because the reinforcing steel holds the cracks tight, evidenced by the fact that the cracks are all low severity.

The limited number of sections makes it difficult to draw any significant conclusions. Again, the PSR was plotted as a function of age, ESAL's, and the product of age and ESAL's. All three plots indicate that the JRCP sections have performed considerably better than the JPCP sections. The PSR of the JPCP sections drops off quickly, whereas the JRCP sections have performed well although they have carried over 60 million ESAL applications.

As mentioned, only six sections from Italy were included, which made the analysis difficult. For the same reason, a PSR prediction model could not be developed for Italy. Likewise, an evaluation of the individual design features and their effect on pavement performance could not be conducted.

### The United Kingdom

The United Kingdom has contributed 17 concrete pavement sections to the European COPES program, representing nine projects. Although the United Kingdom data only represent seven highways, some highways contain more than one project. These highways are divided into different projects because they were constructed at different times with different cross sections and design features.

#### *Design Features*

The COPES sections from the United Kingdom represent a variety of pavement designs, ages, and features. One pavement section is a JRCP with 0.12 percent longitudinal reinforcing steel (expressed as a percentage of the cross-sectional area), and the other 16 sections are JPCP. The sections represents pavements with the following characteristics:

- The sections range from 2 to 24 years old, with an average age of 12.8 years.
- The sections range in thickness from 7.9 to 12.0 in (200 to 305 mm), although the majority (12 sections) are between 9.8 and 11.0 in (250 and 280 mm).
- The pavement sections in the United Kingdom contain three different base types: LCB, AGG, and CTB. Four pavement sections contain an LCB, three are 5.9 in (150 mm thick, and the other one is 8.9 in (225 mm) thick. Six sections contain an aggregate base, with thicknesses ranging from 3.0 to 8.9 in (75 to 225 mm). The remaining seven sections contain a CTB, with thicknesses ranging from 5.1 to 5.9 in (130 to 150 mm).
- The pavement sections consist of three sections with AC shoulders, seven with

PCC shoulders, and two with aggregate shoulders. The type of shoulder is not provided for five pavement sections.

- For the JPCP, 11 sections have 16.4-ft (5.0-m) joint spacings and 5 have 19.7-ft (6.0-m) joint spacings. The JRCP section has a joint spacing of 82.0 ft (25.0 m).
- All sections have dowels that range in diameter from 0.79 and 1.18 in (20 to 30 mm).
- Three different types of joint sealants (asphalt-rubber, PVC coal tar, and polyurethane) are used in these sections.
- All pavement sections contain longitudinal edge drains with a diameter of 5.9 in (150 mm).
- Every section is constructed on an A-6 subgrade with 12-ft (3.65-m) slab widths.
- Every section contains at least two modernity elements—drainage (longitudinal edge drains) and strengthened structure (dowels). The four sections with three modernity elements also have a nonerodible base (LCB).

#### *Climatic Information*

The annual precipitation and the freezing index are both available for the sections from the United Kingdom. Overall, these values indicate little variation in climatic conditions. The freezing index is 140 degree-days (degrees in Fahrenheit) for each pavement section. The annual precipitation is 15.5 in (393 mm) for 6 sections and 18.3 in (464 mm) for the other 11 sections. Based on the given information, these climatic conditions are similar to those experienced in western Kansas.

#### *Traffic Data*

As before, several assumptions were made regarding growth in traffic volumes and truck factors. The ESAL applications range from 8 to 106 million, with more than 30 million ESAL applications on 13 of the 17 sections. Over 20 percent of the axles are over the legal limit in the United States (20,000 lb [9.1 tons] for single axles and 34,000 [15.4 tons] for tandem axles). Due to the higher legal load limit, pavement sections in the United Kingdom can experience considerably more ESAL's over the same design period as compared to sections in the United States.

#### *Pavement Performance*

The only performance indicator consistently provided for each pavement section is the PSR. Although some distress data exist, this information is inconsistent or unavailable for some pavement sections. In addition, the data sheets indicate that only a PSR category (e.g., 3-4 good) was chosen and not a specific value. The value

assigned to each section was the value at the midpoint of the scale. That is, if a section had a serviceability rating of *fair* (PSR = 2-3), a PSR value of 2.5 was assigned to that section. This misinterpretation complicated the analysis of the data.

Some of the data entries require further explanation. For example, the PSR for section 57009\_01 is given as 0 to 1, which indicates the pavement section is impassible. However, this pavement section is only 7 years old and has been exposed to fewer than 10 million ESAL applications. The condition rating appears to be in error, so this section was removed from the pavement performance analysis.

Section 57008\_04 contains 300 m (984 ft) of transverse cracking, whereas the other sections contain less than 25 ft (8 m) of transverse cracking. This section is the only JRCPC section, and JRCPC sections are designed to crack. These cracks relieve the curling stresses in the pavement, but they do not affect pavement performance if the reinforcing steel holds the cracks tight. However, these cracks have deteriorated to a medium-severity level, which may indicate that insufficient steel has been provided.

Section 57008\_02 contains considerably more longitudinal cracking (656 ft [200 m]) than the other pavement sections. The low PSR value for this section supports the high degree of cracking, so the data entry does not appear to be an error. However, no reasonable explanation for this high amount of longitudinal cracking can be deduced from the available information, especially because the other three sections from this project have sustained about the same number of ESAL's and are still in good condition (PSR = 3.5).

The expected trend of decreasing PSR with increasing age, ESAL's, and (age \* ESAL's) occurs, although some scatter is evident. The PSR shows a more defined trend when plotted as a function of ESAL's, which indicates that the performance of these sections is linked more to traffic loading than to aging effects. This effect is most likely caused by the heavy traffic loading experienced on highways in the United Kingdom.

#### *Prediction Model*

The PSR prediction model for the United Kingdom is only applicable to JPCPC sections. In addition, all sections used to develop the model contained longitudinal edge drains and dowel bars ranging from 20 to 30 mm (0.79 to 1.18 in) in diameter. Therefore, the model is limited to sections with these design features. The model is also limited to variables used to develop the equation (e.g., less than 20 years old and 100 million ESAL's and thicknesses between 250 and 305 mm [9.8 and 12 in]). The following model was developed from the available data:

$$PSR = 4.2561 - 0.0264 \text{ ESAL} - 2.460 \left( \frac{AGE}{THICK} \right) \quad (39)$$



$$\begin{aligned}
R^2 &= 0.78 \\
R^2_{\text{adj}} &= 0.74 \\
\text{SEE} &= 0.44 \\
N &= 13
\end{aligned}$$

where:

$$\begin{aligned}
\text{PSR} &= \text{Present serviceability rating.} \\
\text{AGE} &= \text{Time since construction, years.} \\
\text{ESAL} &= \text{Estimated 18-kip (80-kN) ESAL's, millions.} \\
\text{THICK} &= \text{PCC slab thickness, mm.}
\end{aligned}$$

A sensitivity analysis of the variables indicate that the prediction model is most sensitive to ESAL's. Again, the effects of the heavy traffic loadings have had a more pronounced effect on performance than climatic and aging effects. The thickness of the PCC slab is not a significant variable in the model.

#### *Examination of Design Features*

One design feature that affected pavement performance was the base type. All four sections with LCB have a PSR of 3.5, considerably higher than most of the other pavement sections. Every section with an aggregate base has a lower PSR than the sections with an LCB. Although some of the sections with a CTB have a higher PSR than the sections with LCB, their performance is very inconsistent. For example, four sections with a CTB have been exposed to approximately 40 million ESAL's, although the PSR ranges from 1.5 to 3.5. Although insufficient data exists to support a hypothesis, the reason for this phenomenon is probably erosion of the CTB, which leads to loss of support and pumping. The sections with a high PSR may not have eroded, whereas the other sections have eroded to some degree, leading to a drastic decrease in PSR. The sections with an LCB are also the only sections that contain three modernity elements.

The effect of slab thickness on pavement performance was also examined. The 10.8- and 11.8-in (275- and 300-mm) thick slabs follow a trend of decreasing PSR with the number of ESAL applications. However, the 9.8-in (250-mm) thick slabs are more scattered and do not follow this trend. The 9.8-in (250-mm) thick slabs seem to exhibit more longitudinal cracking. Although longitudinal cracking generally only occurs in thinner slabs, the higher axle loads in the United Kingdom may attribute to longitudinal cracking and, therefore, a lower PSR in some 9.8-in (250-mm) thick slabs.

Tied PCC shoulders transfer part of the load on the pavement across the longitudinal joint. However, AC or aggregate shoulders do not provide load transfer across the longitudinal joint, resulting in a free edge loading condition. The pavement sections with tied PCC shoulders have a higher PSR than the sections with AC or aggregate shoulders. Therefore, tied PCC shoulders are a positive design feature for the pavement sections from the United Kingdom.

Joint spacing can have a tremendous effect on the maximum stress that develops in a concrete slab. Longer slab lengths allow more bending in the slab from thermal curling, and therefore exhibit higher combined load and curl stresses. The sections with 16.4-ft (5.0-m) joint spacings follow the expected trend (decreasing PSR with ESAL's). However, the data for sections with 19.4-ft (6.0-m) joint spacings are quite scattered. Although no conclusions can be obtained from the limited data, one possible explanation is that the pavement sections are subjected to different temperatures and therefore exhibit different magnitudes of thermal curling.

## Belgium

Belgium has contributed 25 concrete pavement sections to the European COPES program. These sections represent three projects, located on three different highways. A summary of the design and performance of these sections is provided in the following sections.

### *Design Features*

The COPES sections from Belgium represent a variety of pavement designs, ages, and features. The data consist of 14 JPCP sections and 11 CRCP sections with longitudinal reinforcing steel ranging from 0.63 to 0.85 percent of the cross-sectional area. Initially, the CRCP sections were constructed using 0.85 percent reinforcing steel, which was placed 2.4 in (60 mm) from the surface. A 2.4-in (60-mm) bituminous interlayer was placed between the LCB and CRCP. Due to concerns over close crack spacings, the design was altered by reducing the steel reinforcement to 0.67 percent, moving the steel to 3.5 in (90 mm) below the surface, and removing the bituminous interlayer. Other characteristics of the Belgian pavement sections are described as follows:

- The sections range from 2 to 17 years old, with an average age of 9.1 years. Thirteen of the 25 sections are 10 years old. These sections are all located on the same highway and encounter the same traffic.
- Of the 25 sections, 19 sections have a slab thickness of 7.9 in (200 mm) and 6 sections have a slab thickness of 9.1 in (230 mm).
- The pavement sections contain two different base types: LCB and CTB. Five pavement sections contain an LCB with a thickness of 7.9 in (200 mm). The remaining 20 sections contain a CTB, with thicknesses ranging from 5.9 to 7.9 in (150 to 200 mm). The CRCP sections with 0.85 percent steel have a 2.4-in (60-mm) bituminous interlayer between the LCB and CRCP.
- All sections with available data are constructed on an A-3 subgrade.
- The slab widths range from 11.5 to 16.4 ft (3.5 to 5.0 m), and the joint spacings range from 11.5 to 18.0 ft (3.5 to 5.5 m).

- Twenty-one sections contain AC shoulders, one section contains an aggregate shoulder, and three sections contain turf shoulders.
- The number of modernity elements ranges from 0 to 3. The modernity elements in these sections consist of drainage (transverse or longitudinal edge drains), strengthened structure (CRCP or dowels), and a nonerrodible base (LCB). Three sections contain no modernity elements, five contain one modernity element, 12 contain two modernity elements, and five contain three modernity elements.

### *Climatic Information*

The freezing index is 502 degree-days for 9 sections and 626 degree-days for 16 sections. The higher freezing index value represents a harsher climate (more time below freezing). The annual precipitation is 34.6 in (878 mm) for all the Belgian sections. These climatic conditions are similar to those found in Pennsylvania.

### *Traffic Data*

For each section, only 1 year of traffic data was available, so assumptions were made regarding growth rates in traffic volumes and truck factors. Also, no tandem-axle data were available for determining the truck factor. Base on the limited data and assumptions, the number of ESAL applications ranges from 3 to 38 million, with an average of 22.8 million. The 13 sections in the 30-to-35 million ESAL range are all the same age and are all located on the same highway.

In Belgium, the legal load limit for single axles is 28,660 lb (13 tons), compared to the United States legal load limit of 20,000 lb (9.1 tons).<sup>(63)</sup> Therefore, for the same traffic volumes, pavements in Belgium can experience considerably more ESAL applications than pavements in the United States. Approximately 13 percent of the single axles are over the legal limit in the United States. According to the data, 15.3 percent of all axles encountered in the pavement sections in Belgium are tandem axles, although the distribution of these axles was not provided.

### *Prediction Model*

The Belgian model was developed for both JPCP and CRCP sections and includes a dummy variable to distinguish the pavement type. The sections used in the model included those with and without dowel bars and edge drains, as well as various base types and shoulder types. However, inclusion of these variables in the model did not increase the accuracy. The model is limited to the range of variables used in the development, such as sections less than 17 years old and less than 30 million ESAL's. The following model was developed for Belgium:

$$PSR=4.1826-0.1134AGE-0.00862ESAL+0.00152THICK+0.4763PTYPE \quad (40)$$

$$\begin{aligned}
R^2 &= 0.76 \\
R^2_{\text{adj}} &= 0.71 \\
\text{SEE} &= 0.33 \\
N &= 25
\end{aligned}$$

where:

- PSR = Present serviceability rating.
- AGE = Time since construction, years.
- ESAL = Estimated 18-kip (80-kN) ESAL's, millions.
- THICK = PCC slab thickness, mm.
- PTYPE = Dummy variable for pavement type (0 for JPCP, 1 for CRCP).

Age is the most significant variable in the equation, whereas thickness and ESAL's affect the model to a much lesser extent. CRCP sections have performed better than the JPCP sections, which is also evident in the model.

#### *Pavement Performance*

Section 58002\_14 has a high degree of longitudinal cracking, yet it has a higher PSR than sections on the same highway with the same number of ESAL applications. No reasonable explanation for this phenomenon can be deduced from the available information.

Section 58003\_02 has two modernity elements and has only encountered 8 million ESAL's, yet it has more longitudinal cracking and a lower PSR than any other section on this highway. One possible explanation is that the damage is due to improper joint forming during construction.

The PSR plotted as a function of age, ESAL's, and the product of age and ESAL's all show a trend of decreasing PSR as the variable increases, although some scatter in the data does exist. The trend is most evident in the plot of PSR as a function of age. The pavement sections in Belgium are subjected to a higher freezing index and more precipitation than the sections in the other European countries. Therefore, the PSR for these sections is more dependent on climatic effects.

The original CRCP design in Belgium consisted of 0.85 percent reinforcing steel and a bituminous interlayer. The average crack spacing on these sections were observed to be in the range of 16 to 24 in (400 to 600 mm), which was thought to be too low and would ultimately lead to fragmentation.<sup>(62)</sup> Thus, the design was altered to include 0.67 percent reinforcing steel and no bituminous interlayer. However, after 20 years of service, no fragmentation of the cracks has been observed on the original sections.<sup>(62)</sup> Crack spacings for the new design show a large variation, with an average crack spacing of 4.9 ft (1.5 m).<sup>(62)</sup>

## *Examination of Design Features*

Several design features appeared to have an effect on the performance of the Belgian sections. For instance, pavement type was shown to be a significant variable in the prediction model. The CRCP sections have shown better performance in terms of less distress and a higher PSR.

The effect of slab thickness on PSR was also examined. The 7.9- and 9.1-in (200- and 230-mm) thick slabs follow the same trend, with the PSR decreasing with the number of ESAL applications. The performance of the thicker sections is not superior to those of the thinner sections. Therefore, the extra thickness does not appear to be an effective means of improving performance.

The Belgian sections contain sections with a CTB and with an LCB. The performance of the sections with an LCB is not significantly better than the sections with a CTB, although the data are insufficient for a thorough investigation. Further investigation is needed to determine the effectiveness of the nonerodible base.

As previously mentioned, the Belgian sections are exposed to more severe climatic conditions than the other European sections. One indicator of climatic conditions is the freezing index, which shows a wide variation within the country. The sections with a freezing index of 502 are performing slightly better than the sections with a freezing index of 626. The environmental effects (e.g., frost heave, spring thaw, swelling soils) associated with the harsher climates contribute to the loss of serviceability.

The sections with three modernity elements exhibit better performance than the other sections. Although the total number of modernity elements can affect the overall performance of the sections, the use of certain modernity elements may provide a better indicator of performance.

## Switzerland

Switzerland has contributed 19 concrete pavement projects to the study. Between 2 and 13 sections are represented within each project. However, complete performance data are not available for each particular pavement section. The available performance data represents the mean values of the measurements within each section.

### *Design Features*

The COPES sections in Switzerland consist of a variety of pavement designs, ages, and other features. Two of the 19 pavement projects are JPCP designs (no reinforcing steel in the slab, although the joints contain dowel bars). The remaining 17 sections are JRCP designs containing light reinforcement (wire mesh weighing less than 2.5 kg/m<sup>2</sup> [0.51 lb/ft<sup>2</sup>] of pavement surface). Although exact wire diameters and spacing are not known, this amount of reinforcing steel corresponds roughly to 0.07 to 0.11

percent of the cross sectional area, assuming a lane width of 4 m (13 ft) and a slab thickness of 180 to 230 mm (7 to 9 in). The following design features and conditions are representative of the Swiss sections:

- All the Swiss pavement sections are more than 10 years old, and four sections are more than 40 years old.
- The slab thickness ranges from 170 to 220 mm (6.7 to 8.7 in); the majority of the sections are either 180 or 200 mm (7.1 or 7.9 in) thick. In addition, the majority of the concrete slabs are placed in two layers that differ in composition. The bottom layer has a cement content of 250 kg/m<sup>3</sup> (421 lb/yd<sup>3</sup>), contains rounded aggregates, and is not air entrained. The top layer, which is constructed of higher quality materials in order to control abrasion of the surface, is placed directly on the underlying layer while still fresh. The top layer has a cement content of 350 kg/m<sup>3</sup> (590 lb/yd<sup>3</sup>), contains crushed stone and rounded aggregates, and is air entrained to produce an air content between 4.5 and 5.5 percent.
- A variety of base types are represented by the Swiss pavement sections. Some projects contain more than one base type, although design and performance data for each particular section can not be distinguished given the available data. For example, the project on Highway Erstfeld-Amsteg contains four pavement sections, which contain either an aggregate or asphalt-treated base.
- Most of the Swiss pavement sections have joint spacings of either 5.0, 6.0, or 8.0 m (16.4, 19.7, or 26.2 ft). Two sections have a joint spacing of 10.0 m (32.8 ft), and one section has a joint spacing of 11.5 m (37.7 ft).
- All of the Swiss pavement sections are equipped with dowel bars at the transverse joints. The dowel diameter varies from 16 to 22 mm (0.63 to 0.87 in), which are small compared to those usually used in the United States (typically 32 mm [1.25 in]). Small diameter dowel bars can lead to high faulting levels.
- Most of the projects contain drainage features. Drainage is achieved either through the use of longitudinal edge drains (of diameter varying from 50 to 100 mm [2 to 4 in]) or through the placement of both longitudinal and transverse drains. However, three projects are reported as containing no drainage features, and another five sections are unknown.
- Most of the European COPES projects from Switzerland include either AC or aggregate shoulders; only two projects have concrete shoulders. In addition, five projects do not have any prepared shoulder.
- The Swiss pavement sections contain either one or two modernity elements. These modernity elements include drainage (transverse and longitudinal drains) and strengthened structure (dowel bars).

### *Climatic Information*

The freezing index varies from 100 °C-days (180 °F-days), which corresponds to a mild climate, to 1000 °C-days (1800 °F-days), which corresponds to a very cold climate. The average annual precipitation varies from 790 to 1800 mm (31 to 71 in). The maximum monthly average temperature varies from 14.6 to 21.4 °C (58.3 to 70.5 °F), and the minimum monthly average temperature varies from -3.1 to 2.8 °C (26.4 to 37.0 °F).

### *Traffic Data*

Of the 19 Swiss projects, 15 projects have sustained less than 10 million ESAL applications, with 7 projects sustaining less than 5 million ESAL applications. The mean traffic per year ranges from 20,000 ESAL's to 680,000 ESAL's with a mean of 280,000 ESAL's. These traffic levels are somewhat lower than the traffic levels experienced in other European countries.

### *Pavement Performance*

The performance data for the outer traffic lane (heaviest traveled lane) of the projects in Switzerland are summarized in appendix B of volume IV. For the most part, the expected trends are apparent. The PSR was found to decrease with an increase in age, ESAL's, and (age \* ESAL's). The relationships for Switzerland are not as pronounced as for the other European countries. One possible explanation is that the older projects have been subjected to rehabilitation activities, which would result in higher PSR values.

The previous analyses focused mainly on the performance of the pavement sections in terms of PSR. However, several distress types (pumping, cracking, spalling, and faulting) were also measured. With the exception of faulting, the Swiss pavements do not exhibit a significant amount of distress. Although 8 projects do not exhibit significant faulting levels (less than 2.5 mm [0.10 in]), 9 projects exhibit faulting levels greater than 2.5 mm (0.10 in), with three of these projects exhibiting faulting levels greater than 5.0 mm (0.20 in).

Other distress types were not as prevalent on the Swiss pavement sections. None of the projects exhibited any visual signs of pumping. The measurements given for cracking and spalling represent the amount of distress over the 200 m (650 ft) survey section. The pavement sections do not exhibit a significant amount of transverse or longitudinal cracking. Likewise, the majority of the pavements exhibit spalling at less than 10 percent of the transverse joints.

### *Prediction Model*

Two prediction models were developed for Switzerland: a joint faulting model and a PSR model. The faulting model was developed using both JPCP and JRCP projects, although all pavements were doweled. Thus, the model is only applicable

for doweled pavements. In addition, the model is only valid for the range of design features used in the development, such as slab thickness between 170 and 220 mm (6.7 and 8.7 in). The joint faulting model has the following form:

$$FAULT = ESAL^{0.25} \times AGE \times PRECIP(7.41 - 2.20LONG - 2.10TRANS) \times 10^{-5} \quad (41)$$

$$\begin{aligned} R^2 &= 0.57 \\ SEE &= 1.24 \\ N &= 16 \end{aligned}$$

where:

- FAULT = Joint faulting, mm.
- ESAL = Estimated 80-kN (18-kip) ESAL's, millions.
- AGE = Time since construction, years.
- LONG = Presence of longitudinal drainage (1 if yes; 0 if no).
- TRANS = Presence of transverse drainage (1 if yes; 0 if no).
- PRECIP = Mean annual precipitation, mm.

A sensitivity analysis of the key variables in the model indicate the model is about equally sensitive to changes in age and ESAL's. The addition of longitudinal and transverse drainage was found to reduce faulting significantly.

A model predicting the pavement serviceability (PSR) based on the design factors was also developed. The JPCP pavement sections were not included in the development of the PSR prediction model. Therefore, the model is only applicable for JRCPP with dowel bars. The following PSR prediction model was developed from the available data:

$$PSR = 4.23 - \frac{AGE}{THICK} (3.1 + 0.1 ESAL) \quad (42)$$

$$\begin{aligned} R^2 &= 0.48 \\ SEE &= 0.27 \\ N &= 27 \end{aligned}$$

where the variables are the same as previously defined. The model has an acceptable level of SEE, but the low  $R^2$  indicates that the model accounts for less than half of the variability.

A sensitivity analysis of the key variables in the PSR model shows the model is most sensitive to pavement age, although the effect of ESAL's is also significant. Slab thickness, on the other hand, did not have a major influence on PSR. However, it should be noted that most of the PSR values for the Swiss projects were within a small range (3.5 to 4.5). As a result, the curve is fairly flat. The use of the average



PSR value for all sections within a given project is likely responsible for this smaller range in performance.

### *Examination of Design Features*

The performance models denote a strong correlation between pavement performance and age and ESAL's. The use of longitudinal and transverse drains were also found to significantly influence the amount of faulting on the pavement sections.

Although one might expect pavements with shorter slabs to perform better, the data did not support this conviction. One possible explanation for this phenomenon is that the effect of joint spacing was confounded by other factors affecting pavement performance, such as pavement thickness or base type.

The effect of slab thickness on pavement performance was also examined. Overall, the data indicate a trend of decreasing PSR with increasing age and ESAL's at all thickness levels. The thicker slabs also appear to be performing better. Most of the 210- and 220-mm (8.3- and 8.7-in) slabs are relatively young, however, and long-term comparisons can not be made with the thinner slabs.

### **Overall Evaluation of European Pavement Performance**

This section presents an overall examination of the data collected under the European COPES program. The European practices in concrete pavement design are summarized, along with a discussion of the performance achieved. The discussion includes a comparison of the design features and performance of concrete pavements in Europe to those in the United States. The data for the U.S. sections used in this report were collected under the concrete pavement performance study conducted by Smith et al. <sup>(2-6)</sup>

### Design Features

The European COPES data base includes a wide variety of pavement sections in terms of pavement design, age, and applied traffic. In general, the design practices in Europe do not seem to vary drastically from one country to another, and for the most part, the designs are similar to the ones used in the United States. The following sections illustrate the range of design features encountered in the European COPES sections that were examined.

#### *Pavement Age*

The overall average age of the pavement sections evaluated is 14.3 years. Over half the sections are 10 years old or younger. Most of the sections that are more than 25 years old are located in Switzerland.

### *Pavement Type*

The predominant pavement type among the European COPES sections is JPCP, which account for about two-thirds of the sections evaluated. The JRCP sections make up 22 percent of the sections, with the remaining 11 percent being CRCP. All of the CRCP sections included in the European COPES program are from Belgium. It is unknown whether this distribution is representative of pavement types in other European countries. One source reports that JPCP is the most common type of concrete pavement in Europe, and the use of CRCP is most common in Belgium and France.<sup>(63)</sup>

### *Joint Spacing*

The joint spacings for the JPCP sections typically range from 14.8 to 16.4 ft (4.5 to 5.0 m); however, one section in France has a joint spacing of 32.8 ft (10 m), and four sections in the United Kingdom have a joint spacing of 19.7 ft (6 m). With the exception of the single long-jointed section in France, the joint spacings for the European COPES sections are well within the maximum recommended joint spacing for JPCP (24 times the slab thickness). The joint spacings for the JRCP sections range from 16.4 to 82.0 ft (5 to 25 m).

### *Slab Thickness*

Slab thicknesses range from 6.7 to 20.1 in (170 to 510 mm), but the majority of the sections fall under three thickness categories: less than 8 in (201 mm), 8 to 10 in (201 to 250 mm), and 10 to 12 in (251 to 300 mm). A significant number of sections are also in the (14-to-16 in (350-to-400 mm) range). Considering that a 2-in (50-mm) difference in the slab thickness can mean an order of magnitude difference in fatigue life of concrete pavements, this represents a considerable range in structural capacity. In comparison, 77 percent of the U.S. sections fall under one thickness category (the 8-to-10 in [201-to-250 mm] range).

### *Base Type*

The European COPES sections were constructed with a wide variety of base types. Stabilized bases are used extensively in the European COPES sections; over 70 percent of the sections evaluated have either a stabilized base or a lean concrete base. The most common type of base is the cement-treated base, followed by the lean concrete base, the asphalt-treated base, and the aggregate base. In the United States, the use of aggregate bases is more common than the use of stabilized bases.

### *Dowels and Drainage*

Doweled transverse joints and drainage are highly effective in minimizing the amount of pumping and faulting in jointed concrete pavements. With the exception of the French sections, dowels are provided in the transverse joints of nearly all sections. Generally, the dowel diameter ranges from 0.79 to 1.18 in (20 to 30 mm).

Nearly all of the European COPES sections evaluated were provided with either edge drains or transverse drains.

### *Lane Width and Shoulder Type*

The other design features that can have a significant effect on the performance of concrete pavements include widened traffic lanes and tied concrete shoulders. These design features are effective for extending the fatigue life of concrete pavements by reducing the critical stresses in the slab. The normal lane width for European COPES sections ranges from 11.5 to 12.3 ft (3.5 to 3.75 m), but widened lanes are also used. Six sections in Belgium and two sections in Italy are provided with traffic lanes that are 13.1 to 17.2 ft (4.0 to 5.25 m) wide. Concrete shoulders are also used, but it does not appear to be a common design feature. As in the United States, the majority of the concrete pavements in Europe are provided with AC shoulders, although the use of aggregate shoulders seems quite common in Europe.

### *Modernity Elements*

In comparison to the concrete pavements in the United States, the pavements in Europe are provided with more features that are expected to promote long-term performance (modernity elements). A much greater proportion of the European sections have two or more modernity elements (75 percent for Europe versus 25 percent for the United States). The significance of modernity elements to concrete pavement performance is discussed later.

### Climatic Information

The environmental exposure conditions for all of the sections are similar and are characteristic of wet-freeze environmental conditions. The annual precipitation for the sections ranges from about 400 to 875 mm (15.7 to 34.4 in) with the exception of three sections in Italy. The freezing index for the sections ranges from about 300 to 600. Because of the uniformity in the environmental conditions, special consideration of the environmental effects did not appear to be warranted.

### Traffic Data

As described earlier, the traffic on the European sections is very heavy. Although the truck volumes are similar to those on major U.S. highways, the axle loads are substantially higher. The legal maximum loads for single axles in Europe range from 22,000 to 28,600 lb (98 to 128 kN).<sup>(63)</sup> The legal tandem axle load in Europe ranges from 41,900 to 46,300 lb (186 to 205 kN), and the legal tridem axle load limit is 52,900 lb (235 kN). The consequence of the heavy axle loads and the longer design periods used in Europe is extremely high design ESAL's. About 35 percent of the European sections have sustained more than 30 million ESAL's.

Over 80 percent of highways in the United States receive less than 0.5 million 80-kN (18-kip) ESAL's per year. In comparison, 44 percent of European sections receive

more than 2 million ESAL's per year. The traffic data shown for the U.S. sections are not fully comparable to the European COPES sections because the U.S. pavement sections are not all located on major traffic routes. However, 1 million ESAL's per year is typically considered very heavy traffic in the United States, and the typical design period in the United States is 20 years (as opposed to the design period of 30 to 40 years commonly used in Europe).

### Pavement Performance

As previously mentioned, some limitations in the completeness of the available data prevented extensive analysis of overall pavement performance. Although only a qualitative analysis was made for this report using the PSR, pavement age, and traffic as the principal parameters, a number of interesting performance trends were observed. The possibility of developing PSR-based performance models, much like the AASHTO models, is a consideration for future analysis. Further information regarding the design practices and performance of European concrete pavements can be found in the literature. <sup>(63,83,84)</sup>

#### *PSR Trends*

Because both the environmental effects and the traffic loads are responsible for pavement deterioration, the pavement condition is expected to deteriorate with increasing age and traffic. Plots of PSR as a function of age, ESAL's, and the product of age and ESAL's were developed to analyze the sections. Although the plots did show a general trend, considerable scatter in the data were evident. Some scatter may be expected because the plots include data from all European sections, regardless of the pavement type, slab thickness, or any other design features. Some of these design features are expected to have a significant effect on pavement performance.

Several different design features were examined as to their effect on pavement performance. In some cases, the use of certain design feature resulted in significantly improved performance. However, in most cases, the data were either insufficient or inconclusive to determine the effect of a particular design feature. For example, enough data were not available to determine the effects of reinforcement. Also, because the joint spacing for the majority of JPCP sections falls within a narrow range of 14.8 to 16.4 ft (4.5 to 5 m), the effects of joint spacing on pavement performance could not be examined.

For the sections included in the European COPES data base, the pavement type did not appear to significantly affect pavement performance. The only noticeable trend was that CRCP may give better, and perhaps more consistent, performance than jointed concrete pavements.

The pavement sections with LCB perform better than those with other base types. However, further investigation may be warranted to determine the reason that those particular sections performed better. The majority of the European COPES sections

with the LCB are JPCP, and the use of a very stiff base under JPCP requires a careful evaluation to avoid cracking due to excessive thermal curling stresses.

The effects of slab thickness, dowels, and drainage on concrete pavement performance were also examined. However, none of the factors showed any significant trend. This does not mean that such important design features as slab thickness, dowel bars, and drainage do not have any effect on pavement performance; it only means that the effects of these variables on pavement performance could not be determined with the available data. The distress data required to make such a determination include cracking, spalling, and faulting.

#### *Effects of Modernity Elements on PSR Trends*

Another way to evaluate the data is to group them by the number of modernity elements. The pavement sections with three or more modernity elements give better and more consistent performance than other sections. Unfortunately, 14 of the 15 sections having three or more modernity elements also have an LCB. With the available data, it is not possible to determine whether the LCB or the combination of having three or more modernity elements provided the superior performance. Although it is more likely that having three or more beneficial design features, and not a single design feature, led to the improved performance, this cannot be shown conclusively.

Although the modernity coefficient concept is a useful tool, it does not distinguish between the different design features. Because different design features have different relative effects on pavement performance, the modernity coefficient is only an approximate indicator of the design quality of a concrete pavement, especially if the pavement contains only one or two modernity elements. However, for pavements with three or more modernity elements, the modernity coefficient may be a reasonably consistent measure of design quality.

#### *Comparison of Performance With the U.S. Sections*

Because of the significant differences in pavement age and applied traffic, the only comparison that could be made between the performance of the European COPES sections and the U.S. sections was that of the PSR versus age. Despite all of the differences, the performance of the European sections and the U.S. sections are comparable. The variability associated with the performance of the U.S. sections may appear to be less than that associated with the European sections, but a comparison of the PSR plots shows that the variabilities are about the same. However, the comparisons are not completely valid, as the conditions and design features in Europe and the United States are often very different. For instance, 44 of the 96 European sections (46 percent) have carried more than 20 million ESAL applications, compared to only 4 of 303 sections (1 percent) in the United States.

## Summary of Important Findings

A qualitative analysis was conducted for this report using the PSR, pavement age, and traffic as the principal parameters. Although this was the only detailed analysis conducted for this report, a number of interesting performance trends were observed. The following presents a summary of the observations from the European COPES data and the results of the analysis:

- The most common type of concrete pavement in Europe appears to be JPCP. The JPCP sections made up two-thirds of the sections evaluated for this report.
- Stabilized bases are used extensively in Europe; over 70 percent of the sections evaluated have either a stabilized base or a lean concrete base.
- Nearly all sections are provided with drainage. Except for many sections in France, most sections are also provided with dowels at the transverse joint.
- A much greater proportion of the European sections have two or more modernity elements (75 percent for Europe versus 25 percent for the United States).
- The sections are subjected to similar climatic conditions that are characteristic of a wet-freeze environmental region.
- European highways are subjected to very high traffic loads. The high design ESAL's are a result of the high legal axle loads and long design life (30 to 40 years) that are common in Europe.
- With the available data, the effects of slab thickness, dowels, and drainage on pavement performance could not be established.
- The base type was found to have significant effect on pavement performance. The sections provided with LCB performed better than those provided with other base types; however, further investigation may be needed to determine whether the improved performance is solely attributable to LCB. None of the European sections contain a permeable base.
- The pavement sections with three modernity elements performed better than those with two or fewer; however, 14 of 15 sections having three modernity elements are LCB sections. Although it is suspected that the combination of three beneficial design features, rather than LCB alone, led to the improved performance, this could not be shown conclusively.
- Detailed distress data are available for only Switzerland, thus preventing the development of distress prediction models. However, serviceability data are available for most sections and models predicting the serviceability over time were developed for each country except Italy, which had too few sections for

model development.

- The serviceability of the European sections with time and traffic was compared to the serviceability of a sampling of U.S. sections. The comparison revealed similar trends, although the European sections have been exposed to far greater ESAL applications than the U.S. sections.

The above observations and conclusions were made based on a qualitative analysis of limited data. Further investigations may be needed to verify some of the findings.

### **Evaluation of Chilean Concrete Pavement Performance**

Toward the end of the 1970's, an extensive reconstruction program of the most deteriorated sections of the Chilean highway network was initiated by the Highway Division of the Chilean Ministry of Public Works. In 1984, the Chilean Directorate of Roads initiated a research project for controlling and monitoring both asphalt concrete (AC) and portland cement concrete (PCC) pavements in Chile. The study involved the analysis of the field performance of 39 specific test sections—21 concrete pavements and 18 asphalt pavements. The study was conducted on in-service pavements using ordinary design and construction techniques. Most of the sections were selected after being constructed and opened to traffic.

The main objective of the research project was to develop performance prediction models for feeding economic evaluation systems that are aimed at better allocating financial resources.<sup>(85)</sup> A secondary objective is the development of a rehabilitation schedule (both routine maintenance and major rehabilitation) that can be applied to in-service pavements.<sup>(85)</sup> To meet these objectives, the University of Chile was assigned the task of modeling the structural deterioration of the concrete pavements, which were designed and constructed under general AASHTO guidelines and specifications.

This section provides a summary of the report, *An Evaluation of Chilean Concrete Pavement Performance*, which documents the performance of the 21 concrete pavement sections included in the Chilean monitoring study and is presented in appendix C of volume IV. Unfortunately, monitoring of Chilean concrete pavements was not conducted in accordance with standardized procedures used by other countries. Thus, a complete set of data variables is not available for these sections. However, extensive field measurements were made on these sections that were not performed on the COPES or LTPP sections. The data collected for this report were obtained from various reports documenting the results of the Chilean study.

The Chilean sections represent pavements with a range of design features, including varying slab thickness, different base types, and different drainage elements. In addition, the various sections are exposed to a wide range of climatic conditions (e.g., precipitation and temperature) and traffic loadings. However, every section is a jointed plain concrete pavement (JPCP) design with no dowel bars at the transverse joints. Some sections were constructed on new alignment, and others were

constructed over existing AC or PCC pavements.

### Instrumentation

All of the 21 concrete pavement sections were instrumented. Sensors were installed in each of the sections to measure the temperature distribution through the slab. Deep reference bases were also installed to measure absolute vertical displacements of the slabs. In addition, reference bases were installed at joints to measure horizontal movements and faulting.

Each deep reference base is equipped with a steel bar grouted in the subsoil 11.5 ft (3.5 m) beneath the pavement and is isolated from lateral confinement by a PVC casing. Absolute deflections of the loaded slabs are recorded with  $\pm 0.0004$  in (0.01 mm) accuracy by means of an analog/digital system. Four deep reference bases were installed in the leave slab, and an additional base was installed in the approach slab. The five simultaneous deflection signals are processed and monitored in the field along with the internal temperature signals, which are measured continuously at five levels in the slab with  $\pm 0.4$  °F (0.2 °C) accuracy. The devices and locations are illustrated in appendix C.

### Data Analysis

Given the level of effort that has been expended on the collection of the performance data, considerable interest exists in the analysis of the data. Reports have been published documenting the design and construction of the various concrete pavement sections, as well as annual reports documenting the performance of the sections. In addition, researchers at the University of Chile have published several reports documenting the analysis of various performance data.

### Design Features

Table 142 provides detailed design and construction information for each of the concrete pavement sections. As indicated in this table, the Chilean concrete pavement sections consist of a variety of design features, construction dates, and climatic conditions. The following design features and conditions are representative of the Chilean sections.

- The pavement sections were all constructed between 1975 and 1985, with 19 of the 21 sections constructed during a 5-year period between 1981 and 1985.
- All of the pavement sections are JPCP designs without dowel bars at the transverse joints.
- The slab thicknesses range from 8.3 to 10.2 in (210 to 260 mm), with an average slab thickness of 8.9 in (227 mm). The majority of the sections (17 of 21) have slab thicknesses between 8.3 and 9.1 in (210 and 230 mm).



Table 142. Design information for Chilean concrete pavement sections.

Test Section	Location	Const. Date	Pavement Type	Thickness, mm (in)	Dowels	Slab Width, m (ft)	Joint Spacing, m (ft)	Skew, cm (in)	Base Type	Subbase Type	Drainage	Shldr Type	Subgrade (USCS)
1	Longotoma	1983	JPCP	230 (9.1)	No	3.5 (11.5)	3.7-4.6 (12.1-15.1)	46 (18)	CTB	AC	Edge	AC	ML
2	Las Chilcas	1981	JPCP	230 (9.1)	No	3.5 (11.5)	4.5-5.4 (14.8-17.7)	46 (18)	CTB	PCC	None	AC	CL
3	Lampa	1984	JPCP	240 (9.4)	No	3.5 (11.5)	3.4-3.6 (11.2-11.8)	74 (29)	CSB	PCC	Edge	AC	CH
4	Lo Vásquez	1985	JPCP	260 (10.2)	No	3.5 (11.5)	3.4-3.6 (11.2-11.8)	46 (18)	CSB	GRM	Edge	AC	SM
5	Talagante	1975	JPCP	220 (8.7)	No	3.5 (11.5)	3.4-5.4 (11.2-17.7)	53 (21)	GRB	GRM	None	AC	GC
6	Paine	1983	JPCP	240 (9.4)	No	3.5 (11.5)	4.2-4.6 (13.8-15.1)	66 (26)	GRB	AC	None	AC	SP
7	Graneros	1983	JPCP	250 (9.8)	No	3.5 (11.5)	3.6-4.6 (12.1-14.1)	66 (26)	GRB	PCC	None	AC	GP
8	San Fernando	1983	JPCP	230 (9.1)	No	3.5 (11.5)	3.7-4.3 (12.1-15.1)	-55 (22)	CTB	PCC	None	AC	SM
9	San Rafael	1983	JPCP	230 (9.1)	No	3.5 (11.5)	3.7-4.6 (12.1-15.1)	41 (16)	CTB	AC	Edge	AC	SM
10	Cocharcas	1982	JPCP	210 (8.3)	No	3.5 (11.5)	4.5-4.6 (14.8-15.1)	71 (28)	GRB	PCC	None	AC	GP
11	Concepción	1984	JPCP	230 (9.1)	No	3.5 (11.5)	3.5 (11.5)	0 (0)	CTB	AC	Edge	AC	ML
12	Cabrero	1984	JPCP	220 (8.7)	No	3.5 (11.5)	3.5-3.6 (11.5-11.8)	-66 (26)	CSB	PCC	Edge	AC	SC
13	Laja	1982	JPCP	210 (8.3)	No	3.5 (11.5)	4.4-4.6 (14.4-15.1)	0 (0)	CTB	PCC	None	AC	SP
14	Cta. Esperanza	1979	JPCP	210 (8.3)	No	3.5 (11.5)	4.3-4.8 (14.1-15.7)	59 (23)	CTB	PCC	None	AC	SM
15	Victoria	1984	JPCP	230 (9.1)	No	3.5 (11.5)	4.0 (13.1)	75 (30)	CSB	PCC	Edge	AC	ML
16	Temuco	1981	JPCP	210 (8.3)	No	3.5 (11.5)	4.4-4.6 (14.4-15.1)	59 (23)	CTB	PCC	None	AC	CL
17	Gorbea	1983	JPCP	220 (8.7)	No	3.5 (11.5)	4.5 (14.8)	84 (33)	GRB	GRM	Edge	AC	GM
18	Loncoche	1984	JPCP	220 (8.7)	No	3.5 (11.5)	3.8-4.3 (12.5-14.1)	62 (24)	CTB	GRM	Edge	AC	CL
19	Mariquina	1983	JPCP	230 (9.1)	No	3.5 (11.5)	4.4-5.0 (14.4-16.4)	42 (17)	CTB	PCC	None	AC	ML
20	Mafil	1983	JPCP	230 (9.1)	No	3.5 (11.5)	4.3-4.6 (14.1-15.1)	79 (31)	GRB	GRM	None	AC	GM
21	Ro Bueno	1983	JPCP	220 (8.7)	No	3.5 (11.5)	4.5 (14.8)	59 (23)	CTB	PCC	None	AC	ML

- Three different base types are represented in the Chilean concrete pavement sections. Six sections contain a granular base (GRB), 4 sections contain a cement-stabilized base (CSB), and 11 sections contain a cement-treated base (CTB). Cement-stabilized bases consist of high quality granular materials treated with about 1 to 2 percent portland cement by weight, whereas cement-treated bases typically contain around 3 to 4 percent cement by weight.
- The type of subbase (or layer between the base and subgrade) also varies for the Chilean sections. Five pavements were constructed on a granular subbase (GRM), and the remaining sections were constructed on existing AC pavements (4 sections) or PCC pavements (12 sections).
- Table 142 presents the subgrade type for concrete pavement sections in accordance with the Unified Soil Classification System (USCS). Nine sections are constructed on silty or clayey soils, seven on sandy soils, and five on gravels.
- Most of the sections (17 of 21) employ random joint spacings, with joint spacings ranging from 11.5 to 18.0 ft (3.5 to 5.5 m), although the spacings are often not repeated in a regular pattern, as usual. Some differences in joint spacing are a result of inaccurate sawing and not part of the design. Over half the sections have maximum joint spacings ranging from 14.8 to 16.1 ft (4.5 to 4.9 m).
- The transverse joints range from nonskewed to a skew of one-sixth of the slab width. The joints are created by inserting fiber strips and sawing to a depth of about one-fourth of the slab thickness.
- Nearly half of the Chilean sections contain drainage features. Nine sections contain longitudinal edge drains, and the remaining 12 sections do not incorporate any drainage features.
- All of the Chilean concrete pavement sections employ shoulders consisting of compacted granular material topped with an asphaltic surface treatment.
- The slab widths are all 11.5 ft (3.5 m).
- One section contains 2 modernity elements and 8 sections contain 1 modernity element, whereas the remaining 12 sections do not contain any modernity elements. The sections with at least one modernity element incorporate drainage (specifically, longitudinal edge drains); the section with two modernity elements also contains a strengthened structure (slab thickness greater than 10 in [250 mm]).

## Climatic Information

The amount of precipitation and the thermal conditions at a given location are two properties that influence concrete pavement performance. The amount of precipitation provides an indication of the amount of free moisture to which the pavement is exposed. Although the amount of precipitation is not by itself an indicator of severe moisture conditions (one must also consider the relative evapotranspiration and the drainage characteristics of the pavement), it can provide some insight into the prevailing moisture conditions.<sup>(81)</sup>

Figure 69 shows the location of the Chilean concrete pavement sections and the number of days with heavy rainfall (greater than 0.2 in [5 mm] per day). The number increases southward, varying from less than 15 days at the section farthest north (section 1) to more than 120 days at the section farthest south (section 21). The majority of these heavy rains occur during the winter. Consequently, ambient humidity is far from saturation during the rest of the year, with strong hydro-evaporation conditions predominating.<sup>(86)</sup>

The freezing index indicates the amount of time throughout the year that the pavement is subjected to temperatures below freezing; it is the summation of the number of degrees that the average daily temperature is below freezing for each day throughout a year.<sup>(81)</sup> However, ambient temperatures where the sections are located are mild, with no significant differences along the concrete test sections. As a result, the sections are unaffected by frost conditions, and the freezing index is not a factor for these sections. Based on the climatic data provided, the prevailing climatic conditions in Chile are approximately comparable to those in the southern regions of the United States.

## Traffic Data

Traffic on the Chilean sections consist of a variety of different axle types and weights, which was expressed in terms of an equivalent number of 18-kip (80-kN) ESAL applications. The distribution of axle loads for each axle type on the Chilean sections was available. This information indicated that heavy ESAL loadings are not uncommon, as many are above the legal load limits in the United States. For example, 23 percent of the single axles are greater than 20,000 lb (90 kN), the legal limit for single axles in the United States.

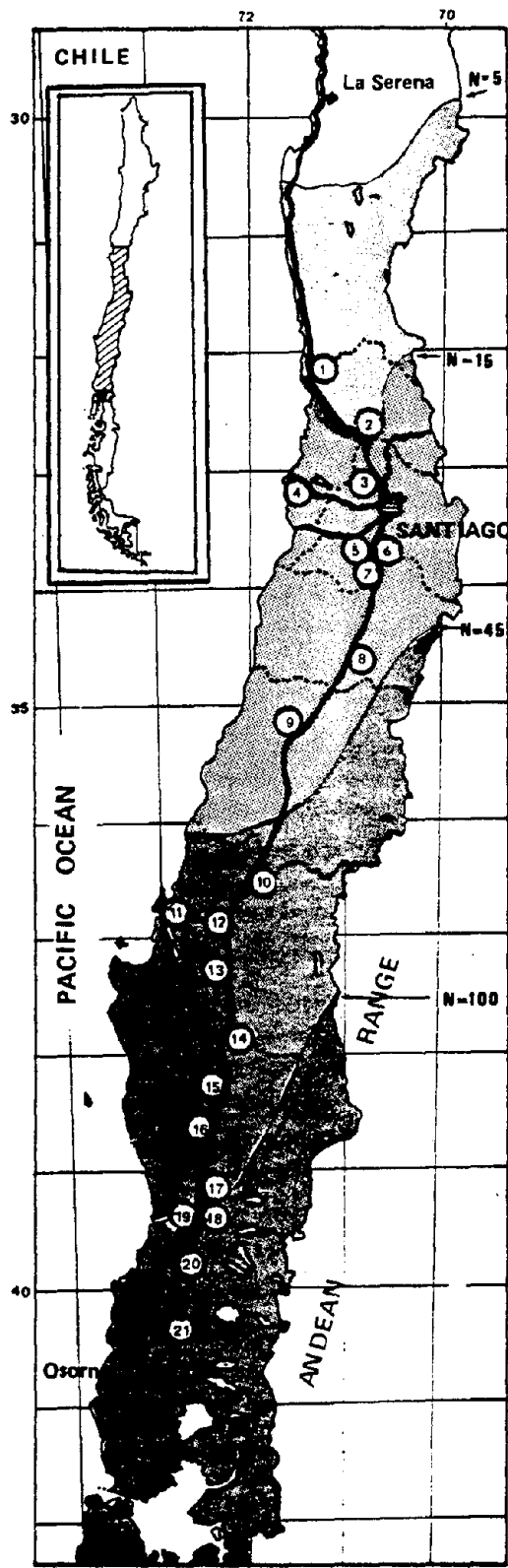


Figure 69. Days per year (N) of heavy rainfall.<sup>(85)</sup>

Based on the given information, the number of ESAL's for each load category and the mean ESAL's for a given axle type were determined. The mean 18-kip (80-kN) ESAL's for a single-axle load is 1.12; that is, the average single-axle load inflicts the same amount of damage as 1.12 18-kip (80-kN) ESAL's. Similarly, the mean 18-kip (80-kN) ESAL's for tandem-axle and tridem-axle loads are 0.40 and 0.83, respectively. This information, in conjunction with the number of each axle type per truck, was used to estimate the average truck factor. For the Chilean sections, the average truck produces the same damage as 2.8 18-kip (80-kN) ESAL's.

In general, adequate information was available for estimating the ESAL's, although assumptions had to be made in some instances. The number of ESAL's through 1991, the time at which most of the distress data were available, was estimated for the Chilean sections. Fourteen of the 20 sections have sustained between 2 and 6 million ESAL's, or approximately 500,000 ESAL's per year. Only three sections have been subjected to more than 10 million ESAL's; these sections are all located near Santiago, where traffic levels are higher than in other parts of the country. Data were not available for test section 14, which is why only 20 sections are represented.

### Pavement Performance

Complete performance data are not available for all of the 21 pavement sections included in the evaluation. For example, the present serviceability rating (PSR), which is an important measure of concrete pavement performance, is not available for any of the Chilean sections. Similarly, some distress measurements are only available for a limited number of the sections. These limitations greatly restrict the extent of the analyses that can be conducted on the pavement sections. On the other hand, some distress measurements, such as transverse cracking and faulting, are available for nearly every pavement section.

Another factor complicating the comparison of the performance of the various pavement sections is that they were not constructed as experimental sections with the sole purpose of evaluating design features. Although many of the sections are located on the same highway, they are often constructed in different years and with similar (if not the same) design features. Direct performance comparisons are infrequent, and even when possible, they are difficult because of differences in traffic loadings and aging/climatic effects. However, the range of traffic loadings and climatic conditions allows these effects to be more adequately evaluated.

Because of the absence of complete performance data, and because of the difficulty in making direct comparisons between different pavement sections, a more general evaluation of the performance of the Chilean concrete pavement sections was conducted. The purpose of this type of evaluation is to examine the overall performance of the various pavement sections and to identify general performance trends.

### *Upward Concavity*

Through several years of periodic monitoring of the Chilean concrete test sections, researchers at the University of Chile are convinced of the existence of an upward concavity in all concrete slabs. This condition has resulted in the slab edges being unsupported most of the time and thus, an increase in the presence of various distress types. The causes of this condition are believed to be the result of a combination of three conditions:

- Negative thermal gradients in the slab.
- Moisture differentials between the top and bottom of the slab.
- Irreversible drying shrinkage immediately after construction.

These factors are all related to climatic conditions that are prevalent in the central region of Chile.

Due to the additive effects of these three conditions, a predominant upward concavity in the concrete slabs is prevalent. This upward concavity appears to be controlling the structural condition of the Chilean concrete pavements. Downward curling of the slabs, often considered as critical, only occurs during the first hours of high solar radiation of a sunny summer day while the edges are free to rotate.<sup>(87)</sup>

Temperature differentials between the top and the bottom of the slab have been shown both experimentally and analytically to cause significant deformation of the slab. This temperature differential is often expressed in terms of a thermal gradient, or a change in temperature per unit length. Positive thermal gradients (warmer at the top of the slab) curl the slab downward at the corners, creating a maximum tensile stress at the bottom of the slab midway between the joints. Negative thermal gradients, on the other hand, cause an upward curling of the corners, producing a tensile stress at the top of the slab midway between the joints.

Measurements of internal slab temperatures were conducted at five depth locations within the slab using thermal sensors. Based on these measurements during a sunny day, a positive thermal gradient was found to exist from approximately 10 a.m. to 6 p.m., with negative thermal gradients occurring the remainder of the time.<sup>(86)</sup> Negative thermal gradients, which cause an upward curling of the slab, occur about two-thirds of the time.

These same temperature changes in the slab also result in horizontal slab movements, with the slab contracting as it cools and expanding as it warms. The horizontal slab movements were measured at transverse joints near the outer edge at 5 times throughout a normal temperature cycle on a sunny day. In general, the joint appears to be more open at the slab surface, with the bottom edges being compressed at several times throughout the day. Toward the late afternoon, when pavement temperatures are at or near maximum, the joint has a tendency to close, thus preventing any rotation.<sup>(86)</sup> On cloudy winter days, lower temperatures persist, causing less variation in thermal gradients and less rotation at the edges. As a result,

the joints generally remain open, with little or no compression at the lower edges.<sup>(86)</sup>

The vertical movements of typical adjacent slabs were also measured. A comparison of the vertical movements with the thermal gradient resulted in the following conclusions:<sup>(86)</sup>

- Vertical movements of slab corners and edges become minimal when the thermal gradient becomes maximum or positive; when a negative thermal gradient exists, the corners and edges remain curled upward.
- The slab remains curled upward as the thermal gradient approaches zero.
- Behavior of the slab center is always contrary to the behavior of the corners and edges.
- Maximum deflections under load behave in a manner similar to deflections due to thermal gradients, with a proportionality between the magnitudes of deflection and edge lifting.

Upward curling appears to occur in all pavement sections to varying degrees. The uplift is greater for the sections in the north (1-9) than in the south (10-21). The northern sections are located in a very dry area with low humidity and precipitation.

As with temperature differentials, differences in moisture content between the top and the bottom of the slab can cause warping in the pavement. Moisture causes the pavement to expand, so if more moisture is present in the upper portion of the slab, the slab tends to warp downward. Conversely, the slab tends to warp upward when more moisture is present in the lower portion of the slab.

The pavement surface is exposed to changing climatic conditions (e.g., wind, humidity, temperature, and rain) and, as a result, a wider variation in moisture conditions. The bottom of the slab, on the other hand, is protected from these elements and remains relatively moist throughout the year. In central Chile, most of the rainfall occurs during Winter, which is followed by prolonged periods of drought and low humidity. Consequently, the moisture differential is minimal during the winter, increasing to a maximum toward the end of autumn.

Investigations of the Chilean concrete test sections indicate the significant effect of moisture on pavement response.<sup>(87)</sup> Seasonal deflection data from a moving 18-kip (80-kN) axle load were measured at the slab corner and at the slab interior during periods of zero thermal gradients. These deflection were compared to the monthly rainfall data over the same period. The corner deflections are highest during the dry periods of the year, indicating that the slab corners are warped upwards. The corner deflections are lowest after periods of heavy rainfall, at which time the upward warping is less pronounced. The deflection at the slab interior is less than the corner deflections and is relatively constant throughout the seasons, indicating the relative stability of the underlying layers (recall that 16 sections were constructed on existing

AC or PCC pavements).

Another indicator of the moisture effects came as a result of measuring the transverse joint openings. At a given temperature, the average opening of 10 consecutive joints was slightly wider in autumn than in winter, due to concrete swelling from the absorbed moisture.<sup>(87)</sup> This behavior is typical of all Chilean concrete pavements, especially those in central Chile, where heavy winter rainfall is followed by prolonged periods of drought.<sup>(87)</sup>

At the time of placement, concrete contains considerably more water than necessary for hydration. Within a few hours, the slab loses water and shrinkage results, especially along the exposed surface. This phenomenon is known as drying shrinkage. When the bottom of the slab contains more moisture than the top, an upward warping of the slab can occur. As this condition persists and hydration continues, equilibrium can occur, resulting in a permanent warping of the slab. In central Chile, where conditions are hot and dry throughout part of the year, this phenomenon can be very common. Warmer climates within the United States, such as Arizona, California, and Florida, have also experienced this type of permanent warping of concrete slabs.

#### *Load Transfer*

Load transfer refers to the ability of the pavement to transfer a wheel load from one slab to the next. Effective load transfer reduces stresses and deflections at transverse joints, thus reducing the potential for pumping and faulting. The Chilean concrete pavement sections do not contain dowel bars or other means of load transfer at the transfer joints, and thus must rely on aggregate interlock (i.e., the interlocking of the aggregate particles of the abutting joint faces).

On sections that rely on aggregate interlock as the sole means of load transfer, the degree of load transfer depends largely on the width of the transverse joint opening. The variation in joint openings for 10 consecutive joints of test section 3 were measured approximately 2 years after construction. The openings are fairly well distributed between the joints. In general, joint openings are greater during the winter, when temperatures are cooler and the slab contracts. In addition, the joint that cracked first remains wider than the other joints.

The magnitude of the opening controls the degree of aggregate interlock at the joint. The wider the opening, the less contact between the aggregate particles. Many researchers believe that aggregate interlock is completely lost if the joint opening exceeds 0.023 in (0.58 mm). Based on this value, most of the joints do not have any aggregate interlock during the winter. However, the openings were measured at the surface and will not be uniform throughout the depth of the slab.

Load transfer on both the approach and leave side of the joint was determined for the Chilean sections. The load transfer values are typically higher during the summer as compared to the winter. During the hot summer months, the pavement



often acts as a continuous slab, with complete locking of the joints.<sup>(88)</sup> Another interesting observation was the difference between load transfer values on the approach and leave side of the joint, especially during the winter when the joint openings are wider. One suggested reason for this phenomenon, which was verified through core samples, is the inclination of the induced crack below the sawed joint.<sup>(88)</sup> If the induced crack was on the approach side of the joint, then the load transfer measured on the approach side would generally be higher, and vice-versa.

### *Faulting*

After 5 years of measurements on the Chilean concrete pavement sections, an analysis and evaluation of the faulting data was conducted.<sup>(85)</sup> Table 143 provides faulting measurements from 1991, as well as the age and applied ESAL's at that time. Faulting continues to increase with age on the newly constructed sections, following an S-shaped curve that appears to be maximizing around the moderate severity level (0.2 in [5 mm]). The older pavement sections, on the other hand, remain at lower faulting levels (0.08 in [2 mm]) after 30 years of service.

The older pavement sections were all constructed on granular bases, whereas many of the newer sections were constructed on cement-treated or cement-stabilized bases. The use of a cement-treated base has not decreased the level of faulting in the pavements. In fact, due to the uplifting of the slabs from the stiff base, the potential for pumping has further increased. In addition, the newer pavements are demonstrating a systematic buildup of faulting during the winter, followed by a decrease during the dry season, which is attributed to a redistribution of the accumulated sandy fines under the approach slab edges.<sup>(85)</sup>

Another way to examine faulting is through its accumulation with traffic loadings, specifically the number of 18-kip (80-kN) ESAL's. This evaluation showed a general trend of higher faulting levels with increasing ESAL's. However, sections 13 and 21 have faulting values around 0.14 in (3.6 mm) after only 4.5 and 2.5 million ESAL's, respectively. Both these sections have two common features that may be attributing to the higher faulting measurements: thin pavement sections (when compared to the other sections) and no drainage elements.

The same faulting measurements were also plotted as a function of the product of age and ESAL's. By using both parameters, the effect of age (a surrogate for climatic effects) and traffic on pavement performance can be considered simultaneously. In this case, the points follow the same general trend as the faulting vs. ESAL's plot. As before, sections 13 and 21 deviate from this general trend.

The effect of edge drains on faulting was examined using a plot of faulting as a function of ESAL's, with the data separated into two categories: those with edge drains and those with no drainage features. In general, the sections with edge drains are exhibiting less faulting than those without drainage. None of the sections with edge drains have faulting levels greater than 0.10 in (2.5 mm).

Table 143. Performance data for Chilean sections.

Test Section	Location	Age, years	ESAL's, millions	Backcalculated k-value, kPa/mm (psi/in)	Faulting, mm (mils)	Percent Cracking
1	Longotoma	8	3.69	147 (540)	1.0 (39)	81
2	Las Chilcas	10	5.31	169 (624)	1.1 (43)	95
3	Lampa	7	7.82	38 (140)	2.2 (87)	0
4	Lo Vásquez	6	4.64	24 (90)	1.5 (59)	0
5	Talagante	16	22.21	75 (275)	1.0 (39)	45
6	Paine	8	12.68	49 (179)	3.2 (126)	0
7	Graneros	8	13.02	28 (102)	1.7 (67)	74
8	San Fernando	8	7.01	77 (286)	0.2 (8)	44
9	San Rafael	8	5.04	181 (665)	1.9 (75)	23
10	Cocharcas	9	6.35	132 (485)	1.9 (75)	15
11	Concepción	7	4.58	100 (369)	0.8 (31)	0
12	Cabrero	7	3.45	138 (508)	0.6 (24)	0
13	Laja	9	4.46	103 (379)	3.6 (142)	22
14	Cta. Esperanza	12				
15	Victoria	7	2.41	83 (306)	0.9 (35)	0
16	Temuco	10	4.37	183 (675)	1.9 (75)	12
17	Gorbea	8	2.34	24 (87)	0.8 (31)	0
18	Loncoche	7	2.05	63 (232)	1.4 (55)	0
19	Mariquina	8	2.34	65 (239)	1.1 (43)	0
20	Mafil	8	2.34	26 (96)	0.7 (28)	0
21	Rio Bueno	8	2.52	68 (252)	3.7 (146)	0

The k-values shown in table 143 were backcalculated using deflections measured from the deep reference bases and represent the effect of all layers beneath the concrete slab. Thus, this parameter incorporates the effect of the base, subbase, and subgrade into a single value. The sections with k-values below 400 psi/in (110 kPa/mm) generally have higher faulting values. All sections with k-values in excess of 400 psi/in (110 kPa/mm) have faulting levels below 0.08 in (2.0 mm).

## Cracking

Another important measure of concrete pavement performance is transverse cracking, which is mainly associated with fatigue of the pavement due to traffic loadings (although curling and warping can contribute to fatigue). Table 143 provides the percentage of cracked slabs for each section. Based on the estimated ESAL computations, a fatigue analysis was conducted to predict the amount of cracking in the concrete sections. The following fatigue model was used:<sup>(89)</sup>

$$\log N = 2.13 SR^{-1.2} \quad (43)$$

where:

- N = Number of stress applications to failure.
- SR = Stress ratio (tensile stress/flexural strength).

The number of applications to failure was then used in the following cracking model to predict the percentage of cracked slabs:<sup>(3)</sup>

$$P = \frac{1}{0.01 + 0.03 \left[ 20^{-\log(n/N)} \right]} \quad (44)$$

where:

- P = Percent of slabs cracked.
- n = Actual number of ESAL's.
- N = Allowable number of ESAL's (from previous equation).

The results from this equation were plotted against the actual cracking. The fatigue model predicted cracking with some accuracy for most sections. However, the model severely underpredicted the amount of cracking on sections 1, 2, 7, and 8. This error is probably a result of the cracking occurring from reasons other than normal fatigue, in which cracking initiates at the bottom of the slab. Many of the Chilean sections were observed to have cracking that initiated at the top of the slab due to the upward concavity. The fatigue model cannot be used to predict cracking of this nature.

The percentage of slabs cracked was plotted as a function of age, ESAL's, and the product of age and ESAL's. Because most of the sections are between 8 and 10 years old, the aging effects are impossible to quantify accurately. The plot of cracking as a function of ESAL's shows a wider variation in the data, with a higher degree of cracking for increasing ESAL's. However, sections 1 and 2 have 81 and 95 percent cracking, respectively, which cannot be explained by this plot. The same trend is

evident in the plot of cracking as a function of the product of age and ESAL's.

Slab length can influence the initiation of slab cracking, especially on pavements subjected to temperature and moisture differentials. Longer slabs allow more bending due to curling and warping and, thus, develop higher tensile stresses at the bottom of the slab. An analysis of the effect of joint spacing on cracking showed some interesting results. Eight of the eleven sections with a maximum joint spacing greater than 15 ft (4.6 m) are exhibiting some cracking. On the other hand, only one of the nine sections with a maximum joint spacing less than 15 ft (4.6 m) has cracked, and that section has been exposed to more than 12 million ESAL applications. Based on these results, the increased effect of warping and curling on the longer slabs has resulted in higher amounts of fatigue cracking.

Although not as prevalent as slab length, other features are also common in the sections exhibiting transverse cracking. For instance, most of the cracked sections have backcalculated k-values in excess of 400 psi/in (110 kPa/mm). The softer sections allow some settlement of the stabilized layers, resulting in improved support. Conversely, the stiffer layers do not allow much settlement, resulting in more unsupported areas. Another common feature of the cracked sections involves the drainage design. Seven of the nine cracked sections do not incorporate any drainage feature into the design. Likewise, most of the sections with edge drains have not experienced any transverse cracking.

### Summary of Chilean Concrete Pavement Performance

The Chilean test sections offer an ideal opportunity to investigate concrete pavement performance. They offer a range of design features and climatic conditions. The results of several studies, conducted by the Chilean researchers, are available and should be consulted for further details and observations. Moreover, the Chilean research project will continue for at least 3 more years and should provide additional data on these sections. An evaluation and analysis of the current published research reports and data resulted in the following observations:

- As a result of thermal gradients, moisture differentials, and irreversible drying shrinkage, a predominant upward concavity in the concrete slabs is prevalent.
- A positive thermal gradient occurs about one-third of the time, with a negative gradient existing two-thirds of the time. The positive gradients reach higher values than the negative gradients.
- The moisture differential is minimal during the winter, increasing to a maximum toward the end of autumn.
- Joint load transfer values are much lower during the winter, when the joints are open wider, due to the slabs contracting from cooler temperatures.
- Many sections are demonstrating a systematic buildup of faulting during the

winter, followed by some decrease during the dry season.

- Improved support and the incorporation of edge drains have resulted in a reduction in faulting when compared to otherwise similar sections.
- A few sections showed large amounts of cracking, indicating that some unusual curling or warping, which cannot be explained by traffic or design, may have occurred during construction.
- The longer jointed sections had considerably more cracking, mainly due to the increase in curling and warping. Softer support conditions and the use of edge drains also resulted in a reduction of cracking.

1  
2  
3  
4  
5  
6  
7  
8  
9  
10  
11  
12  
13  
14  
15  
16  
17  
18  
19  
20  
21  
22  
23  
24  
25  
26  
27  
28  
29  
30  
31  
32  
33  
34  
35  
36  
37  
38  
39  
40  
41  
42  
43  
44  
45  
46  
47  
48  
49  
50  
51  
52  
53  
54  
55  
56  
57  
58  
59  
60  
61  
62  
63  
64  
65  
66  
67  
68  
69  
70  
71  
72  
73  
74  
75  
76  
77  
78  
79  
80  
81  
82  
83  
84  
85  
86  
87  
88  
89  
90  
91  
92  
93  
94  
95  
96  
97  
98  
99  
100

## 6. SUMMARY AND CONCLUSIONS

### Overview of Report

In 1986, the FHWA sponsored a research study on the evaluation of 95 concrete pavement sections located throughout North America.<sup>(2-7)</sup> The goal of that study was to gain insight on the performance of inservice concrete pavements. That study, completed in 1990, provided much useful information on the performance of concrete pavements, including the development of prediction models for several concrete pavement performance indicators (faulting, spalling, cracking, and serviceability loss).

This study is a follow up to the original study and is designed to address the deficiencies (e.g., limited number of sections, no time series data, and young age and low traffic levels of some sections) while building upon and extending the original study. Not only were the original 95 pavement sections reinspected and reevaluated after receiving 5 more years of traffic loadings, but 208 additional pavement sections were added to the study, thus greatly strengthening the data base used for analysis. Furthermore, many of the new sections that were added to the study contain newer design elements, such as widened lanes or permeable bases. The result is that a total of 303 concrete pavement sections located throughout North America and representing a broad range of pavement designs were studied.

This report focuses on the evaluation of pavement design features on concrete pavement performance and contains six chapters including this one. Chapter 1 provides a brief introduction to the project, including the background, objectives, and approach. Chapter 2 summarizes briefly the sections included in the study and gives an overview of the range of designs and design features available for analysis.

Chapter 3 provides an evaluation of the effect of pavement design features on concrete pavement performance. The design features evaluated in this section include the following:

- Slab thickness.
- Joint spacing.
- Joint orientation.
- Joint load transfer.
- Joint sealant.
- Base type.
- Drainage.
- Shoulder type.
- Widened slabs.
- Steel reinforcement type and content.
- Coarse aggregate size and quality.
- PCC pavement type.

Where applicable, three types of evaluations are conducted for each pavement type. The first type of evaluation is a direct comparison of sections within the same project in which only the design feature in question is varied. Secondly, an overall evaluation of all sections is conducted; this type of evaluation is often confounded by variations in other design features and differences in climatic conditions and traffic loadings. Lastly, past studies are reviewed to examine results obtained by other researchers that may be useful in this analysis.

Chapter 4 describes the methodology of the new backcalculation procedure and the steps taken to verify and further refine the backcalculation results. The chapter begins with a presentation of the theoretical background of the new procedure, followed by a discussion of the validation results. Finally, the evaluation of bonding conditions between the slab and base are evaluated. This ability to distinguish between bonded and nonbonded systems gives rise to the "equivalent thickness" concept, which is also described in chapter 4.

Chapter 5 summarizes the results of an investigation conducted on the performance of concrete pavements in Europe and in Chile. France, Italy, the United Kingdom, Belgium, and Switzerland have collectively conducted evaluations on 96 concrete pavements under the European COPES program. These sections are exposed to much greater and heavier truck loadings than pavements in the U.S. A similar research program in Chile includes the evaluation and analysis of the performance of 21 concrete pavements. Together, the results of these studies provide additional information and insight on the effect of design variables on concrete pavement performance.

## **Review of Significant Findings**

This report presents a vast amount of information on the performance and behavior of a variety of concrete pavement designs under different environmental and traffic loading conditions. A summary of the significant findings and conclusions presented throughout this report is provided in the following sections.

### Effect of Design Features on Pavement Performance

A major evaluation was conducted on examining the effect of pavement design features on concrete pavement performance. Significant findings and observations are presented below by design feature. In interpreting these findings, it must be kept in mind that while the majority of the sections are greater than 15 years old, only four have sustained more than 20 million ESAL applications.

#### *Slab Thickness*

With the available data, the effect of slab thickness on concrete pavement performance is often confounded or obscured by other factors. For example, many of the thicker pavement sections included in the study were placed directly on the subgrade (without benefit of a base course), as compared to thinner sections



constructed on a well-prepared base. Thus, conclusions regarding the effect on performance of adding additional slab thickness are not always clear.

In direct comparisons between thicker and thinner slabs, increased slab thickness did appear to reduce the amount of transverse slab cracking. However, increased slab thickness does not appear to reduce faulting or pumping of the transverse joints. Moreover, it was observed that thicker slabs placed directly on grade perform no better than thinner slabs constructed on a base course, and in some cases actually perform worse in terms of faulting and pumping. These latter two observations reinforce the need for a comprehensive pavement design, one that includes ample consideration of structural support requirements, drainage provisions, and load transfer needs.

It is worth noting that in several of the comparisons, the difference in slab thickness was only 1 in (25 mm). The effect of such a small increase in slab thickness may be obscured by other effects, such as the inherent variability in performance or the normal variability in the actual as-constructed thickness of the pavement.

### *Joint Spacing*

Joint spacing is a variable on several of the projects. For the JPCP designs, sections with shorter joint spacings exhibit less transverse cracking. Longer-jointed JPCP designs (greater than about 15 ft [4.6 m]) are generally more susceptible to greater curling stresses (particularly when they are placed on a very stiff base course), which can lead to the development of transverse cracking. However, joint spacing did not appear to have a significant effect on other distress types, such as pumping or faulting.

Some interesting trends are observed when transverse cracking is plotted against the ratio of the JPCP joint spacing,  $L$ , to the radius of relative stiffness,  $\ell$ , where  $\ell$  is defined as follows:

$$\ell = \left[ \frac{Eh^3}{12(1-\mu^2)k} \right]^{0.25} \quad (45)$$

For sections with aggregate base courses, it is observed that significant transverse cracking occurs when  $L/\ell$  exceeds about 6, whereas for sections with treated base courses, significant transverse cracking occurs when  $L/\ell$  exceeds about 4.

Many of the JPCP sections contained randomly spaced transverse joints. It was frequently observed that the longer segments in the pattern (for example, the 18- and 19-ft [5.5- and 5.8-m] segments in the 12-13-19-18-ft [3.7-4.0-5.8-5.5-m] random joint spacing pattern) exhibit much more transverse cracking than the shorter segments, as would be expected. Many agencies have now adopted shorter random joint spacing to reduce transverse cracking on the longer panels (for example, California has used a 12-13-15-14-ft [3.7-4.0-4.6-4.3-m] random joint spacing pattern since the late 1970's,

and Washington State uses joint spacings of 9-10-14-13 ft [2.7-3-4.3-4.0 m] and 12-13-15-14 ft [3.7-4.0-4.6-4.3-m] for their nondoweled and doweled pavements, respectively).

The effect of shorter joint spacings on the performance of JRCP is not as apparent as on JPCP. Many of the shorter-jointed JRCP designs (with joint spacing less than 30 ft [9.1 m]) display good performance with few deteriorated transverse cracks. However, some short-jointed JRCP designs have not performed very well. In addition, many longer-jointed JRCP designs (including some with 78.5-ft [23.9 m] joint spacing) also exhibit very few deteriorated transverse cracks. It appears that the other factors (e.g., base type, climate, and reinforcing content) may have a greater affect on the development of deteriorated transverse cracks than joint spacing alone.

### *Joint Orientation*

Joint orientation refers to the angle of the transverse joint with respect to the centerline of the pavement. Perpendicular joints are constructed perpendicular to the centerline, whereas skewed joints are placed at an angle to the centerline, usually offset about 2 ft (0.6 m) per 12-ft (3.7-m) lane in the counterclockwise direction.

In three projects allowing direct comparisons between perpendicular and skewed transverse joints, two of the projects showed that skewed joints perform better than perpendicular joints, primarily in terms of faulting (all sections were nondoweled). Furthermore, in an overall evaluation, skewed joints appear to reduce faulting and spalling for JPCP, particularly for nondoweled designs. However, sections with skewed joints are also more susceptible to corner breaks, and these appear to suggest the need to maintain skews of no more than 2 ft (0.6 m) per 12-ft (3.7-m) lane. When used, the FHWA recommends a skew of 1 in 10, although past performance data do not indicate the need for skewed joints, especially on doweled pavement sections (38).

### *Transverse Joint Load Transfer*

Positive load transfer, provided by steel dowel bars placed across transverse joints at mid-depth of the slab, have a pronounced beneficial effect on the performance of jointed concrete pavements. It was observed that nondoweled sections develop significant levels of faulting regardless of pavement design or climate. On the other hand, pavement sections containing dowel bars at the transverse joints exhibit much less faulting than sections without dowel bars. Similarly, the load transfer efficiency of doweled transverse joints is greater than that of nondoweled joints.

However, many pavement sections containing small diameter (1 in [25 mm]) dowel bars exhibit significant levels of faulting, although the faulting on these sections is still less than that of adjacent, nondoweled sections. This indicates the need for sufficiently sized dowel bars (minimum 1.25 in [32 mm] diameter) for heavy truck loading. It is of interest to note that several sections containing large diameter dowel bars (1.38 in [35 mm] or greater) display very small amounts of joint faulting.

The dowel bars used in many of the pavement projects are coated with a protective covering (such as epoxy or plastic) to prevent corrosion. Sections with coated dowels generally have less spalling, and in some cases less faulting, than sections with noncoated dowels. This observation suggests that the coating of the dowel bars is keeping the dowel from corroding, thereby allowing free movement at the joint and preventing a reduction in the effective diameter of the bar.

### *Joint Sealant Type*

A variety of joint sealant materials is used in the transverse joints of the pavement sections evaluated under this study. For purposes of categorization, three main groupings are made: hot-poured, asphaltic-based sealant materials; silicone sealant materials; and preformed compression seal materials. In addition, some of the sections evaluated under the study are purposely not sealed, the joints being sawed about 0.125 in (3 mm) wide and left unsealed.

On projects providing direct comparisons between sealed and nonsealed transverse joints, those sections containing sealed joints generally exhibit less spalling than sections with nonsealed joints, although the difference in spalling is not always significant. Many of these projects were young and the long-term effects of sealing joints are not clear. Climatic effects are evident, however, as many nonsealed sections in a mild environment (California) display small amounts of transverse joint spalling, some even after nearly 20 years. The benefits of the mild environment include smaller joint movements, less free moisture available to infiltrate the pavement at the joint, and the absence of deicing chemicals or abrasives.

More difficult to evaluate is the effect of joint sealing on moisture-related aspects of pavement performance (pumping, faulting, loss of support). There is some evidence to suggest that sealed joints show less faulting, but this effect is often difficult to isolate because of confounding variables. However, significant pumping and loss of support (resulting in corner breaks and transverse cracking) did develop on some nonsealed California sections where dowel bars and tie bars were not used. California noted that better overall faulting performance was derived on pavements containing tied PCC shoulders and sealed transverse joints.<sup>(90)</sup>

In comparisons between the different joint sealant types, sections containing preformed compression seals display the best performance in terms of joint spalling. Where material durability (D-cracking) is not a problem, joints containing preformed compression seals are generally clean and free from spalling, in at least one case for up to 21 years of service. Although many of the sections containing preformed joint seals are less than 10 years old, this material does appear to hold the promise of providing long-term performance. A potential problem with preformed sealants occurs with nonuniform joint openings (i.e., intermediate joints remain uncracked causing cracked joints to open wider than normal), as the wider openings can cause the preformed sealant to drop into the joint.

## *Base Type*

Base type has a substantial effect on the performance of the pavement, both through the support it provides to the slab and through its contribution to pavement drainage. A variety of base types is included in this evaluation, including aggregate (granular) bases, cement-treated bases, asphalt-treated bases, lean concrete bases, and permeable (both treated and nontreated) bases. In addition, several pavement sections contain no base, with the slab placed directly on the prepared subgrade.

In evaluating the performance of the concrete pavements placed over different base courses, the overall quality of the base must be considered. For aggregate base courses, the base should be nonfrost susceptible and restrictions should be placed on the total fines content (material passing the No. 200 sieve) of the base. For asphalt- and cement-treated bases, as well as for lean concrete bases, adequate amounts of stabilizing agent should be added to increase the erosion resistance of the material; a minimum of 8 percent cement and 6 percent asphalt are recommended for strong erosion resistance.<sup>(44,46)</sup>

The results of the evaluation show that sections constructed on aggregate bases exhibit fair to good performance. These sections are somewhat susceptible to faulting, probably because of the erodibility of the base material. However, JPCP sections containing aggregate bases often exhibit less cracking than other base types, due to reduced friction at the slab/base interface and lower thermal curling stresses. In addition, JRCP sections with aggregate bases often have less deteriorated transverse cracking, again probably due to the lower friction levels between the slab and base.

The performance of sections constructed on ATB and CTB vary considerably. Although several sections are performing very well, many of the sections constructed on ATB and CTB display excessive levels of faulting and transverse cracking. The high levels of joint faulting are believed to be the result of the erodibility of both the ATB and CTB materials that were evaluated. Even though the bases are stabilized, research has shown that at stabilizing levels less than about 5 to 7 percent, the treated materials are still susceptible to erosion. Most of the sections with ATB and CTB in this study had stabilizing levels less than 6 percent. In order to obtain good performance from these base courses, they must represent high-quality mixtures (plant-mixed, adequate stabilizer contents, strong, durable aggregates).

In comparison to aggregate bases, the relative stiffness of the ATB and CTB is believed to be the reason for their higher levels of JPCP transverse cracking (lower quality, erodible mixtures also contribute). The greater stiffness leads to increased thermal curling stresses that can result in greater slab cracking. Other design measures such as reduced joint spacing must be considered if the stiffer bases are to be used.

Another factor affecting the performance of several of the sections placed on ATB and CTB is the cross-sectional design of the substructure. In addition to being placed

beneath the mainline pavements, the treated base course material in several cases was also placed beneath the shoulders, thus creating a "bathtub" design that does not allow free moisture to drain. This presence of free moisture in the pavement structure is believed to have accelerated the development of distress on several sections.

The performance of sections constructed on LCB ranges from fair to good. While these sections generally show little faulting and few deteriorated transverse cracks, a few of the sections did show substantial transverse cracking and significant joint faulting (nondoweled joints only). However, these are often JPCP designs that have relatively long slab lengths (say, greater than 16 ft [4.9 m]) in a random joint spacing pattern which, in combination with the stiff LCB base, created large curling stresses and subsequent slab cracking.

Pavements constructed directly on grade without benefit of a base course show poor to fair performance. Although these were often thicker slabs, these designs are susceptible to pumping and faulting and exhibit excessive levels of faulting even under relatively low traffic. None of the sections constructed directly on the subgrade contain dowel bars at the transverse joints.

Sections constructed on permeable bases display the best overall performance. When properly designed, these sections show little pumping and joint faulting, and also exhibit a reduction in other moisture-related distresses, such as D-cracking. This good performance is exhibited by all three permeable base types (permeable aggregate, permeable asphalt-treated, and permeable cement-treated), and no distinction in the relative performance of these base course materials can be made at this time. However, some permeable bases are showing loss of support at the corners which may indicate future problems.

Although the sections constructed on permeable bases typically are very young (about half are less than 5 years old) and have been exposed to few ESAL applications, they hold strong promise for the future. However, several aspects of permeable base design and construction are critical to their performance, including:

- Placement of the permeable base directly beneath the slab.
- Use of separator layer beneath the permeable base course to prevent migration of fines from below.
- Proper location of the collector pipes within the permeable base course.
- Adequate depth of ditches.
- Effective design and spacing of drainage outlets to ensure proper drainage and to allow maintenance inspections and cleanouts.

## *Drainage*

Nearly one-half of the pavement sections evaluated in this study incorporate some form of pavement drainage. Most commonly this is accomplished through the use of longitudinal pipe edge drains, with or without permeable bases. However, daylighted cross sections, longitudinal fin drains, and transverse pipe drains are also present.

The examination of the performance data shows that these different forms of drainage are not equivalent. It was generally observed that sections constructed on permeable bases are performing better than sections containing other drainage designs. As previously stated, direct comparisons between sections with permeable and nonpermeable bases indicate that the permeable base sections generally show better performance. This enhanced performance is generally manifested in lower faulting and fewer transverse cracks. In some cases, joint spalling is also less for the permeable base sections, probably due to the joints being less saturated over the year.

Pavement sections containing longitudinal pipe edge drains (and not accompanied by a permeable base) did not show any significant advantage in pavement performance when compared to nondrained systems, and in some cases even showed worse performance. This could be due to free moisture being unable to migrate to the longitudinal drain because of the relative impermeability of the base course. If this is the case, free moisture remains in the pavement structure, which then behaves more like a nondrained system. Furthermore, inadequate maintenance of the pipe drain system may also hinder the removal of moisture from the pavement.

Daylighted cross sections are another type of pavement subsurface drainage. In these designs, the aggregate base course extends out beyond the shoulders to the ditches as a means of removing excess moisture. However, the daylighted base courses included in the study are all dense-graded, allowing little movement of free moisture.

An examination of the performance data from the daylighted sections show that the daylighting does not appear to provide any benefit to the structural performance of the pavement. That is, the amount of transverse cracking and faulting are about the same between daylighted and adjacent nondaylighted and nondrained sections, and in some cases the daylighted sections show worse performance. However, as observed at the OH 2 sections, daylighting did appear to have an effect on reducing or delaying the development of D-cracking, even though the base was dense-graded and did not appear to have an effect on faulting.

In addition to the relative impermeability of the daylighted sections included in this study, another factor reducing the effectiveness of the daylighted configuration is that it is a "nonmaintainable" design. The "outlet" portion of the daylighted base frequently clogs with dirt, grass, and other debris, which serves to keep free moisture within the pavement system and accelerates the development of pavement distress.

Another way to evaluate the relative effect of drainage on pavement performance is to rank the overall drainability of each section. This is accomplished using the AASHTO Drainage Coefficient ( $C_d$ ), which accounts for a combination of factors that influence the drainability of the pavement, including drainage design factors, cross-sectional design factors, subgrade characteristics, and climatic indices. Sections with relatively good drainability typically will have a  $C_d$  greater than 1, whereas sections with relatively poor drainability will have a  $C_d$  less than 1.

The results show that the performance of the pavements generally improves with increasing  $C_d$ . This is particularly true for faulting, which, on average, is much lower for sections with  $C_d$  values greater than 1. The effect is also more pronounced for nondoweled pavement sections.

### *Shoulder Type*

Many pavement sections included in this study contain a PCC shoulder as a means of providing lateral support to the mainline pavement. When effectively tied to the mainline pavement, the provision of this lateral support can significantly reduce critical stresses in the mainline pavement slab when the edge or corner is loaded. Asphalt or aggregate shoulders provide no such lateral support so that edge and corner loading on pavements with these types of shoulders represent “free edge” loading conditions.

Overall, it was observed that tied PCC shoulders are structurally in better condition than AC shoulders. The AC shoulders typically exhibit extensive deterioration and lane-shoulder dropoff, whereas tied PCC shoulders exhibited little or no deterioration. However, of greater interest is the effect of the shoulder on the performance of the mainline pavement. In this case, the benefits of tied PCC shoulders (or any other tied, lateral support fixture—traffic lane, edge beam, or curb and gutter) to concrete pavement performance are not as clear. In many cases, sections with lateral support exhibit the same levels of faulting and transverse cracking as sections without lateral support. In other cases, the sections with lateral support show lower levels of faulting and transverse cracking, but not to the extent that is expected. This perhaps speaks to inadequacies in the tie system securing the shoulder to the mainline pavement. Generally, sections that are tied using anything smaller than No. 5 (16-mm) bars, or with tie bars spaced farther than 36 in (914 mm) apart, did not perform well.

Many sections with tied PCC shoulders contain intermediate joints that do not align with joints in the mainline pavement. In these cases, “sympathetic” cracking in the mainline pavements at the location of the intermediate shoulder joints was observed. It is recommended that joints placed in JPCP shoulders match those in the mainline pavement.

An examination of the deflection data taken in 1992 generally shows good load transfer across the lane-PCC shoulder joint. Similarly, corner deflections and the percentage of corners with voids are usually reduced for tied sections. However,

much of the deflection data was collected at elevated temperatures during which load transfer provided by aggregate interlock would be greater. All of the sections with lateral edge support included in this evaluation were placed independently of the mainline pavement.

Sections with *nontied* PCC shoulders appear to offer no benefits to performance over sections with AC shoulders. In fact, the performance is considerably worse in some cases.

Another common trend is the effect of shoulder thickness on performance. Tied PCC shoulders that are thinner than the mainline pavement did not perform as well as full-depth PCC shoulders. Both the mainline pavement and the shoulder exhibit higher distress levels than corresponding sections with thicker shoulders.

#### *Widened PCC Slabs*

The use of widened PCC slabs is another method of reducing critical edge and corner loading stresses. By constructing the outer lane slab 13 to 14 ft (4.0 to 4.3 m) wide but maintaining the painted traffic lane width at 12 ft (3.7 m), a more interior loading condition is produced.

No direct comparisons between sections with and without widened slabs are available. However, an examination of those sections constructed with widened slabs indicates outstanding performance for pavements up to 9 years old and over 9 million ESAL applications. The faulting on these sections is very low and their overall rideability is very good. A few sections display some longitudinal cracking, emphasizing perhaps the importance of proper joint sawing and the need to limit the slab widths to about 14 ft (4.3 m) or less.

#### *JRCP Steel Reinforcing Content*

Although many different JRCP designs are included in the study, few direct comparisons are available for analyzing the effects of reinforcement on PCC pavement performance. The two projects from Illinois indicate that a hinge joint design, in which a greater amount of reinforcement is concentrated at a controlled crack, provides superior performance in terms of the number of deteriorated cracks (although more roughness, likely due to higher number of joints) compared to the conventional design, in which the reinforcement is distributed through the entire length of the slab. This type of design is not common practice outside of Illinois, but its current performance warrants further consideration.

An overall evaluation of the JRCP sections indicates that the sections with higher steel percentages are performing better, especially in terms of the number of deteriorated transverse cracks. Sections with reinforcing contents above 0.17 percent exhibit outstanding performance, with very few deteriorated transverse cracks and overall good rideability. On the other hand, sections with less than 0.10 percent reinforcing steel have a much higher risk of the transverse cracks becoming



deteriorated. These results appear to be in line with recent research that recommends JRCP steel percentages in the range of 0.20 to 0.30 percent. The use of deformed welded wire fabric (or deformed bars) is also recommended over smooth welded wire fabric, as the deformed wire is more effective at holding the cracks tightly together.

#### *CRCP Steel Reinforcing Content*

A few CRCP sections are included in the study, primarily because they are part of the experimental pavement project in which jointed concrete pavements were evaluated. These pavements range in age from 6 to 21 years, and the reinforcing content varies from 0.56 to 0.73 percent. However, because of the relatively small number of sections and because of their good performance, it is not practical to draw meaningful conclusions on the effect of steel content on pavement performance. One of the two CRCP sections containing deformed welded wire fabric is not performing well, exhibiting deteriorated transverse cracks and punchouts.

#### *Maximum Coarse Aggregate Size*

The maximum coarse aggregate size refers to the smallest sieve opening through which a selected aggregate sample passes. Recent years have seen a movement to the use of smaller maximum coarse aggregate sizes as a means of increasing the durability of concrete mixtures containing D-cracking susceptible aggregate.

The results of this study do indicate that, for D-cracking susceptible aggregates, sections with smaller maximum coarse aggregate size do display lower levels of D-cracking (and in some cases the D-cracking is eliminated entirely). However, the results of this study also show that maximum coarse aggregate size does have an effect on the development of deteriorated transverse cracking; sections with larger maximum coarse aggregate sizes exhibit less deteriorated transverse cracking than sections with smaller maximum coarse aggregate size. There is also some evidence that sections with smaller maximum coarse aggregate exhibit greater crack and joint faulting than sections with larger size aggregate. This is believed to be due to the straightness of the cracks that occur in sections with small maximum coarse aggregate sizes; the cracks extend very straight both vertically through and laterally across the slab, reducing the effectiveness of aggregate interlock of the abutting joint or crack faces.

The selection of the most suitable maximum coarse aggregate size may present a conflict in some situations in which larger sizes are desired for structural performance, yet a smaller size may be needed for durability of certain D-cracking susceptible aggregates. In these cases, a balance must be struck between the structural performance and durability requirements. It may be that if smaller sized aggregate is required for durability, a pavement design that eliminates the potential adverse performance effects of smaller sized aggregate should be selected (e.g., a doweled JPCP pavement in which short joint spacings are employed to eliminate

mid-panel cracking and dowels at the transverse joints to provide positive load transfer).

### *Overall Summary of the Effect of Design Features*

An overall summary of the effect of the design features on pavement performance is provided in table 144. In addition, other factors that are closely tied to the effectiveness of each individual design feature are also listed in the table. This is in recognition of the many different factors that influence the performance of the pavement. Indeed, the results of this evaluation highlight the importance of designing the pavement as a system and not as a collection of individual design features. The contributions of many of the design features are closely related and the maximum benefits may not be realized if the entire pavement structure is not considered as a whole. In some cases, certain design features may actually have opposing effects, with the result being no real enhancement to pavement performance. Modifying or adding one design feature will not necessarily by itself improve the performance of the pavement.

### Comparison of Performance By PCC Pavement Type

Several experimental projects evaluated under the study include different pavement types (i.e., JPCP, JRCP, and CRCP), allowing direct comparisons of the performance of each type. In order for such comparisons to be meaningful, it must be recognized that:

- Many variables are confounded (for example, joint spacing for JPCP will typically be shorter than that for JRCP).
- Each pavement type performs differently, exhibiting different types of distress.

An ideal comparison would consider the life-cycle costs of each pavement type, based on the life expectancy of each design. However, since the pavements are being evaluated at only one point in time, and in recognition of the above factors, the overall rideability of each pavement type is the primary performance parameter that can be compared.

Two sites provide direct comparisons between all three pavement types. At these locations, the CRCP designs are performing very well, slightly better than the average performance of the JPCP design. However, both sites have at least one JPCP design that exhibited about the same level of performance as the CRCP sections. The JRCP designs typically perform worse than the JPCP designs, particularly in more severe climates where D-cracking and inadequate steel contents hinder the performance of the JRCP designs.

Table 144. Summary of effect of design features.

Design Feature	Effect of Design Feature on Pavement Performance	Other Factors Influencing Effectiveness
Slab Thickness	<p>Thicker slabs reduce cracking, but not faulting.</p> <p>Thick slab-on-grade designs perform no better than thinner slabs on a base.</p>	<p>Base Type Joint Spacing Load Transfer</p>
JPCP Joint Spacing	<p>For JPCP, shorter spacings (&lt; 16 ft) have less transverse cracking.</p> <p>Long segments of random JPCP joint spacing pattern exhibit more transverse cracking.</p>	<p>Base Type Climate</p>
JRCP Joint Spacing	<p>For JRCP, many short-jointed (&lt;30 ft) pavements perform well, but some longer-jointed pavements (&gt; 60 ft) also perform well.</p>	<p>Base Type Steel Content &amp; Type Climate</p>
Joint Orientation	<p>For nondoweled pavements, there is some evidence that joint skewing reduces faulting.</p>	<p>Load Transfer Base Type</p>
Joint Load Transfer	<p>Doweled joints exhibit much less faulting than nondoweled joints.</p> <p>Small diameter dowels (1 in) are not always effective in reducing faulting.</p> <p>Pavements with coated dowel bars show less spalling and, in some cases, less faulting.</p>	<p>Drainage Climate</p>
Joint Sealant	<p>Sealed joints perform slightly better than nonsealed joints, although differences in performance are not always significant. Some nonsealed joints in mild climates perform well, in terms of joint spalling.</p> <p>Some evidence to suggest that nonsealed sections exhibit more pumping and loss of support.</p> <p>Preformed compression seals display the best performance of all sealant types, although most sections are less than 10 years old.</p>	<p>Climate Deicing Materials Drainage Load Transfer Concrete Durability</p>
Base Type	<p>Pavements with aggregate bases perform fair to good, showing less transverse cracking than sections with treated bases.</p> <p>Sections with ATB and CTB perform poor to good, with extensive cracking and some faulting. Performance is tied to the stabilizer content, and many are less than 5 percent.</p> <p>Performance of lean concrete bases ranges from fair to good. Faulting levels generally low, but a few sections have significant cracking.</p> <p>Sections without a base are often susceptible to pumping and faulting.</p> <p>Sections with permeable bases show good performance, generally with little faulting. However, most of these sections are relatively new and have not been exposed to significant ESAL applications.</p>	<p>Joint Spacing Drainage Climate</p>

1 in = 25.4 mm; 1 ft = 0.305 m

Table 144. Summary of effect of design features (continued).

Design Feature	Effect of Design Feature on Pavement Performance	Other Factors Influencing Effectiveness
Drainage	Sections with longitudinal edge drains (and no permeable base) did not show any significant enhancement to pavement performance and sometimes showed worse performance.  Dense-graded daylighted systems perform about the same as or worse than nondrained systems, although they may delay the onset of D-cracking.  Drainage provided by permeable base and edge drains has the most pronounced effect on pavement performance, although these sections are still relatively young.	Base Type Climate
Shoulder Type	While PCC shoulders are in better condition than AC shoulders, their use is not always beneficial to the performance of the mainline pavement, perhaps due to inadequate tie bar system.	Tie System Shoulder Thickness
Widened Slabs	Sections with widened lanes (14 ft or less) display outstanding performance with minimal faulting and a small amount of slab cracking.	Width of Widening
JRCP Steel Content	Pavements with steel contents greater than about 0.17 percent show the best overall performance. The use of deformed welded wire fabric (or deformed bars) is recommended.	Joint Spacing Climate Base Type Steel Type
CRCP Steel Content	No conclusions on the effect of steel content. Contents ranged from 0.56 to 0.73, with most sections performing very well with exception of one section containing deformed welded wire fabric.	Climate Base Type Steel Type
Maximum Coarse Aggregate Size	Smaller aggregate size reduces durability problems such as D-cracking.  Larger aggregate size prevents deterioration of transverse cracks and faulting of joints and cracks.	Aggregate Quality Joint Spacing Load Transfer

1 in = 25.4 mm; 1 ft = 0.305 m

Several sites contain direct comparisons between JPCP and JRCP designs, but no clear trends are evident. This is perhaps due to the fact that each design can contain certain design elements (joint spacing, load transfer, steel content, base type) that can have a pronounced effect on the performance of that pavement type. Thus, the difference in performance is related more to the specific design elements than to the pavement type.

Two sites provide direct comparisons of the performance of a CRCP to a jointed design (either JPCP or JRCP). In both instances, the performance of the CRCP is superior to the jointed design.

Overall, the CRCP sections included in the study provide good performance, perhaps slightly better than the JPCP sections. The JRCP designs typically perform poorer than both the CRCP and the JPCP designs, perhaps because of inadequate steel reinforcing contents. However, not all of the pavements evaluated in the study

represent “good” design practices, meaning that the “best” design of each pavement type is not always being compared.

Each of the different pavement types can provide excellent performance, provided that they are effectively designed and constructed. Design considerations of particular interest for each pavement type are given below:

- Jointed Plain Concrete Pavements
  - Slab Thickness
  - Load Transfer Design (dowels and tie bars)
  - Joint Spacing Considerations
  - Joint Sealant Design
  - Base Type Selection
  - Drainage Design
  - Edge Support
  - Subgrade/Subbase Support
  
- Jointed Reinforced Concrete Pavements
  - Slab Thickness
  - Load Transfer Design (dowels and tie bars)
  - Joint Spacing Considerations
  - Joint Sealant Design
  - Base Type Selection
  - Drainage Design
  - Edge Support
  - Steel Reinforcing Design
  - Subgrade Subbase Support
  
- Continuously Reinforced Concrete Pavements
  - Slab Thickness
  - Steel Reinforcing Design
  - Base Type Selection
  - Drainage Design
  - Edge Support
  - Terminal Joint Design
  - Subgrade/Subbase Support

### Two-Layer System Backcalculation Procedure

A new backcalculation procedure has been developed that allows for evaluation of two-layer systems. This ability permits the identification of bonded and nonbonded conditions, which results in the more accurate representation of the pavement structures.

The backcalculation procedure was applied to the sections evaluated under this study and the effective slab thickness was calculated for those pavements placed on a stabilized base course. The effective slab thickness is calculated directly from the

backcalculated  $l$  value and is representative of the structural capacity of all pavement layers above the subgrade. By calculating this effective thickness, the structural contributions of the base course are considered and a more accurate representation of the pavement behavior is obtained. For example, if the base is bonded to the slab, the critical stress at the edge or the corner of the slab is less than that determined using a conventional Westergaard analysis. By knowing the effective thickness, a more realistic assessment of the actual critical stress can be made, which in turn leads to an improved assessment of the load-carrying capacity of the pavement structure.

### Performance of European Concrete Pavement Sections

Several European countries—namely France, Italy, the United Kingdom, Belgium, and Switzerland—have been monitoring the performance of their concrete pavements for several years and have provided data to this study for evaluation. Following are some of the highlights of the evaluation of that data:

- About 70 percent of the European pavement sections evaluated are JPCP. Most of these sections are in a wet-freeze climatic zone, and over 70 percent of the sections evaluated contained either a stabilized or lean concrete base.
- Nearly all sections are provided with some sort of drainage system (commonly a longitudinal edge drain). Except for many sections in France, most sections are also provided with dowels at the transverse joint. Slab thicknesses are generally in the 8- to 11-in (203- to 279-mm) range.
- Nearly three-quarters of the European sections have two or more modernity elements. Modernity elements are specific design features (such as nonerodible bases, subsurface drainage, strengthened structures [doweled joints, thickened slabs], and material/loading optimization [widened lanes]) that are expected to contribute to the performance of a concrete pavement. An examination of the U.S. sections evaluated in this study indicates that only about one-quarter contain two or more modernity elements.
- European highways are subjected to very high traffic loads, with accumulated ESAL applications exceeding 100 million for a few sections. The high ESAL values are a result of the high legal axle loads (26,500 to 28,600 lb [118 to 127 kN] single-axle loads) and long design lives (30 to 40 years) that are common in Europe. Of the 96 European sections, 44 sections (46 percent) have carried more than 20 million ESAL applications, compared to only 4 of 303 sections (1 percent) in the United States.
- Although the effects of slab thickness, dowels, and drainage on pavement performance could not be established with the available data, the base type was found to have a significant effect on pavement performance. The sections constructed on an LCB perform better than sections constructed on other base types.

- The pavement sections with three modernity elements perform better than those with two or fewer; however, 14 of 15 sections having three modernity elements are LCB sections.
- Detailed distress data are available for only Switzerland, thus preventing the development of distress performance prediction models. However, serviceability data are available for most sections and models predicting the serviceability of the sections over time were developed for each country except Italy, which had too few sections for model development.
- The serviceability of the European sections over time and traffic was compared to the serviceability of a sampling of U.S. sections. The comparison revealed similar trends, although the European sections have been exposed to far greater ESAL applications than the U.S. sections.

### Performance of Chilean Concrete Pavement Sections

Beginning in 1984, the Chilean Ministry of Public Works initiated a monitoring program of both their AC and PCC pavements. The purpose of this monitoring was to develop performance prediction models and to develop pavement rehabilitation schedules. From that monitoring program, design, construction, and performance data for 21 Chilean PCC pavements have been provided to this study for evaluation. The highlights of that evaluation are summarized below:

- The pavement sections were all constructed between 1975 and 1985, with 19 of the 21 sections constructed during a 5-year period between 1981 and 1985. The sections are located in a relatively mild climate, similar to California.
- All of the pavement sections are JPCP designs without dowel bars at the transverse joints. The slab thicknesses range from 8.3 to 10.2 in (210 to 260 mm), and are constructed on one of three different base types: granular, cement-stabilized, and cement-treated. Most of the sections employ random joint spacings, with joint spacings ranging from 11.5 to 18.0 ft (3.5 to 5.5 m).
- The Chilean sections are constructed on 3 different subbase materials beneath the base course): granular subbase (5 sections), existing AC pavement (4 sections), and existing PCC pavement (12 sections).
- Nearly half of the Chilean sections contain subsurface drainage in the form of longitudinal edge drains. Nine sections contain longitudinal edge drains, and the remaining 12 sections do not incorporate any positive drainage features.
- Accumulated ESAL applications for the Chilean sections range from 2 to 13 million, with the majority between 2 and 6 million. Only 3 sections have over 10 million accumulated ESAL applications.

- One section contains 2 modernity elements and 8 sections contain 1 modernity element, whereas the remaining 12 sections do not contain any modernity elements. The sections with at least one modernity element incorporate subsurface drainage (specifically, longitudinal edge drains); the section with two modernity elements also contains a strengthened structure (slab thickness greater than 10 in [250 mm]).
- As a result of thermal gradients, moisture differentials, and irreversible drying shrinkage, a predominant upward concavity in the concrete slabs is prevalent.
- A positive thermal gradient occurs about one-third of the time, with a negative gradient existing two-thirds of the time. The positive gradients reach higher absolute values than the negative gradients.
- The moisture differential is minimal during the winter (wet season) and increases to a maximum value toward the end of autumn (dry season).
- Joint load transfer values are much lower during the winter, when the joints are open wider, due to the slabs contracting from cooler temperatures.
- Many sections are demonstrating a systematic buildup of faulting during the winter, followed by some decrease during the dry season.
- Improved support and the incorporation of edge drains have resulted in a reduction in faulting when compared to otherwise similar sections.
- A few sections show large amounts of cracking, indicating that curling or warping of the slabs may have occurred during construction.
- The longer jointed sections have considerably more cracking, mainly due to the increase in curling and warping. Softer support conditions and the use of edge drains also resulted in a reduction of cracking.

## Closure

The primary findings and significant results of a major field study on concrete pavement performance are summarized in this chapter. Data collected from 303 pavement sections are evaluated to provide insight into the effectiveness of pavement design features (e.g., joint spacing, load transfer, drainage) on pavement performance. The relative performance of the various concrete pavement design types is also examined, and a new approach to backcalculation is described. Finally, the results of concrete pavement performance monitoring studies being conducted in Europe and Chile are discussed. Taken together, this information forms a foundation for the development of guidelines and recommendations for the design and construction of concrete pavements, material that is presented in volume III of this series of reports.



## REFERENCES

1. *The Long-Term Pavement Performance Program Guide*, Federal Highway Administration, LTPP Division, Washington, DC, December 1993.
2. Smith, K. D., D. G. Peshkin, M. I. Darter, A. L. Mueller, and S. H. Carpenter, *Performance of Jointed Concrete Pavements, Volume I: Evaluation of Concrete Pavement Performance and Design Features*, FHWA-RD-89-136, Federal Highway Administration, Washington, DC, March 1990.
3. Smith, K. D., A. L. Mueller, M. I. Darter, and D. G. Peshkin, *Performance of Jointed Concrete Pavements, Volume II: Evaluation and Modification of Concrete Pavement Design and Analysis Models*, FHWA-RD-89-137, Federal Highway Administration, Washington, DC, July 1990.
4. Smith, K. D., D. G. Peshkin, M. I. Darter, and A. L. Mueller, *Performance of Jointed Concrete Pavements, Volume III: Summary of Research Findings*, FHWA-RD-89-138, Federal Highway Administration, Washington, DC, November 1990.
5. Smith, K. D., D. G. Peshkin, M. I. Darter, A. L. Mueller, and S. H. Carpenter, *Performance of Jointed Concrete Pavements, Volume IV: Appendix A—Project Summary Reports and Summary Tables*, FHWA-RD-89-139, Federal Highway Administration, Washington, DC, March 1990.
6. Smith, K. D., D. G. Peshkin, M. I. Darter, A. L. Mueller, and S. H. Carpenter, *Performance of Jointed Concrete Pavements, Volume V: Appendix B—Data Collection and Analysis Procedures*, FHWA-RD-89-140, Federal Highway Administration, Washington, DC, March 1990.
7. Mueller, A. L., D. G. Peshkin, K. D. Smith, and M. I. Darter, *Performance of Jointed Concrete Pavements, Volume VI: Appendix C—Synthesis of Concrete Pavement Design Methods and Analysis Models, and Appendix D—Summary of Analysis Data for the Evaluation of Predictive Models*, FHWA-RD-89-141, Federal Highway Administration, Washington, DC, July 1990.
8. *Long-Term Pavement Performance Information Management System—Data User's Guide*, FHWA-RD-93-094, Federal Highway Administration, LTPP Division, Washington, DC, July 1993.
9. Delton, J. P., "Non-Conventional Versus Conventional Concrete Pavements in Arizona," *Proceedings*, Second International Conference on Concrete Pavement Design and Rehabilitation, Purdue University, April 1981.

10. Mueller, P. E. and L. A. Scofield, "An Expanded Evaluation of Arizona's Ten-Mile Concrete Test Roadway," *Proceedings, Fourth International Conference on Concrete Pavement Design and Rehabilitation*, Purdue University, April 1989.
11. Spellman, D. L., J. H. Woodstrom, B. F. Neal, and P. E. Mason, *Recent Experimental PCC Pavements in California*, Research Report CA-HY-MR-5180-1-73-01, California Department of Transportation, Sacramento, CA, June 1973.
12. Neal, B.F., *Evaluation of Design Changes and Experimental PCC Construction Features*, FHWA/CA/TL-85/07, California Department of Transportation, Sacramento, CA, July 1987.
13. Wells, G. K. and W. A. Nokes, *Field Review—10-SJ-5 PCCP Test Sections (Jointed PCCP Performance)*, Minor Research Report 65332-637391-31104, California Department of Transportation, Sacramento, CA, December 20, 1991.
14. Page, G. C., and L. W. Harper, *Florida Econocrete Test Road Post Construction and Materials Report*, Research Report FL/DOT/OMR-80/221, Florida Department of Transportation, Gainesville, FL, November 1980.
15. Larsen, T. J., and J. M. Armaghani, "Florida Econocrete Test Road: A 10-Year Progress Report," *Proceedings, Fourth International Conference on Concrete Pavement Design and Rehabilitation*, Purdue University, April 1989.
16. *Evaluation of the Performance of Doweled Contraction Joints Placed on Three Types of Subbase Course*, Report No. 1, February 1972; Report No. 2, December 1972; Report No. 3, February 1974; Georgia Department of Transportation.
17. Barenberg, E. J. and D. G. Zollinger, "Validation of Concrete Pavement Responses Using Instrumented Pavements," *Transportation Research Record 1286*, Transportation Research Board, Washington, DC, 1990.
18. Green, T. M. and E. C. Novak, Jr., *Drainage and Foundation Studies for an Experimental Short Slab Pavement*, Research Report R-1041, Michigan Department of Transportation, Lansing, MI, February 1977.
19. Arnold, C. J. and M. A. Chiunti, *Experimental Concrete and Bituminous Shoulder Construction Report*, Research Report R-844, Michigan Department of Transportation, Lansing, MI, January 1973.
20. Raisanen, D. L. and D. D. Anderson, *Concrete Pavements on Treated Bases*, Investigation No. 193, Minnesota Department of Highways, Minneapolis, MN, 1972.
21. Halverson, A. D., *Concrete Pavements on Treated Bases, Long-Term Performance Report—1986* Investigation No. 193, Minnesota Department of Transportation, Minneapolis, MN, 1986.

22. Tayabji, S. D., C. G. Ball, and P. A. Okamoto, *Effect of Concrete Shoulders on Concrete Pavement Performance*, FHWA/MN/RD-83/05, Minnesota Department of Transportation, Minneapolis, MN, October 1983.
23. Korfhage, G. R., *Effect of Concrete Shoulders, Lane Widening and Frozen Subgrade on Concrete Pavement Performance*, FHWA/MN/RD-88/02, Minnesota Department of Transportation, Minneapolis, MN, July 1988.
24. *Report on Joint Spacing of Concrete Pavement on T.H. 36*, Investigation No. 167, S.P. 6212-62, Minnesota Department of Transportation, Minneapolis, MN, 1990.
25. *Investigation of Roadway Design Variables to Reduce D-Cracking*, Final Report 78-1, Missouri Highway and Transportation Department, Jefferson City, MO, December 1987.
26. Bryden, J. E. and R. G. Phillips, *The Catskill-Cairo Experimental Rigid Pavement: A Five-Year Progress Report*, Research Report 17, New York State Department of Transportation, Albany, NY, November 1973.
27. Vyce, J. M. and R. G. Phillips, *The Catskill-Cairo Experimental Rigid Pavement: A Ten-Year Progress Report*, FHWA/NY/RR-81/91 (NYSDOT Research Report 91), New York State Department of Transportation, Albany, NY, July 1981.
28. Vyce, J. M., *Short-Slab Unreinforced Concrete Pavement and Shoulders: A Five-Year Performance Summary*, FHWA/NY/RR-82/95 (NYSDOT Research Report 95), New York State Department of Transportation, Albany, NY, May 1982.
29. *Experimental Project-Concrete Pavement Interstate 95, Nash and Halifax Counties, North Carolina*, Internal Departmental Memos, 1968-1984, North Carolina Department of Transportation, Raleigh, NC.
30. Wu, Shie-Shin, "Concrete Pavement Performance: A 23-Year Report," *Transportation Research Record 1370*, Transportation Research Board, Washington, DC, 1992.
31. Wu, Shie-Shin and T. M. Hearne, Jr, "Performance of Concrete Pavement with Econcrete Base," *Proceedings, Fourth International Conference on Concrete Pavement Design and Rehabilitation*, Purdue University, April 1989.
32. Minkarah, I. A. and J. P. Cook, *A Study of the Effect of the Environment on an Experimental Portland Cement Concrete Pavement*, OHIO-DOT-19-75, Ohio Department of Transportation, Columbus, OH, October 1975.
33. Stark, D., *The Significance of Pavement Design and Materials in D-Cracking*, FHWA/OH/91/009, Ohio Department of Transportation, Columbus, OH, June 1991.

34. Kazmierowski, T. J. and G. A. Wrong, "Six Year's Experience with Experimental Concrete Pavement Sections in Ontario," *Proceedings, Fourth International Conference on Concrete Pavement Design and Rehabilitation*, Purdue University, April 1989.
35. Kazmierowski, T. J. and A. Bradbury, "Ten Years Experience with Experimental Concrete Pavement Sections in Ontario," *Proceedings, Fifth International Conference on Concrete Pavement Design and Rehabilitation*, Purdue University, April 1993.
36. Highlands, K. L. and G. L. Hoffman, "Subbase Permeability and Pavement Performance," *Transportation Research Record 1159*, Transportation Research Board, Washington, DC, 1988.
37. Hall, M., *Cement Stabilized Open Graded Base: Strength Testing and Field Performance Versus Cement Content*, Project 0624-32-65, Wisconsin Concrete Pavement Association, Madison, WI, 1990.
38. Kelleher, K., and R. M. Larson, "The Design of Plain Doweled Jointed Concrete Pavement," *Fourth International Conference on Concrete Pavement Design and Rehabilitation*, Purdue University, 1989.
39. McGhee, K. H., *NCHRP Synthesis of Highway Practice—Design, Construction, and Maintenance of PCC Pavement Joints*, National Cooperative Highway Research Program, Washington, DC, 1995.
40. Vyce, J. M., *Performance of Load Transfer Devices*, FHWA/NY/RR-87/140 (NYSDOT Research Report 140), New York State Department of Transportation, Albany, NY, July 1987.
41. Crovetti, J. A., *Analysis of Support Conditions Under Jointed Concrete Slabs Along USH 18/151*, WI/SPR-01-95, Wisconsin Department of Transportation, Madison, WI, January 1995.
42. Shoher, S. F., "The Great Unsealing: A Perspective on PCC Joint Sealing," *1997 Transportation Research Board Annual Meeting*, (in press).
43. Wells, G. K., *Evaluate Stripping of Asphalt Treated Permeable Base*, Minor Research Report 65332-638047-39303, California Department of Transportation, Sacramento, CA, 1993.
44. Van Wijk, A. J., and C. W. Lovell, "Prediction of Subbase Erosion Caused by Pavement Pumping," *Transportation Research Record 1099*, Transportation Research Board, Washington, DC, 1986.

45. De Beer, M., "Erodibility of Cementitious Subbase Layers in Flexible and Rigid Pavements," *2nd International Workshop on the Theoretical Design of Concrete Pavements*, Sigüenza, Spain, 1990.
46. Ray, M., and J. P. Christory, "Combatting Concrete Pavement Slab Pumping, State of the Art and Recommendations," *Proceedings, Fourth International Conference on Concrete Pavement Design and Rehabilitation*, Purdue University, April 1989.
47. Federal Highway Administration, *Drainable Pavement Systems*, Participant's Notebook, Demonstration Project 87, FHWA-SA-92-008, Washington, DC, March 1992.
48. Cedegren, H. R., J. A. Arman, and K. H. O'Brien, *Development of Guidelines for the Design of Subsurface Drainage Systems for Highway Pavement Structural Sections*, FHWA-RD-73-14, Federal Highway Administration, Washington, DC, 1973.
49. Crovetti, J. A. and B. J. Dempsey, *Pavement Subbases*, Department of Civil Engineering, University of Illinois at Urbana-Champaign, Report Number UILU-ENG-91-2005, Illinois Department of Transportation, Springfield, IL, 1991.
50. Koslov, G. S., V. Mottola, and G. Mehalchick, *Improved Drainage and Frost Action Criteria for New Jersey Pavement Design, Volume I—Investigations for Subsurface Drainage Design*, New Jersey Department of Transportation, Federal Highway Administration, Washington, DC, 1983.
51. Darter, M. I., K. T. Hall, and C. Kuo, *Support Under Portland Cement Concrete Pavements*, NCHRP Report 372, National Cooperative Highway Research Program, Washington, DC, 1995.
52. Federal Highway Administration, *Concrete Pavement Joints*, Technical Advisory No. 5040.30, Washington, DC, 1990.
53. Tayabji, S. D., C. G. Ball, and P. A. Okamoto, *Effect of Concrete Shoulders on Concrete Pavement Performance*, FHWA/MN/RD-83/05, Minnesota Department of Transportation, St. Paul, MN, October 1983.
54. Yu, T. H., K. D. Smith, and M. I. Darter, *Field and Analytical Evaluation of the Effects of Tied PCC Shoulder and Widened Slabs on Performance of JPCP*, ERES Consultants, Inc., Colorado Department of Highways, Denver, CO, 1995.
55. Sehr, M., *Lateral Load Distribution and the Use of PCC Extended Pavement Slabs for Reduced Fatigue*, Federal Highway Administration, Washington, DC, June 1989.
56. American Association of State Highway and Transportation Officials, *AASHTO Guide for Design of Pavement Structures*, Washington, DC, 1986.

57. American Association of State Highway and Transportation Officials, *AASHTO Guide for Design of Pavement Structures*, Washington, DC, 1993.
58. Kunt, M. M., and B. F. McCullough, *Improved Design and Construction Procedures for Concrete Pavements Based on Mechanistic Modeling Techniques*, Research Report 1169-5F, Center for Transportation Research, University of Texas, Austin, TX, June 1992.
59. Bruinsma, J. E., Z. I. Raja, M. B. Snyder, and J. M. Vandenbossche, *Factors Affecting Deterioration of Transverse Cracks in Jointed Reinforced Concrete Pavements*, Michigan Department of Transportation, 1995.
60. S. Iwama, *Experimental Studies on the Structural Design of Concrete Pavement*, Public Works Research Institute, Japan, 1964.
61. Nakamura, T., and T. Iijima, "Evaluation of Performance and Structural Design Methods of Cement Concrete Pavements in Japan," *7th International Symposium on Concrete Roads*, Vienna, 1994.
62. Verhoeven, K., "Cracking and Corrosion in Continuously Reinforced Concrete Pavements," *Fifth International Conference on Concrete Pavement Design and Rehabilitation*, Purdue University, West LaFayette, IN, 1993.
63. Federal Highway Research Program, *Report on the 1992 U.S. Tour of European Concrete Highways*, FHWA-SA-93-012, Federal Highway Administration, Washington, D.C., 1993.
64. Bradbury, R. D., *Reinforced Concrete Pavements*, Wire Reinforcement Institute, Washington, DC, 1938.
65. Cashell, H. D., and W. E. Teske, "Continuous Reinforcement in Concrete Pavements," *Proceedings of the 34th Annual Meeting of the Highway Research Board*, Washington, DC, January 1955.
66. Fordyce, P, and W. E. Teske, *Some Relationships of the AASHO Road Test to Concrete Pavement Design*, Portland Cement Association, Chicago, IL, 1963.
67. McCullough, B. F., M. Won, and K. Hankins, "Long-Term Performance Study of Rigid Pavements," *Fourth International Conference on Concrete Pavement Design and Rehabilitation*, Purdue University, West LaFayette, IN, April 1989.
68. Blum, R. C., and C. E. Solberg, "Plain Pavement; An Economic Alternative," *International Conference on Concrete Pavement Design*, Purdue University, West LaFayette, IN, February 1977.

69. Darter, M. I., J. M. Becker, M. B. Snyder, and R. E. Smith, *Portland Cement Concrete Pavement Evaluation System (COPEs)*, NCHRP Report No. 277, Transportation Research Board, Washington, D.C., 1985.
70. Korenev, B. G. *Problems of analysis of beams and plates on elastic foundation*. Gosudarstvennoe Izdatel'stvo Literatury po Stroitel'stvu i Arkhitekture, Moscow, 1954 (in Russian).
71. Ioannides, A. M., L. Khazanovich, and J. L. Becque, "Structural Evaluation of Base Layers in Concrete Pavement Systems," *Transportation Research Record 1370*, Transportation Research Board, Washington, DC, 1992.
72. Ioannides, A. M. and L. Khazanovich, "Backcalculation Procedure For Three-Layered Concrete Pavements," *Proceedings, Fourth International Conference on Bearing Capacity of Roads and Airfields*, Minneapolis, MN, 1994.
73. Losberg, A., "Structurally Reinforced Concrete Pavements," *Doktorsavhandlingar Vid Chalmers Tekniska Högskola*, Göteborg, Sweden, 1990.
74. Ioannides, A. M., "Dimensional Analysis in NDT Rigid Pavement Evaluation," *Journal of Transportation Engineering*, ASCE, Vol. 116, No. 1, New York, NY, 1990.
75. McLachlan, N. W., *Bessel Functions for Engineers*, 2nd Ed. Clarendon Press, Oxford, U.K., 1955
76. Hoffman, M. S., and M. R. Thompson, "Mechanistic Interpretation of Nondestructive Testing Deflections," *Civil Engineering Studies*, Transportation Engineering Series No. 32, Illinois Cooperative Highway and Transportation Research Program Series No. 190, University of Illinois, Urbana, IL, 1981.
77. Hall, K. T., *Backcalculation Solutions for Concrete Pavements*, technical memo prepared for SHRP Contract P-020, Long-Term Pavement Performance Analysis, 1992.
78. Yoder, E. J., and M. W. Witczak, *Principles of Pavement Design*, John Wiley & Sons, Inc., New York, NY, 1975.
79. Uzan, J., R. Briggs, and T. Scullion, "Backcalculation of Design Parameters for Rigid Pavements," *Transportation Research Record 1377*, Transportation Research Board, Washington, DC, 1992.
80. Highway Research Board, *The AASHO Road Test*, Special Report 61E, Highway Research Board, Washington, D.C., 1962.
81. Carpenter, S. H., M. I. Darter, and B. J. Dempsey, *A Pavement Moisture Accelerated Distress (MAD) Identification System—Volume I*, FHWA/RD-81/079, Federal Highway Administration, Washington, D.C., September 1981.

82. Christory, J. P., "COPEs System, Europe—USA Cooperation," *Proceedings, Volume 190.7.B, XIXth World Road Congress, September 22–28, 1991*.
83. CEMBUREAU, *6th International Symposium on Concrete Roads*, Madrid, Spain, October 1990.
84. PIARC, *2nd International Workshop on the Theoretical Design of Concrete Pavements*, Siquenza, Spain, October 1990.
85. Poblete, M., C. Videla, and G. Echeverria, "Question III: Operation and Management—Chile," *National Report Presented to the 19th World Congress, Marrakesh, 1991*.
86. Poblete, M., R. Salsilli, R. Valenzuela, A. Bull, and P. Spratz, "Field Evaluation of Thermal deformations in Undoweled PCC Pavement Slabs," *Transportation Research Record 1207*, Transportation Research Board, Washington, DC, 1988.
87. Poblete, M., A. Garcia, J. David, P. Ceza, and R. Espinosa, "Moisture Effects on the Behavior of PCC Pavements," *Proceedings of the 2nd International Conference on the Design and Evaluation of Concrete Pavements*, Siquenza, Spain, 1990.
88. Poblete, M., R. Valenzuela, and R. Salsilli, "Load Transfer in Undoweled Transverse Joints of PCC Pavements," *Transportation Research Record 1207*, Transportation Research Board, Washington, DC, 1988.
89. Darter, M. I., *A Comparison Between Corps of Engineers and ERES Consultants, Inc. Rigid Pavement Design Procedures*, Technical Report for United States Air Force SAC Command, Savoy, IL, 1988.
90. Wells, G. K. and W. A. Nokes, *Field Review—PCCP Shoulder Performance Near Geyserville*, Minor Research Report 65328-637378-30088, California Department of Transportation, Sacramento, CA, 1990.